A Study on Operational Characteristics of Bubble Column Fermentors under Foam Control

March, 1994

Satoshi Takesono

Course of Industrial Science
Graduate School of Science and Technology
Niigata University

CONTENTS

CHAPTER 1

INTRODUCTION

1-1. Preface

Although aerated stirred-tank fermentors, i.e., aerated agitated vessels, have been commonly used in microbial process industries, they often encounter serious limitations, for example, high power requirement per unit volume, gas phase back mixing, shaft seal leaks, and difficulty in scaling up. Recently, bubble column fermentors (Refs.30, 52, 98, 120, 122) are being researched as alternative bioreactor types. In particular, these types are preferable for the processing of shear-sensitive cultures since in aerated stirred-tank fermentors shear intensities close to the impeller are usually very high. Scaling up is also easier to carry out due to the absence of moving parts such as the mixing impeller, etc. Thus, much attention has recently been received on application of bubble column fermentors to various aerobic microbiological reaction systems. On the other hand, in fermentation operations in such a fermentor, it has been recognized that foam formation during microbial fermentations is an undesirable but generally unavoidable evil (Refs.1, 65, 129). The foam has a negative effect including (Refs. 19, 23, 54, 59, 85, 101, 125, 126, 128, 134):

1) Reduction of the filling volume of the fermentor and increase of the likelihood of affecting the process;

2) creation of additional non-homogeneity of the mixture due to floatation of separate types of microorganisms;

3) loss of product due to foam ejection or disturbance of the technological conditions upon suppression of the foaming activity, the latter operation requiring a decrease of aeration and addition of liquid foam suppressors;

4) complication of the entire technology;

5) disturbance of the quality of the medium due to the presence of an antifoam agent, which hampers its further purification (bleaching); in the case of concentrates their physicochemical qualities decrease (agglutination, hygroscopicity, etc.).

Taking into account the fact that foam formation of most production media cannot be avoided, it becomes necessary to control the foam in some way.

Two typical methods, namely chemical and mechanical means, are available for foam control in bubble column fermentors. The chemical method is the one using antifoam agents (AFs) and has been extensively employed in fermentation industries because of simplicity and reliableness. However, as frequently pointed out, the addition of AFs to a process solution involves the following problems (Refs.2, 9, 10, 14, 15, 22, 34, 35, 37, 38, 43, 49, 54, 58, 59, 70, 81, 82, 86, 91, 106, 108, 109, 112, 113, 117, 119, 123, 130, 133, 134, 136, 137):

1) AFs have toxicity to microorganisms.

2) AFs are assimilated by microorganisms.

3) Oxygen supply is disturbed.

4) AFs are low in heat-resistant.

5) Subsequent procedures are affected.

6) Products or production metabolites are damaged.

7) High activity is not obtained by a small dose.

8) High concentration of AFs is necessary for reliable control.

9) Long duration of activity is not obtained.

10) Contamination such as adhesion occurs.

11) Cost of AFs is considerably high.

In view of these problems, the chemical method using AFs is by no means recommendable. On the contrary, foam-breaking by mechanical means without the addition of antifoam agents (AFs) has long ago attracted much attention as the method that is free from the problems as seen when the foaming was controlled by antifoam agents (AFs). A suitably developed mechanical means, i.e., foam-breaker, can provide benefit of not only holding down the running cost but also facilitating oxygen supply due to the increased gas holdup, i.e., the increased specific gas-liquid interfacial area. There is also no problem such as complication in separation and purification operations of products as seen when AFs were added to the process solution. Supported by these potential advantages, a number of mechanical foam-breakers have so far been proposed for the control of foam (Refs.24, 28, 29, 51, 24, 54, 56, 57, 59, 68, 129, 134, 135, 145). Development of practicable higher performance foam-breakers is still continued. In spite of all these painstaking efforts, however, most of

those foam-breakers failed to prove effective on large-scale foam mass or foam grown by high aeration and mixing, unless combined with the use of AFs together. Thus, they are hardly practical. In other words, none of the mechanical foam-breakers proposed so far is entirely satisfactory or universally applicable to fermentation foams. This may be partially attributable to the situation that the immediate effect on foam-breaking, where foaming is regarded as a secondary phenomenon, has been the matter of the highest priority. However, it seems mainly due to the following reasons:

1) Most of the foam-breakers thus far developed is the products of empirical approaches without fundamental analysis of the mechanism of mechanical foam-breaking. In addition, access to the comparative quantitative data and guide-lines for selection of a mechanical foam-breaker has not also been provided.
2) In spite of the wide variety of foaming liquids actually used in production processes, foam-breaking experiments have been carried out using only a restricted range of foaming liquids.
3) There has been little quantitative discussion on the relationship between the performance of the foam-breaker and the nature of foam to be treated.
4) Quantitative analysis on the performance of mechanical foam-breakers have been almost totally ignored with the natural consequence of failure in establishing the effective foam-breaker which could have

been derived from the above mentioned analytical quantification.

5) Methods for complete calculations of mechanical foam-breakers and full foam control systems are not adequately developed.

Prior to practical application of a mechanical foam-breaker, sufficient studies on clarification of these problems have to be carried out. In other words, it is necessary that the performance of the foam-breaker to be employed should have been examined with various foaming systems and also that its operational characteristics should have been clarified in respect of the nature of foams in the liquids to be treated. It is also important to obtain correlations useful for the design and operation of the foam-breaker fitted to the bubble column fermentor or its scaling-up.

The ultimate objective of bubble column fermentors is to supply oxygen enough for aerobic cultivation of microorganisms. Oxygen supply changes largely depending on the magnitude of the oxygen transfer rate. Thus, information on the gas holdup ϕ_g and the volumetric mass transfer coefficient k_La relating to oxygen transfer rate is indispensable for the design and operation of bubble column fermentors under foam control. The volumetric mass transfer coefficient k_La is obtained as the product of the liquid-phase mass transfer coefficient k_L and the specific gas-liquid interfacial area a. Knowing the dependence of the individual parameters, k_L and a, on liquid properties and operating conditions leads us to a better

design and operation of bubble column fermentors. Therefore, it is also necessary to discuss separately these constituent parameters of the volumetric mass transfer coefficient, i.e., k_L and a. A large number of studies on ϕ_g and k_La of bubble column fermentors without foaming have been reported (Refs.4, 5, 11, 12, 33, 40, 44, 48, 53, 55, 61-63, 69, 75, 78, 79, 84, 87, 90, 92, 94, 96, 99, 102, 121, 122). These data have been utilized effectively as the basis for the design and operation of bubble column fermentors not only in laboratories but also in industrial plants. Many studies have also dealt with the effect of antifoam agents (AFs) on the hydrodynamic and mass transfer characteristics in bubble column fermentors (Refs.2, 7, 9, 14, 22, 31, 49, 64, 81, 82, 91, 108, 117, 119, 123, 130, 136, 137). The differences in ϕ_g and k_La between bubble column fermentors with and without the addition of AFs have been discussed. In most of these existing studies, however, liquids or media of less foaming tendency, for which the addition of AFs is not necessarily required, were employed. Experiments were also carried out using bubble column fermentors without foam-breaker. In contrast, practically no information is available in the literature on the characteristics such ϕ_g and k_La of bubble column fermentors in a mechanical foam control system because of the difficulty of foam control or the lack of an appropriate foam-breaker effective for foam control. In order to confirm the superiority of operation using the bubble column fermentor without the addition of AFs where the foaming

is controlled mechanically, clarification of the differences in ϕ_g and k_La between bubble column fermentors when the foaming is controlled by the foam-breaker and AFs is desired. Liquids in bubble column fermentors contain surfactants, antifoam agents or both. The overall changes in volumetric mass transfer coefficient k_La due to the presence of these materials depends on the relative magnitude of their effects on the liquid-phase mass transfer coefficient k_L and the specific gas-liquid interfacial area a. The relative balance between the changes in k_L and a determines whether k_La increases or decreases. Concerning the changes in k_L in the nonfoaming system i.e., bubble column fermentors without foaming, many studies have been carried out (Refs.3, 6, 8, 16, 25-27, 31, 32, 36, 39, 45-47, 50, 66, 67, 72, 74, 76, 77, 80, 83, 88, 89, 93, 97, 100, 103, 110, 118, 124, 132, 142, 143) and various types of correlations for predicting k_L in such a system have been proposed so far (Refs.6, 27, 67, 118). Most of these correlations, however, are those obtained in liquids or media of less foaming tendency, for which the addition of AFs is not necessarily required. In other words, their correlations are not those obtained in liquids or media of high foaming tendency, for which control of foaming by either AFs or the mechanical foam-breaker becomes necessary. A direct application of these existing correlations to k_L data in foaming systems which are of more practical interest is difficult due to a large difference in the hydrodynamic behavior or bubble dynamics between the foaming

and nonfoaming systems. Thus, information on k_L under mechanical or chemical foam control and correlations for k_L in both systems are indispensable for a better design and operation of bubble column fermentors, treating various foaming liquids of high foaming tendency or foaminess, under foam control.

As introduced in the above, studies on operational characteristics of bubble column fermentors with mechanical foam-breaker which include foam-breaking, flow and mass transfer are scarce, and understanding of the design and operational procedures of bubble column fermentors under foam control is also far from adequate. In fact, the usage of bubble column fermentors treating various foaming systems is at present mostly empirical. The circumstances that this branch of investigation is considerably underdeveloped in comparison with the studies on the new production techniques of microorganic cell mass and production metabolites, analysis of biological reaction processes and new type of bubble column fermentors are also a serious problem. Development and application of bubble column fermentors having a mechanical foam-breaking mechanism or advancement of their practical value as a new aeration technique, useful for effectively treating a foaming system without using antifoam agents (AFs), largely depend on the systematic study on the foam-breaking operation by means of a mechanical foam-breaker that permits quantitative evaluation of performance or quantitative analysis of the effects of operational conditions on foam-breaking and the relation be-

tween the nature of foam and difficulty in foam-breaking procedure. In this thesis, the problems related to design and operational characteristics of bubble column fermentors under foam control which has so far remained without quantitative analysis were studied systematically on the basis of the experimental data using the foam-breaker of the type in which the impact force of dispersed liquid particles is incorporated for mechanically controlling foam.

1-2. Purpose and plan of the study

The present study is concerned with operational characteristics of bubble column fermentors, i.e., bubble columns (BCs), under foam control. The main objective is to obtain correlations useful for the design and operation or scale-up of BCs treating various foaming systems under mechanical foam control. It is also a purpose of this thesis to clarify the difference in performance and operational characteristics of BCs when the foaming is controlled by a rotating-disk mechanical foam-breaker (MFRD), which facilitates foam-breaking action by the impact between the liquid particles dispersed from the disk and the ascending foam, and antifoam agents (AFs). Firstly, as a step forward to a series of studies on various characteristics of BCs under mechanical foam control, foam-breaking performance of the MFRD fitted to the BC, its usefulness as a foam controlling apparatus in the BC with a foaming system and superiority of mechanically controlled foaming were attempted to clarify. Operational

characteristics of MFRDs fitted to BCs treating various foaming liquids were then evaluated. A new foaming characteristic term that reflects the dynamic foaming capacity (intensity) of BCs containing various liquids and is related to difficulty or ease of mechanical foam-breaking with MFRDs regardless of the kind of foaming liquid or its concentration was sought. Applicability of this foaming characteristic term to design and operation of BCs with MFRDs, treating various complex solutions and biological media, was also examined. The gas holdup, the volumetric liquid-phase mass transfer coefficient and the liquid-phase mass transfer coefficient in BCs under foam control with MFRDs were further studied. The difference in these characteristic values between BCs where the foaming is controlled by MFRDs and an AF was also attempted to clarify quantitatively.

1-3. Construction of the thesis

This thesis consists of 10 chapters and a conclusion.

Chapter 1 describes the aim and scope of the present study.

Chapter 2 not only introduces the circumstances of studies on the design and operation of bubble column fermentors, i.e., bubble columns, having a mechanical foam-breaking mechanism but also describes the situation that this field of investigation is underdeveloped, thus defining the significance of this study.

Chapter 3 is concerned with performance characteristics of a bubble column (BC) with mechanical foam control. The

characteristics of a rotating-disk mechanical foam-breaker (MFRD) fitted to the BC treating various liquids are first examined. Foaming behavior in the BC and foam-breaking behavior of the MFRD under varying operating conditions are also studied in terms of the changes in liquid holdup in foam. The differences in flow and mass transfer characteristics between two BCs when the foaming is controlled by the MFRD and an antifoam agent (AF) is then evaluated. Furthermore, from a comparison of the volumetric liquid-phase mass transfer coefficient between the mechanical foam control system and the nonfoaming system in terms of the specific power input, the superiority of mechanically controlled foaming will be demonstrated.

Chapter 4 is concerned with design and operation of MFRDs fitted to BCs. The main objective of this chapter is to investigate operational characteristics of BCs with MFRDs of different sizes treating various foaming liquids and to develop design parameters and empirical equations for scale-up of the MFRD as a foam controlling apparatus fitted to BC. The foam-breaking behavior of MFRDs fitted to BCs and the foaming behavior of BCs are first investigated respectively from the changes in the required critical disk rotational speed and those in liquid holdup in the foam. The empirical equations for predicting the critical disk rotational speed and the liquid holdup in foam-breaking regions, useful for the design and operation of MFRDs fitted to BCs, are then proposed. The level of the required foam-breaking power of MFRDs is further clarified in relation to the level of liquid holdup which

reflects the foaming intensity of BCs and is related to the difficulty of mechanical foam-breaking.

Chapter 5 deals with relation between mechanical foam-breaking difficulty and foaming characteristics of solutions. Using a small foaming apparatus, liquid foaming characteristics such as liquid holdup in foamate flow, rate of liquid drainage from foam, foam velocity and foam size are first examined. The relationship among their values and liquid holdup in foam in BCs with MFRDs is then investigated. Furthermore, on the basic of the relationship obtained, a new correlation for predicting liquid holdup in foam under any operating conditions independently of the kind of foaming liquid and its concentration is discussed.

Chapter 6 is concerned with relation between critical disk rotational speed for foam-breaking of MFRDs and foaming characteristics of solutions. For BCs treating various foaming liquids, the critical disk rotational speed required for foam-breaking of MFRDs fitted BCs is discussed in relation to the foaming characteristics of liquids. A new empirical equation that prediction of critical disk rotational speed of MFRDs fitted to BCs treating various liquids is possible regaradless of the type of foaming liquid or its concentration has been described.

Chapter 7 deals with design and operation of BCs fitted with MFRDs treating various complex solutions and biological media. For a small BC treating mixed solutions, the foaming behavior of the BC and foam-breaking behavior of the MFRD are first evaluated respectively from changes in

liquid holdup in foam and required critical disk rotational speed for foam-breaking. The differences in liquid holdup and critical disk rotational speed among mixed solutions are then discussed in relation to the values of foaming characteristic term of respective solutions, which colud be determined on the basis of the results measured by using the foaming apparatus. Usefulness of the empirical correlations for the prediction of liquid holdup in the small BC and critical disk rotational speed of the MFRD fitted to its BC is also examined. Similar investigations are then carried out for the small BC with the MFRD treating biological media. It is further checked whether the empirical correlations for the prediction of liquid holdup in foam and critical disk rotational speed and the power for foam-breaking obtained in chapters 5 and 6 is applicable to larger BCs with MFRDs treating mixed solutions and biological media. On the basis of the correlations obtained, the operational procedure of MFRD based on changes in foaming characteristics of liquid in the BC during the operation is also discussed.

Chapter 8 is concerned with the gas holdup in BCs treating various foaming liquids under foam control. The effects of operating conditions such as the air sparge rate, the liquid or the column size on the gas holdup in BCs under mechanical foam control with MFRDs is first investigated. Similar investigations are then carried out for BCs with the addition of AF. Correlations for predicting the gas holdups in a mechanical foam control system (MFS) and a nonfoaming system (NS) are also described.

Chapter 9 deals with the volumetric liquid-phase mass transfer coefficient in BCs under foam control. As the foaming liquid for the evaluation of the oxygen transfer characteristics of the BC, 0.15M sodium sulfite solutions containing various foaming agents have been employed. The volumetric liquid-phase mass transfer coefficients in a mechanical foam control system (MFS) and a nonfoaming system (NS) is first measured according to the sulfite oxidation method. Comparison of the volumetric liquid-phase mass transfer coefficients between the MFS and NS in terms of the specific power input is then carried out. The superiority of the MFS not only in oxygen transfer performance but also in power input economy will be demonstrated.

Chapter 10 is concerned with liquid-phase mass transfer coefficients in BCs under foam control. The bubble diameter in BCs when the foaming is controlled by the MFRD and an AF is first measured. From these results and those of the gas holdup measured in chapter 8, the specific gas-liquid interfacial area in respective foam control systems are then evaluated. The value of the liquid-phase mass transfer coefficient is also determined by using the value of specific gas-liquid interfacial area and that of volumetric liquid-phase mass transfer coefficient obtained in the preseding chapter. The difference in volumetric liquid-phase mass transfer coefficients between BCs when the foaming is controlled by the MFRD and the AF, demonstrated in chapter 9, is discussed in relation to the changes in liquid-phase mass tranfer coefficent

and specific gas-liquid interfacial area. Furthermore, correlations for predicting the liquid-phase mass transfer coefficient in the mechanical foam control and non-foaming systems are sought.

Chapter 11 as the conclusion summarized the results obtained in the foregoing chapters. Problems that need further investigations are proposed and further course of development is also suggested in this chapter.

CHAPTER 2

REVIEW OF EXISTING STUDIES ON FOAM CONTROL IN SUBMERGED FERMENTATION AND CHARACTERISTICS OF BUBBLE COLUMN FERMENTORS UNDER FOAM CONTROL

In this chapter, the outline of the existing studies on foam formation and control in submerged fermentation, mechanical foam-breaking methods and equipments and measure for foam-breaking is shown together with problems involved. Circumstances of the existing studies on gas holdup, volumetric liquid-phase mass transfer coefficient and liquid-phase mass transfer coefficient in bubble column fermentors under foam control are also reviewed briefly in turn.

2-1. Effect of foam in fermentation

Foam formation in fermentations or aerobic cultures of microorganisms, which occurs extensively not only in a laboratorial scale but also in industrial plants, is undesirable because of its many adverse effects (Refs.19, 23, 54, 59, 85, 101, 125, 126, 128, 134) (Table 2-1). The problems posed by foams fall into two categories (Ref. 59). There are those caused by its presence within the fermentor and those caused by its escape if uncontrolled. In the former, the most obvious disadvantage is the head space occupied by the foam, which reduces the filling volume of the fermentor and the yield. A further disadvantage with a very rapidly forming foam is the limit im-

posed on the allowable aeration rates. This limit becomes a serious problem in the cultivation of a microorganic cell mass and production of metabolites that require higher aeration rates. Concerning the latter problem, the most immediate consequence of foam escape is the wetting of the outlet air filters and lines. This causes contamination and results in failure of the normal fermentation operation. There are also adverse effects resulting from foam separation and froth floatation. Foam separation is due to the selective adsorption of solutes at a gas-liquid interface. Froth floatation is the phenomenon that fine solids (cells) are floated out of the bulk solution and into the foam layer during aeration. Both these phenomena occur simultaneously and a fermentation foam thereby becomes enriched in solid (cell) and surfactant concentration relative to the broth. This results in promotion of lysis of cells and creation of non-homogeneity in fermentation system. Loss of cellular material from the culture broth by froth floatation is also clearly undesirable in any fermentation, and this can occur, even if no foam escapes, by deposition on the walls, baffles and top of the fermentor during periods of active foaming. This deposited material also undergoes lysis and liberates proteins which act as catalysts for additional foam formation. Thus, the problems caused by foam have microbiological, economical and chemical engineering aspects, and an efficient foam control system should take all of them into account.

2-2. Effect of antifoam agents

Antifoam agents (AFs) are commonly used to control foaming in submerged aerobic fermentations. However, attention should be paid to the fact that the use of AFs for control of foam during fermentation leads to many adverse effects (Refs.2, 9, 10, 14, 15, 22, 34, 35, 37, 38, 43, 49, 54, 58, 59, 70, 81, 82, 86. 91, 106, 108, 109, 112, 113, 117, 119, 123, 130, 133, 134, 136, 137) such as the reduction of oxygen transfer rate, the reaction inhibition and toxicity, adverse effects on separation or purification of cell mass or production metabolites from the fermentation broth, etc (Table 2-2).

Many studies have reported remarkable effect of AFs on oxygen transfer rate in fermentors (Refs.2, 9, 14, 22, 49, 81, 82, 91, 108, 117, 119, 123, 130, 136, 137). In some cases of fermentation, the oxygen transfer rate decreases by more than 50% on using AFs. The lowing of oxygen transfer rate has a serious negative effect on the cultivation of a microorganic cell mass which is very sensitive to oxygen or the production of metabolites which requires exceedingly high aeration rates. As to the toxic effect of AFs, for example, Plichon et al. (Ref. 109) reported that addition of an AF, a silicone, provokes an interruption of bacterial growth. Berovič and Cimerman (Ref.15) also observed that some AFs inhibited mould growth. Furthermore, the presence of AFs in the system also causes difficulty in extraction and purification of the product and the necessity for extra separation stage for the removal of AFs from the product, there-

Table 2-1 Adverse effects of foam in fermentation.

	Effect	Reference
(1)	Reduction in working capacity	(Ref.23)
(2)	Loss of culture fluid and cells through air line	(Ref.125)
(3)	Contamination of the atmosphere	(Ref.19)
(4)	Increased chances of fermentor contamination	(Ref.125)
(5)	Barrier to oxygen transfer	(Ref.126)
(6)	Promotion of lysis of cells	(Ref.19)
(7)	Invalid fermentation data	(Ref.23)
(8)	Deposition of cells on upper part of fermentor	(Ref.19)
(9)	Shutdown of the plant	(Ref.23)
(10)	Preferential removal of surface-active agents from medium	(Ref.19)
(11)	Additional expenses for foam control	(Ref.23)
(12)	Creation of additional non-homogeneity in fermentation system	(Ref.134)

Table 2-2 Adverse effects of antifoam agents (Ref.54).

	Effect
(1)	Changed pattern of dissolved gases
(2)	Change in air bubble size
(3)	Gradual drop in mixing power and consequent changed pattern of agitation
(4)	Sharp increase in power requirement
(5)	Changes in pH pattern
(6)	Production of totally different metabolite (antibiotic)
(7)	Preferential utilization of antifoams as carbon source
(8)	Decrease in product/biomass, reduced fermentation rate, delayed onset of metabolite production

by making the process more expensive. Thus, there is a demand for mechanical foam-breaking method without using antifoam agents (AFs).

2-3. Methods and equipments for mechanical foam control

The action of mechanical foam-breaking methods is based on mechanisms such as rapid pressure change, shear force, compressive force and impact force, either alone or in combination. Among the mechanical methods, mechanical foam-breakers with rotating installations (Refs.24, 28, 51, 54, 56, 59, 68, 134, 135, 145) are most popular. They can be of various types ranging from simple to complex designs. The simplest apparatus consists of either a bent, rotating stirring rod (Ref.56), rotating paddle, or rotating vanes (Ref.19) which are attached to the stirrer shaft. These apparatuses break the foam by a combination of impact and shear forces (Ref.56). Another widely used foam-breaker with rotating installations is the centrifugal or basket foam-breaker, which brings about sudden pressure changes and the shear of bubbles in the spinning bowl (Ref.56). Apparatuses based on conical dishes (Ref.134) or disks (Refs.28, 68) have also been reported. Reviewing these, however, most reports offer only qualitative considerations. In other words, they do not mention the physicochemical properties of foams, the relation between their properties and the performance of mechanical foam-breakers or their design, operation and scale-up, etc. Recently, the rotating-disk mechanical foam-breaker (MFRD) (Refs.104, 105) has developed as a

high performance foam-breaking apparatus. The performance of the MFRD as a foam control apparatus and the design and operation of MFRDs fitted to stirred-tank fermentors, i.e., aerated agitated vessels, have already been characterized by Yasukawa et al (Refs.139-141). This apparatus, which facilitated foam-breaking action by the impact between the dispersed liquid particles from the disk and the ascending foam, is expected to be one of potential value in controlling foaming in a bubble column fermentor that operates at high aeration rate conditions. The performance of the MFRD fitted to a bubble column fermentor treating various foaming liquids or the various characteristics such as the gas holdup, the oxygen transfer rate, etc., however, have not yet been investigated. In order to provide a more sound and generalized basis for the design and operation of a bubble column fermentor with the MFRD treating various liquids, quantitative studies on the performance of the MFRD fitted to the bubble column fermentor and various characteristics of the bubble column fermentor with the MFRD are necessary.

2-4. Measure for mechanical foam-breaking

More effective design and operation of the foam-breaker to be employed for mechanical foam control are important to base on the nature of the foam generated or on the foaming characteristics of liquids to be treated. Various methods for measuring the nature of foam such as foaminess, foam lifetime, etc. have been proposed so far (Refs.17, 20, 21, 71, 73, 114-116). Most of these meth-

ods, however, could allow measurements under considerably restricted conditions that were different from actual gas bubbling and foaming. This, in other words, implies that a direct application of the existing methods to a mechanical foam-breaking system, i.e., a fermentor having a foam-breaking mechanism, operating under high gas throughput is difficult. Efforts have also been done to find parameters which characterize the foam-forming ability of liquids and to apply their parameters for design or operation of mechanical foam-breakers (Refs.54, 59, 134). However, such attempts seem to have yet been unsuccessful. In order to carry out effective design and operation of the mechanical foam-breaker, a measure which reflects foaming behavior (intensity) of the fermentor and the foam-breaking behavior of the foam-breaker and is also related to the difficulty or ease of mechanical foam-breaking independently of the kind of foaming liquid or its concentration becomes important. However, little information has yet been available on such a measure.

2-5. Gas holdup in bubble column fermentors

The gas holdup is an important parameter in the design and operation of a bubble column fermentor because their values are closely related to the changes in oxygen transfer rate. Many studies on the effect of operational conditions on gas holdup of bubble column fermentors, i.e., bubble column (BCs), without foam formation have been reported (Refs.5, 11, 12, 44, 53, 55, 61, 62, 69, 78, 84, 87, 92, 94, 96, 121). A large number of correlations for

gas holdups are also available in the literature. Some of the important correlations are shown in Table 2-3. These have been utilized effectively for the design and operation of BCs without foaming, not only in laboratories but also in industrial plants. However, all of these correlations do not consider the effect of foaming. In other words, it is difficult to apply the existing correlations to BCs with a foaming system. In the operation of BCs with a foaming system, foam is controlled by either antifoam agents (AFs) or mechanical foam-breakers. According to the difference in foaming behavior in BCs with and without the addition of AFs, it is suggested that gas holdups between two BCs when the foaming is controlled by a mechanism foam-breaker and an AF may differ largely. However, quantitative information on such a difference has not yet been reported. Systematic studies on the gas holdup of the BC under foam control are desired.

2-6. Mass transfer in bubble column fermentors

In aerobic submerged fermentations using a bubble column fermentor, i.e., a bubble column (BC), productivity of microorganic cell mass and metabolites is largely affected by the dissolved oxygen concentration in the bulk liquid, in other words, the absorption rate of oxygen into the medium. Therefore, it is important to understand beforehand the level of oxygen absorption rate of the BC employed actually. The oxygen absorption rate can be evaluated in terms of the overall volumetric oxygen transfer coefficient $k_L a$. It can be said that $k_L a$ is a most

Table 2-3 Gas holdup correlations in literature.

System	Range of Parameters	Correlation Proposed	Reference
(1) Air-Water Air-Kerosene Air-Na_2SO_3 aq. soln. Air-Glycerol Air-Light Oil Air-$ZnCl_2$ aq. soln. ρ, kg/m^3: 780-1700 μ, Pas: 0.0009-0.0152 σ, N/m: 0.025-0.076	U_g, m/s: 0.004-0.45 D_T, m > 0.1	$\varepsilon_g=\frac{1}{2+(0.35/U_g)(\rho\sigma/72)^{1/3}}$	(Ref. 67)
(2) Air-Water	U_g, m/s: 0-0.3 u_L, m/s: 0-0.015 D_T, m: 0.066-0.214 H_f, m: 2.01-4.05	$\varepsilon_g=\frac{2.51U_g}{0.78+\beta U_g^{0.8}(1-e^{\gamma})}$ $\beta=4.5-3.5-2.548D_T^{1.8}$ $\gamma=717U_g^{1.8}/\beta$	(Ref. 78)
(3) Air-Water Air-Glycol aq. soln. Air-Methanol O_2-Water He-Water CO_2-Water ρ, kg/m^3: 800-1600 μ, Pas: 0.00058-0.021 σ, N/m: 0.022-0.0742	U_g, m/s: 0.003-0.4 u_L, m/s: 0-0.044 D_T, m: 0.152-0.6 H_f, m: 1.26-3.5	$\frac{\varepsilon_g}{(1-\varepsilon_g)^4}=C\left(\frac{gD_T^2\rho}{\sigma}\right)^{1/8}\left(\frac{gD_T^3}{\nu^2}\right)^{1/12}\left(\frac{U_g}{\sqrt{gD_T}}\right)$ C = 0.2 for pure liquids and non-electrolytes C = 0.25 for electrolytes	(Ref. 5)
(4) Air-Water Air-Methanol aq. soln. ρ, kg/m^3: 910-1200 μ, Pas: 0.0007-0.0138 σ, N/m: 0.0375-0.0748	U_g, m/s: 0.042-0.38 D_T, m: 0.1-0.19 H_f, m: 0.6-1.35	$\varepsilon_g=0.505U_g^{0.47}(0.072/\sigma)^{2/3}(0.001/\mu)^{0.05}$	(Ref. 61)
(5) Air-Different Liquids ρ, kg/m^3:800-1600 μ, Pas:0.00043-0.0 σ, N/m:0.0214-0.0728	U_g, m/s: 0.01-0.08 D_T, m: 0.0756-0.61 H_f, m: 0.02-3.5	$\varepsilon_g=0.89\left(\frac{H_f}{D_T}\right)^{0.036(-15.7\log K)}\left(\frac{d_{bj}}{D_T}\right)^{0.3}\times\left(\frac{U_g}{d_{bg}}\right)^{20.025(2.6+\log K)}K^{0.047}-0.05$ $K=\rho\sigma^3/\mu^4 g$	(Ref. 53)
(6) Air-Water Air-Glycerol aq. soln Air-Kerosene ρ, kg/m^3: 800-1100 μ, Pas: 0.0009-0.0115 σ, N/m: 0.0312-0.072	U_g, m/s: 0.0014-0.14 D_T, m: 0.05 and 0.1	$\varepsilon_g=0.728U-0.458U^2+0.0975U^3$ $U=U_g(\rho^2/\sigma(\rho-\rho_g)g)^{1/4}$	(Ref. 92)

(7) Air-Ethanol-Solids
Air-Glycerol aq. soln. Solids
Air-Methanbol-Solids
Air-water-Solids
ρ, kg/m^3:790-1210
μ, Pas:0.001-0.062
σ, N/m:0.0223-0.0728

U_g, m/s: 0.05-4.0
D_T, m: 0.05 and 0.1
d_p, m: 0.011-0.0287
H_f, m: 0.05-0.2

$$\frac{\varepsilon_g}{\left\{\varepsilon_g(1-\varepsilon_g)^2\right\}^{0.44}} = 0.5\left(\frac{D_T U_g^2 \rho}{\sigma}\right)^{0.11} \times \left(\frac{U_g}{\sqrt{gD_T}}\right)^{0.22}$$

(Ref. 87)

(8) Air-Water-Solids

U_g, m/s: 0-0.173
u_L, m/s: 0-0.12
D_T, m: 0.076 and 0.152
H_f, m: 0.22-0.45

$$\varepsilon_g = (1.612\pm0.023)U_g^{0.720\pm0.028} \times d_p^{0.168\pm0.061} D_T^{-0.125\pm0.088}$$

(Ref. 12)

(9) Air-Alcohols
Air-Halogenated Hydrogents

U_g, m/s: 0-0.1
D_T, m: > 0
H_f, m: >1.2

$$\frac{\varepsilon_g}{(1-\varepsilon_g)} = 0.115\left(\frac{U_g^3}{\nu g(\rho-\rho_g)/\rho}\right)^{0.23}$$

(Ref. 11)

(10) Gas-Liquid

Ranges are not defined (semitheoretical equation)

$$\frac{\varepsilon_g}{(1-\varepsilon_g)^4} = 0.14 U_g \left(\frac{\rho^2}{\sigma(\rho-\rho_g)g}\right)^{1/4} \times \left(\frac{\rho^2\sigma^3}{\mu^4(\rho-\rho_g)g}\right)^{1/24}\left(\frac{\rho}{\rho_g}\right)^{5/72}\left(\frac{\rho}{\rho-\rho_g}\right)^{1/3}$$

(Ref. 96)

(11) Different Gases (Air, H_2, CO_2, CH_4, C_3H_8, N_2)-Water
Air-Organic Liquids
Air-Electrolyte Soln.
ρ, kg/m^3: 790-1170
μ, Pas: 0.0009-0.0178
σ, N/m: 0.0229-0.0796
ρ_g, kg/m^3: 0.84-1.84

U_g, m/s: 0.042-0.38
D_T, m: 0.1
H_f, m: 0.65

$$\varepsilon_g = 0.672 f\left(\frac{U_g\mu}{\sigma}\right)^{0.578}\left(\frac{\mu^4 g}{\rho\sigma^3}\right)^{-0.131} \times \left(\frac{\rho_g}{\rho}\right)^{0.062}\left(\frac{\mu_g}{\mu}\right)^{0.107}$$

f = 1.0 for nonelectolyte solutions
$f = 10^{0.04141}$ I < 1.0kgion/m^3
f = 1.1 I > 1.0kgion/m^3
I = Ionic strength of the solution

(Ref. 62)

(12) Gas-Liquid

Theoretical

$$\frac{\varepsilon_g}{(1-\varepsilon_g^{1/3})} = \frac{U_g}{U_b}$$

(Ref. 69)

(13) Downflow bubble Column

Air	Water	$148 < I < 336$
Ar	CCl_4	$0.003 < \varepsilon^* < 0.24$
H_2	Glycerol aq. soln.	$184 < \rho/\rho_g < 5.340$
CCl_2F_2		$37 < \mu/\mu_g < 2220$
	CMC	$0.055 < \sigma < 0.07$

$$\varepsilon_g = \left\{1+0.0685\frac{(1-\varepsilon_g^*)^{3.112}}{\varepsilon_g^{*0.395}}\left(\frac{\rho}{\rho_g}\right)^{0.0346} \times \left(\frac{\mu}{\mu_g}\right)^{0.25} Fr^{0.36} We^{0.543}\right\}^{-1}$$

$$\varepsilon_g^* = \frac{U_g}{U_g+u_L}$$

(Ref. 44)

important parameter which characterizes oxygen transfer performance of BCs. Many studies have been carried out on mass transfer characteristics of BCs without foam formation (Refs.4, 5, 33, 40, 48, 55, 63, 75, 79, 90, 99, 102). As summarized in Table 2-4, various correlations for k_La have also been reported. In contrast, practically no information is available in the literature on the mass transfer characteristics of BCs with a foaming system. Therefore, there have been no data on oxygen transfer rate in the BC under mechanical foam control or on the difference in oxygen transfer rates between BCs when the foaming is controlled by a mechanical foam-breaker and an antifoam agent (AF). It is expected that in BCs with a foaming system the gas holdup may be considerably large and as a result of its phenomenon higher values of the mass transfer rate would also be attained. In order to confirm this, i.e., the superiority of mechanically controlled foaming, quantitative studies are necessary on oxygen transfer rates in not only BCs having a foam-breaking mechanism but also BCs with an added AF.

2-7. Liquid-phase mass transfer coefficients in bubble column fermentors

Liquids in fermentors, i.e., fermentation broths, contain surface-active materials such as surfactants, antifoam agents or both. It is known that these materials in liquids retard mass transfer from a single bubble. The overall change in volumetric liquid-phase mass transfer coefficient k_La due to the addition of these materials

Table 2-4 Reported studies for k_La.

System	Range of Parameters	Correlation Proposed	Reference
(1) Water-Air Glycol-Air Methanol-Air Glycol aq. soln.-Air Methanol aq. soln-Air Water-O_2 Water-He Water-CO_2	U_g, m/s: 0.003-0.4 u_L, m/s: 0.0-0.44 D_T, m: 0.152-0.6 H_f, m: 0.126-0.35 ρ, kg/m^3: 800-1600 μ, Pas: 0.00058-0.021 σ, N/m: 0.022-0.0742	$\frac{k_La D_T^2}{D_L} = 0.6 \left(\frac{\nu}{D_L}\right)^{0.5} \left(\frac{g D_T^2 \rho_l}{\sigma}\right)^{0.62} \times \left(\frac{g D_T^3}{\nu^2}\right)^{0.31} \varepsilon_g^{1.1}$	(Ref. 5)
(2) Gas-Liquid	Theoretical Equation	$k_La = 3.31 \frac{D_L \varepsilon_g}{d_b^2} \left(\frac{\mu}{\rho D_L}\right)^{1/3}$	(Ref. 40)
(3) Water-Air Sucrose aq. soln.-Air CMC aq. soln.-Air Sodium polyacrylate aq. soln. -Air	U_g, m/s < 0.1 ρ, kg/m^3: 995-1230 μ, Pas: 0.005-0.06 C=0 for unelastic liquids C=0.133 for elastic liquids m=0.55 λ =characteristic relaxation time	$\frac{k_La D_T^2}{D_L} = 0.09 \left(\frac{\nu}{D_L}\right)^{0.5} \left(\frac{g D_T^2 \rho}{\sigma}\right)^{0.75} \times \left(\frac{g D_T^3}{\nu^2}\right)^{0.39} \left(\frac{U_g}{g D_T}\right) \left(1+C\left(\frac{U_b \lambda}{d_{vs}}\right)\right)^{m-1}$	(Ref. 99)
(4) Water-Air Water-O_2 Water-H_2 Water-CH_4 Water-CO_2 Sucrose solns.-Air n-butanol-Air Methanol solns.-Air Electrolyte solns.-Air	U_g, m/s: 0.042-0.38 H_f, m: 0.13-0.22 D_T, m: 0.1-0.19 ρ, kg/m^3: 998-1230 μ, Pas: 0.0008-0.011 σ, N/m: 0.025-0.082 D_L, m^2/s: 4.6-26.0	$k_La = \frac{14.9gf}{U_g} \left(\frac{U_g \mu}{\sigma}\right)^{1.76} \left(\frac{\mu^4 g}{\rho \sigma^3}\right)^{-0.248} \times \left(\frac{\mu_g}{\mu}\right)^{0.243} \left(\frac{\mu}{\rho D_L}\right)^{-0.604}$ f=1.0 for nonelectrolytes $f = 10^{0.0681 I} < 1.0 \frac{Kgion}{m^3}$ $f = 1.114 \times 10^{0.021 I} > 1.0 \frac{Kgion}{m^3}$	(Ref. 63)
(5) Aqueous CMC solu. (1.0-2.0wt%)	U_g, m/s: 0.08 D_T, m: 0.14 H_f, m: 2.6	$k_La = 0.00315 U_g^{0.59} \mu_{ef}^{-0.84}$	(Ref. 33)

depends on the relative magnitudes of their effects on liquid-phase mass transfer coefficient k_L and specific gas-liquid interfacial area a. The relative balance between the changes in k_L and a determines whether $k_L a$ will increase or decrease. A number of studies on k_L in nonfoaming system, i.e., bubble column fermentors (BCs) without foam formation, have been carried out (Refs.3, 6, 8, 16, 25-27, 32, 36, 39, 45-47, 50, 66, 67, 72, 74, 76, 77, 80, 83, 88, 89, 93, 97, 100, 103, 110, 118, 124, 132, 142, 143). Calderbank and Moo-Young (Ref.27), Hughmark (Ref.67), Akita and Yoshida (Ref.6), and Schugerl et al. (Ref.118) have proposed correlations for k_L or Sherwood number. Some of the widely used correlations for k_L or Sherwood number are listed in Table 2-5. These correlations have been utilized effectively as the bases for the design and operation of BCs without foaming, not only in laboratories but also industrial plants. Most of these correlations, however, are those obtained in liquids or media without foaming tendency. There is a large difference in the hydrodynamic behavior or bubble dynamics between the foaming and nonfoaming systems. Hence, a direct application of these existing correlations to k_L data in foaming systems is difficult. The mechanism of the effect of antifoam agents (AFs) on bubble dynamics and mass transfer in BCs is still largely unresolved. The effect of AFs on the mass transfer coefficient is also sometimes confusing. For a better design and operation of bubble column fermentors under foam control, treating various foaming liquids of high foaming tendency or

Table 2-5 Reported studies for k_L

	System	Range of Parameters	Correlation Proposed	Reference
(1)	(A) for large bubbles aqueous glycol solns.-CO_2 Water-CO_2 Water-O_2 Brine-O_2 Polyacrylamide soln.-CO_2	ρ, kg/m^3: 1000-1178 $\rho - \rho_g$, kg/m^3: 1000-1178 μ, Pas: 0.0006-0.0897 $d_b > 2.5$mm	$k_L = 0.42\left(\frac{(\rho-\rho_g)\mu g}{\rho^2}\right)^{1/3}\left(\frac{\mu}{\rho D_L}\right)^{-1/2}$	(Ref. 27)
	(B) for small bubbles aqueous glycol solns.-CO_2 Brine-O_2 Wax-H_2 Aqueous ethanol soln. -C_6H_6	ρ, kg/m^3: 698-1160 $\rho - \rho_g$, kg/m^3: 1000-1178 μ, Pas: 0.00084-0.001 $d_b < 2.5$mm	$k_L = 0.31\left(\frac{(\rho-\rho_g)\mu g}{\rho^2}\right)^{1/3}\left(\frac{\mu}{\rho D_L}\right)^{-1/2}$ $Re = \frac{d_{vs}U_g\rho}{\mu}$ $Sc = \frac{\mu}{\rho D_L}$	
(2)	Air-Water Air-Na_2CO_3 soln. Air-Varsol Air-Glycerol solns. Air-$ZnCl_2$ soln.	D_T, m: 0.025-1.1 ρ, kg/m^3: 776-1696 μ, Pas: 0.0009-0.152 σ, N/m: 0.025-0.076	$\frac{k_L d_b}{D_L} = 2+0.0187\left\{Sc^{0.339}Re^{0.484}\right.$ $\left.\times\left(\frac{d_{vs}g^{1/3}}{D_L^{2/3}}\right)^{0.072}\right\}^{1.61}$	(Ref. 67)
(3)	Water-Air Glycol-Air Methanol-Air Aqueous solns. of Glycol-Air Aqueous solns. of Methanol-Air Water-O_2 Water-He Water-CO_2	U_g, m/s: 0.003-0.4 u_L, m/s: 0.0-0.44 D_T, m: 0.152-0.6 H_f, m: 0.126-0.35 ρ, kg/m^3: 800-1600 μ, Pas: 0.00058-0.021 σ, N/m: 0.022-0.0742	$k_L = 0.5\frac{D_L}{d_{vs}}\left(\frac{\nu}{D_L}\right)^{1/2}\left(\frac{g d_{vs}}{\nu^2}\right)^{1/4}\left(\frac{g d_{vs}^2\rho}{\sigma}\right)^{3/8}$	(Ref. 6)
(4)	Aqueous alcohol soln.-Air Electrolytes-Air	U_g, m/s < 0.08 ρ, kg/m^3: 996-1006 μ, Pas: 0.00089-0.001 σ, N/m: 0.053-0.073	$k_L = \frac{0.15D_L}{d_{vs}}\left(\frac{\nu}{D_L}\right)^{1/2}\left(\frac{d_{vs}U_g\rho}{\mu}\right)^{3/4}$	(Ref. 118)

foaminess, quantitative information on k_L under mechanical or chemical foam control and correlations for k_L in both systems are indispensable.

As reviewed in the above, few systematic studies have been carried out on operational characteristics of bubble column fermentors, i.e., bubble columns (BCs), under foam control. Quantitative performance data are scarce, and our understanding of the mechanisms of the operation is also far from adequate. In fact, the design and operation of BCs under mechanical or chemical foam control are at present mostly empirical. In addition, due to the lack of basic information on operational problems in a foaming system, BCs with a foaming system seem to have been operated based on the parameters of nonfoaming systems, even though antifoam agents (AFs) were added to suppress foam. Still, there is the risk that an AF induces considerable changes in the physical properties of the culture broth, and may even deteriorate various operational characteristics of the bubble column fermentor. The marked decline of fermentor performance due to this kind of negligence is rather common. Therefore, it is apparent that analysis of all the characteristics of the bubble column fermentor is necessary, especially when the bubble column fermentor is a foaming system in which foaming is controlled mechanically without the use of AFs. It should be also recognized that although there is much need for such studies concerning the cultivation of a microorganic cell mass and production of metabolites that require exceedingly high aeration rates, or when fermentation using a

substrate of high foaminess such as molasses, yeast extract, malt extract, peptone, hydrocabons, etc. has been advocated (Refs.54, 59, 129, 134), this branch of investigation is considerably underdeveloped in comparison with the studies in other branches of the fermentation industry.

In view of the above, the problems related to design and operational characteristics of bubble column fermentors, i.e., bubble columns (BCs), under foam control which have so far remained without quantitative analysis were studied on the basis of the experiment with the foam-breaker that utilized the impact force of the dispersed liquid particles, i.e., the rotating-disk mechanical foam-breaker (MFRD), in accordance with the following plans.

1) Experimental study on the performance of the MFRD as a foam controlling apparatus in the BC and the flow and mass transfer characteristics of the BC with the MFRD.
2) Evaluation of the foam-breaking characteristics of MFRDs fitted to BCs treating various foaming liquids and the power consumption required for foam-breaking.
3) Analysis of the nature of foam that reflects the foaming capacity (intensity) of BCs containing various foaming liquids and the difficulty or ease of mechanical foam-breaking with MFRDs.
4) Prediction of the minimum (critical) disk rotational speed for foam-breaking of MFRDs fitted to BCs based on the nature of foam, i.e., the foaming characteristics of liquids to be treated.

5) Establishment of guide-line for the design and operation of BCs with MFRDs treating mixed solutions and biological media whose composition is complex.
6) Quantitative study on the gas holdup in BCs treating various liquids under foam control.
7) Quantitative study on the volumetric liquid-phase mass transfer coefficient in BCs treating various liquids under foam control.
8) Evaluation and analysis of the liquid-phase mass transfer coefficient in BCs under mechanical or chemical foam control.

CHAPTER 3

PERFORMANCE CHARACTERISTICS OF A BUBBLE COLUMN WITH MECHANICAL FOAM CONTROL

3-1. Introduction

Bubble columns (BCs) are the bioreactors commonly used for aerobic biological reactions. As described in chapter 2, a number of experimental and theoretical studies on the various characteristics of BCs used for aerobic biological reactions without foam formation have been reported (Refs.30, 52, 98, 120, 122). Theses data have been utilized effectively as the basis for the design and operation of BCs without foaming not only in laboratories but also in industrial plants. However, considering the differences in hydrodynamics, bubble dynamics or foam forming and foam-breaking behavior, etc. between bioreactors with and without foaming a direct application of the existing results to the foaming system, i.e., the mechanical foam-control system (MFS), where the foam-breaking operation forces foam to be enclosed within a limited head-space between the aerated liquid surface and the foam-breaking apparatus and the generation and collapse of foam are maintained in a dynamic equilibrium state, may have difficulties. This suggests the necessity of carrying out systematic studies on the various characteristics of BCs when foaming is controlled mechanical by the foam-breaking apparatus. Previously, Ohkawa et al. (Refs.104, 105) developed a rotating-disk mechanical foam-

breaker (MFRD) as a foam controlling apparatus, which facilitated foam-breaking action by the impact between the dispersed liquid particles from the disk and the ascending foam. The MFRD has already been proved to be useful in controlling foaming in stirred-tank fermentors, i.e., aerated agitated vessels (Refs.139-141), without the addition of antifoam agents (AFs). This apparatus is expected to be one of potential value in controlling foaming in a BC that operates at high aeration rate conditions. Prior to a series of studies on various characteristics of the BC under foam control, it is necessary to investigate foam-breaking performance of the MFRD fitted to the BC and to confirm its usefulness as a foam control apparatus in the BC with a foaming system. From a comparison of flow and mass transfer characteristics between BCs when the foaming is controlled by the MFRD and an AF, it is also necessary to demonstrate clearly the superiority of mechanically controlled foaming.

In this chapter, foaming characteristics in the BC with the MFRD treating various liquids are first examined. Foaming behavior in the BC and foam-breaking behavior of the MFRD are also studied in terms of the volume fraction of liquid in the foam, i.e., the liquid holdup in the foam. The differences in the gas holdup and the volumetric mass transfer coefficient between the two BCs when the foaming is controlled by the MFRD and an AF are then evaluated. From a comparison of power input between the BCs with and without the addition of the AF, the advantage of mechanically controlled foaming is further dis-

cussed.

3-2. Experimental

Apparatus The flow diagram of the experimental apparatus is shown in Fig.3-1. For studies of measurements of foaming or foaming behavior in the BC, foam-breaking behavior of the MFRD and gas holdup in the liquid, only the BC shown in the left side of the figure, which is operated in liquid batchwise, was used. The BC, 0.19m in diameter D_T and 1.0m in height, was equipped with four baffles ($0.1D_T$ in width and 0.30m in length) and four porous glass ball filters (0.015m in diameter with average pore openings of 25μm) for air-sparging. The working liquid volume V_L was held constant at 0.017m^3. The air sparge rate ranged from 1.0 to 5.0vvm, corresponding to 1.0×10^{-2} to 5.0×10^{-2}m/s as the gas superficial velocity U_g. The MFRD was set at a height of 0.9m from the bottom. For the rotating disk, a disk, 0.15m in diameter D_d, which was set close to the upper limit of $D_T/D_d=1.2$ (Ref. 105), was employed throughout the experiments. The liquid feed rate W onto the rotating disk was varied from 1.0×10^{-5} to $3.0\times10^{-5}m^3/s$. Additional details of the MFRD, including foam-breaking principles and the operational procedure, have been reported (Ref.105). In experiments for mass transfer, two BCs, i.e., the absorber and stripper, as shown in Fig.3-1 were used. The absorber ($D_T=0.19$m) was connected to the stripper ($D_T=0.19$m) which was fed continuously, at the bottom, with N_2. One positive dis-

placement pump drove liquid continuously, at a measured flow rate F between 7.92×10^{-5} and 8.52×10^{-5} m^3/s, from the absorber to the stripper, and under the steady state the same flow rate was being sent back to the absorber by the other pump. The working liquid volume and the range of the air sparge rate in oxygen absorption experiments or the MFRD (D_d=0.15m) fitted to the absorber and the stripper under mechanical foam control, were the same as those in foam-breaking experiments described above.

Determination of critical disk rotational speed In the experiments with a given air sparge rate, the disk rotational speed was measured at the transient state from the foam-breaking to the nonfoam-breaking regions, i.e., the critical state for foam-breaking, brought about by step variation of the disk rotational speed at the liquid feed rate prescribed by the flow controller (Ref.105). The changes in foaming characteristics of the BC and foam-breaking characteristics of the MFRD under various operational conditions were studied on the basis of the changes in this critical disk rotational speed.

Liquid holdup in foam Foam withdrawn through a glass tube (0.01m diameter) fitted on the wall between two adjacent baffles was collected in a graduated container of constant volume v_F (Ref.138). The glass tube A was kept at a level 0.02m lower than the disk level, along with a middle axis in an annular section between the disk and the column wall, i.e., along with the vertical axis at a distance of $(D_T-D_d)/4$ from the wall. The liquid holdup in the foam, ϕ_L, was determined by Eq.(3-1) (Refs.60, 114):

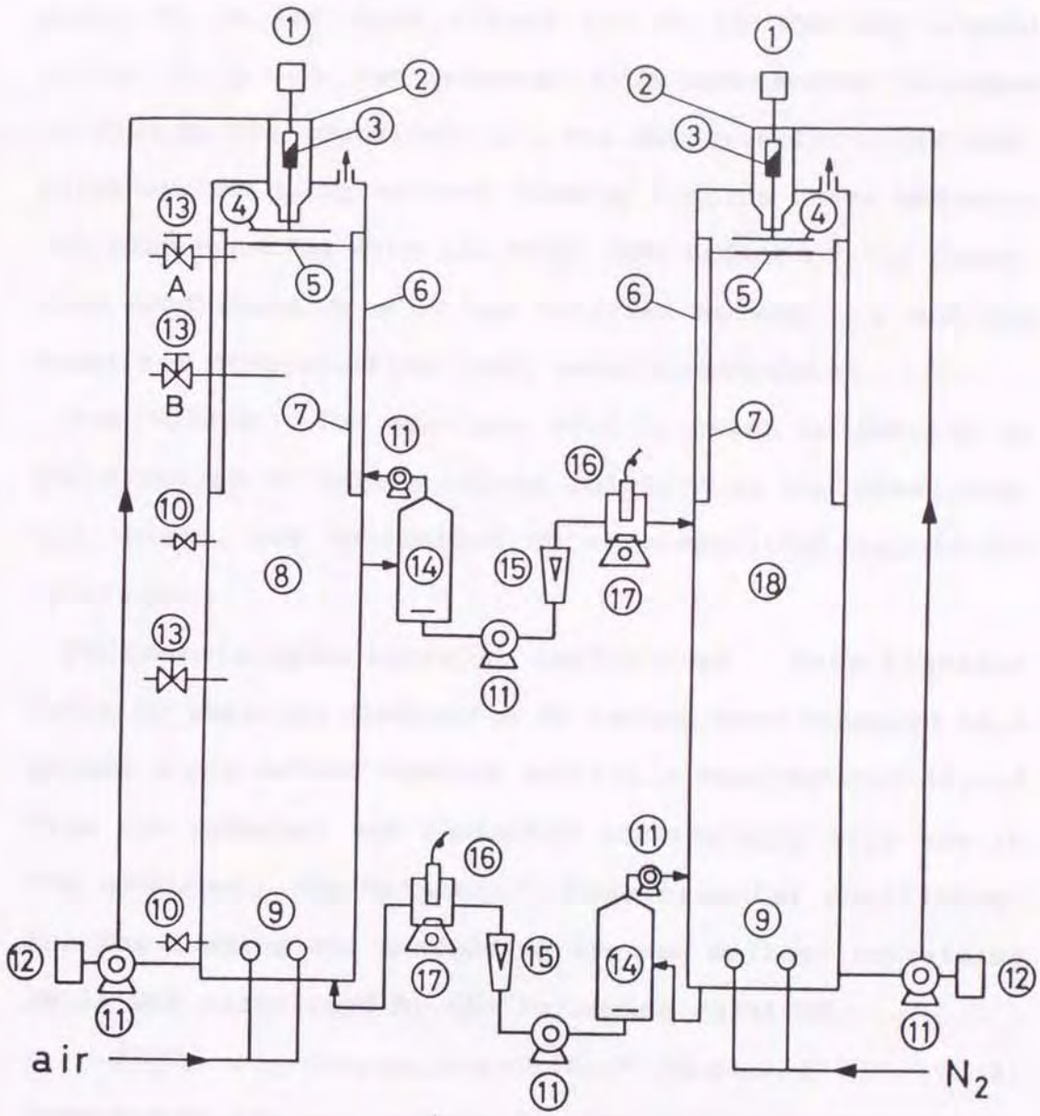

Figure 3-1. Schematic flow diagram of the experimental apparatus used for the run of foam-breaking, flow characteristics and mass transfer: (1)motor, (2)liquid feeder, (3)torque meter, (4)rotating disk, (5)fixed disk, (6)bubble column, (7)baffle plate, (8)absorber, (9)ball sparger, (10) pressure tap, (11)pump, (12)flow controller, (13)sampling tap, (14)tank for bubble-liquid separation, (15)flow meter, (16)DO probe, (17)magnetic stirrer, and (18)sttipper.

$$\phi_L = V_L / V_F \qquad (3\text{-}1)$$

where V_F is the foam volume and V_L is the net liquid volume in V_F. V_L was measured from spontaneous collapse of foam in the container. ϕ_L was measured for a gas-bubbling system using various foaming liquids under mechanical foam-breaking with the MFRD. The effect of the operating conditions on ϕ_L, the relation between ϕ_L and the power for foam-breaking, etc. were investigated.

Gas holdup The mean gas holdup, which is defined as the fraction of bubble volume relative to the clear liquid volume, was determined by a conventional manometric technique.

Volumetric mass transfer coefficient Mass transfer rates by physical absorption of oxygen were measured by a steady state method whereby partially deoxygenated liquid from the desorber was contacted continuously with air in the absorber. The volumetric mass transfer coefficient $k_L a$ for foaming and nonfoaming systems without containing cells was calculated by the following equation.

$$F[(C_{DO})_{out} - (C_{DO})_{in}] = k_L a V_L [C_{DO}^* - (C_{DO})_{out}] \qquad (3\text{-}2)$$

Complete mixing was assumed for the liquid in the absorber and stripper. $(C_{DO})_{in}$ and $(C_{DO})_{out}$ are the oxygen concentration in the liquid at the inlet and outlet, respectively. Oxygen concentration was measured with an oxygen analyzer (Beckman, Field-lab). The dissolved oxygen concentration in foaming and nonfoaming liquids at saturation, C_{DO}^*, was determined by sparging air through the liquid in the BCs with and without the MFRD for a sufficient length of time. In calculating $k_L a$ for foaming and

nonfoaming systems containing living cells (commercial baker's yeast, Chuetsu Yeast Co. Ltd.), the amount of oxygen taken up by cells in the liquid was further taken into consideration, and k_La values were calculated from Eq.(3-3):

$$F[(C_{DO})_{out}-(C_{DO})_{in}]=k_LaV_L[C_{DO}^*-(C_{DO})_{out}]-R \qquad (3\text{-}3)$$

where R is the oxygen uptake rate which changes depending on the cell concentration and was determined by using an apparatus for the respiration rate measurement (Ref.130).

Foaming and nonfoaming liquids Three kinds of foaming liquids were used at 293K. Table 3-1 shows the properties of the foaming liquids. These same solutions to which an AF, silicon oil (KM70, Shin-Etsu Chemical Co.Ltd.), was added at various concentrations were used as the nonfoaming liquids.

3-3. Results and Discussion

3-3-1. Foaming characteristics in bubble column in terms of changes in required disk rotational speed

The change in disk rotational speed of the MFRD with varying operating variables such as W and U_g was measured for respective liquids at the critical foam-breaking state. As shown in Fig.3-2, the effects of W and U_g on the critical disk speed N_c at which foam-breaking was carried out were almost the same as those observed previously (Ref.105). That is, the smaller is W (i.e., the smaller is the liquid feed rate per unit disk circumference) and the larger is U_g, the higher N_c becomes. Higher

Table 3-1 Physical Properties of Foaming Liquids at 293K.

Liquid			ρ (kg/m^3)	μ x10^3 (Pa·s)	σ x10^3 (N/m)
Detergent*	F-D(1)	0.005[a]	998.2	1.00	63.85
	F-D(2)	0.010[a]	998.2	1.00	53.94
[Detergent(0.0075 vol.%) +Corn-syrup]**	F-DS(1)	10.0[b]	1035.8	1.25	58.44
	F-DS(2)	20.0[b]	1075.8	1.59	59.63
	F-DS(3)	30.0[b]	1116.0	2.23	60.83
	F-DS(4)	40.0[b]	1150.0	3.60	63.21
[Detergent(0.010 vol.%) +baker's yeast]**	F-DC(1)	1.0[c]	998.5	1.01	49.36[d]
	F-DC(2)	2.0[c]	998.7	1.02	49.36[d]
	F-DC(3)	3.0[c]	998.8	1.02	49.45[d]
	F-DC(4)	5.0[c]	999.2	1.03	50.02[d]
	F-DC(5)	10.0[c]	999.4	1.04	51.53[d]
	F-DC(6)	20.0[c]	1000.5	1.06	54.37[d]
	F-DC(7)	40.0[c]	1002.6	1.12	56.87[d]
	F-DC(8)	80.0[c]	1007.3	1.23	57.22[d]

*Lipon F, manufactured by Lipon Corp. (Non-ionic surfactant 23%, Sodium alkylbenzensulfonate, Sodium alkylethersulfuricester); ** These foaming liquids were used in experiments after mixing respective liquids containg detergent and corn-syrup or baker's yeast for 12 hours.; a)Vol.%; b)Corn-syrup, wt.%; c)Wet yeast, kg/m^3; d)Value for liquid filtered baker's yeast.

values of N_c at smaller W and larger U_g may be attributed respectively due to the decreased number of liquid particles dispersed per unit disk circumference and the increased foaming intensity. Figure 3-3 shows a plot of N_c against the viscosity μ of foaming liquids. N_c tends to gradually decrease with increasing μ . This means that there occurs a more foam-breakable tendency due to the decreased foaming intensity with increase in μ . The relation between N_c and the cell concentration X_L [the concentration (wet weight basis) of the cells per unit working liquid volume] is shown in Fig.3-4. N_c rapidly decreased with the initial increase in X_L. However, when X_L exceeds a certain level, N_c was almost free from the effect of X_L. Almost constant values of N_c in the high X_L region may be attributed to the same level of foaming intensity. Moreover, under foaming conditions, cells in the bulk liquid layer are carried into the foam layer together with the foam generated (Refs.85, 101). In a dynamic equilibrium state under mechanical foam control, the cells are considered to have been distributed in a certain proportion between the bulk liquid and foam layer. What degree is the enrichment of the cells in the foam, i.e., what amount of the cells exists in the foam and bulk liquid layer, is discussed in a later section.

3-3-2. Foaming behavior in bubble column and foam-breaking behavior of rotating-disk mechanical foam-breaker in terms of changes in liquid holdup in foam

The MFRD achieves foam-breaking by means of the impact

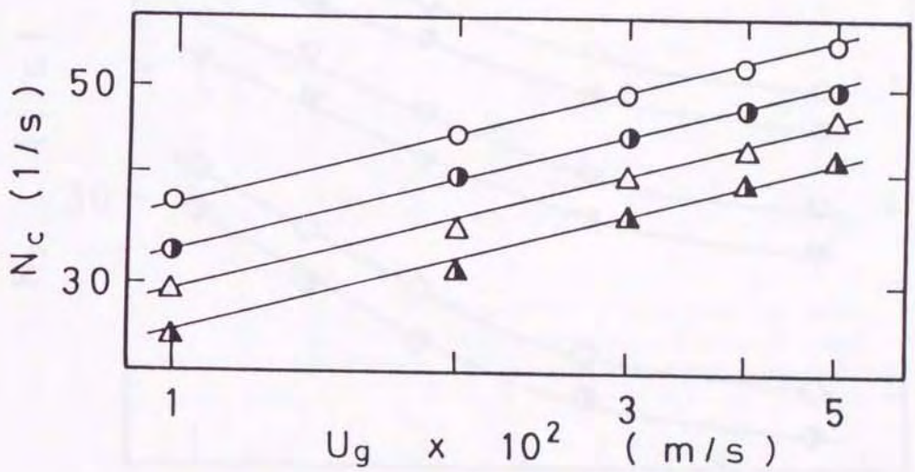

Figure 3-2. Effect of U_g on N_c: F-D(1) solution; W (x10^{-5} m^3/s): △ ; 1.0, ▲ ;1.5, F-D(2) solution; W (x$10^{-5}m^3/s$): ○ ; 1.0, ◑ ; 1.5.

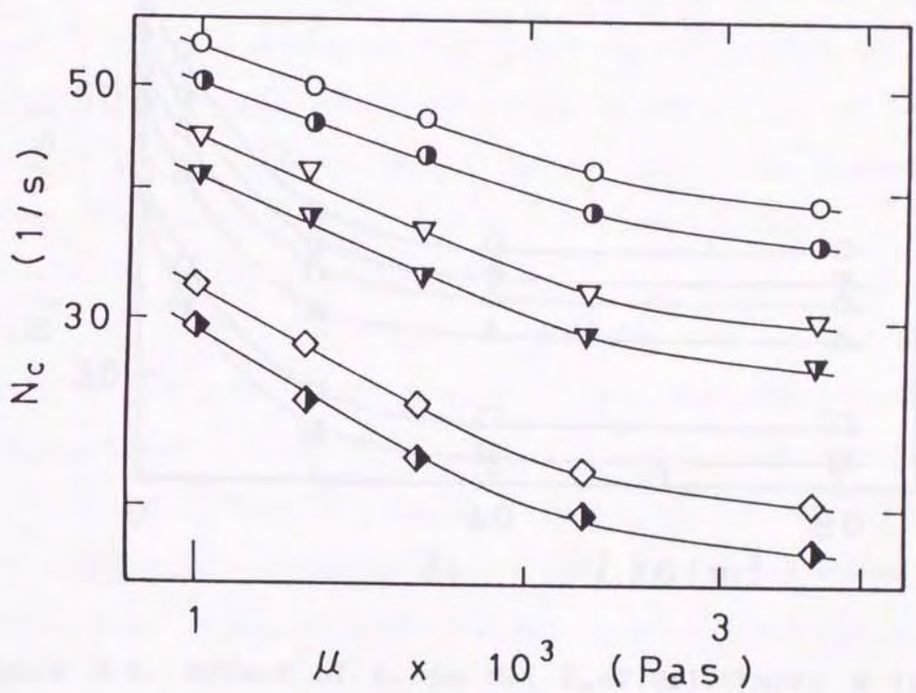

Figure 3-3. Effect of μ on N_c: U_g=1.0x10^{-2}m/s; W (x10^{-5} m^3/s): ◇ ; 1.0, ◈ ; 1.5, U_g=3.0x10^{-2}m/s; W (x10^{-5}m^3/s): ▽ ; 1.0, ▼ ; 1.5, U_g=5.0x10^{-2}m/s; W (x10^{-5}m^3/s): ○ ; 1.0, ◑ ; 1.5.

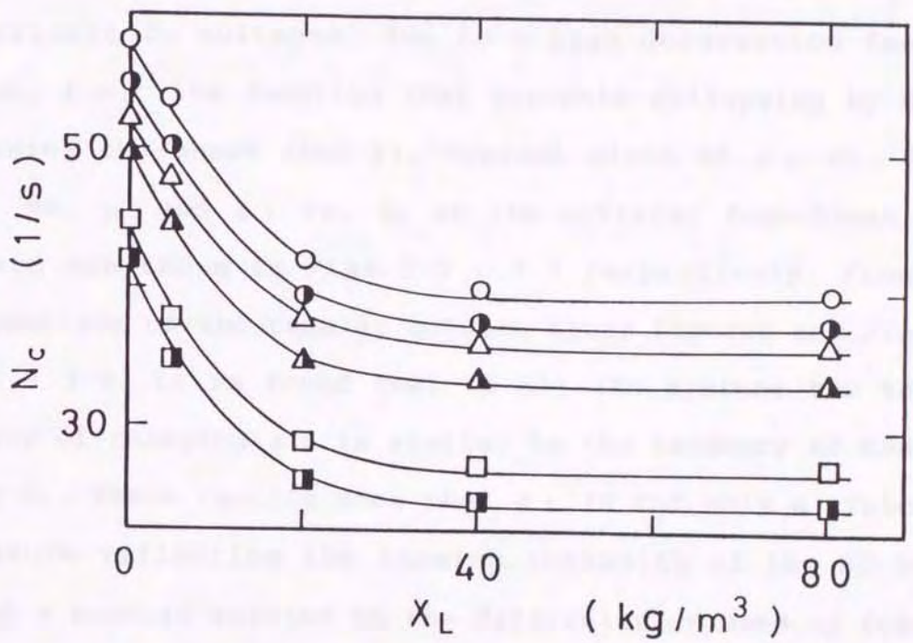

Figure 3-4. Effect of X_L on N_c: U_g=2.0x10^{-2}m/s; W (x10^{-5} m^3/s): □ ; 1.0, ◨ ; 1.5, U_g=4.0x10^{-2}m/s; W (x10^{-5}m^3/s): △ ; 1.0, ◭ ; 1.5, U_g=5.0x10^{-2}m/s; W (x10^{-5}m^3/s): ○ ; 1.0, ◑ ; 1.5.

action of liquid particles from the disk against the foam (Ref.105). According to this mechanism, the liquid holdup in the foam, ϕ_L, may be pointed out as a measure that reflects the foaming intensity of the BC and is also related to difficulty or ease of mechanical foam-breaking (Ref.138). The reason is that foam with larger ϕ_L may be difficult to collapse, due to a high deformation function, i.e., the function that prevents collapsing by deforming the shape (Ref.1). Typical plots of ϕ_L vs. U_g, ϕ_L vs. μ and ϕ_L vs. X_L at the critical foam-breaking state are shown in Figs.3-5 - 3-7 respectively. From a comparison of the results between these figures and Figs. 3-2 - 3-4, it is found that in all the systems the tendency of changing ϕ_L is similar to the tendency of changing N_c. These results show that ϕ_L is not only a typical measure reflecting the foaming intensity of the BC but also a measure related to the difficulty or ease of foam-breaking in terms of the changes in the required disk speed.

3-3-3. Relation between liquid holdup in foam and power for foam-breaking

The relation between ϕ_L and the power for foam-breaking (power P_{kc} required for liquid dispersion by the rotating disk) was investigated. The power P_{kc} in the critical foam-breaking state was determined from both the torque meter readings and the values of N_c. Fig.3-8 shows the relation between P_{kc} and ϕ_L for all of the data. On the whole, good correspondence was seen between the in-

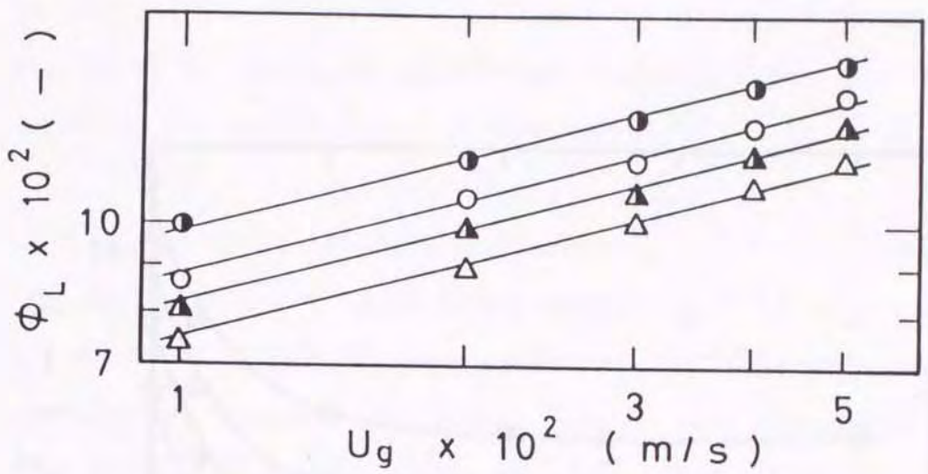

Figure 3-5. Effect of U_g on ϕ_L (keys are the same as in Fig.3-2).

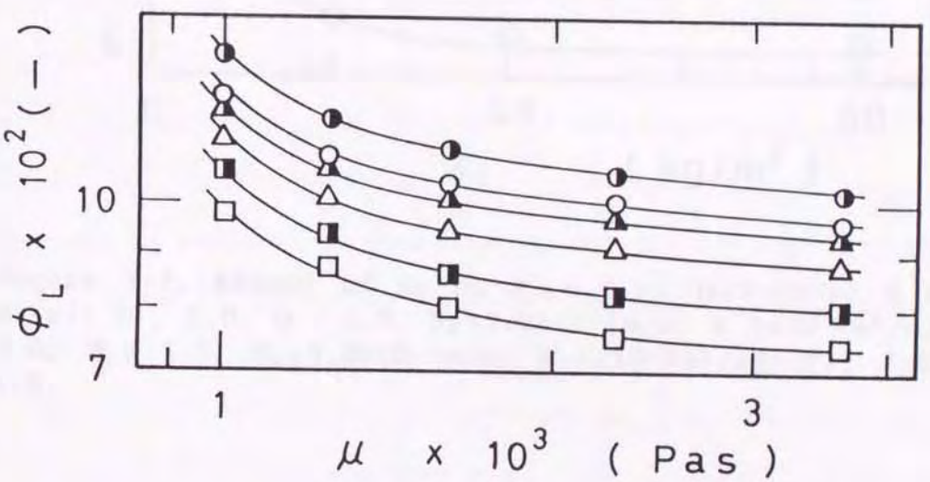

Figure 3-6. Effect of μ on ϕ_L: U_g=2.0x10^{-2}m/s; W (x10^{-5} m^3/s): □ ; 1.0, ◨ ; 1.5, U_g=4.0x10^{-2}m/s; W (x10^{-5}m^3/s): △ ; 1.0, ▲ ; 1.5, U_g=5.0x10^{-2}m/s; W (x10^{-5}m^3/s): ○ ; 1.0, ◑ ; 1.5.

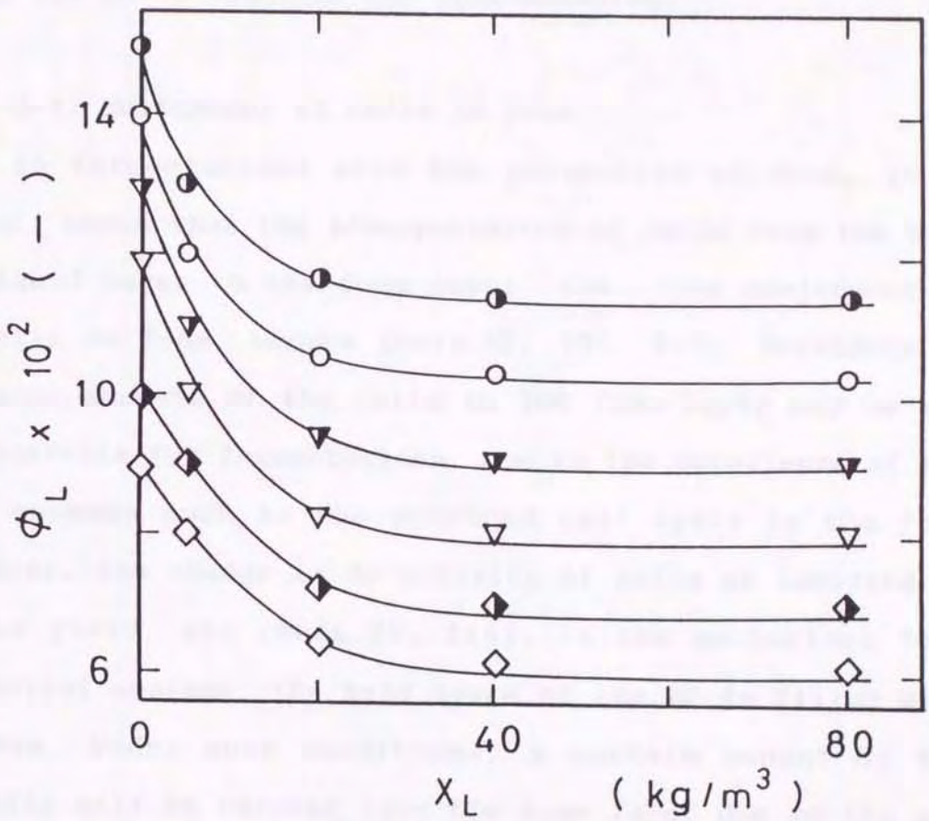

Figure 3-7. Effect of X_L on ϕ_L: U_g=1.0x10^{-2}m/s; W (x10^{-5} m^3/s): ◇ ; 1.0, ◈ ; 1.5, U_g=3.0x10^{-2}m/s; W (x10^{-5}m^3/s): ▽ ; 1.0, ▼ ; 1.5, U_g=5.0x10^{-2}m/s; W (x10^{-5}m^3/s): ○ ; 1.0, ◑ ; 1.5.

creases of P_{kc} and ϕ_L. According to this result, it may be pointed out that regardless of being with or without the cells, the value of ϕ_L can be also related to the difficulty or ease of mechanical foam-breaking in terms of the power required for foam-breaking.

3-3-4. Enrichment of cells in foam

In fermentations with the generation of foam, it is well known that the transportation of cells from the bulk liquid layer to the foam layer, i.e., the enrichment of cells in foam, occurs (Refs.85, 101, 119). Existence of large amounts of the cells in the foam layer may be undesirable for fermentations, due to the occurrence of the phenomena such as the enhanced cell lysis in the foam layer, the change in an activity of cells or lowering of the yield, etc (Refs.85, 119). In the mechanical foam control systems, the head space of the BC is filled with foam. Under such conditions, a certain amount of the cells will be carried into the foam layer due to the effect of liquid entrainment in foam. An attempt was made to estimate the absolute amounts, W_l and W_f, of the cells that existed in the foam and bulk liquid layers respectively when the MFRD was operated at the critical foam-breaking state, on the basis of the following cell mass balance equation:

$$X_L V_L = V_l X_l \ (=W_l) + V_f \overline{X}_f \ (=W_f) \qquad (3\text{-}4)$$

where the product, $X_L V_L$, is the total amount (wet weight basis) of the cells suspended in the liquid, V_l and V_f are the net liquid volume in the bulk liquid and foam

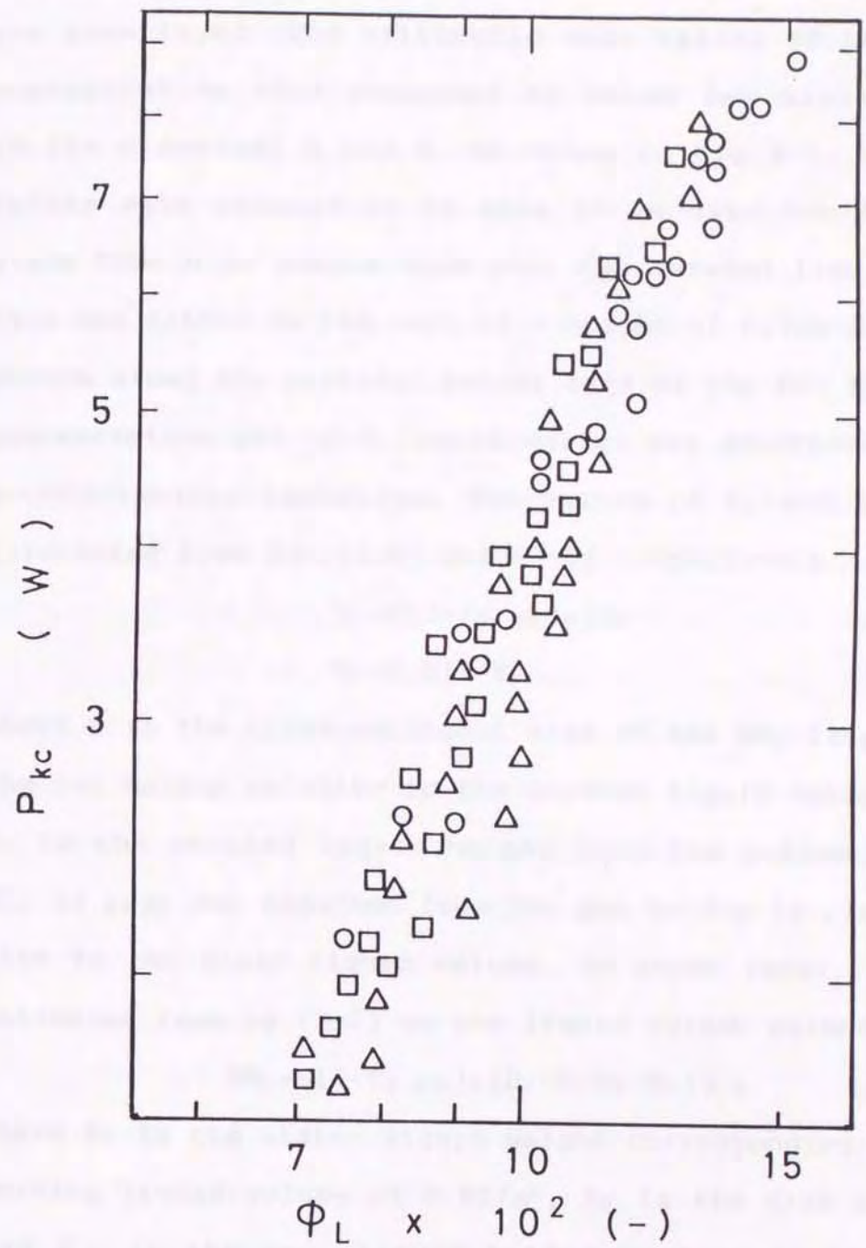

Figure 3-8. Relation between ϕ_L and P_{kc} at U_g=1.0x10^{-2}-5.0x10^{-2}m/s and W=1.0x10^{-5}-1.5x10^{-5}m^3/s: ○ ; F-D solutions, △ ; F-DS solutions, □ ; F-DC solutions.

layer respectively, X_l is the cell concentration in the bulk liquid layer, $\overline{X}_f$ is the mean cell concentration in the foam layer. The arithmetic mean values of the cell concentration were measured by using two glass tubes (0.01m diameter) A and B, as shown in Fig.3-1, and the values were assumed to be able to be used for $\overline{X}_f$. The glass tube B to sample foam near the aerated liquid surface was fitted to the wall at a height of 0.72m from the bottom along the vertical center axis of the BC. The cell concentration per unit liquid volume was determined with a colorimetric technique. The values of V_l and V_f were calculated from Eqs.(3-5) and (3-6) respectively:

$$V_l = S[1-(\varepsilon_{gm})_M]H_f \qquad (3\text{-}5)$$

$$V_f = 0.017 - V_l \qquad (3\text{-}6)$$

where S is the cross-sectional area of the BC, $(\varepsilon_{gm})_M$ is the gas holdup relative to the aerated liquid volume, and H_f is the aerated liquid height from the bottom of the BC. $(\varepsilon_{gm})_M$ was obtained from the gas holdup $(\varepsilon_g)_M$ relative to the clear liquid volume, as shown later. H_f was estimated from Eq.(3-7) on the liquid volume balance:

$$SH_L = S[1-(\varepsilon_{gm})_M]H_f + S(H_d - H_f)\overline{\phi}_L \qquad (3\text{-}7)$$

where H_L is the static liquid height corresponding to the working liquid volume of $0.017m^3$, H_d is the disk height, and $\overline{\phi}_L$ is the mean liquid holdup in foam in the foam layer. $\overline{\phi}_L$ was the arithmetic mean between two liquid holdup values measured for samples withdrawn from the glass tubes A and B.

As a result of calculation, the amount W_f of cells that existed in the foam layer was found to be considerably

smaller compared to the amount W_l of the cells in the bulk liquid layer, that is, to be under 5% of W_l. In the operations of the BC with the MFRD, perpetual exchange of the liquid and cells between the foam and bulk liquid layer occurs because of recirculation of the liquid due to the use of the pump to feed the liquid onto the rotating disk. This recirculation contributes also to making uniform the concentrations of components such as substrates, oxygen, etc. throughout the whole BC. Thus, when the MFRD is employed as a foam control apparatus in a BC treating a foaming biological reaction system, an effective fermentation operation may be expected to be able to be carried out without having to worry about any changes in the activity of the cells, yield of cell mass or products, etc. in contrast to the effects that have been seen when enrichment of the cells into the foam is very large and the exchange of cells and substrates between the foam and bulk liquid layer is insufficient.

3-3-5. Gas holdup

For the gas holdup $(\varepsilon_g)_M$ in a mechanical foam-control system (MFS) with the MFRD, Figure 3-9 shows the results of $(\varepsilon_g)_M$ plotted against W. $(\varepsilon_g)_M$ tends to increase slightly with increasing W at the low U_g region, but is almost independent of W at the high U_g region. In the BC with the MFRD, the collapsed foam liquid produced by foam-breaking flows downward along with the column wall. At the low U_g region, this flow tended to entrain foam ascending from the aerated liquid surface near the wall

into the bulk liquid. The larger is W, the larger is the amount of foam entrained into the liquid, which also contributes to an increase in the gas holdup in the bulk liquid. The increase of $(\varepsilon_g)_M$ with W in the low U_g region may be attributed to enhancement of such a foam entrainment phenomenon. Figure 3-10 shows the relationship between $(\varepsilon_g)_M$ and the viscosity μ of the liquid. The results of the gas holdup ε_g in the nonfoaming liquids without including detergent and AF are also plotted. As shown in the figure, $(\varepsilon_g)_M$ was affected only a small amount by μ, but ε_g tended to decrease gradually with increasing μ. In the MFS, the bubble size was considerably small and distribution of bubbles also was almost uniform regardless of μ. On the other hand, in the nonfoaming liquids, bubble coalescence was observed and its frequency tended to be high with increasing μ. The differences in $(\varepsilon_g)_M$ and ε_g in Fig.3-10 seem to be mainly attributed to the difference in the situation as to whether or not bubble coalescence occurs. Figure 3-11 shows a plot of $(\varepsilon_g)_M$ against the cell concentration X_L. $(\varepsilon_g)_M$ rapidly decreased with the initial increase in X_L, but when X_L exceeds a certain concentration $(\varepsilon_g)_M$ was almost independent of X_L. When the cells were added to the foaming liquid, bubble coalescence and large bubble formation were liable to occur. The decrease in $(\varepsilon_g)_M$ in the low X_L region and almost constant values of $(\varepsilon_g)_M$ in the high X_L region may be attributed to the increased frequency of bubble coalescence and the same level of coalescence frequency respectively.

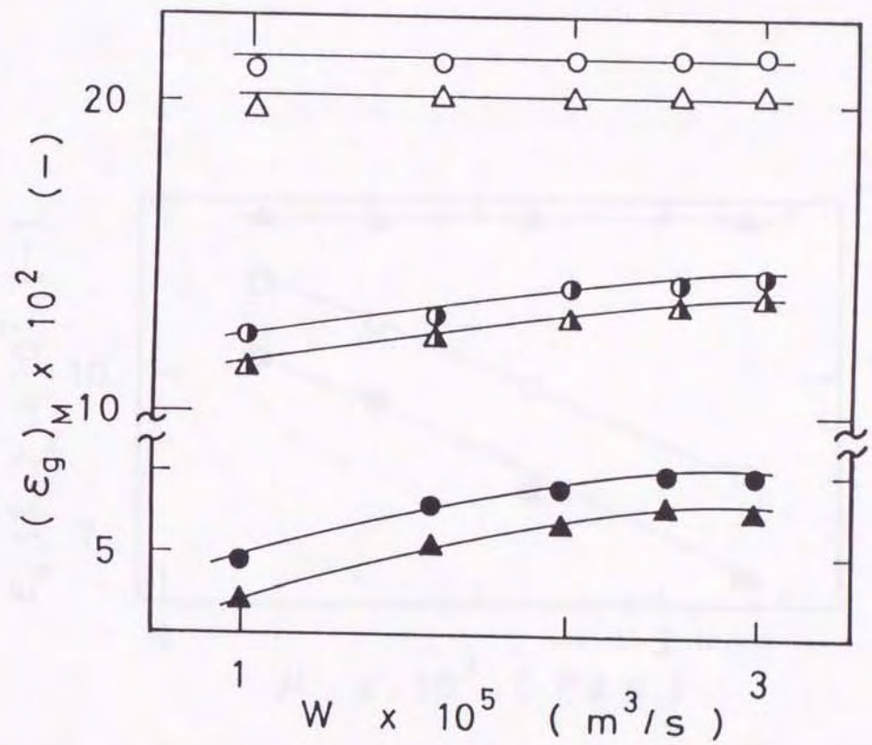

Figure 3-9. Effect of W on $(\varepsilon_g)_M$: F-D(1) solution; U_g (x 10^{-2}m/s): ▲ ; 1.0, ◭ ; 2.0, △ ; 5.0, F-D(2) solution; U_g (x 10^{-2}m/s): ● ; 1.0, ◑ ; 2.0, ○ ; 5.0.

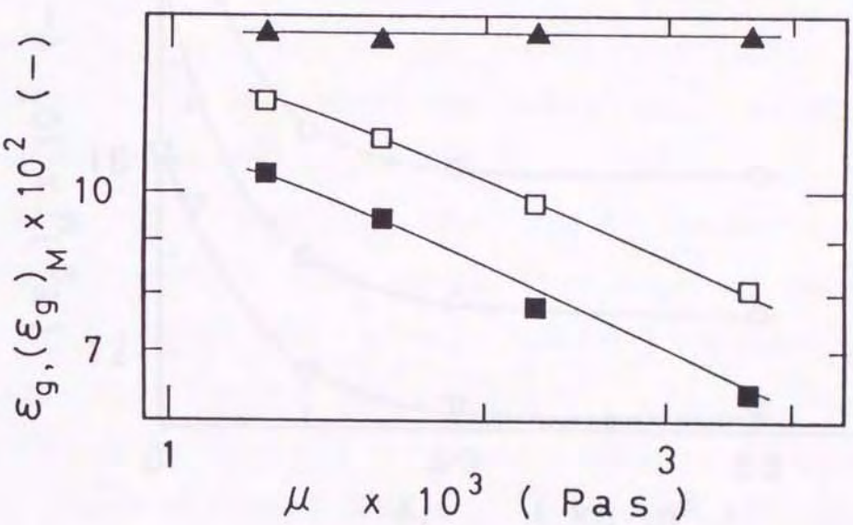

Figure 3-10. Effect of μ on $(\varepsilon_g)_M$ at W=1.0x10^{-5} m^3/s and ε_g: F-DS solution [$(\varepsilon_g)_M$]; U_g (x10^{-2} m/s): ▲ ; 2.0, Corn-syrup solutions (ε_g); U_g (x10^{-2}m/s): ■ ; 2.0, □ ; 4.0.

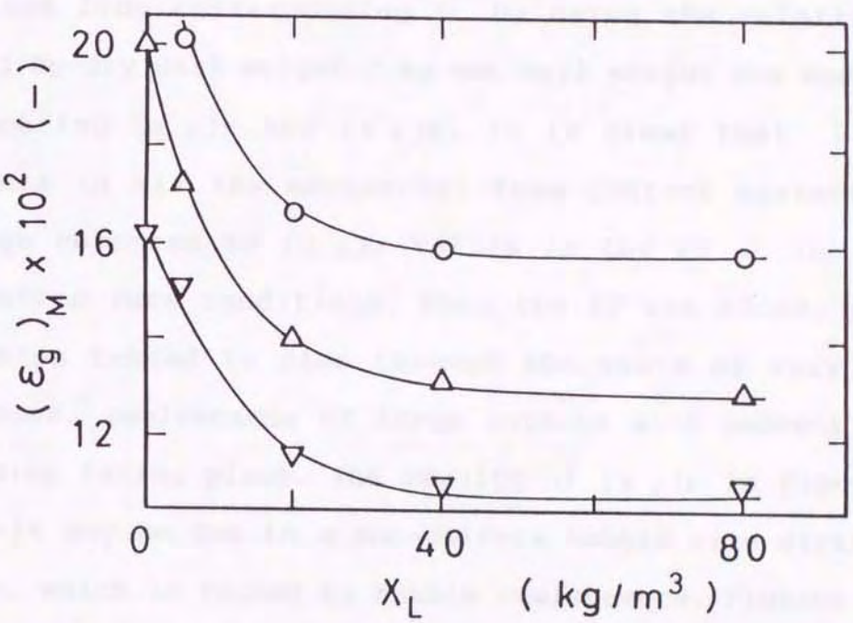

Figure 3-11. Effect of X_L on $(\varepsilon_g)_M$ (keys are the same as in Figs.3-4 and 3-7).

The gas holdup $(\varepsilon_g)_F$ in a nonfoaming system (NS) including an AF was then measured and compared with $(\varepsilon_g)_M$ in the MFS. Typical results of $(\varepsilon_g)_F$ and $(\varepsilon_g)_M$ plotted against U_g, μ and the cell concentration respectively are shown in Figs.3-12 - 3-14. In Fig.3-14, in order to compare our results with those in the literature (Ref. 137), the dry cell weight concentration X_d which was obtained from corresponding X_L by using the relation of 0.33 kg-dry cell weight / kg-wet cell weight was employed. Comparing $(\varepsilon_g)_F$ and $(\varepsilon_g)_M$, it is clear that $(\varepsilon_g)_M$ values in all the mechanical foam control systems are large compared to $(\varepsilon_g)_F$ values in the NS at the same aeration rate conditions. When the AF was added, large bubbles tended to rise through the swarm of very fine bubbles, coalescence of large bubbles with ambient fine bubbles taking place. The results of $(\varepsilon_g)_F$ in Figs.3-12 - 3-14 may be due to a non-uniform bubble size distribution, which is caused by bubble coalescence. Figures 3-15 and 3-16 shows the values of the gas holdup ratio $(\varepsilon_g)_F/(\varepsilon_g)_M$, plotted against the concentration C_F of the AF added. Oblique-lined areas in the low C_F range represent the region of nonfoam-controlling, i.e., the region where the foam control by the AF is difficult due to a gradual increase in the foam layer. Although $(\varepsilon_g)_F/(\varepsilon_g)_M$ values varied in a wide range depending on the liquids, the tendency of leveling off the value of $(\varepsilon_g)_F/(\varepsilon_g)_M$ above a certain concentration of the AF was common for all the systems.

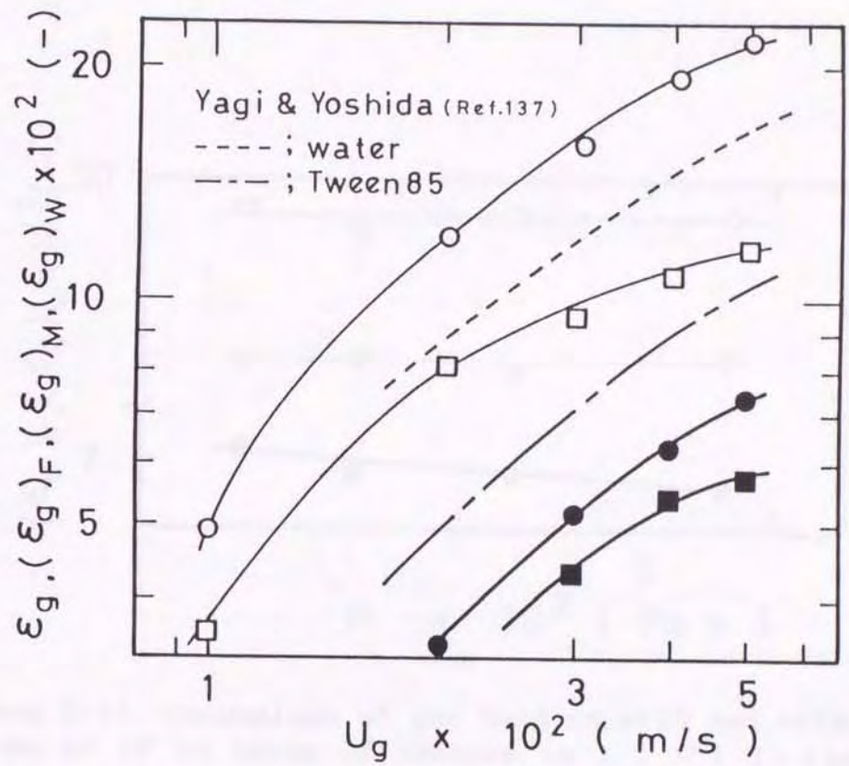

Figure 3-12. Comparison of gas holdups with and without addition of AF in terms of changes in U_g: ○ ; $(\varepsilon_g)_M$, F-D(2) solution at $W=1.0\times10^{-5}$ m³/s, ● ; $(\varepsilon_g)_F$, F-D(2) solution with AF (C_F=120ppm), □ ; $(\varepsilon_g)_W$, water, ■ ; $(\varepsilon_g)_F$, water with AF (C_F=120ppm).

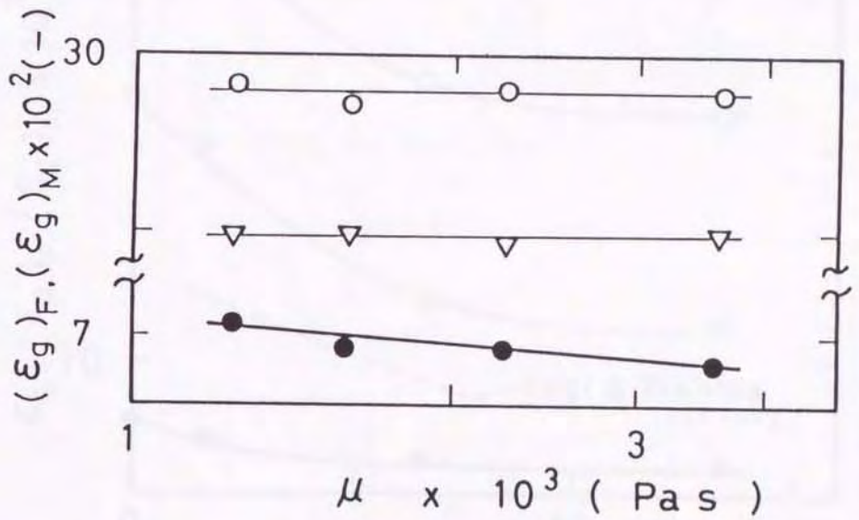

Figure 3-13. Comparison of gas holdups with and without addition of AF in terms of changes in μ : ∇ ; $(\varepsilon_g)_M$, F-DS solutions, $U_g = 3.0 \times 10^{-2}$ m/s, $W = 1.0 \times 10^{-5}$ m^3/s ○ ; $(\varepsilon_g)_M$, F-DS solutions, $U_g = 5.0 \times 10^{-2}$ m/s, $W = 1.0 \times 10^{-5}$ m^3/s ● ; $(\varepsilon_g)_F$, F-DS solutions with AF (C_F = 120ppm), $U_g = 5.0 \times 10^{-2}$ m/s.

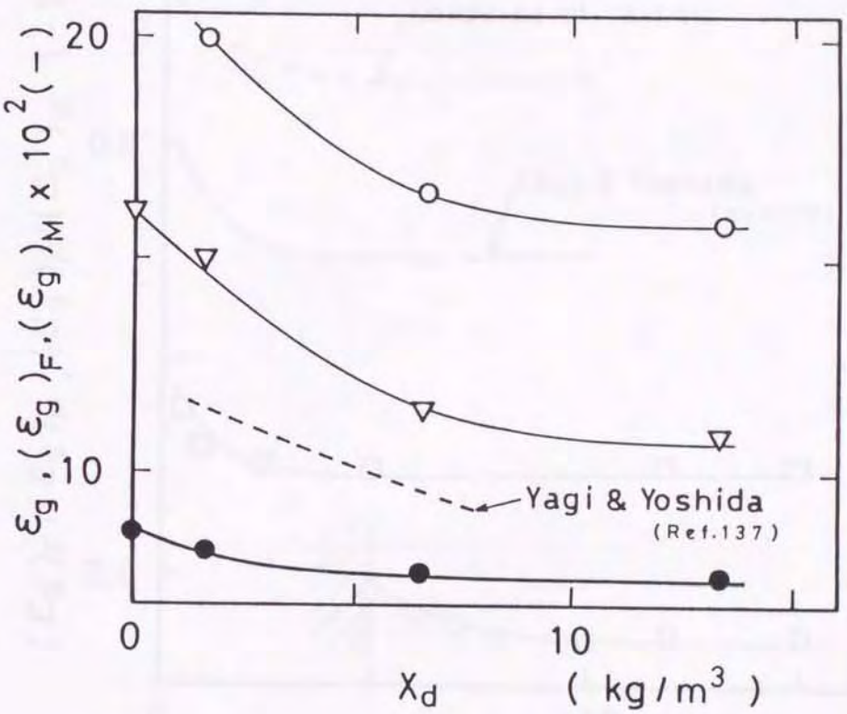

Figure 3-14. Comparison of gas holdups with and without addition of AF in terms of changes in X_d: ▽ ; $(\varepsilon_g)_M$, F-DC solutions, $U_g = 3.0 \times 10^{-2}$ m/s, $W = 1.0 \times 10^{-5}$ m^3/s ○ ; $(\varepsilon_g)_M$, F-DC solutions, $U_g = 5.0 \times 10^{-2}$ m/s, $W = 1.0 \times 10^{-5}$ m^3/s ● ; $(\varepsilon_g)_F$, F-DC solutions with AF (C_F = 120ppm), $U_g = 5.0 \times 10^{-2}$ m/s.

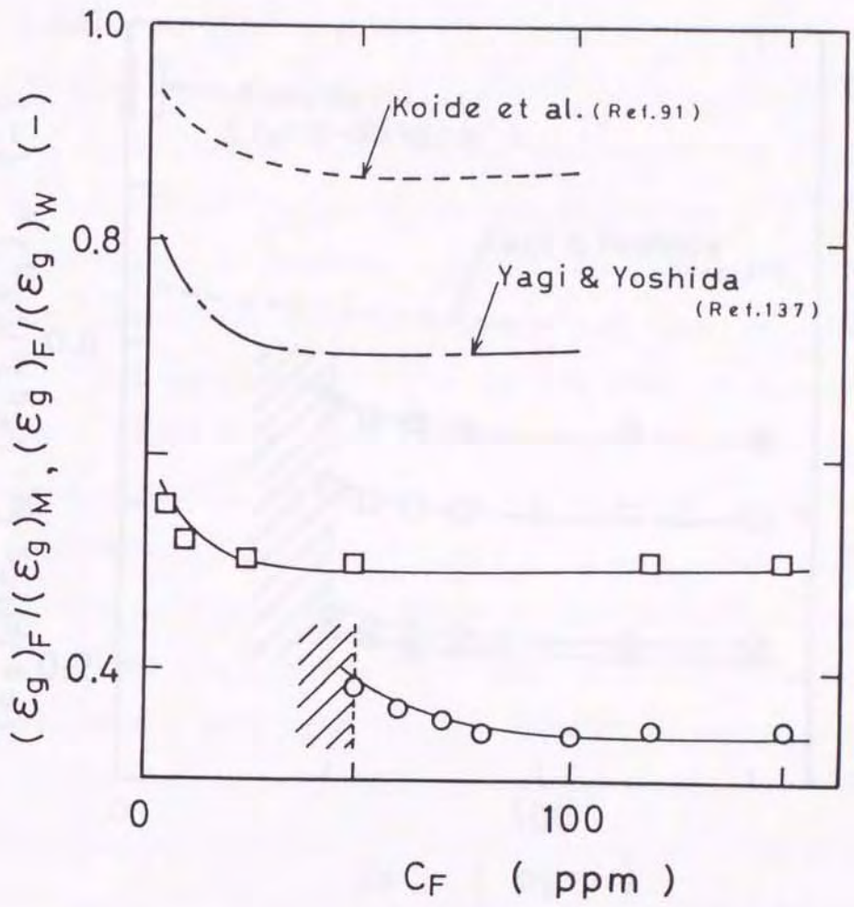

Figure 3-15. Relative changes of gas holdup with addition of AF at $U_g=5.0\times10^{-2}$ m/s (oblique-lined areas in the figures show the region of nonfoam-controlling): ○ ; $(\varepsilon_g)_F/(\varepsilon_g)_M$, F-D(2) solution, $W=1.0\times10^{-5}$ m^3/s, □ ; $(\varepsilon_g)_F/(\varepsilon_g)_W$, water.

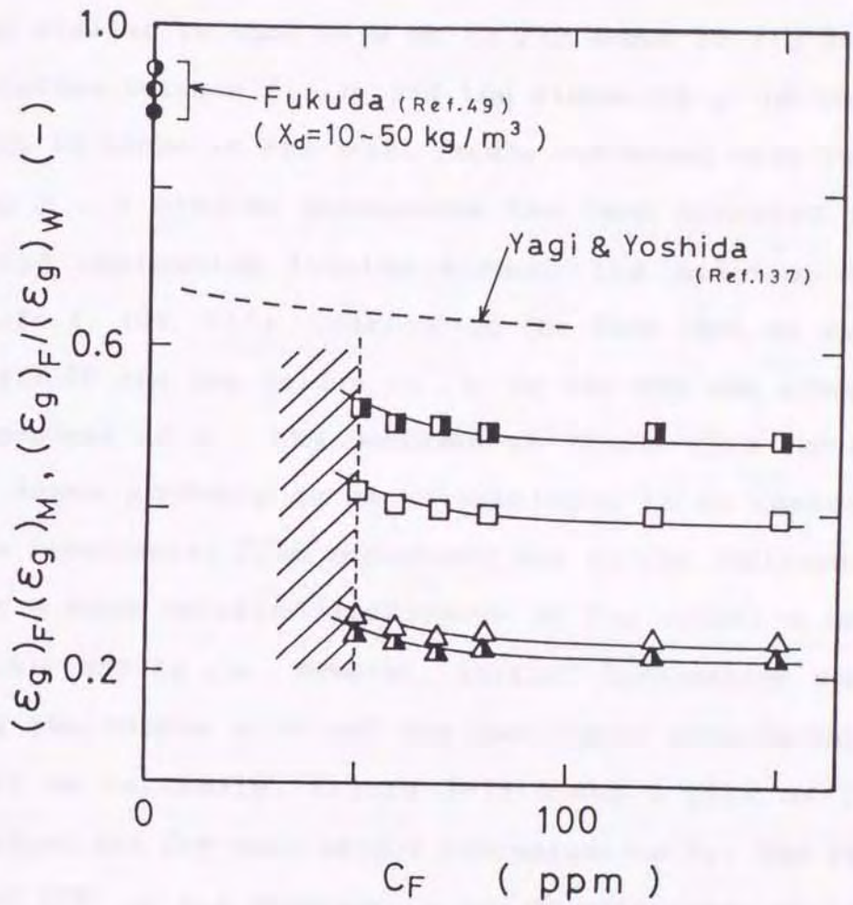

Figure 3-16. Relative changes of gas holdup with addition of AF at $W=1.0\times10^{-5}$ m³/s and $U_g=5.0\times10^{-2}$ m/s (oblique-lined areas in the figures show the region of nonfoam-controlling): $(\varepsilon_g)_F/(\varepsilon_g)_M$: △ ; F-DS(1) solution, ▲ ; F-DS (4) solution, □ ; F-DC(4) solution (X_d=1.65 kg/m³), ◨ ; F-DC(6) solution (X_d=6.6kg/m³).

3-3-6. Volumetric mass transfer coefficient

Figure 3-17 shows the results of the volumetric mass transfer coefficient $(k_La)_M$ measured in the MFS at the critical foam-breaking state. The effect of W on $(k_La)_M$ was similar to that of W on $(\varepsilon_g)_M$ shown in Fig.3-9. The relation between $(\varepsilon_g)_M$ and the viscosity μ of the liquids is shown in Fig.3-18. $(k_La)_M$ decreased with increasing μ. A similar phenomenon has been observed in BCs using nonfoaming liquids without the addition of AFs (Refs.4, 102, 117). Considering the fact that as shown in Fig.3-10 the gas holdup $(\varepsilon_g)_M$ in the MFS was almost independent of μ, the decrease of $(k_La)_M$ with increasing μ seems probably to be attributable to an increase in the interfacial film resistance due to the increase in μ. For a more detailed discussion on the relation between $(k_La)_M$ and $(\varepsilon_g)_M$, however, further information concerning the bubble size and the gas-liquid interfacial area will be necessary. Figure 3-19 shows a plot of $(k_La)_M$ against the dry cell weight concentration X_d. The results (Ref.137) of k_La measured in the BC with water containing baker's yeast are also shown in the figure. In the same manner as that observed by Yagi and Yoshida (Ref.137), $(k_La)_M$ rapidly decreased with the initial increase in X_d, but when X_d exceeds a certain concentration $(k_La)_M$ was almost free from the effect of X_d. The tendency that the decrease of k_La with X_d levels off above a certain value of X_d has also been reported in actual fermentations using stirred-vessels (Refs.18, 42). Concerning the dependency of X_d on k_La, Yagi and Yoshida (Ref.137) have

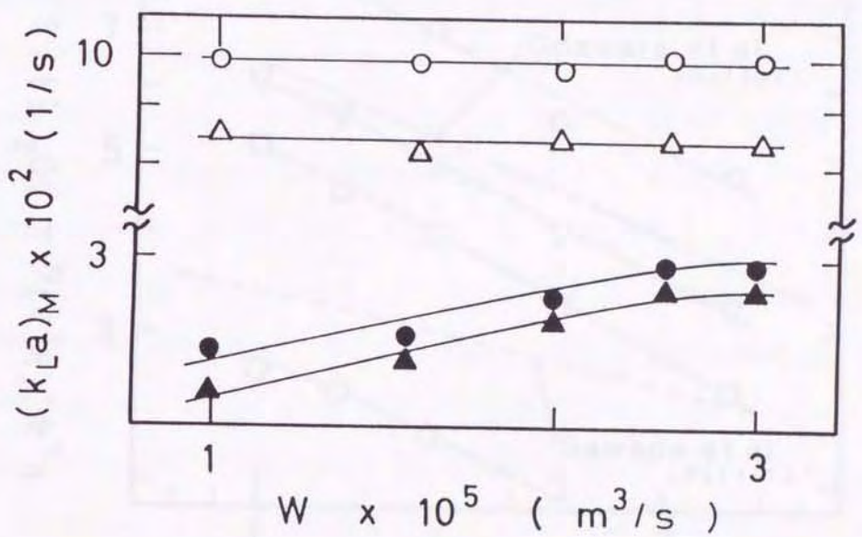

Figure 3-17. Effect of W on $(k_La)_M$ (keys are the same as in Fig.3-9).

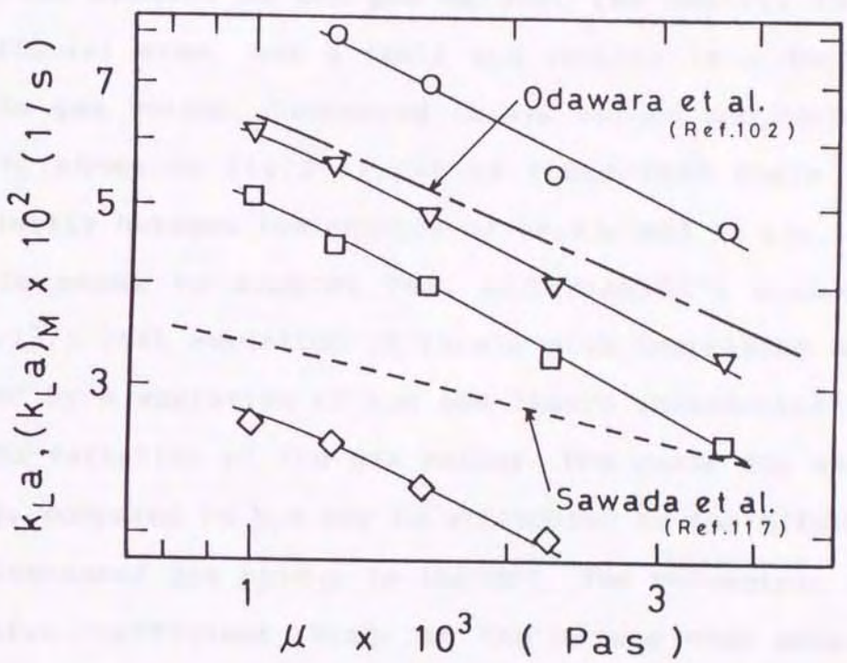

Figure 3-18. Effect of μ on $(k_La)_M$ and k_La: W=1.0x10^{-5} m^3/s; Ug (x10^{-2}m/s): ◇ ; 1.0, □ ; 2.0, ▽ ; 3.0, ○ ; 5.0.

discussed the cause on the basis of the results observed in a stirred-vessel with known interfacial area. They showed that variation of k_L due to the presence of cells was within the accuracy of experiments and variation of k_La with increasing X_d was mainly caused by variation of the interfacial area and not of k_L. It is generally known that the smaller is the gas holdup, the smaller is the interfacial area, and a small k_La results in a decrease of the gas holdup. Comparing $(k_La)_M$ values and those of $(\varepsilon_g)_M$ shown in Fig.3-11, it is found that there is a similarity between the changes of $(k_La)_M$ and $(\varepsilon_g)_M$. This result seems to support Yagi and Yoshida's mechanism (Ref.137) that variation of $(k_La)_M$ with increasing X_d is caused by a variation of the gas-liquid interfacial area due to variation of the gas holdup. The cause for larger $(k_La)_M$ compared to k_La may be attributed to the effect of the increased gas holdup in the MFS. The volumetric mass transfer coefficient $(k_La)_F$ in the NS was then measured and compared with $(k_La)_M$ values in the MFS. The typical results of $(k_La)_F$ plotted against U_g are shown in Figs.3-20 and 3-21, together with the results of $(k_La)_M$. As for the difference in the volumetric mass transfer coefficient between the MFS and the NS, as might be expected, $(k_La)_M$ in the MFS was large compared with $(k_La)_F$ in the NS under the same aeration rate conditions, which was also similar to the tendency observed in gas-liquid contacting systems including surfactant (Ref.137) or biosurfactant (Ref.123). This phenomenon may be mainly attributed to the increased gas holdup in the MFS compared

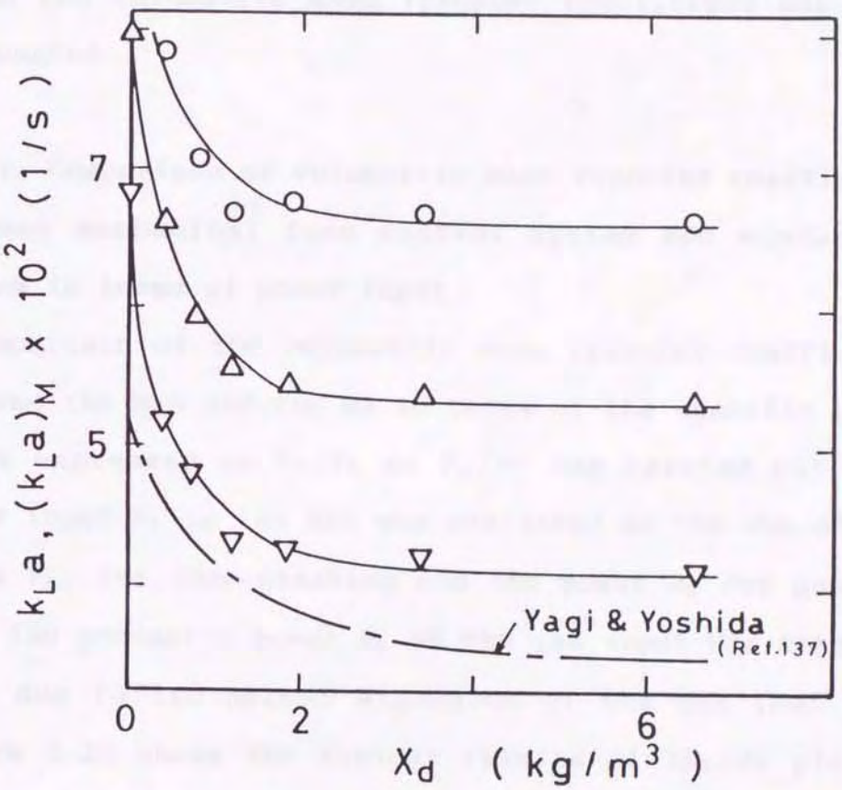

Figure 3-19. Effect of X_d on $(k_La)_M$ (keys are the same as in Figs.3-4 and 3-7).

to that in the NS, as demonstrated in Figs.3-12 - 3-14. Figures 3-22 and 3-24 shows the values of the volumetric mass transfer coefficient ratio $(k_La)_F/(k_La)_M$, plotted against the concentration of the AF added. As is clear from the results shown in the figures, the effect of the AF on the volumetric mass transfer coefficient was very pronounced.

3-3-7. Comparison of volumetric mass transfer coefficient between mechanical foam control system and nonfoaming system in terms of power input

Comparison of the volumetric mass transfer coefficient between the MFS and the NS in terms of the specific power input expressed as P_T/V_L or P_g/V_L was carried out. The power input P_T in the MFS was evaluated as the sum of the power P_{kc} for foam-breaking and the power P_g for gas input. The pneumatic power P_g of the gas input was taken as that due to isothermal expansion of the gas (Ref.13). Figure 3-25 shows the typical results of $(k_La)_M$ plotted against P_T/V_L and those of $(k_La)_F$ plotted against P_g/V_L. As can be seen from the figure, $(k_La)_M$ values in the MFS are on the whole large compared with those in the NS at the same level of the specific power input. It is also found that in order to obtain the same values of volumetric mass transfer coefficient between the two BCs the specific power input in the NS must be increased compared to the MFS.

The mechanical foam-control method is free of problems such as the reaction inhibition and toxicity and adverse

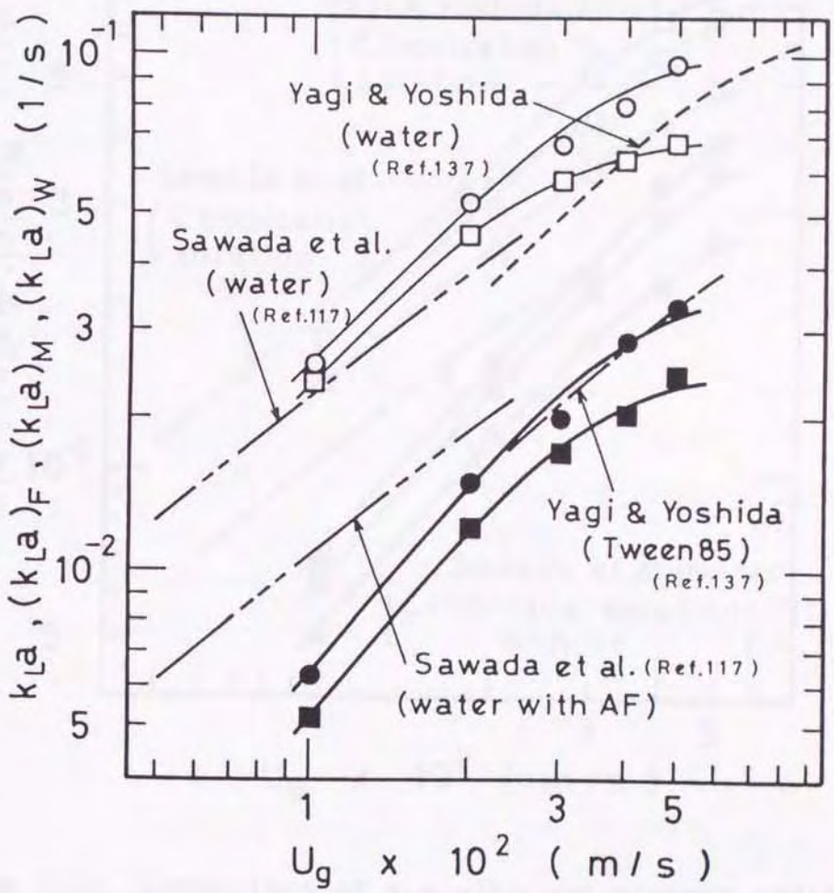

Figure 3-20. Comparison of k_La with and without addition of AF among water and F-D solution in terms of changes in U_g (keys are the same as in Fig.3-12).

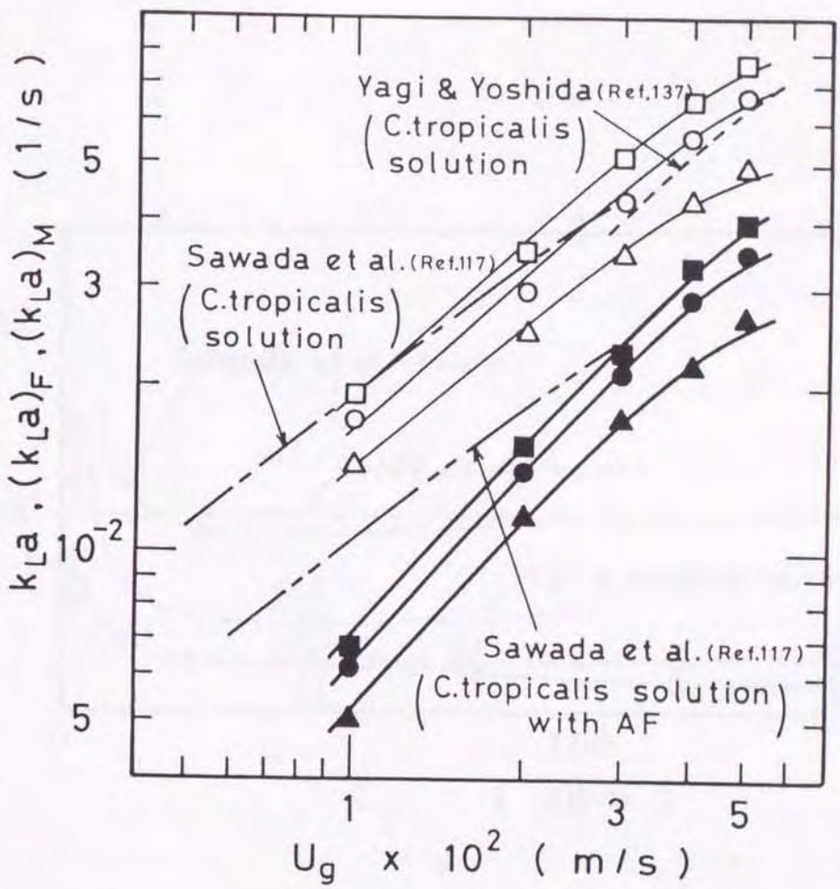

Figure 3-21. Comparison of k_La with and without addition of AF among F-DS solution and F-DC solution in terms of changes in U_g: □ ; $(k_La)_M$, F-DC(1) solution (X_d=0.33kg/m³), W=1.0x10⁻⁵m³/s, ■ ; $(k_La)_F$ F-DC(1) solution with AF (C_F=120ppm), ○ ; $(k_La)_M$, F-DC(3) solution (X_d=0.99kg/m³), W=1.0 x10⁻⁵m³/s, ● ; $(k_La)_F$, F-DC(3) solution with AF (C_F=120 ppm), △ ; $(k_La)_M$, F-DS(4) solution, W=1.0x10⁻⁵m³/s, ▲ ; $(k_La)_F$, F-DS(4) solution with AF (C_F=120ppm).

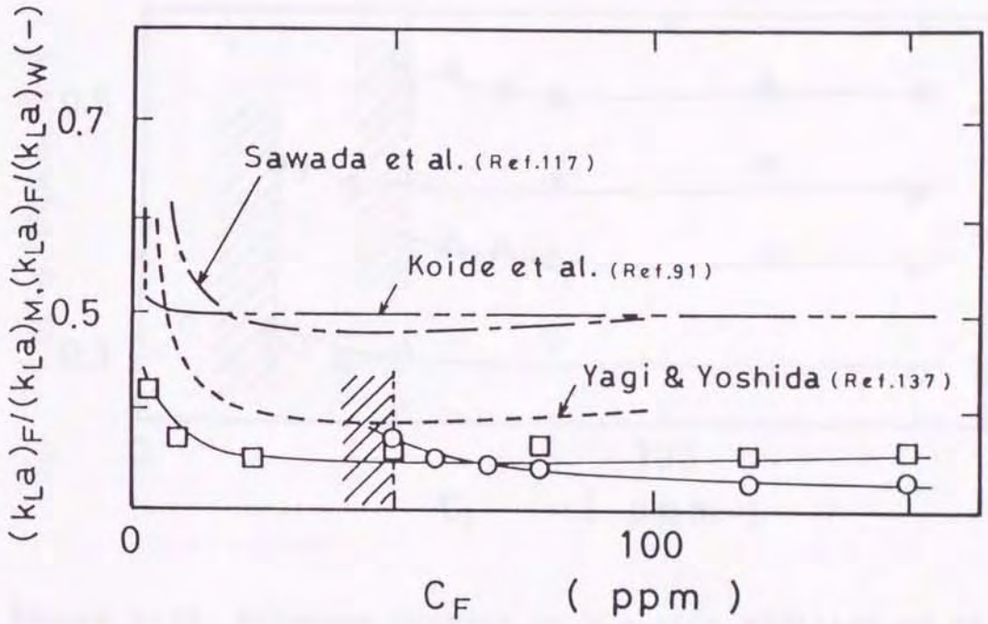

Figure 3-22. Relative changes in k_La with addition of AF in F-D(2) solution and water (oblique-lined areas show the region of nonfoam-controlling): ○ ; $(k_La)_F/(k_La)_M$, W=1.0 x10^{-5}m^3/s, U_g=5.0x10^{-2}m/s, □ ; $(k_La)_F/(k_La)_W$, U_g=5.0x10^{-2} m/s.

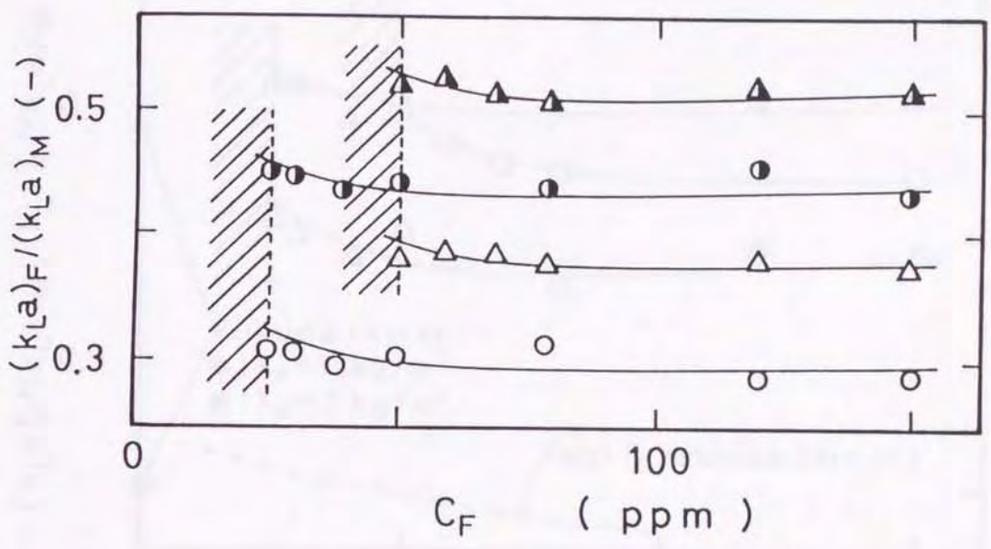

Figure 3-23. Relative changes in k_La with addition of AF in F-DS solutions at $W=1.0\times10^{-5}m^3/s$ (oblique-lined areas show the region of nonfoam-controlling): $(k_La)_F/(k_La)_M$; F-DS(1) solution; U_g ($\times10^{-2}$m/s): ○ ; 2.0, △ ; 5.0. F-DS(4) solution; U_g ($\times10^{-2}$m/s): ◑ ; 2.0, ◭ ; 5.0.

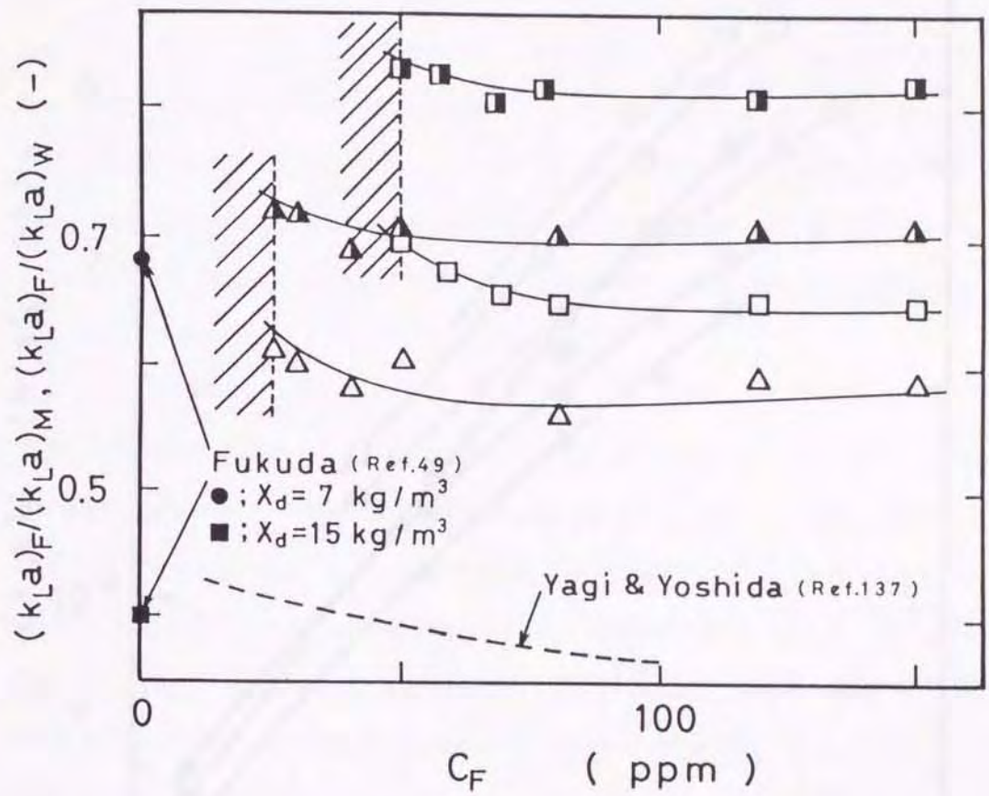

Figure 3-24. Relative changes in k_La with addition of AF in F-DC solutions at W=1.0x10^{-5}m^3/s (oblique-lined areas show the region of nonfoam-controlling): $(k_La)_F/(k_La)_M$; F-DC(3) solution (X_d=0.99kg/m^3); U_g (x10^{-2}m/s): △ ; 2.0, □ ; 5.0. F-DC(6) solution (X_d=6.6kg/m^3); U_g (x10^{-2}m/s^1): ◭ ; 2.0, ◨ ; 5.0.

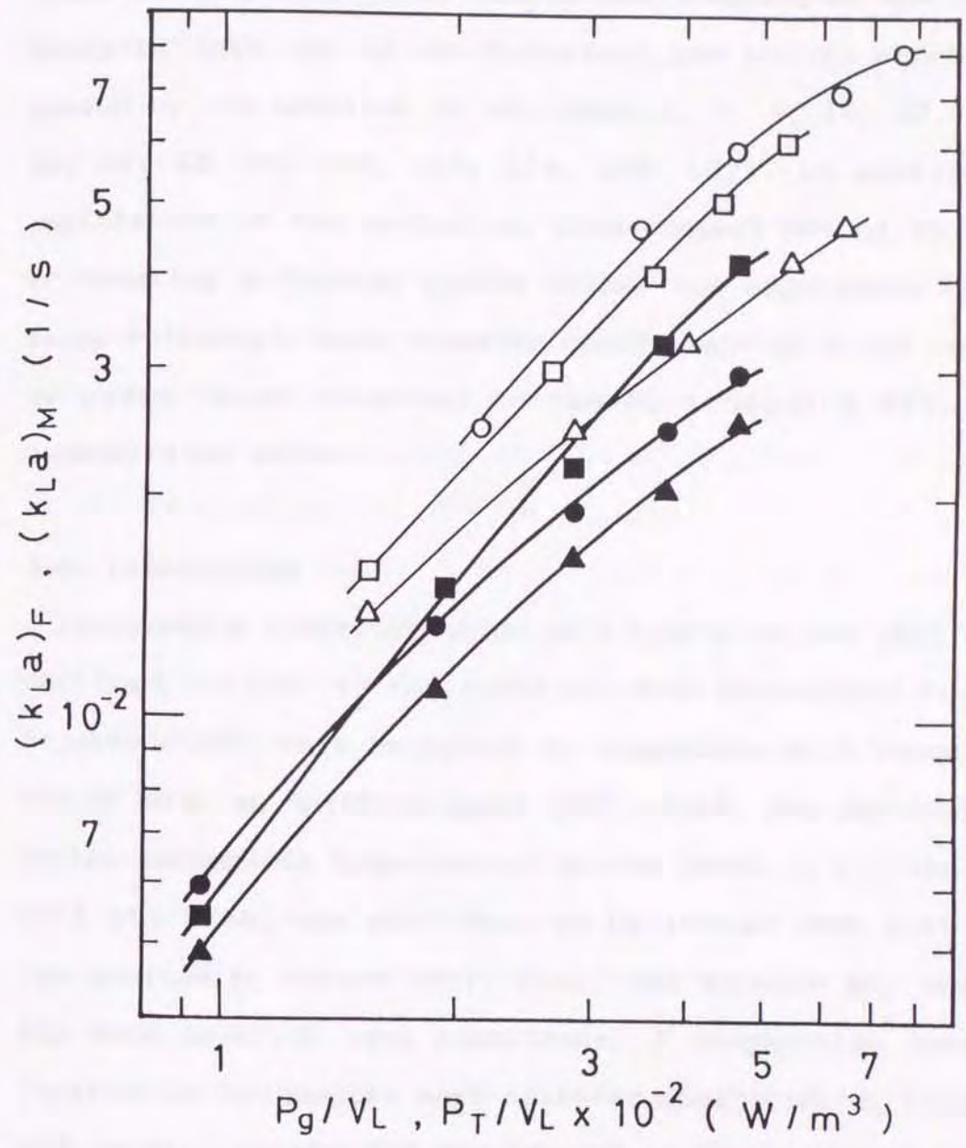

Figure 3-25. Comparison of k_La with and without addition of AF in terms of specific power input: ○ ; $(k_La)_M$ vs. (P_T/V_L), F-D(1) solution, $W=1.0\times10^{-5}\,m^3/s$, ● ; $(k_La)_F$ vs. (P_g/V_L), F-D(1) solution with AF (C_F=120ppm), △ ; $(k_La)_M$ vs. (P_T/V_L), F-DS(4) solution, $W=1.0\times10^{-5}\,m^3/s$, ▲ ; $(k_La)_F$ vs. (P_g/V_L), F-DS (4) solution with AF (C_F=120ppm), □ ; $(k_La)_M$ vs. (P_T/V_L), F-DC(7) solution (X_d=13.2kg/m³), $W=1.0\times10^{-5}\,m^3/s$, ■ ; $(k_La)_F$ vs. (P_g/V_L), F-DC(7) solution with AF (C_F=120ppm).

effects on separation and purification of products seen when foaming is controlled by AFs (Refs.54, 59, 134). There is also no problem such as the lowering of the mass transfer rate due to the decreased gas holdup which is caused by the addition of AFs (Refs.2, 7, 9, 14, 22, 49, 64, 81, 82, 91, 108, 117, 119, 130, 137). In addition, application of the mechanical foam-control method to the BC treating a foaming system allows the appearance of a large volumetric mass transfer coefficient at a low level of power input compared to the NS including AFs, as demonstrated above.

3-4. Conclusions

Performance characteristics of a bubble column (BC) under foam control by the rotating-disk mechanical foam-breaker (MFRD) were evaluated in comparison with those in the BC with an antifoam agent (AF) added. The gas holdup in the mechanical foam-control system (MFS), i.e., the BC with the MFRD, was confirmed to be larger than that in the nonfoaming system (NS), i.e., the BC with AF, under the same aeration rate conditions. A comparative investigation of volumetric mass transfer coefficients, $(k_La)_M$ and $(k_La)_F$, in the MFS and the NS in terms of the specific power input showed higher level of the MFS in respect not only to oxygen transfer rate but also to saving power requirements.

CHAPTER 4

DESIGN AND OPERATION OF ROTATING-DISK MECHANICAL FOAM-BREAKERS FITTED TO BUBBLE COLUMNS

4-1. Introduction

In chapter 3, for a bubble column (BC) treating diluted detergent solutions and those containing a certain amount of corn-syrup or living cells (baker's yeast), the performance of a rotating-disk mechanical foam-breaker (MFRD) fitted to its BC was examined. The MFRD proved to be useful in controlling foam in the BC without the addition of antifoam agents (AFs). From a comparative investigation of the oxygen transfer performance between the two BCs when foaming was controlled by the MFRD and AFs, the superiority of mechanically controlled foaming was also demonstrated. In order to provide a basis for the design and operation of the MFRD fitted into the BC, however, further quantitative studies using various kinds of foaming liquids or BCs with MFRDs of different sizes were necessary.

In this chapter, for foaming systems using various liquids, the foam-breaking behavior of MFRDs fitted to BCs, which is represented by the changes in the required critical disk rotational speed N_c, is first examined. The foaming behavior of BCs is then investigated from the changes in the liquid holdup in the foam, ϕ_L, relating to the difficulty of mechanical foam-breaking. On the basis of the results obtained, empirical equations for

predicting N_c and ϕ_L in foam-breaking regions are also sought. Furthermore, the power consumption P_{kc} for foam-breaking with MFRDs is attempted to evaluate in relation to the level of ϕ_L in BCs.

4-2. Experimental

A schematic flow diagram of the apparatus used in this experiment and the dimensions of BCs with MFRDs are shown in Figs.4-1(a) and 4-1(b) respectively. In addition to the apparatus used in chapter 3, two BCs, 0.256 and 0.31m in diameter D_T, equipped with four baffles ($0.1D_T$ in width and $H_d/3$ in length) were used. They were geometrically similar to the BC of D_T=0.19m. For air sparging, four, eight and twelve porous sintered glass bead filters were used respectively for BCs of D_T=0.19, 0.256 and 0.31m. The number of filters was chosen so that the ratio of the total surface area of filters to the cross-sectional area of the column was almost equal. The filters in the BC of D_T=0.19m were set at an equal distance on the coaxial circle at the position of $D_T/4$ from the center of the column bottom. In the BCs of D_T=0.256m and 0.31m, four filters were set respectively at an equal distance on the coaxial circles at the position of $D_T/6$ and the remaining filters on those at the position of $D_T/3$. The gas superficial velocity U_g ranged from 1.0×10^{-2} to 5.0×10^{-2}m/s. The working liquid volume was varied from 1.3×10^{-2} to 7.5×10^{-2}m^3 depending on D_T. The MFRD was set in the head space of each BC to maintain the ratio of the disk height H_d to D_T (4.737 in H_d/D_T) and nine rotating

disks, 0.13 to 0.24m in diameter D_d, were employed. The ratio of D_T/D_d in three BCs was in the range of 1.267 to 1.476. The liquid feed rate W onto the rotating disk was varied from 1.0×10^{-5} to $4.8\times10^{-5}m^3/s$. Additional details of the MFRD, including the experimental procedure of foam-breaking with the MFRD, have been reported in chapter 3. The critical disk rotational speed N_c, the power P_{kc} required for foam-breaking and the liquid holdup in foam, ϕ_L, were measured according to the respective methods in the previous chapter. The height H_f of the aerated liquid surface from the bottom in the low U_g region below $3.0\times10^{-2}m/s$ was mainly measured by a scale fitted to the column wall. H_f values in the high U_g region were determined approximately on the basis of the change in pressure distribution measured along the height of the BC. As seen in Fig.4-2(a), the value of the pressure in the foam layer deviates from the linear solid line for the vertical pressure distribution in the bulk liquid. The height H_f was determined as the mean value between the position (A) and the position (B), as shown in a magnifying example of Fig.4-2(b). The foam-ascending distance h_f from the aerated liquid surface to the MFRD was then obtained from the difference between the value of H_d and that of H_f: $H_d - H_f$. Table 4-1 shows the properties of the foaming liquids used at 293K.

4-3. Results and Discussion

4-3-1. Critical disk rotational speed required for foam-

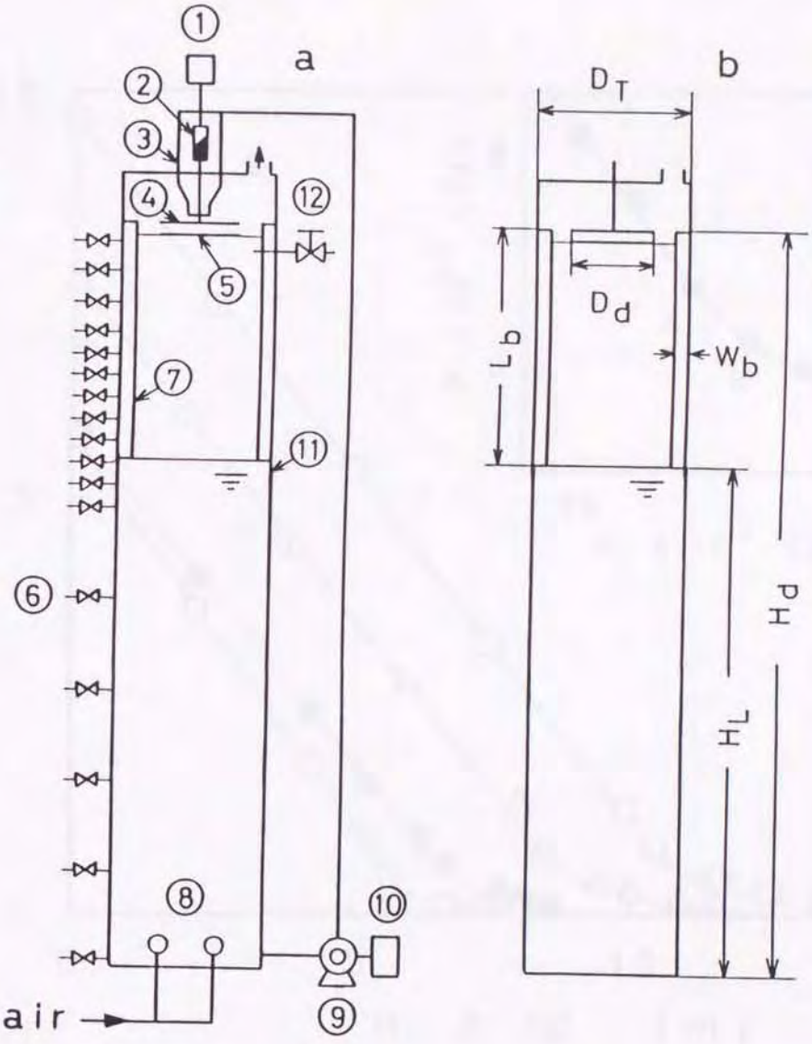

Figure 4-1. (a)Schematic flow diagram of experimental apparatus: (1)motor, (2)torque meter, (3)liquid feeder, (4)rotating disk, (5)fixed disk, (6)pressure tap, (7)baffle plate, (8)ball sparger, (9)pump, (10)flow controller, (11)bubble column, and (12)sampling tap. (b)Geometric design of BC with MFRD. Dimensions are D_T=0.19-0.31m; H_d=4.737D_T; D_d=0.678D_T-0.789D_T; W_b=D_T/10; L_b=H_d/3; H_L=0.511H_d-0.667H_d.

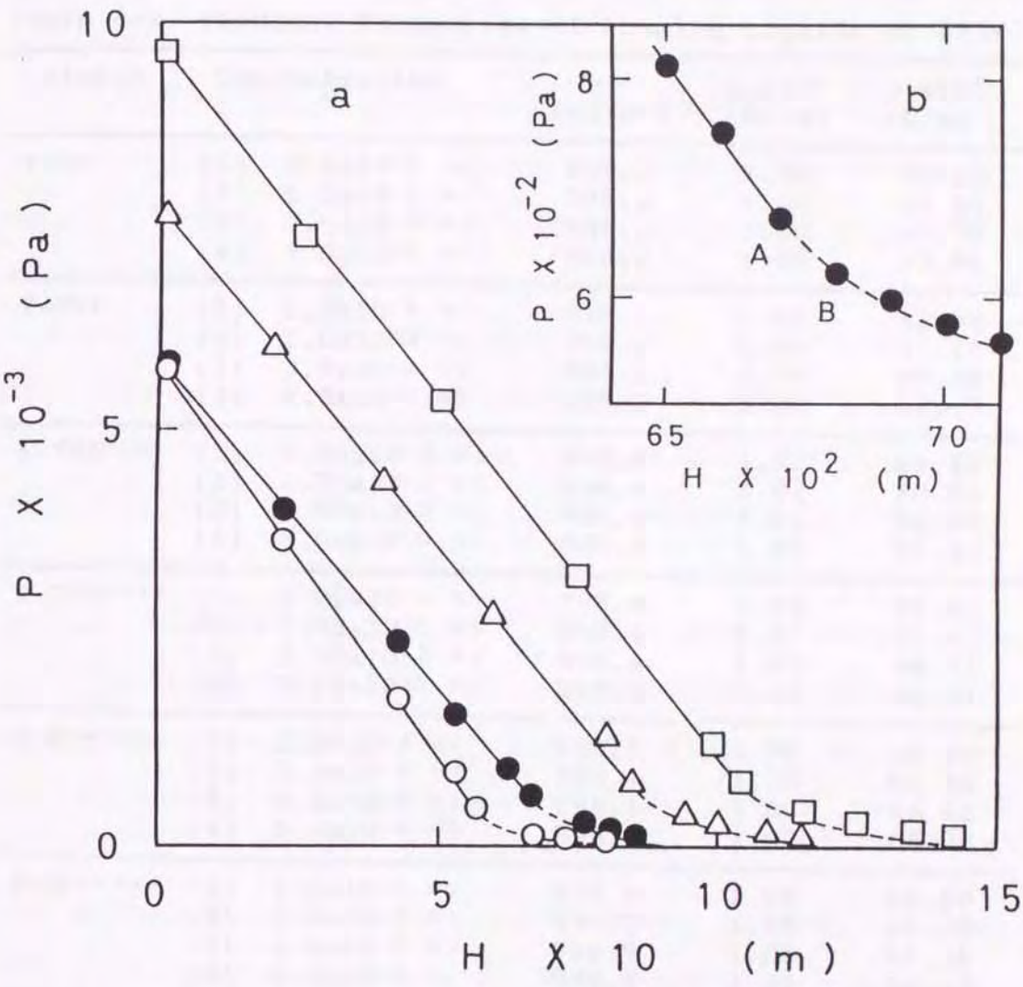

Figure 4-2. Vertical pressure distribution measured along the height of the BC: D_T=0.19m, F-D(4) solution, Γ =2.122 x10^{-5}m^2/s; U_g (x10^{-2}m/s): ○ ; 1.0, ○ ; 5.0, △ ; D_T=0.256m, F-E(4) solution, U_g=3.0x10^{-2}m/s, Γ =3.183x10^{-5}m^2/s, □ ; D_T= 0.31m, F-T(4) solution, U_g=2.0x10^{-2}m/s, Γ =2.122x10^{-5}m^2/s.

Table 4-1 Physical Properties of Foaming Liquids at 293K.

Liquid	Concentration		ρ (kg/m^3)	μ x10^3 (Pa·s)	σ x10^3 (N/m)
F-D*	(1)	3.0x10^{-3} a)	998.2	1.00	70.25
	(2)	5.0x10^{-3} a)	998.2	1.00	63.85
	(3)	7.5x10^{-3} a)	998.2	1.00	57.70
	(4)	1.0x10^{-2} a)	998.2	1.00	53.94
F-T**	(1)	1.0x10^{-3} b)	998.2	1.00	52.82
	(2)	2.0x10^{-3} b)	998.2	1.00	51.15
	(3)	3.0x10^{-3} b)	998.2	1.00	49.40
	(4)	4.0x10^{-3} b)	998.2	1.00	47.75
F-T40***	(1)	1.00x10^{-2} b)	998.4	1.02	61.46
	(2)	1.75x10^{-2} b)	998.4	1.02	60.03
	(3)	2.50x10^{-2} b)	998.4	1.02	58.85
	(4)	5.00x10^{-2} b)	999.4	1.02	55.20
F-T60****	(1)	1.00x10^{-2} b)	998.4	1.02	51.43
	(2)	1.75x10^{-2} b)	998.4	1.02	49.45
	(3)	2.50x10^{-2} b)	998.4	1.02	48.72
	(4)	5.00x10^{-2} b)	998.4	1.02	46.41
F-S*****	(1)	2.0x10^{-3} b)	998.1	1.00	68.40
	(2)	3.0x10^{-3} b)	998.1	1.00	66.48
	(3)	4.0x10^{-3} b)	998.1	1.00	65.62
	(4)	5.0x10^{-3} b)	998.1	1.00	65.22
F-E******	(1)	1.0x10^{-1} b)	998.4	1.05	66.50
	(2)	2.0x10^{-1} b)	998.7	1.05	65.10
	(3)	3.0x10^{-1} b)	998.9	1.06	57.36
	(4)	5.0x10^{-1} b)	999.4	1.06	50.17

*Detergent(Lipon F, manufactured by Lipon Corp.); **Triton X-100; ***Tween 40; ****Tween 60; *****Saponin; ******Egg albumin; a)Vol.%; b)Wt.%.

breaking

It was suggested that the operational variables affecting the foam-breaking capacity of the MFRD, i.e., the critical disk rotational speed N_c, when the diameter D_T of the BC, the height H_d and the diameter D_d of the disk and the working liquid volume V_L are held constant were the liquid feed rate per unit disk circumference, Γ (which is related to the number of liquid particles dispersed per unit disk circumference), and the gas superficial velocity U_g. For the present system where BCs with MFRDs of different sizes are used and the kinds of foaming liquids and their concentrations are varied, it becomes necessary to consider further the effect of the variables such as D_T, D_d, V_L, the foam-ascending distance h_f (relating to the change in the nature of foam by gravity) and the concentration C of solute in the liquid. Prior to investigation of the relationship between these operating variables and N_c, consideration of the choice of parameters to be employed in plotting the data was made.

The size of an annular foam-breaking section between the disk and the column wall is determined by the magnitude of D_T and D_d. As the parameter reflecting its size, the ratio of D_T to D_d, D_T/D_d, was chosen. Since the change in V_L results in a change of h_f, the effect of V_L is represented by h_f. The change in h_f also means that the time required for movement of foam from the aerated liquid surface to the MFRD, the change of which affects the liquid holdup in foam, ϕ_L, due to the effect of liq-

uid drainage from the foam by gravity (Ref.17), varies. Such a time is possible to evaluate in terms of the parameter h_f/U_g. In the present work, it was assumed that N_c may be affected by all the above parameters including Γ and C, namely that N_c may be expressed as a function of their parameters as follows:

$$N_c = \text{func.}(\Gamma,\ C,\ D_T/D_d,\ h_f/U_g) \qquad (4\text{-}1)$$

4-3-1-1. Effect of liquid feed rate per unit disk circumference

The change in N_c was measured for each BC at a transient state, which is in the regime of foam-breaking to nonfoam-breaking as a critical state for foam-breaking. The typical relation between N_c and the liquid feed rate per unit disk circumference, Γ, is shown in Fig.4-3. Solid lines represent the critical state (the areas below the lines show the nonfoaming-breaking regions). Dotted lines represent the transition boundary at which the liquid disintegration pattern by a rotating disk changes from the region of ligament formation to the region of liquid film formation, estimated by the following equation (Ref.95).

$$N_\Gamma^+ = 0.141(Re)^{2/3}(We)^{-0.883} \qquad (4\text{-}2)$$

From a comparison between the solid and dotted lines, the position where the decrease in N_c with the increase in Γ levels off coincides on the whole with the region of Γ_T determined by Eq.(4-2) where film formation (which is non-effective for foam-breaking, due to a lower frequency (Ref.95) of liquid particle formation per unit circumfer-

ence width of a disk) is initiated. It is also shown that within the Γ_T range which could be predicted by Eq.(4-2), N_c decreases linearly with increasing Γ. This may be attributed the increased number of liquid particles dispersed from the disk. As for the dependence of Γ on N_c, it was found that their relation was expressed in the form of $N_c \propto \Gamma^{-0.27}$ regardless of D_T, D_d, U_g and the foaming liquid.

4-3-1-2. Effect of concentration of solute

To investigate the effect of concentration C of solute on N_c within the effective upper limit of Γ, i.e., the Γ_T range which could be predicted by Eq.(4-2), $N_c/\Gamma^{-0.27}$ was plotted against C. The typical results are shown in Fig.4-4. Although there is a difference in the value of $N_c/\Gamma^{-0.27}$, depending on D_T/D_d, U_g and the kind of the liquid, all the system had a tendency that $N_c/\Gamma^{-0.27}$ increased linearly with increasing C. For different $N_c/\Gamma^{-0.27}$ values at the same level of C, the main cause may be probably due to a difference in foaming characteristics among the liquids. Concerning this difference, further studies on characterization of foam-forming ability of the liquids by using a small foaming tester and the relation between their changes and these in N_c will be necessary in the future. For the dependence of C on $N_c/\Gamma^{-0.27}$, from the results shown in Fig.4-4, their relation for respective kinds of foaming liquids can be expressed as follows:

$$N_c/\Gamma^{-0.27} \propto C^{\alpha} \qquad (4\text{-}3)$$

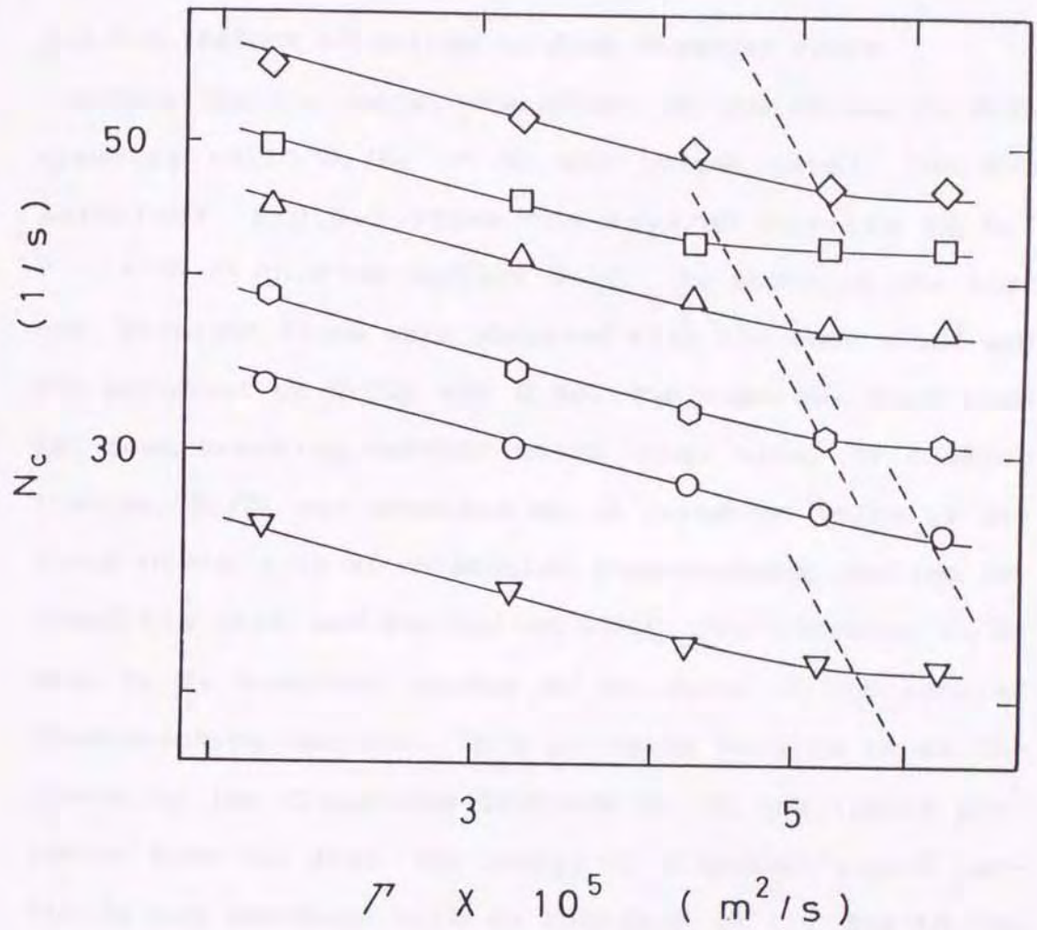

Figure 4-3. Effect of Γ on N_c at H_L/H_d=0.667: D_T=0.19m: ⬡; F-E(4) solution, U_g=1.0x10^{-2}m/s, D_T/D_d=1.267, △ ; F-T40(4) solution, U_g=2.0x10^{-2}m/s, D_T/D_d=1.476, ◇ ; F-S(3) solution, U_g=5.0x10^{-2}m/s, D_T/D_d=1.267, D_T=0.256m: □ ;F-E(3) solution, U_g=3.0x10^{-2}m/s, D_T/D_d=1.267, D_T=0.31m: ▽ ; F-T(4) solution, U_g=1.0x10^{-2}m/s, D_T/D_d=1.267, ○ ; F-D(2) solution, U_g=2.0x10^{-2}m/s, D_T/D_d=1.267.

where α is empirical constants which change depending on the kind of the foaming liquid. The values of α determined were 0.21, 0.12, 0.20, 0.20, 0.24 and 0.10, respectively for F-D, F-T, F-T40, F-T60, F-S and F-E solutions.

4-3-1-3. Effect of column to disk diameter ratio

Within the Γ_T range, the effect of the column to disk diameter ratio D_T/D_d on N_c was investigated. For F-D solutions, Fig.4-5 shows the typical results of $N_c/\Gamma^{-0.27}C^{0.21}$ plotted against D_T/D_d. As shown in the figure, straight lines were observed with the same slope and the exponent of D_T/D_d was 0.90. The same was confirmed for foam-breaking systems using other kinds of foaming liquids. D_T/D_d was selected as a parameter which is related to the size of an annular foam-breaking section between the disk and the column wall. The increase in D_T when D_d is constant causes an increase of the annular foam-breaking section. This increase results in an increase of the dispersion distance l_f of the liquid particles from the disk. The energy of dispersed liquid particles may decrease with an increase in l_f, due to the increased frequency of impact between the liquid particles and the ascending foam. In order to avoid a lowering of the impact force of the liquid particles with l_f and to carry out foam-breaking effectively, the disk rotational speed, the increase of which contributes to an increase of the kinetic energy of the liquid particles, must be increased compared to cases using the BC of small D_T. The results shown in Fig.4-5 may be attributed to the

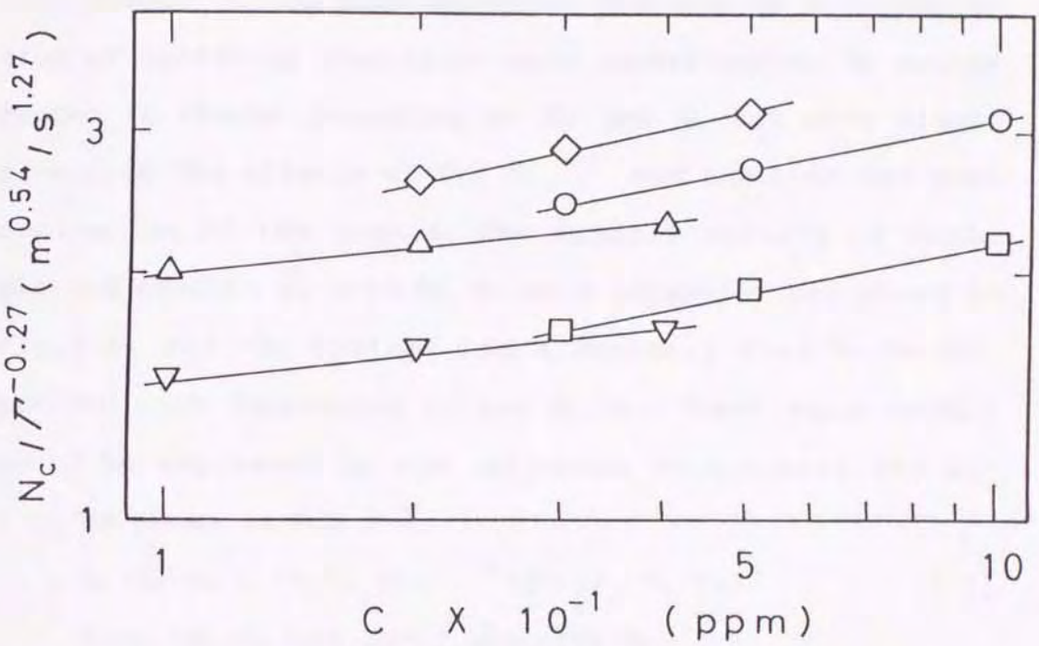

Figure 4-4. Relation between $N_c / \Gamma^{-0.27}$ and C: F-D(1-4) solutions: ○ ; D_T =0.19m, U_g =5.0x10^{-2}m/s, D_T / D_d =1.267, □ ; D_T =0.31m, U_g =2.0x10^{-2}m/s, D_T / D_d =1.476, F-T(1-4) solutions: ▽ ; D_T =0.19m, U_g =1.0x10^{-2}m/s, D_T / D_d =1.267, △ ; D_T =0.256m, U_g =2.0x10^{-2}m/s, D_T / D_d =1.476, F-S(1-4) solutions: ◇ ; D_T = 0.19m, U_g =5.0x10^{-2}m/s, D_T / D_d =1.267.

increased dispersion distance of liquid particles from the disk due to the increase of D_T.

4-3-1-4. Effect of foam-ascending distance to gas superficial velocity ratio

Prior to investigation of the effect of h_f/U_g on N_c, the changes in the foam-ascending distance h_f with variation of operating conditions were investigated. h_f values tended to change depending on U_g and H_L but were almost free from the effects of D_T, D_d, Γ and the kind and concentration of the liquid. The typical results of h_f/D_T plotted against U_g with H_L/H_d as a parameter are shown in Fig.4-6. All the systems had a tendency that h_f/D_T decreased with increasing U_g and H_L/H_d. Their relationship could be expressed by the following form within 10% error, as shown in Fig.4-7.

$$h_f/D_T = U_g^{-2.54(H_L/H_d)^{5.76}} 10^{func.(H_L/H_d)} \qquad (4\text{-}4)$$

$$func.(H_L/H_d) = -2.25 - 15.30\log(H_L/H_d) - 22.65\log(H_L/H_d)^2 \qquad (4\text{-}5)$$

The relationship between $N_c/\Gamma^{-0.27}C^{\alpha}(D_T/D_d)^{0.90}$ and h_f/U_g was then examined. As the value of h_f, those obtained from Eqs.(4-4) and (4-5) were employed. Figure 4-8 shows such a relationship for F-D solutions (α =0.21) and F-T40 solutions (α =0.20). The values of $N_c/\Gamma^{-0.27}C^{\alpha}(D_T/D_d)^{0.90}$ tended to decrease gradually with increasing the foam ascending distance to gas superficial velocity ratio h_f/U_g. The liquid holdup in foam is known to reduce with increasing the vertical ascending distance, due to the effect of liquid drainage from the foam by gravity. The

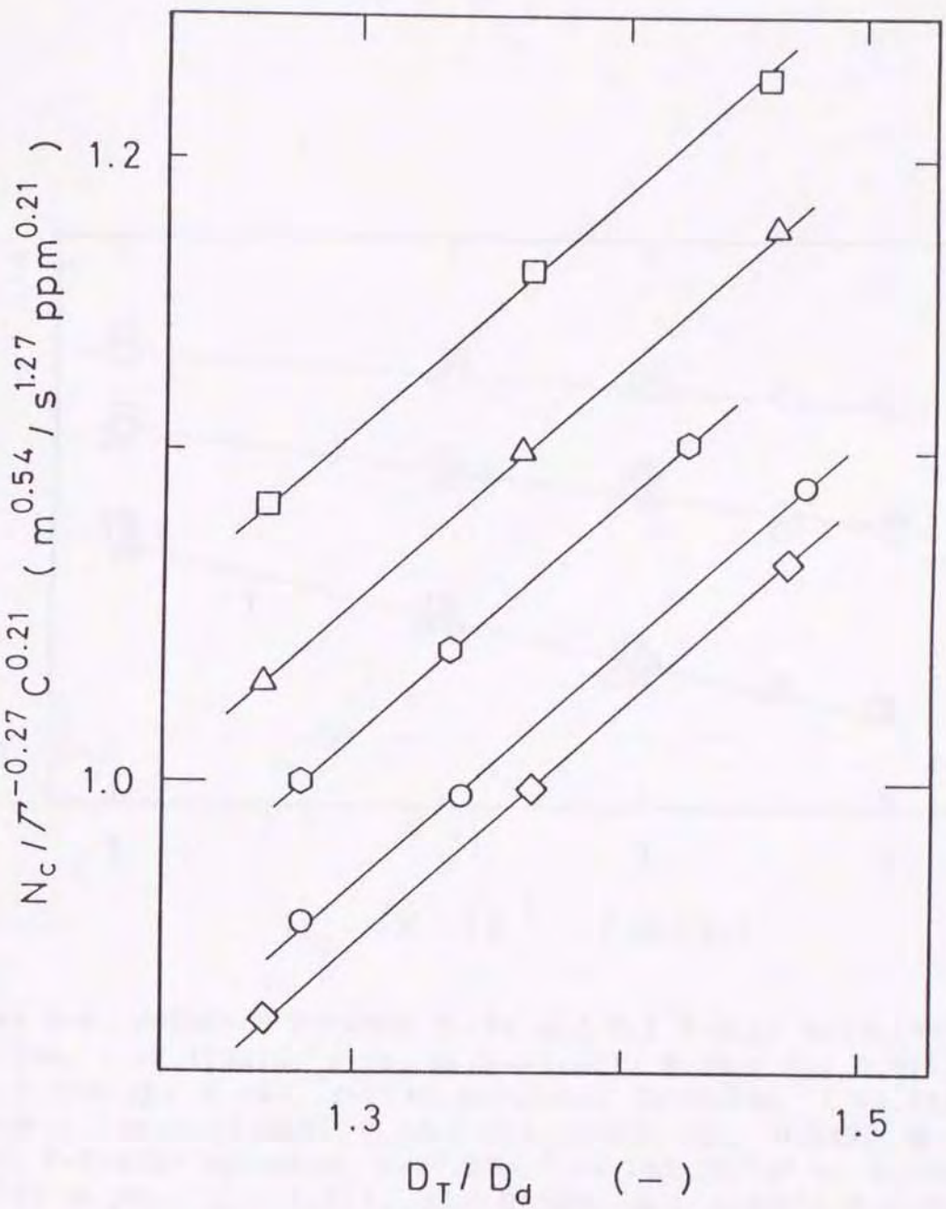

Figure 4-5. Relation between $N_c / \Gamma^{-0.27} C^{0.21}$ and D_T / D_d for F-D solutions: D_T=0.19m: ◇ ; U_g=2.0x10^{-2}m/s, △ ; U_g=3.0x10^{-2}m/s, □ ; U_g=4.0x10^{-2}m/s, D_T=0.256m: ⬡ ; U_g=3.0x10^{-2}m/s, D_T=0.31m: ○ ; U_g=3.0x10^{-2}m/s.

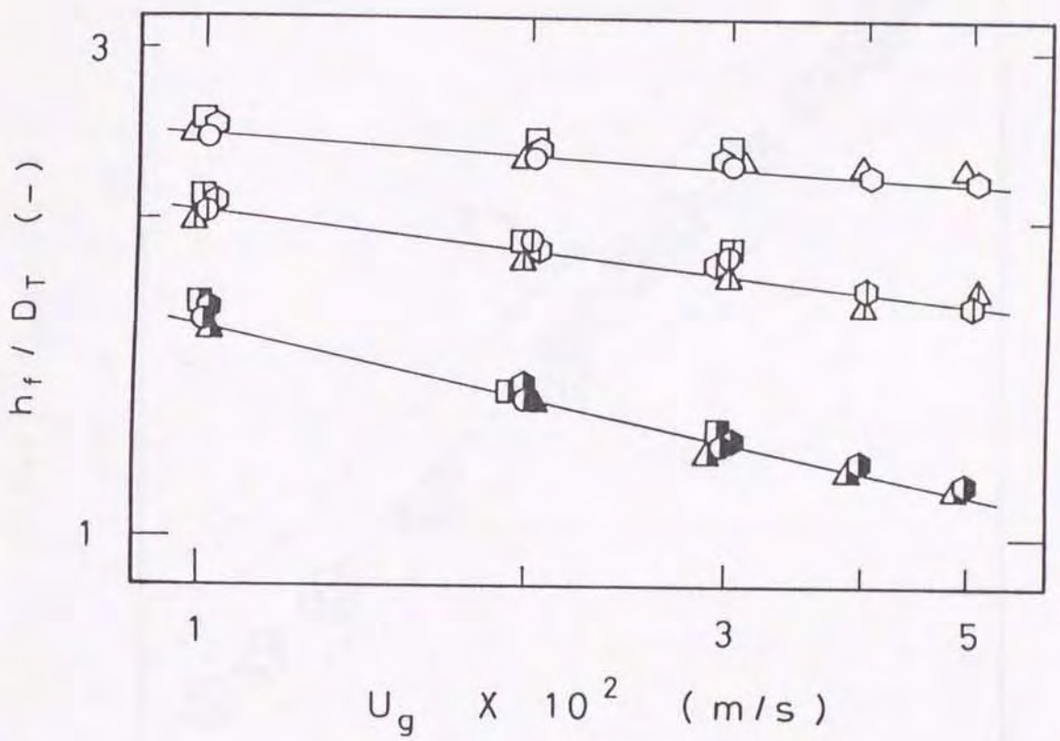

Figure 4-6. Relation between h_f/D_T and U_g : F-D(1) solution, D_T=0.19m, Γ =2.122x10^{-5}m^2/s, D_T/D_d=1.267; H_L/H_d : ○ ; 0.511, ◐ ; 0.589, ◑ ; 0.667, F-D(4) solution, D_T=0.31m, Γ =3.183 x10^{-5}m^2/s, D_T/D_d=1.267; H_L/H_d : ○ ; 0.511, ◐ ; 0.589, ◑ ; 0.667, F-T60(3) solution, D_T=0.19m, Γ =3.183x10^{-5}m^2/s, D_T/D_d =1.476; H_L/H_d : △ ; 0.511, ◭ ; 0.589, ▲ ; 0.667, F-E(4) solution, D_T=0.256m, Γ =2.122x10^{-5}m^2/s, D_T/D_d=1.476; H_L/H_d : □ ; 0.511, ◫ ; 0.589, ◨ ; 0.667.

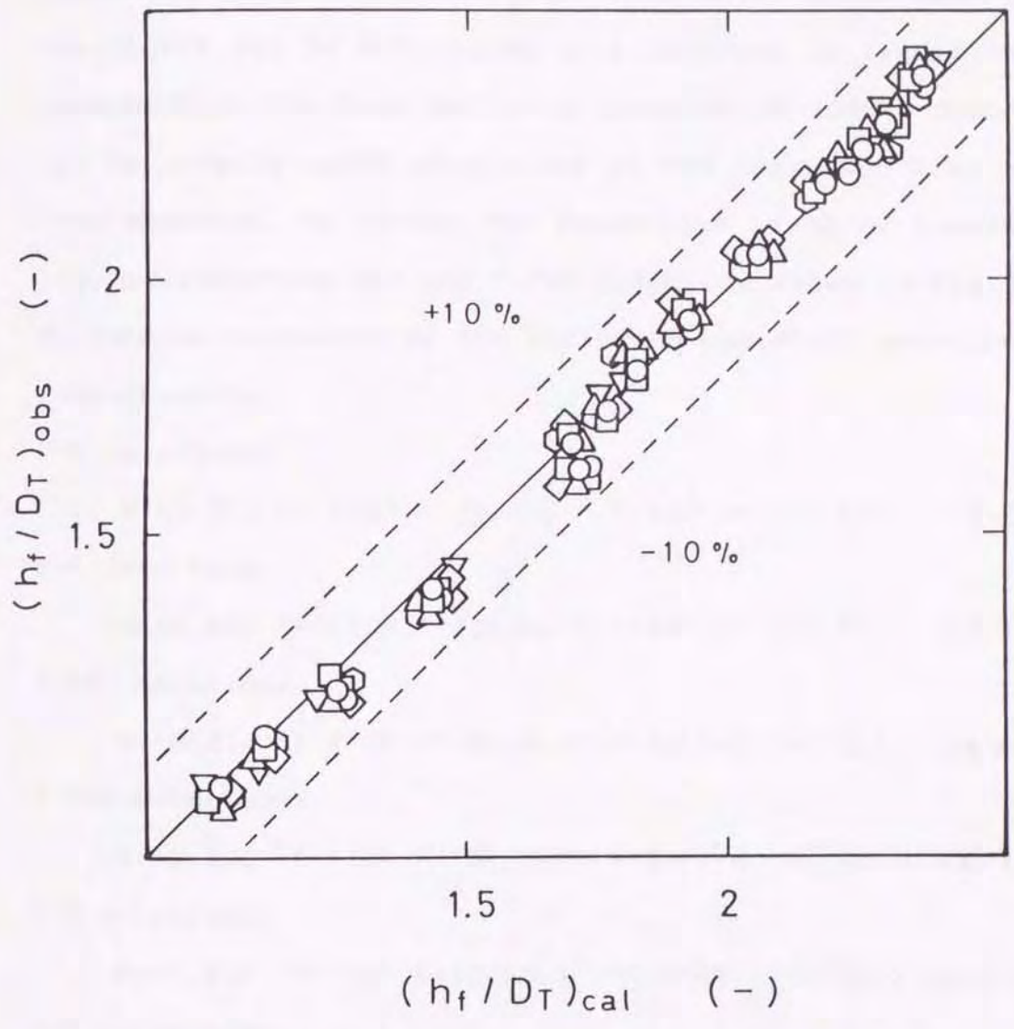

Figure 4-7. Comparison of observed and calculated values of h_f/D_T : ○ ; F-D(1-4) solutions, △ ; F-T(1-4) solutions, ▽ ; F-T40(1-4) solutions, ⬡ ; F-T60(1-4) solutions, ◇ ;F-S(1-4) solutions, □ ; F-E(1-4) solutions.

increase in h_f in the present system may result in a decrease in the liquid holdup in foam. It was shown previously that the decrease in the liquid holdup in ascending foam, ϕ_L, contributed to reduction of N_c. The decrease in $N_c/\Gamma^{-0.27}C^{\alpha}(D_T/D_d)^{0.90}$ with h_f/U_g as seen in the figure may be attributed to a decrease in liquid entrainment in the foam due to an increase of liquid drainage by gravity under conditions of the increased time of foam movement. N_c values for respective kinds of foaming liquids including F-D and F-T40 solutions shown in Fig.4-8 could be expressed by the following empirical equations respectively.

F-D solutions:

$$N_c=0.31\Gamma^{-0.27}C^{0.21}(D_T/D_d)^{0.90}10^{func.(h_f/U_g)} \quad (4\text{-}6)$$

F-T solutions:

$$N_c=0.48\Gamma^{-0.27}C^{0.12}(D_T/D_d)^{0.90}10^{func.(h_f/U_g)} \quad (4\text{-}7)$$

F-T40 solutions:

$$N_c=0.21\Gamma^{-0.27}C^{0.20}(D_T/D_d)^{0.90}10^{func.(h_f/U_g)} \quad (4\text{-}8)$$

F-T60 solutions:

$$N_c=0.19\Gamma^{-0.27}C^{0.20}(D_T/D_d)^{0.90}10^{func.(h_f/U_g)} \quad (4\text{-}9)$$

F-S solutions:

$$N_c=0.32\Gamma^{-0.27}C^{0.24}(D_T/D_d)^{0.90}10^{func.(h_f/U_g)} \quad (4\text{-}10)$$

F-E solutions:

$$N_c=0.34\Gamma^{-0.27}C^{0.10}(D_T/D_d)^{0.90}10^{func.(h_f/U_g)} \quad (4\text{-}11)$$

$Func.(h_f/U_g)$ in Eqs.(4-6) - (4-11) is the same in its functional form and was expressed by the form of Eq.(4-12) independently of the kind of the foaming liquid.

$$func.(h_f/U_g)=0.511+0.062\log(h_f/U_g)-0.144[\log(h_f/U_g)]^2 \quad (4\text{-}12)$$

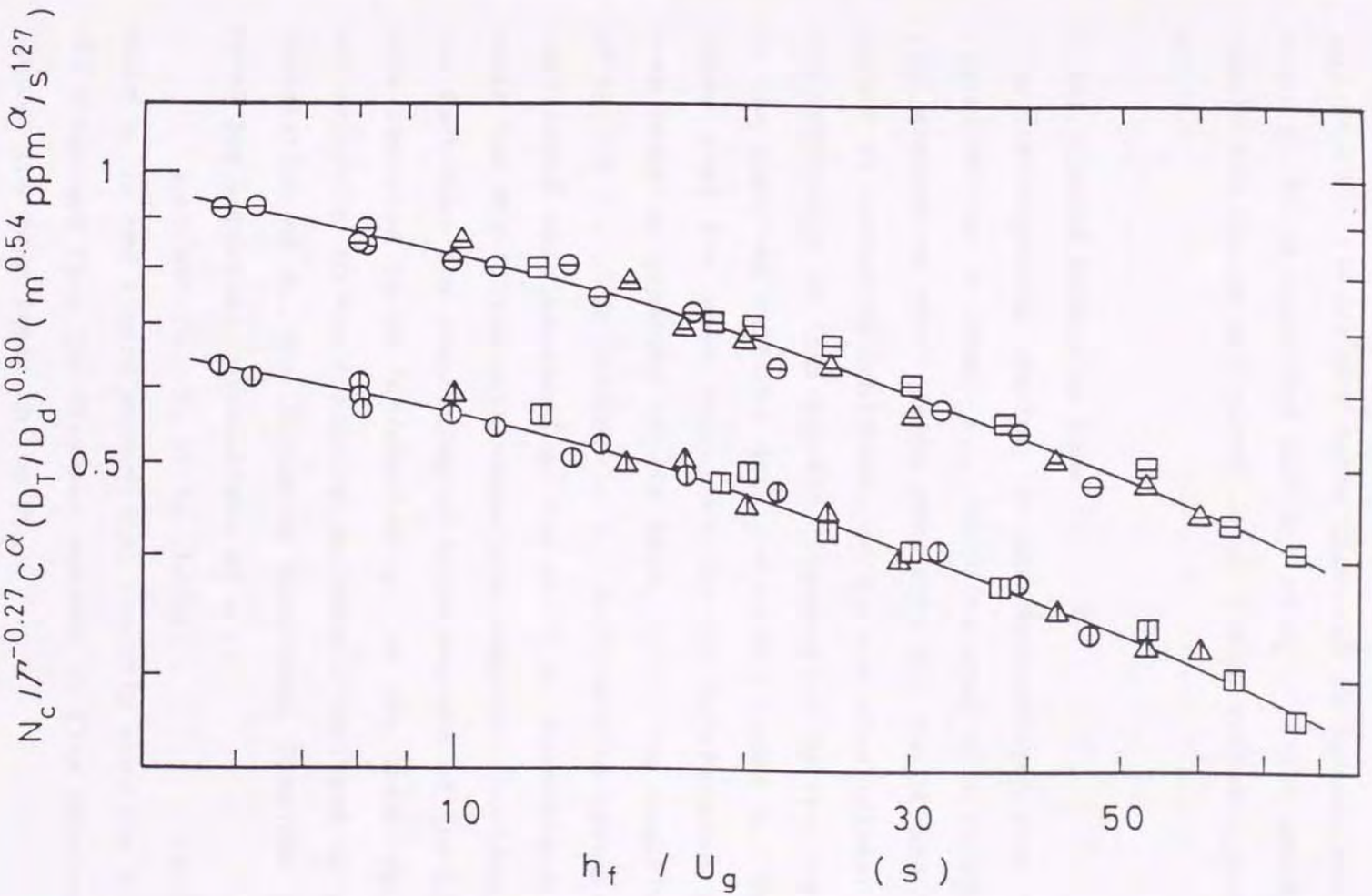

Figure 4-8. Relation between $N_c/\Gamma^{-0.27}C^{\alpha}(D_T/D_d)^{0.90}$ and h_f/U_g: F-D(1-4) solutions (α =0.21); D_T(m): ⊖ ; 0.19, △ ; 0.256, ⊟ ; 0.31, F-T40(1-4) solutions (α =0.20); D_T(m): ⊕ ;0.19, ◭ ; 0.256, ◫ ;0.31.

The relationship between the values of N_c calculated by Eqs.(4-4) - (4-12) and those observed is summarized in Fig.4-9. It is concluded that Eqs.(4-4) - (4-12) would be usable for design and operation of a MFRD fitted into the BC.

4-3-2. Liquid holdup in foam

In the preceding chapter, it was demonstrated that the liquid holdup in foam, ϕ_L, could be used as a substantial measure of the foaming intensity for the BC and the effect of operating conditions on ϕ_L was also related to the difficulty of foam-breaking represented by the change in the required critical disk rotational speed N_c. This means that the most important factor determining the foam-breaking capacity of the MFRD, i.e., the magnitude of N_c, is ϕ_L. The changes in ϕ_L with varying operating conditions were measured at the critical foam-breaking state for BCs filled with respective liquids. Considering the fact that the dispersing of large amounts of the liquids resulted in an increase of ϕ_L in the foam layer, and referring to the foregoing parameters employed in the correlation of N_c, the following functional form was assumed for empirical correlations of ϕ_L:

$$\phi_L = \text{func.}(U_L,\ C,\ D_T/D_d,\ h_f/U_g) \qquad (4\text{-}13)$$

where U_L is the liquid superficial velocity when the liquid dispersed from the disk was assumed to flow downwards through the foam layer in the BC.

The effect of U_L on ϕ_L was first investigated. As shown in Fig.4-10, the values of ϕ_L were found to in-

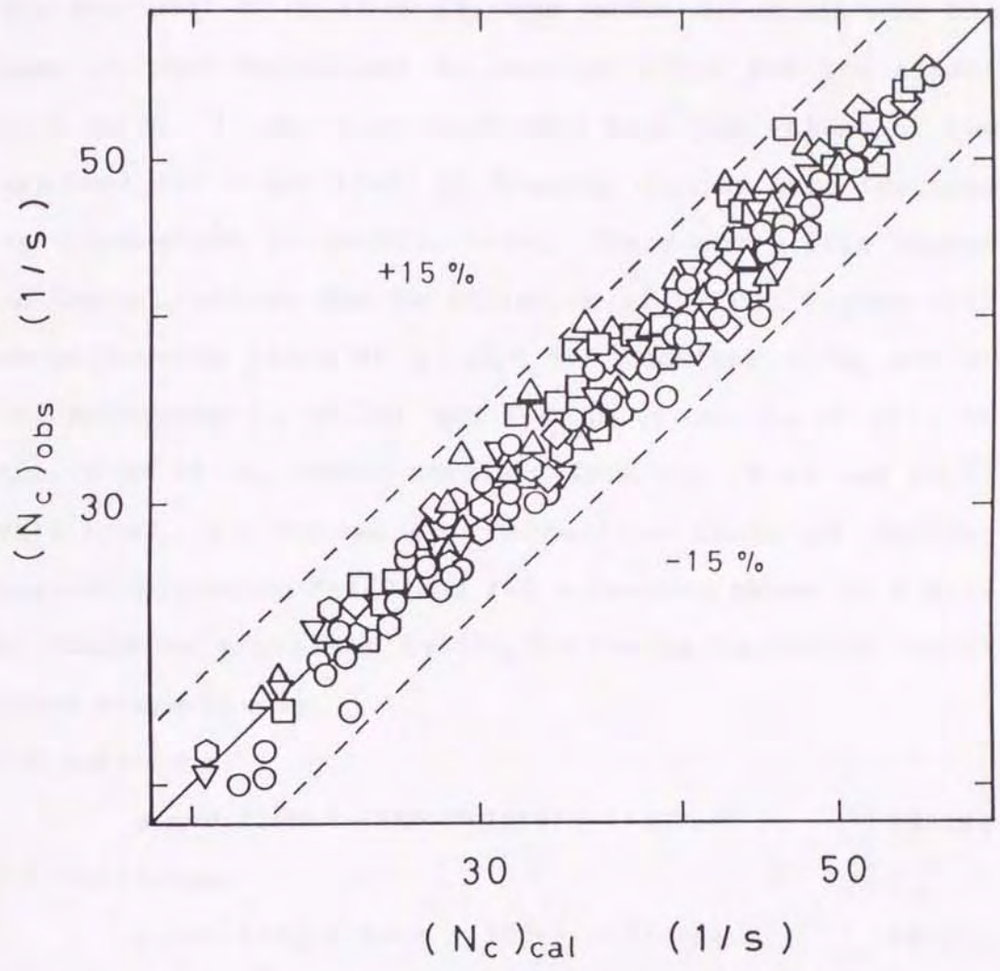

Figure 4-9. Comparison of observed and calculated values of N_c (keys are the same as in Fig.4-7).

crease with increase in U_L in the form of $\phi_L \propto U_L^{0.24}$ for all the systems used. To investigate the effect of C on ϕ_L, $\phi_L/U_L^{0.24}$ was then plotted against C. Examples of such a plot for F-E solutions is shown in Fig.4-11. The exponent of C is 0.10, the value of which was the same to that determined in section 4-3-1 for the effect of C on N_c. It was also confirmed that the values of the exponent for other kinds of foaming liquids were the same as those shown in section 4-3-1. There was little change in the ϕ_L values due to variation of D_T/D_d. Figure 4-12 shows log-log plots of $\phi_L/U_L^{0.24}C^{\alpha}$ against h_f/U_g for F-T60 solutions (α =0.20) and F-E solutions (α =0.10). As the value of h_f, those obtained from Eqs.(4-4) and (4-5) were used. ϕ_L values for respective kinds of foaming liquids including F-T60 and F-E solutions shown in Fig.4-12 could be expressed by the following empirical equations respectively.

F-D solutions:

$$\phi_L = 0.110 U_L^{0.24} C^{0.21} 10^{func.(h_f/U_g)} \qquad (4\text{-}14)$$

F-T solutions:

$$\phi_L = 0.174 U_L^{0.24} C^{0.12} 10^{func.(h_f/U_g)} \qquad (4\text{-}15)$$

F-T40 solutions:

$$\phi_L = 0.070 U_L^{0.24} C^{0.20} 10^{func.(h_f/U_g)} \qquad (4\text{-}16)$$

F-T60 solutions:

$$\phi_L = 0.068 U_L^{0.24} C^{0.20} 10^{func.(h_f/U_g)} \qquad (4\text{-}17)$$

F-S solutions:

$$\phi_L = 0.112 U_L^{0.24} C^{0.24} 10^{func.(h_f/U_g)} \qquad (4\text{-}18)$$

F-E solutions:

$$\phi_L = 0.120 U_L^{0.24} C^{0.10} 10^{func.(h_f/U_g)} \qquad (4\text{-}19)$$

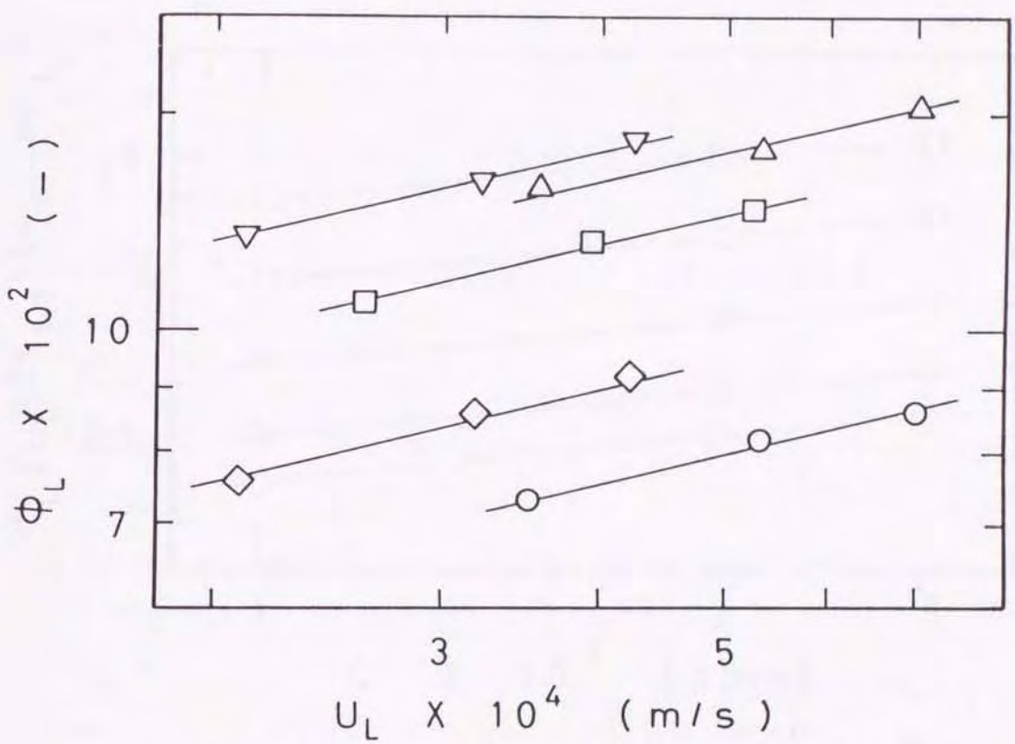

Figure 4-10. Effect of U_L on ϕ_L: D_T=0.19m: ○ ; F-T60(1) solution, U_g=4.0x10^{-2}m/s, △ ; F-S(3) solution, U_g=5.0x10^{-2} m/s, D_T=0.256m: □ ; F-T(4) solution, U_g=3.0x10^{-2}m/s, D_T= 0.31m: ▽ ; F-D(4) solution, U_g=3.0x10^{-2}m/s, ◇ ; F-E(4) solution, U_g=1.0x10^{-2}m/s.

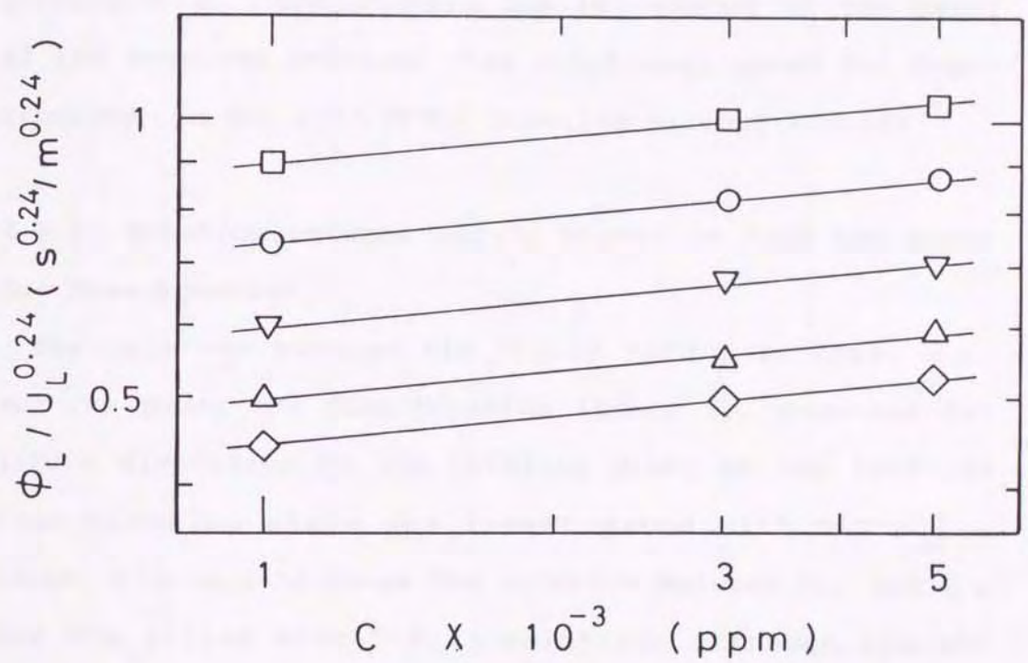

Figure 4-11. Relation between $\phi_L/U_L^{0.24}$ and C for F-E solutions: D_T=0.19m: ▽ ; U_g=2.0x10^{-2}m/s, ○ ; U_g=4.0x10^{-2}m/s D_T=0.256m:△ ; U_g=1.0x10^{-2}m/s, D_T=0.31m: ◇ ; U_g=1.0x10^{-2}m/s, □ ; U_g=3.0x10^{-2}m/s.

The functional form of func.(h_f/U_g) in Eqs.(4-14) - (4-19) is the same as that of Eq.(4-12).

A comparison between ϕ_L values calculated and those observed within the Γ_T range which could be predicted by Eq.(4-2) is shown in Fig.4-13. It is concluded that Eqs.(4-4), (4-5) and (4-12) and Eqs.(4-14) - (4-19) would be useful for the prediction of ϕ_L, which reflects the difficulty of foam-breaking and is related to the level of the required critical disk rotational speed for foam-breaking, in BCs with MFRDs treating various liquids.

4-3-3. Relation between liquid holdup in foam and power for foam-breaking

The relation between the liquid holdup in foam, ϕ_L, and the power for foam-breaking (power P_{kc} required for liquid dispersion by the rotating disk) at the critical foam-breaking state was investigated within the Γ_T range. Figure.4-14 shows the relation between P_{kc} and ϕ_L for BCs filled with F-D(4) solution. Although the absolute values of ϕ_L and P_{kc} differ depending on the operating conditions such as U_g, D_T, D_d, etc., on the whole, good correspondence is seen between the increases of P_{kc} and ϕ_L in respective BCs, indicating that foam with larger ϕ_L requires more power for foam-breaking. The same was confirmed for foam-breaking systems using other liquids. These results show that ϕ_L is also a measure that reflects the difficulty of foam-breaking in terms of the power required for foam-breaking. Regarding the fact that P_{kc} values tend to be high in the large BC,

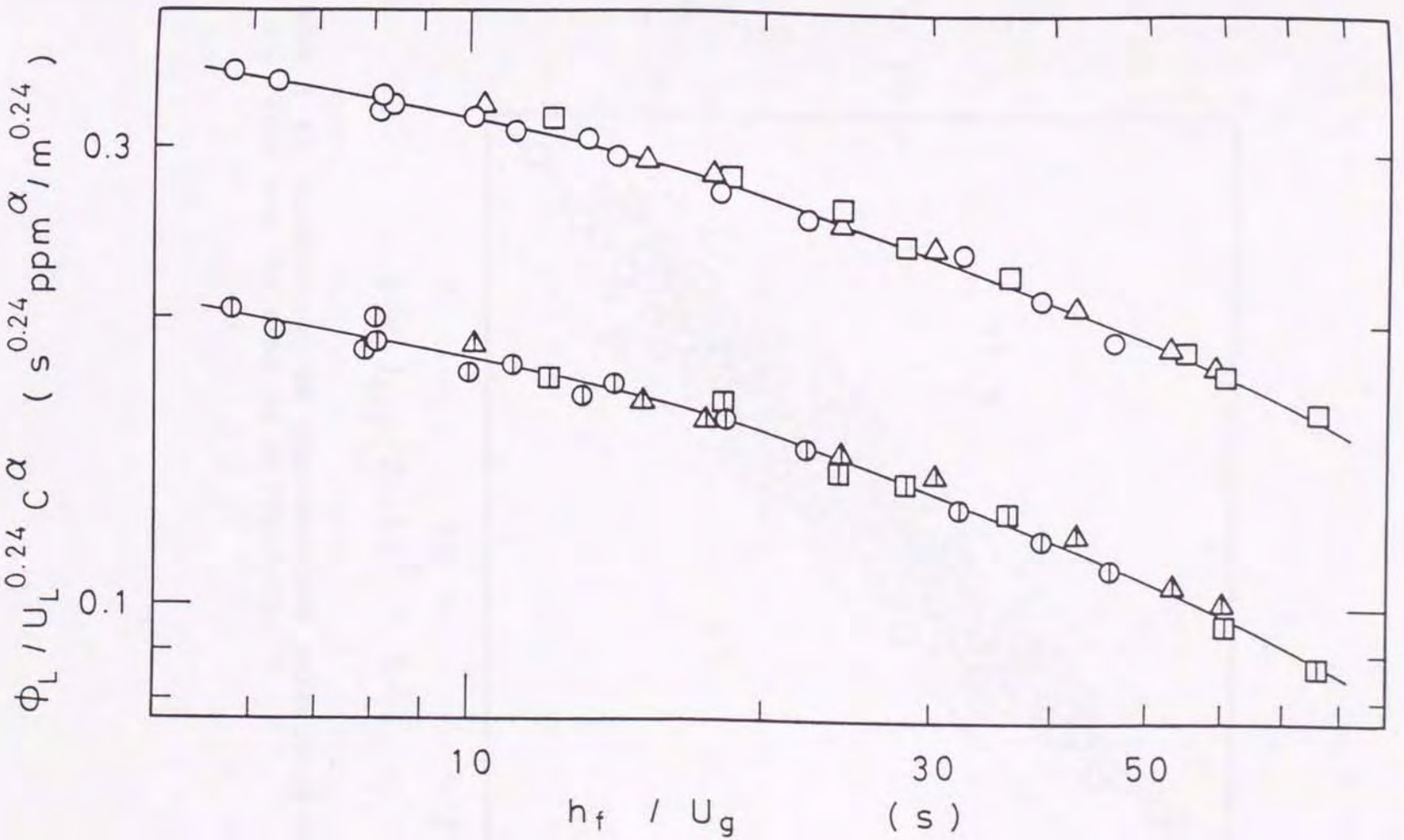

Figure 4-12. Relation between $\phi_L/U_L^{0.24}C^{\alpha}$ and h_f/U_g: F-T60(1-4) solutions (α =0.20); D_T (m): ◑ ; 0.19, ◭ ; 0.256, ◫ ; 0.31, F-E(1-4) solutions (α =0.10); D_T (m): ○ ; 0.19, △ ; 0.256, □ ; 0.31.

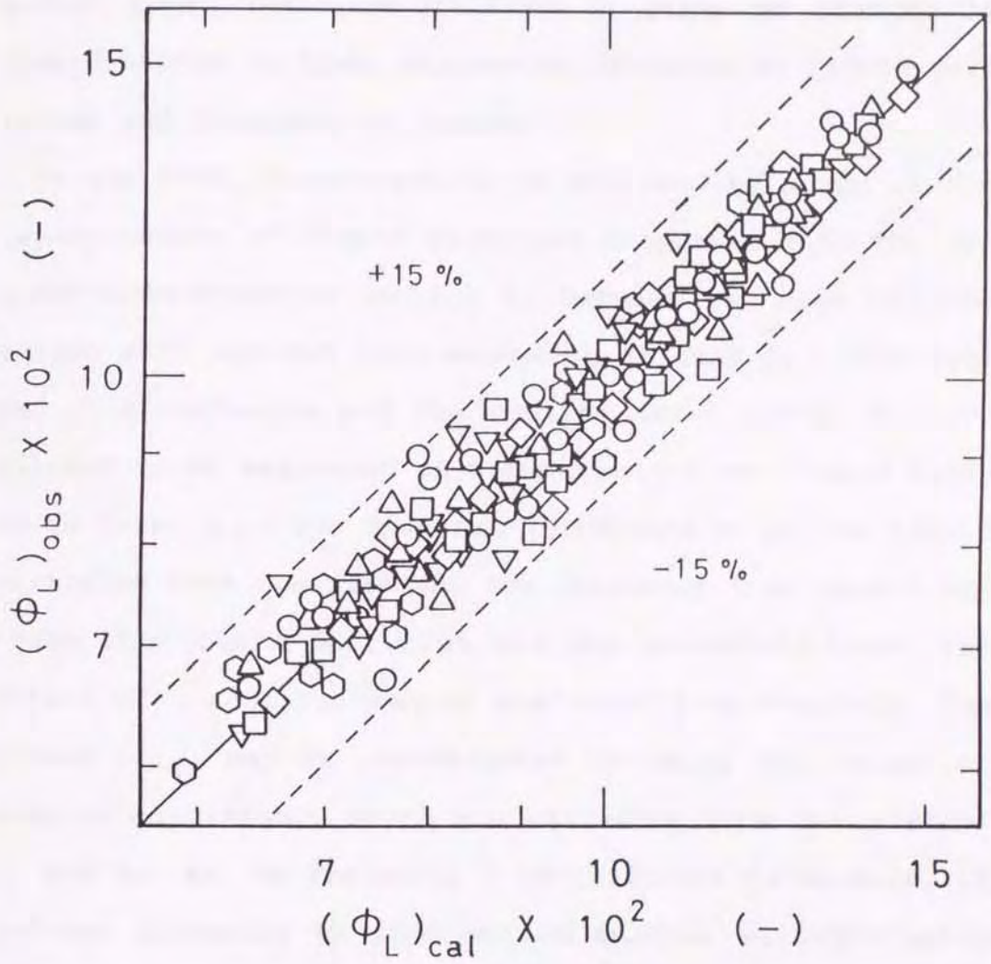

Figure 4-13. Comparison of observed and calculated values of ϕ_L (keys are the same as in Fig.4-7).

the main cause may be related to the increased dispersion distance of the liquid particles and the increased impact frequency of their particles due to the increase of D_T.

4-3-4. Power for foam-breaking in terms of changes in liquid holdup in foam, dispersion distance of liquid particles and frequency of impact

In the MFRD, foam-breaking is achieved by means of the impact action of liquid particles dispersed into the annular foam-breaking section S_a between the disk and the column wall against foam ascending through S_a. Considering this mechanism and the results shown above, P_{kc} are assumed to be expressed as a function of the liquid holdup in foam, ϕ_L, the dispersion distance l_f of the liquid particles from the disk and the frequency f of impact between the liquid particles and the ascending foam. The effect of ϕ_L on P_{kc} can be evaluated from Fig.4-14. The effect of l_f may be investigated by using the values of dispersion distance which are estimated from the size of D_T and D_d. As the frequency f is difficult to measure, it becomes necessary to find out an another variable which is related to f. Referring to the previously-mentioned foam-breaking mechanism, the change in the gas superficial velocity U_{ga} through S_a, the change of which also depends on the gas superficial velocity U_g on the cross-sectional area of the BC, may be pointed out as a measure reflecting the frequency f of impact. The reason is that if U_{ga} is high the number of foams passing through S_a per unit time may be large and that such an increase may re-

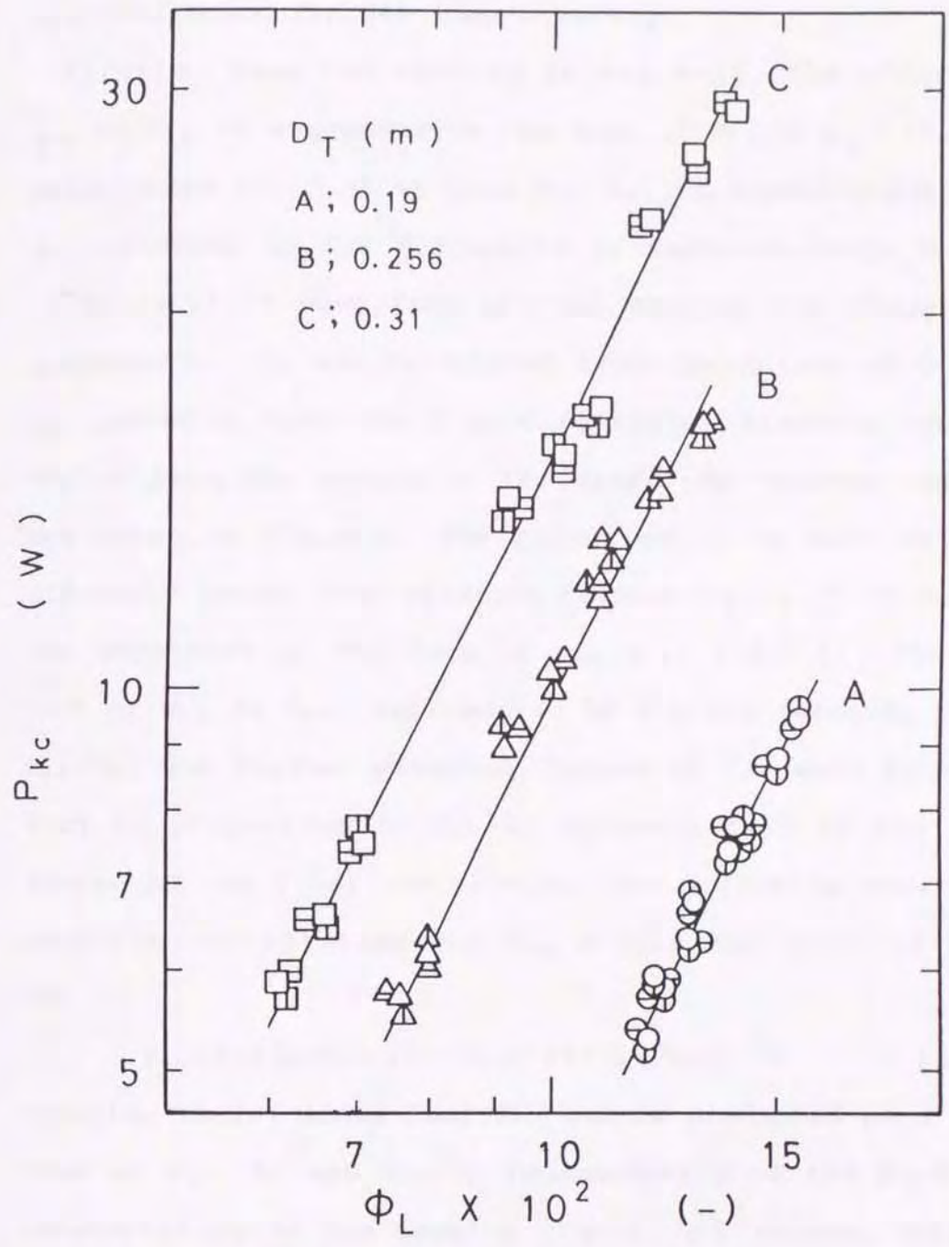

Figure 4-14. Relation between ϕ_L and P_{kc} in F-D(4) solution at H_L/H_d=0.667: D_T=0.19m; D_d(m): ○ ; 0.13, ⊖ ; 0.14, ⏀ ;0.15, D_T=0.256m; D_d(m): △ ; 0.18, ◬ ; 0.19, ⏃ ; 0.20, D_T=0.31m; D_d(m): □ ; 0.21, ⊟ ; 0.23, ◫ ; 0.24.

sult in an increase of f which causes an increase of the required power P_{kc} for foam-breaking.

Firstly, from the results in Fig.4-14, the effect of ϕ_L on P_{kc} is expressed in the form of $P_{kc} \propto \phi_L^{2.14}$, the relation of which shows that P_{kc} values depend largely on ϕ_L relating to the difficulty of foam-breaking. Values of $P_{kc}/\phi_L^{2.14}$ were then plotted against the dispersion distance l_f. l_f was calculated from the values of D_T and D_d, assuming that the liquid particles disperse tangentially from the margin of the disk. The typical results are shown in Fig.4-15. The effect of l_f as well is considerably large. The relation between $P_{kc}/\phi_L^{2.14}$ and l_f was expressed in the form of $P_{kc}/\phi_L^{2.14} l_f^{2.65}$. The effect of U_{ga} on P_{kc}, represented by the gas velocity ratio U_{ga}/U_g, was further examined. Values of P_{kc} were found to vary in proportion to U_{ga}/U_g approximately to the 1.60 power. As the final correlation, the following empirical equation was obtained for P_{kc} within 25% error (Fig.4-16).

$$P_{kc}=2.15\times10^5 \phi_L^{2.14} l_f^{2.65} (U_{ga}/U_g)^{1.60} \qquad (4\text{-}20)$$

Equation (4-20) shows that P_{kc} can be predicted as a function of ϕ_L, l_f and U_{ga}/U_g independently of the kind and concentration of the foaming liquid. ϕ_L values, related to the difficulty of foam-breaking as viewed from the changes in the foaming intensity of BCs, are estimated from Eqs.(4-4), (4-5) and (4-12) and Eqs.(4-14) - (4-19), respectively. l_f, U_g and U_{ga} values are determined from the operating conditions. It is concluded that Eq.(4-20) would be useful for the prediction of the power for foam-

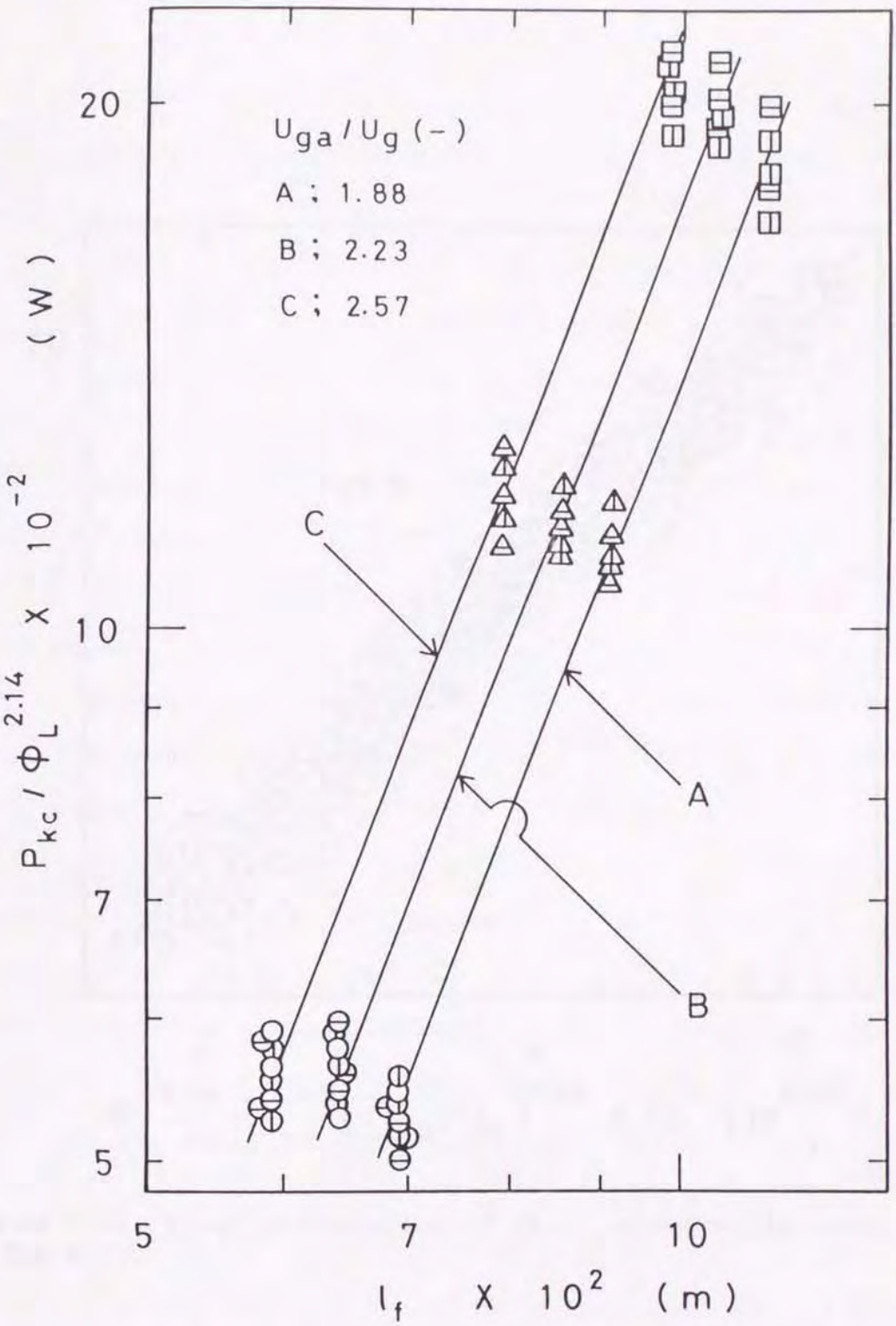

Figure 4-15. Relation between $P_{kc}/\phi_L^{2.14}$ and l_f at H_L/H_d = 0.667: F-D(4) solution; D_T(m): ○ ; 0.19, F-E(4) solution; D_T(m): ◐ ; 0.19, ◭ ; 0.256, ◫ ; 0.31, F-T(4) solution; D_T(m): ⊖ ; 0.19, △ 0.256, ⊟ ; 0.31.

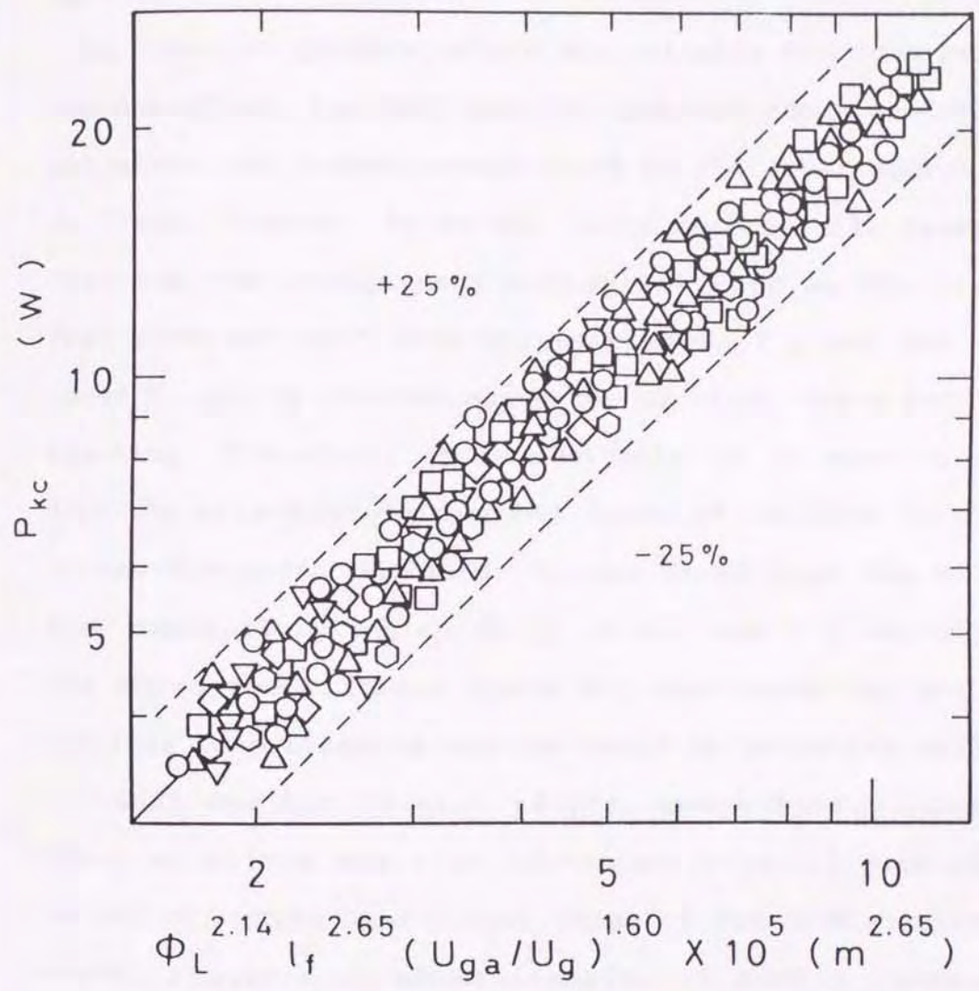

Figure 4-16. Final correlation of P_{kc} (keys are the same as in Fig.4-7).

breaking of MFRDs fitted to BCs.

4-3-5. Prediction of effective operational range of rotating-disk mechanical foam-breakers fitted to bubble columns

In order to perform safely and reliably the foam-breaking operation, the MFRD must be operated above the critical state for foam-breaking which is the lower operational limit. However, to do so, it is necessary to preestimate how the independent variables, such as the liquid feed rate per unit disk circumference, Γ, and the disk speed N, can be changed above the critical state for foam-breaking. Therefore, it is desirable to be able to predict the effective operational range of the MFRD in a BC. In the foregoing sections, it was shown that the effective upper limit region of Γ (i.e., the Γ_T region) at and above the critical state for foam-breaking and the critical foam-breaking regions could be estimated well by Eq.(4-2) and Eqs.(4-4) - (4-12), respectively. Use of these equations may also conveniently permit prediction of the effective operational range of the MFRD mentioned above. Figure 4-17 shows examples of such a range. In this figure, the oblique-lined areas enclosed with the curves drawn by Eq.(4-2) and the N_c-Γ curves drawn by Eqs.(4-4) and (4-5) and Eqs.(4-7) and (4-10) are the operational range under which foaming can be controlled effectively and economically with the MFRD. With these diagrams, it is easy to know how the operational variables such as Γ and N can be changed at the region above

the critical state for foam-breaking. A similar diagram can be shown in other foam-breaking systems by varying the operating conditions. In addition to these diagrams, the knowledge of the capacity of an electric motor for driving a rotating disk and a pump for liquid feeding onto the disk may also contribute to more accurate prediction of the effective operational range of the MFRD. Prior preparation of a diagram such as that shown in Fig. 4-17 will be useful as one of guides for preestimating the conditions when designing and operating a tower fermentor with a MFRD or when foam-breaking experiments with MFRDs are planned.

4-4. Conclusions

The design and operation of rotating-disk mechanical foam-breakers (MFRDs) fitted to bubble columns (BCs) treating various foaming liquids were studied. The foam-breaking capacity, i.e., the disk rotational speed required for foam-breaking, that changes depending on the operational conditions were first evaluated. The critical disk rotational speed N_C required for foam-breaking with MFRDs under any operating conditions of BCs treating respective kinds of foaming liquids could be predicted by Eqs.(4-4) - (4-12), respectively. The foaming behavior of BCs, which is represented by the changes in the liquid holdup in the foam, ϕ_L, that reflects the foaming intensity of BCs and is related to the difficulty of foam-breaking as a function of N_C, was then evaluated. The values of ϕ_L in BCs with MFRDs treating respective kinds

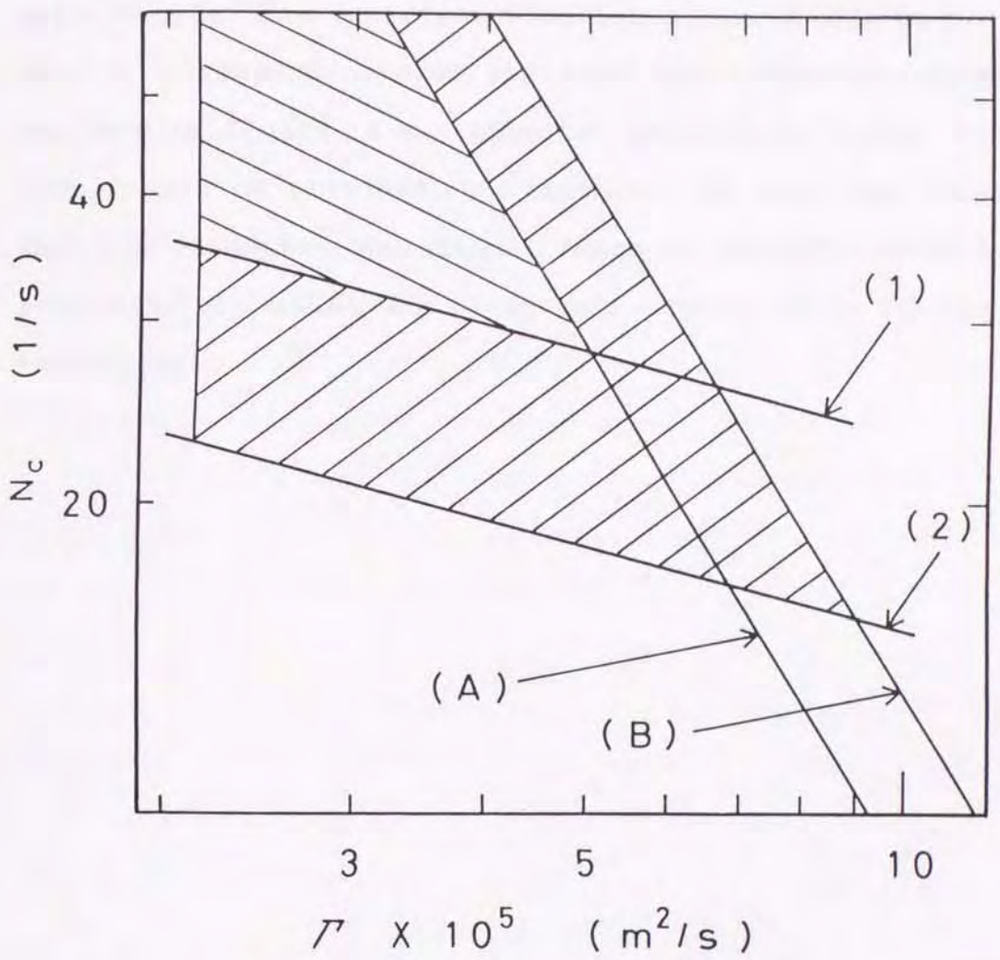

Figure 4-17. Effective operational range of MFRD fitted to BC: V_L=7.5x10^{-2}m^3: line (1); F-T(1) solution: Eq.(4-7) for D_T=0.31m, D_d=0.24m, U_g=3.0x10^{-2}m/s, line (2); F-S(1) solution: Eq.(4-10) for D_T=0.31m, D_d=0.24m, U_g=1.0x10^{-2}m/s, line (A); Eq.(4-2) for F-T(1) solution, D_d=0.24m, line (B); Eq.(4-2) for F-S(1) solution, D_d=0.24m.

of foaming liquids could be predicted by Eq.(4-12) and Eqs.(4-14) - (4-19), respectively. The level of the required foam-breaking power P_{kc} of MFRDs was also clarified in relation to the changes in ϕ_L, the dispersion distance l_f of liquid particles and the gas velocity ratio U_{ga}/U_g. The empirical equation of Eq.(4-20) to predict P_{kc} independently of the kind and concentration of the foaming liquid (i.e., physical properties of the liquids) could be obtained. Furthermore, it was also shown that the effective operational range of the MFRD could be predicted by using Eq.(4-2) and Eqs.(4-4) - (4-12), respectively.

CHAPTER 5

RELATION BETWEEN MECHANICAL FOAM-BREAKING DIFFICULTY AND FOAMING CHARACTERISTICS OF SOLUTIONS

5-1. Introduction

For a more effective design and operation of a foam-breaking apparatus, information on the nature of the foam generated or on the foaming characteristics of solutions to be treated is important. Various methods have been proposed for measuring the nature of foam (Refs.17, 20, 21, 71, 73, 115, 116). Most of these methods, however, only permit measurement under considerably restricted conditions that are different from actual gas bubbling and foaming. Therefore, direct application of these methods to a mechanical foam-breaking system under high gas throughput is difficult. This suggest the necessity for finding new parameters which reflect foaming behavior in the fermentor and the foam-breaking behavior of the foam-breaker. In chapter 3, it was shown that foaming behavior in BCs and the foam-breaking behavior of MFRDs were related to the changes in the liquid holdup in foam, ϕ_L. Values of ϕ_L in identical bubbling conditions, however, differed considerably depending on the kind and concentration of foaming liquids, although independent of physical properties. It is suggested that the differences were caused by differences in the foaming characteristics of the respective liquids. It is possible to evaluate the foaming characteristics of liquids by using a small ap-

paratus which is different from the gas-bubbling apparatus actually employed, i.e., the BC. If a relation which is independent of the kind and concentration of liquid can be found between their parameters measured as standard values and ϕ_L, it is expected that the relationship will be useful for evaluating the mechanical foam-breaking difficulty due to the liquids.

In this chapter, the liquid holdup in foamate flow, ϕ_t, rate of liquid drainage from foam, v, foam velocity u_f and foam size d_f, which reflect the foaming characteristics of liquids, are measured under constant gas-bubbling and foaming conditions using a small foaming apparatus. A parameter ϕ_f which reflects the changes in ϕ_t, v and u_f is sought. The relationship among ϕ_f, d_f and liquid holdup in foam, ϕ_L, in BCs with MFRDs is also investigated. Furthermore, a new correlation for predicting ϕ_L under any operating condition is developed on the basis of this relationship.

5-2. Experimental

Foaming apparatus The equipment shown in Fig.5-1 was designed for measuring the foaming characteristics of liquids. The diameter and length of the foaming column were 5.0×10^{-2} and 6.0×10^{-1}m, respectively. Foaming was carried out by dispersing air bubbles through a ball filter of sintered glass (diameter: 1.5×10^{-2}m, average pore size: 25μm). The superficial gas velocity and the aerated liquid height in the column were held constant at 1.0x

10^{-2}m/s and 4.0×10^{-1}m, respectively. Under these conditions the foam ascended uniformly through the head space of the column without foam coalescence or foam break-up. The aerated liquid height was adjusted by feeding liquids continuously from a reservoir to the column.

Liquid holdup in foamate flow Liquid holdup ϕ_t in foamate discharging through a tube was calculated using Eq.(5-1):

$$\phi_t = Q_L/(Q_g + Q_L) \qquad (5\text{-}1)$$

where Q_g is the volumetric gas flow rate corresponding to a superficial gas velocity of 1.0×10^{-2}m/s and Q_L is the volumetric rate of liquid in foamate flow. Mass of foamate collected in a container was first measured continuously with an auto-electric balance. The mass was then converted to volume, under the assumption that the density of the liquid collected was the same as that of the bulk liquid in the column. The time at which foamate flowing out of the tube contacted the bottom of the container was defined as t=0. The value of Q_L was determined from the slope of straight line for plots of volume against time t elapsed.

Rate of liquid drainage from foam The initial drainage rate (Ref.17) used was the rate of liquid drainage from the foam. Air sparging and liquid feeding from the reservoir were stopped simultaneously after foamate mass measurements discharged through the tube were obtained. The time at which bubbles remaining in the bulk liquid disappeared (within 3-5 seconds) was defined as zero time (t=0), and an increase in the liquid level h_l in the col-

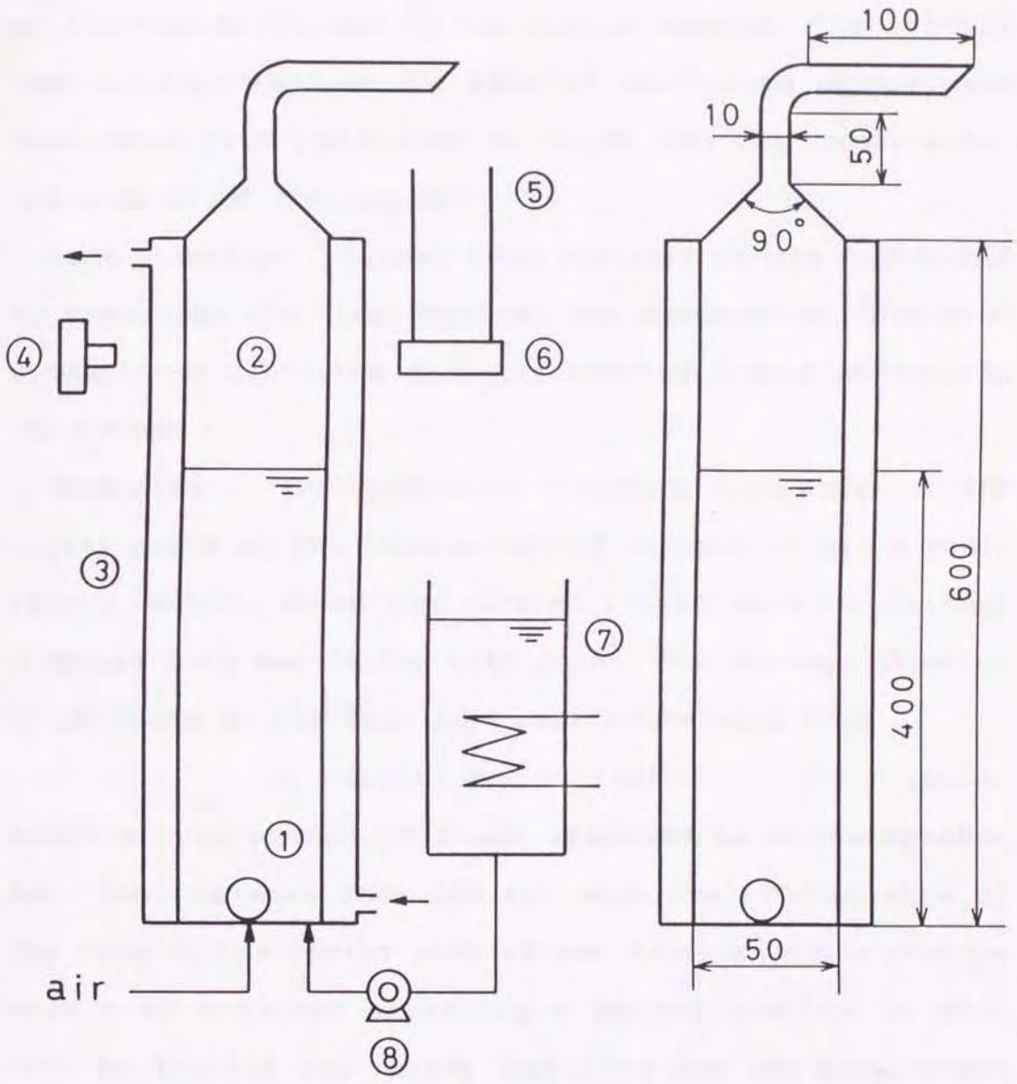

Figure 5-1. Schematic diagram of the experimental apparatus used to measure foaming characteristics of solutions: (1)ball sparger, (2)foaming column, (3)square water bath, (4)camera, (5)container, (6)auto-electric balance, (7)reservoir, and (8)peristaltic pump.

umn was measured with a reading microscope. Drainage diagrams were then obtained by plotting h_l against time elapsed, and the initial rate of increase in h_l, dh_l/dt, at t=0 was evaluated by the mirror method. The initial rate v, expressed as the rate of the volume change, was determined from the values of dh_l/dt and the cross-sectional area A_f of the column.

Foam velocity Linear foam velocity u_f was determined by measuring the time required for movement of foam over a length of 2.0×10^{-1} m from the aerated liquid surface in the column.

Foam size Photographs of the foam were taken at the midway point of the foam-ascending section, i.e., a position 1.0×10^{-1} m above the aerated liquid surface, through a square bath box filled with water. The average diameter d_f of foams in the foam layer was calculated from

$$d_f = [(\sum_{j=1}^{n} 6v_{bj}/\pi)/n]^{1/3} \qquad (5\text{-}2)$$

where n, the number of foams observed in a photograph, was taken as more than 100 for each run. Photographs of the foam at the center part of the foam-ascending section were also obtained employing a method similar to that used by Yoshida and Yamada (Ref.144) for the measurement of oil drop diameters in hydrocarbon fermentors. Foams samples were withdrawn through a tube inserted into the column and passed through a photographic section made of transparent acrylic resin, to which a camera was attached. Under the present bubbling conditions there was little difference between the d_f values of foam near the wall and those of foam at the center part.

Foaming solution As the foaming liquids, twenty four kinds of solutions shown in Table 4-1 in the preceding chapter were used at 293K.

5-3. Results and Discussion

5-3-1. Relationship between foaming characteristics of solutions and liquid holdup in foam in bubble column under foam control

To investigate whether respective foaming characteristic values measured in the foaming apparatus can be used as a measure of foam-breaking difficulty, the values were compared with those of ϕ_L observed in BCs with MFRDs in chapter 4.

5-3-1-1. Relationship between liquid holdup in foamate discharging through tube in small foaming apparatus and liquid holdup in foam in bubble column under mechanical foam comtrol

An increase of the liquid volume v_f in the container with time t elapsed was measured for each foaming liquid. Figure 5-2 shows the typical results of v_f plotted against t. From slopes of straight lines as shown in the figure and A_f of the column, Q_L was obtained, and the liquid holdup in foamate flow discharging through the tube in the small foaming apparatus, ϕ_t, was calculated according to Eq.(5-1). In preceding chapters, the liquid holdup in foam in the BC under foam control, ϕ_L, has been shown to be related to the difficulty of mechanical

foam-breaking. If ϕ_t can be applied as measure of mechanical foam-breaking to a gas-bubbling system using the BC, a definite proportional relation may be found between the increase of ϕ_L and ϕ_t. Figure 5-3 shows the plot of ϕ_L against ϕ_t. The rate of increase in ϕ_L with an increase of ϕ_t differed considerably depending on the kind of foaming liquid. This result indicates that ϕ_L can not simply be correlated by ϕ_t only.

5-3-1-2. Relationship between rate of liquid drainage from foam and liquid holdup in foam in bubble column under mechanical foam control

The typical results of increase in the liquid level h_l measured are shown in Fig.5-4, in which h_l is plotted against time t. h_l rapidly increased with the initial increase in t, but rates of their increase tended to reduce gradually as the time proceeds. The relationship between the liquid holdup in foam in the BC, ϕ_L, and the rate of liquid drainage from foam, v, obtained from the slope of the tangent line which makes contact with the drainage curve, is shown in Fig.5-5. It was difficult to express the relationship using a single correlation due to different rates of increase in ϕ_L with an increase in v.

5-3-1-3. Relationship between foam velocity and liquid holdup in foam in bubble column under mechanical foam control

Figure 5-6 presents a plot of the liquid holdup in foam in the BC, ϕ_L, against the foam velocity u_f. Although on

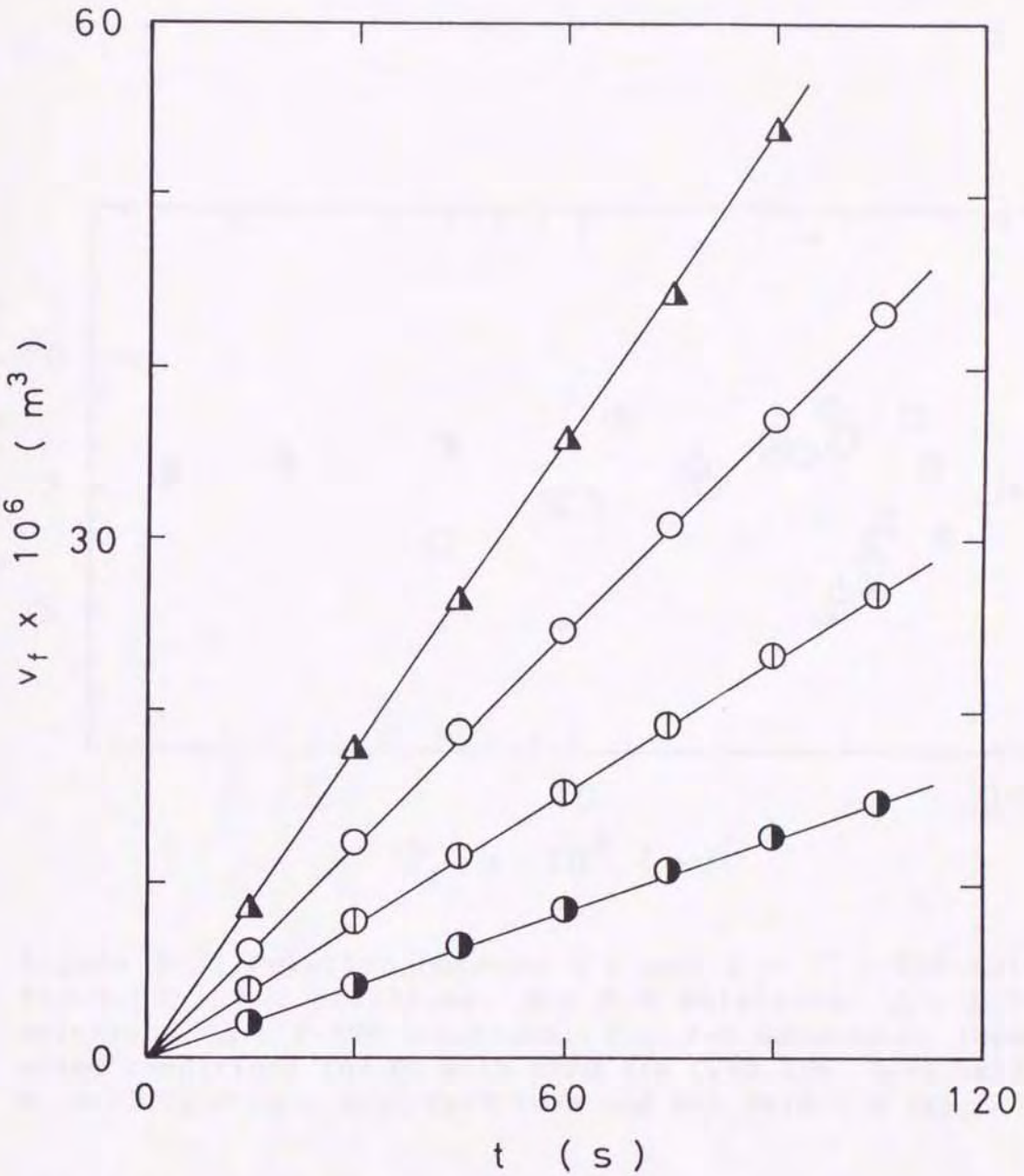

Figure 5-2. Relation between v_f and t: ○ ; F-D(4) solution, ◍ ; F-S(2) solution, ◑ ; F-E(2) solution, △ ; F-T60(4) solution.

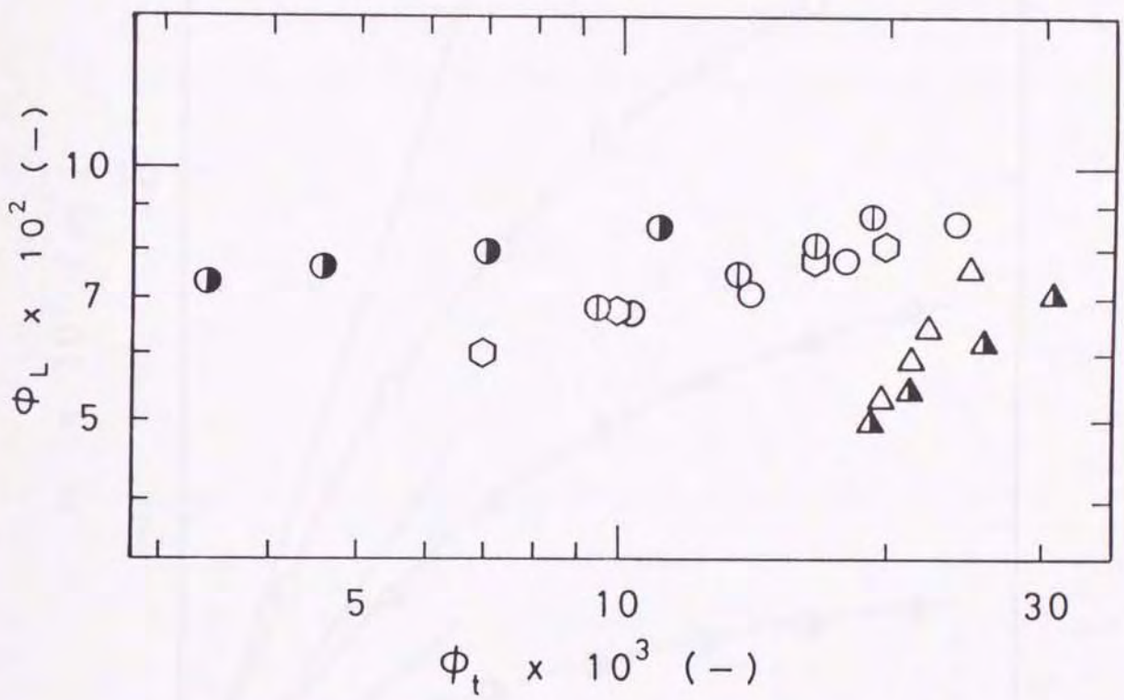

Figure 5-3. Relation between ϕ_t and ϕ_L: ○ ; F-D solutions, ◫ ; F-S solutions. ◑ ; F-E solutions, △ ; F-T40 solutions, ▲ ; F-T60 solutions, ⬡ ; F-T solutions. (operating conditions for BC with MFRD are D_T=0.19m, D_d=1.5x10^{-1} m, V_L=1.7x10^{-2}m^3, U_g=1.0x10^{-2}m/s and W=1.0x10^{-5} m^3/s).

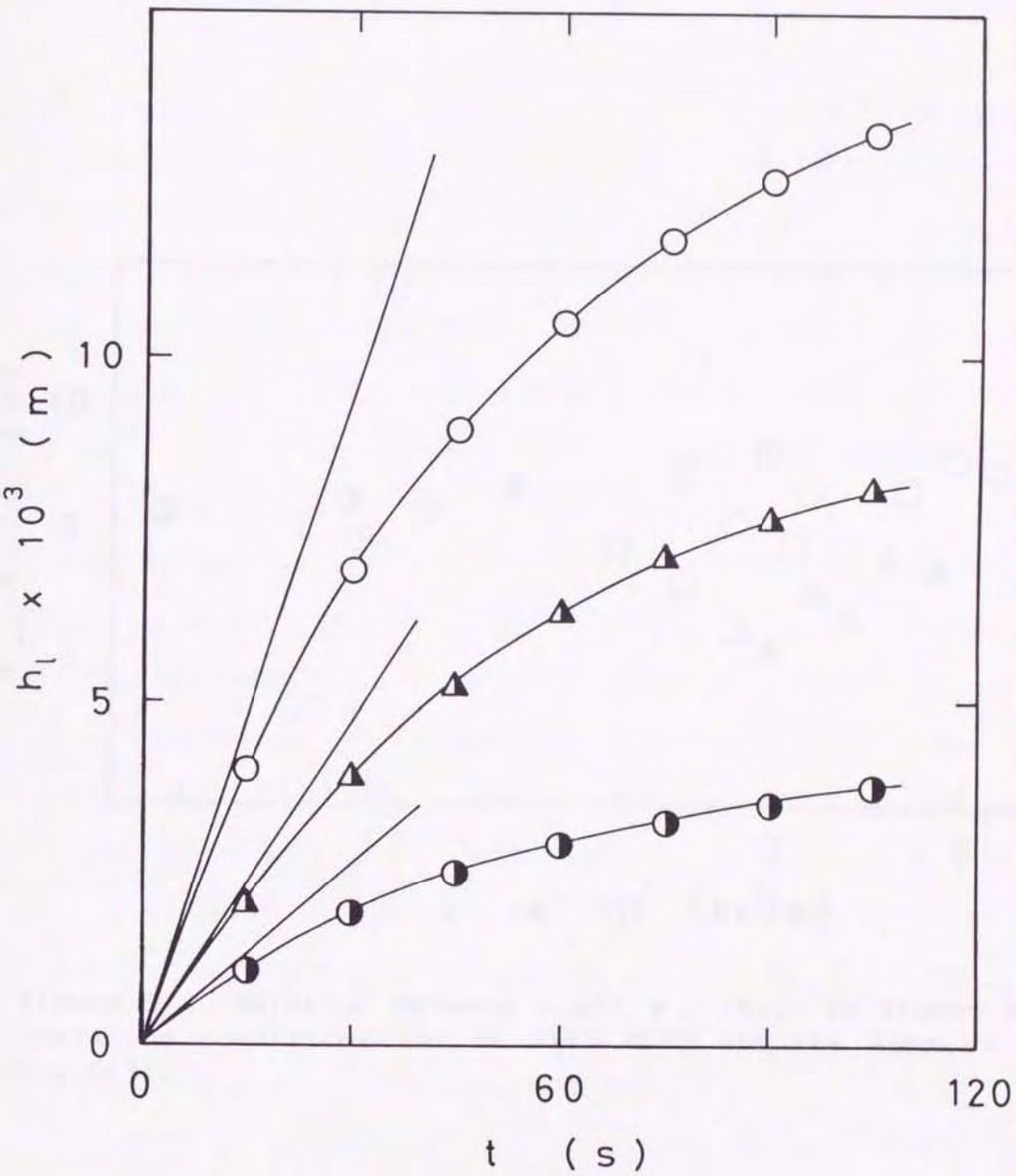

Figure 5-4. Relation between h_l and t: ○ ; F-D(4) solution, ◑ ; F-E(3) solution, ▲ ; F-T60(2) solution.

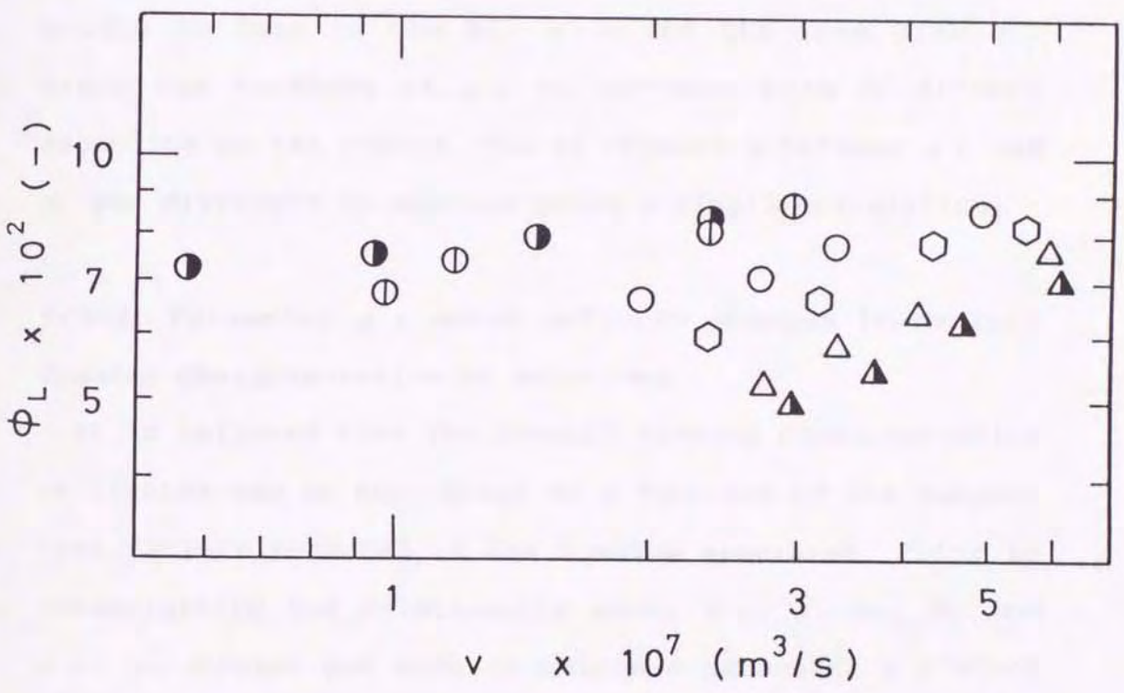

Figure 5-5. Relation between v and ϕ_L (keys in figure and operating conditions for BC with MFRD are the same as in Fig.5-3).

the whole there is a common tendency for ϕ_L to increase with an increase in u_f, it is difficult to obtain a simple correlation, due to different rates of increase in ϕ_L with u_f among the various kinds of foaming liquids.

5-3-1-4. Relationship between foam size and liquid holdup in foam in bubble column under mechanical foam control

Figure 5-7 shows the relationship between the liquid holdup in foam in the BC, ϕ_L, and the foam size d_f. Since the tendency of ϕ_L to decrease with d_f differs depending on the liquid, the relationship between ϕ_L and d_f was difficult to express using a single correlation.

5-3-2. Parameter ϕ_f which reflects changes in overall foaming characteristics of solutions

It is believed that the overall foaming characteristics of liquids may be determined as a function of the respective factors measured in the foaming apparatus. Prior to investigating the relationship among ϕ_t, v, u_f, d_f and ϕ_L, an attempt was made to obtain a parameter ϕ_f which includes the factors ϕ_t, v and u_f.

5-3-2-1. Derivation of new parameter ϕ_f

Figure 5-8 presents a model for foam flow at the top part of the foaming column, i.e., at a level 2.0×10^{-1} m above the aerated liquid surface. Assuming that the size of foams ascending through the head space of the column is uniform and that the flow type is plug flow, the following relation is derived under steady-state conditions:

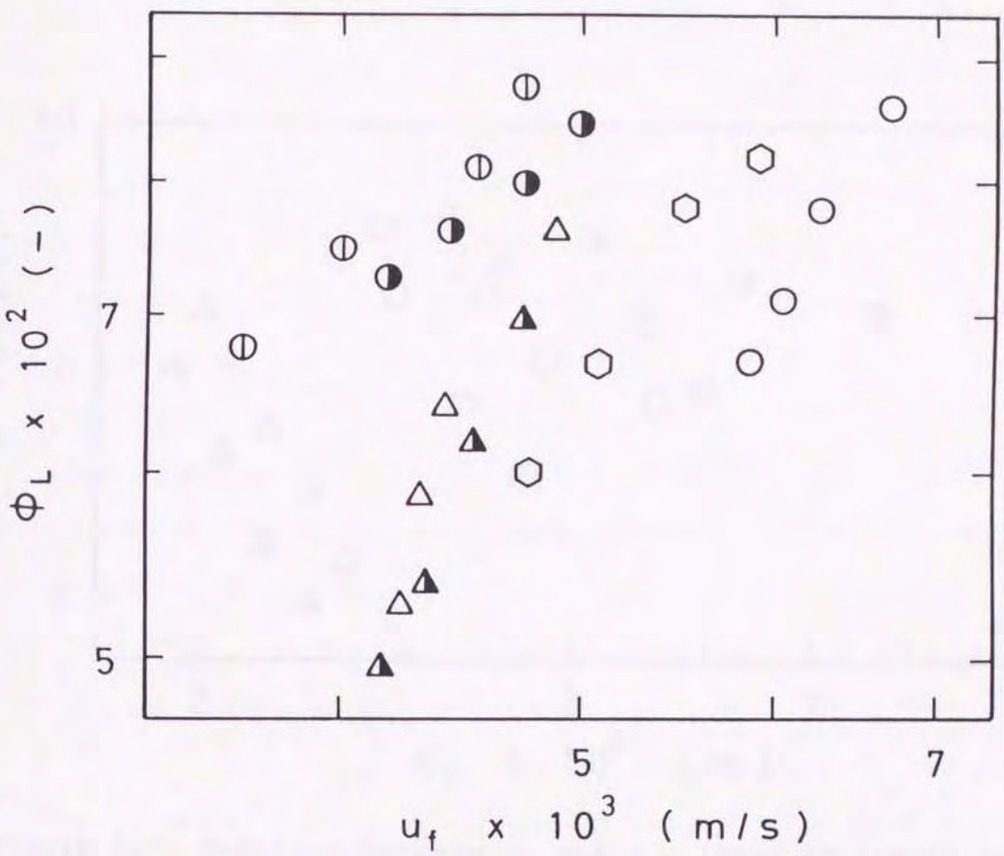

Figure 5-6. Relation between u_f and ϕ_L (keys in figure and operating conditions for BC with MFRD are the same as in Fig.5-3).

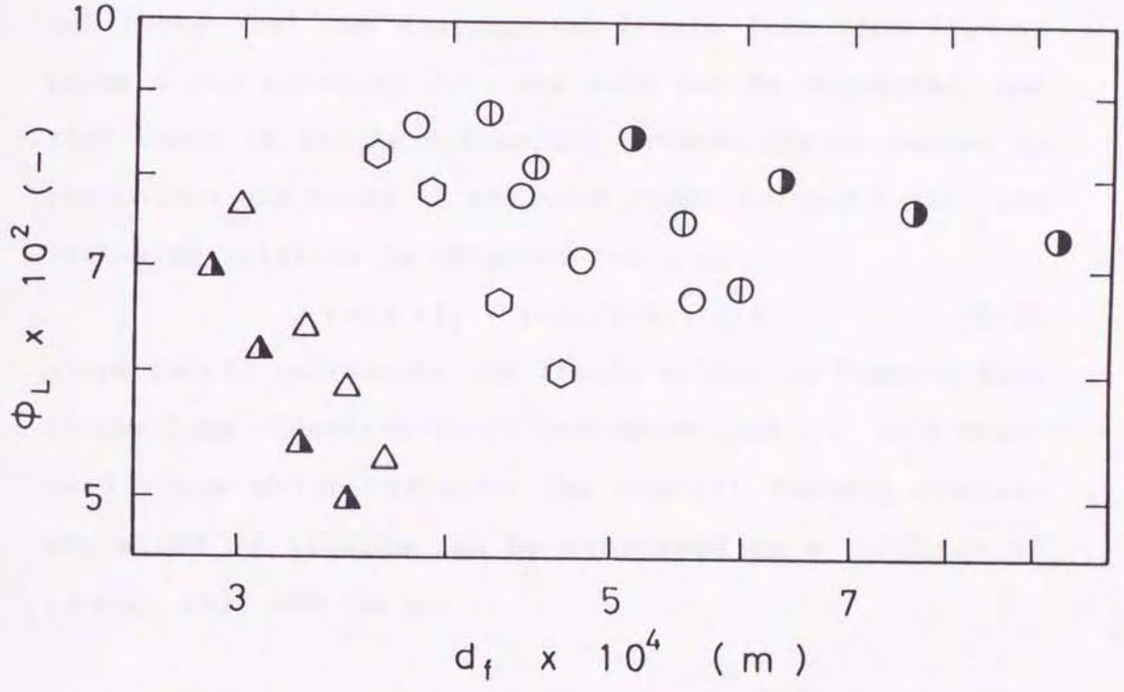

Figure 5-7. Relation between d_f and ϕ_L (keys in figure and operating conditions for BC with MFRD are the same as in Fig.5-3).

$$(\phi_f)_i (u_f)_i A_f = \phi_f (u_f)_i A_f - (v)_i \qquad (5\text{-}3)$$

where ϕ_f represents the liquid holdup in foam entering the plane i of a height of 2.0×10^{-1}m from the aerated liquid surface, $(\phi_f)_i$, $(u_f)_i$ and $(v)_i$ represent the liquid holdup in foam leaving the plane i, foam velocity and the rate of liquid drainage from the foam at its plane, respectively, and A_f is the cross-sectional area of the foaming column. Taking into consideration the experimental facts that the drainage of liquid from foam leaving plane i and entering into the tube can be neglected, and that there is little difference between the d_f values in the column and those in the tube (Figs.5-9 and 5-10), the following relation is obtained for ϕ_f:

$$\phi_f = (\phi_f)_t + (v)_i / [(u_f)_i A_f] \qquad (5\text{-}4)$$

where $(\phi_f)_t$ represents the liquid holdup in foamate flow in the tube. Equation (5-4) indicates that ϕ_f as a standard value which reflects the overall foaming characteristics of liquids can be expressed as a function of $(\phi_f)_t$, $(v)_i$ and $(u_f)_i$.

5-3-2-2. Relationship among parameter ϕ_f, foam size and liquid holdup in foam in bubble columns

For calculations of ϕ_f the values of ϕ_t, v and u_f shown in Figs.5-3, 5-5 and 5-6 were used as $(\phi_f)_t$, $(v)_i$ and $(u_f)_i$ in Eq.(5-4). The values of ϕ_f for the respective foaming liquids were then determined by Eq.(5-4). When describing the changes between ϕ_f and ϕ_L, the ratio ϕ_L/ϕ_f (ϕ_L to ϕ_f as the standard value), was employed. The relationship between ϕ_L/ϕ_f and d_f was

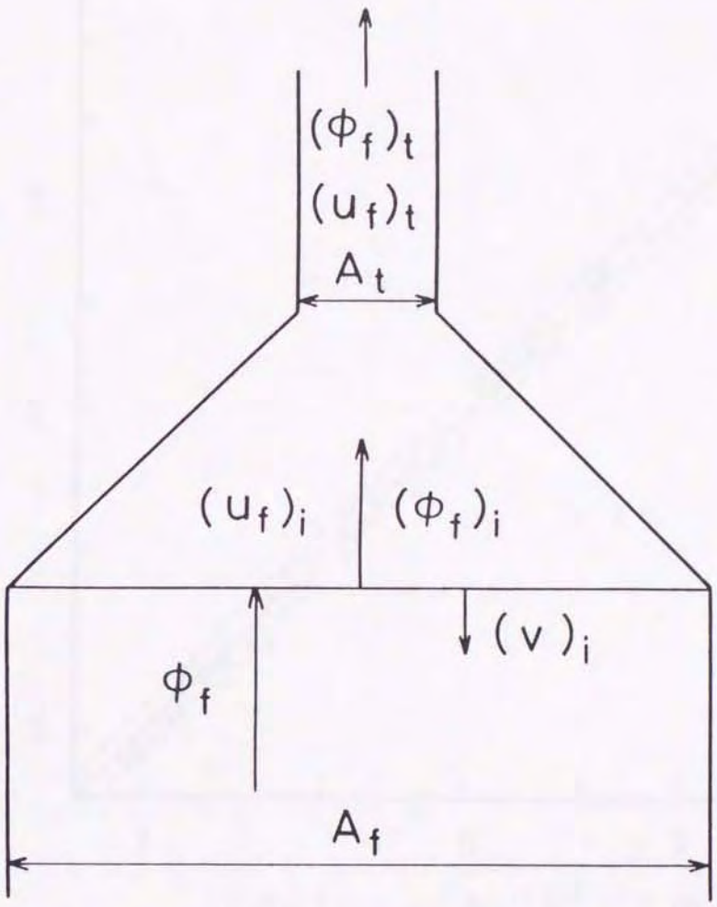

Figure 5-8. Foam flow model.

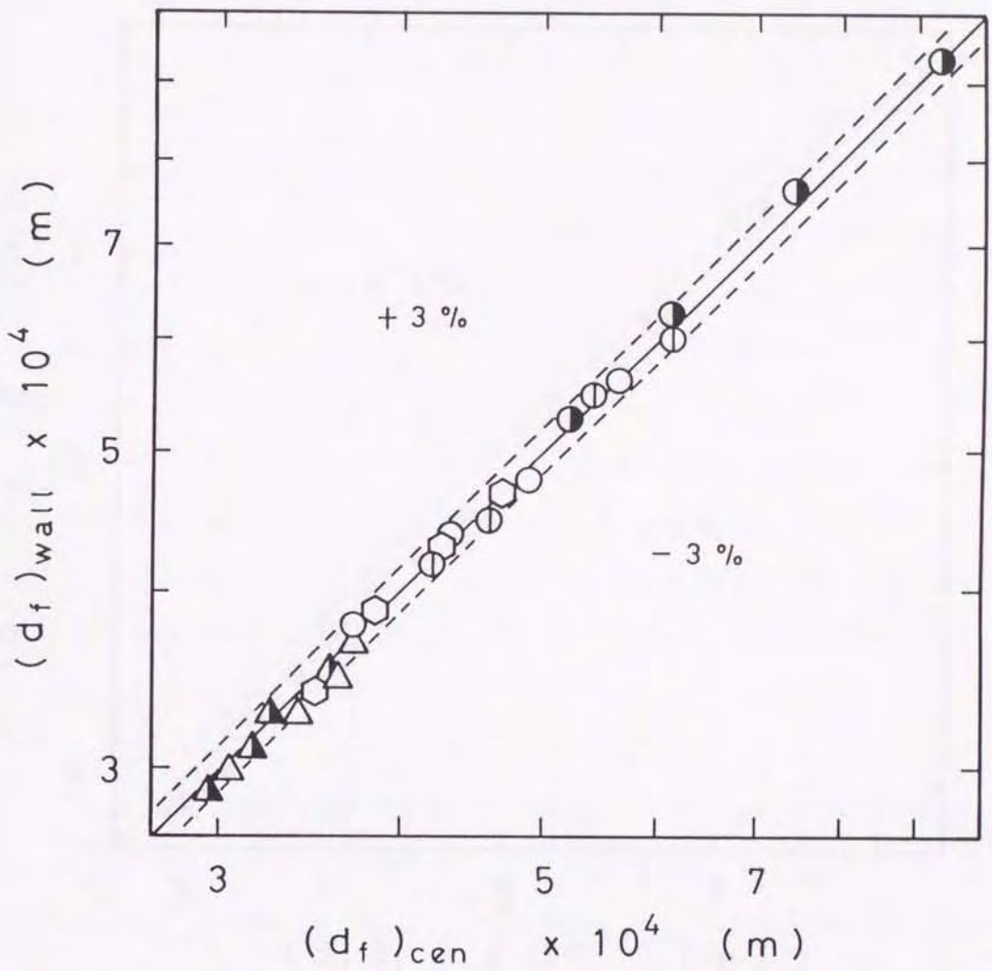

Figure 5-9. Comparison of d_f values of foam near wall in foaming column and those of foam at the center part in foaming column (keys are the same as in Fig.5-3).

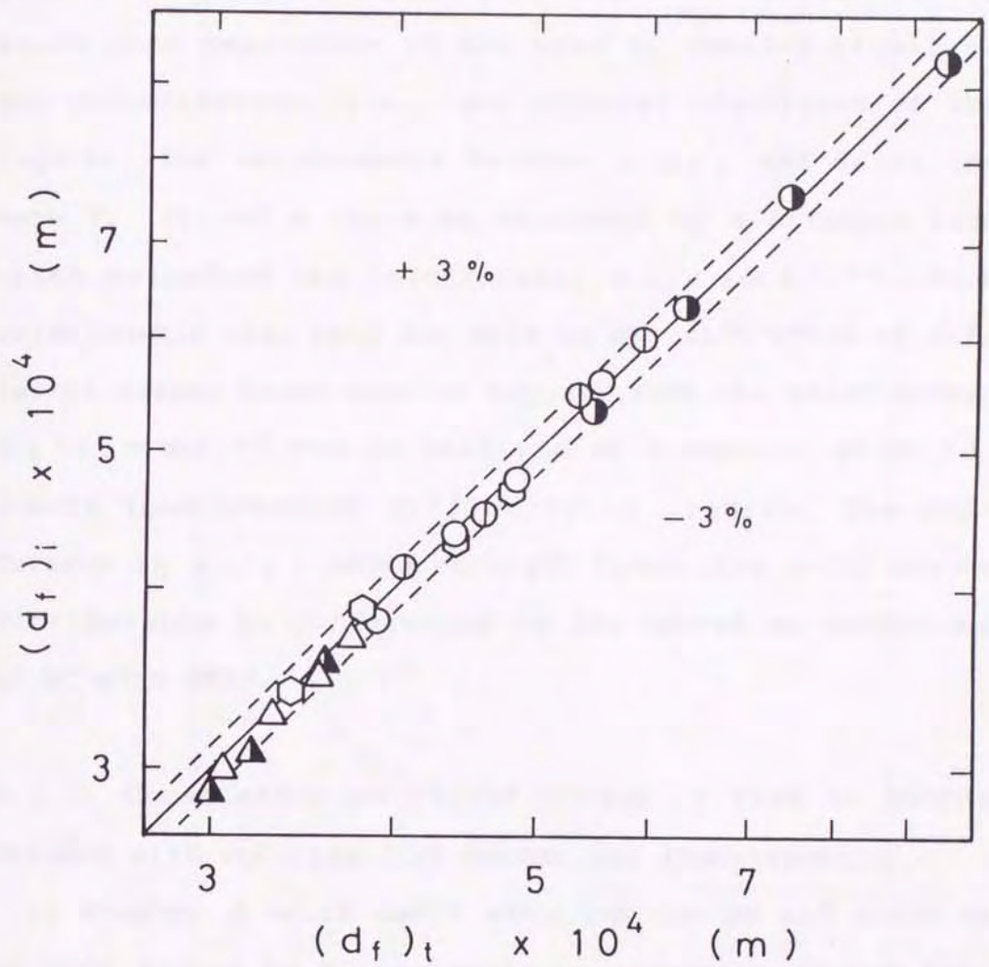

Figure 5-10. Comparison of d_f values of foam in tube and those of foam at plane i in foaming column (keys are the same as in Fig.5-3).

then investigated. A plot of ϕ_L/ϕ_f vs. d_f is shown in Fig.5-11 for ϕ_L data in BC with MFRD (0.19m in column diameter D_T and 0.15m in disk diameter D_d) when the working liquid volume (V_L), superficial gas velocity (U_g) and liquid feed rate (W) onto the disk were varied. It was found that regardless of the kind of foaming liquid or the concentration, i.e., the physical properties of the liquids, the relationship between ϕ_L/ϕ_f and d_f at the same V_L, U_g and W could be expressed by a straight line which satisfied the relationship $\phi_L/\phi_f \propto d_f^{1.83}$. This relationship also held for data in BCs with MFRDs of different sizes. These results suggest that the relationship $\phi_L/\phi_f \propto d_f^{1.83}$ can be utilized as a measure which reflects foam-breaking difficulty in liquids. The difference in ϕ_L/ϕ_f among straight lines (Fig.5-11) may be attributable to differences in the operating conditions of BC with MFRD.

5-3-3. Correlation of liquid holdup in foam in bubble columns with rotating-disk mechanical foam-breakers

In chapter 4 which dealt with the design and scale-up of MFRD fitted to BC, an empirical equation of the following type to predict ϕ_L was obtained.

$$\phi_L = \alpha\ 10^{\mathrm{func.}(h_f/U_g)} \cdot U_L^{0.24} C^{\beta} \qquad (5\text{-}5)$$

where α and β are empirical constants which changed according to the kind of liquid. On the basis of the fact that at the same operating conditions of BC with MFRD the relation $\phi_L/\phi_f \propto d_f^{1.83}$ is maintained regardless of the kind of foaming liquid, it is postulated that the effect

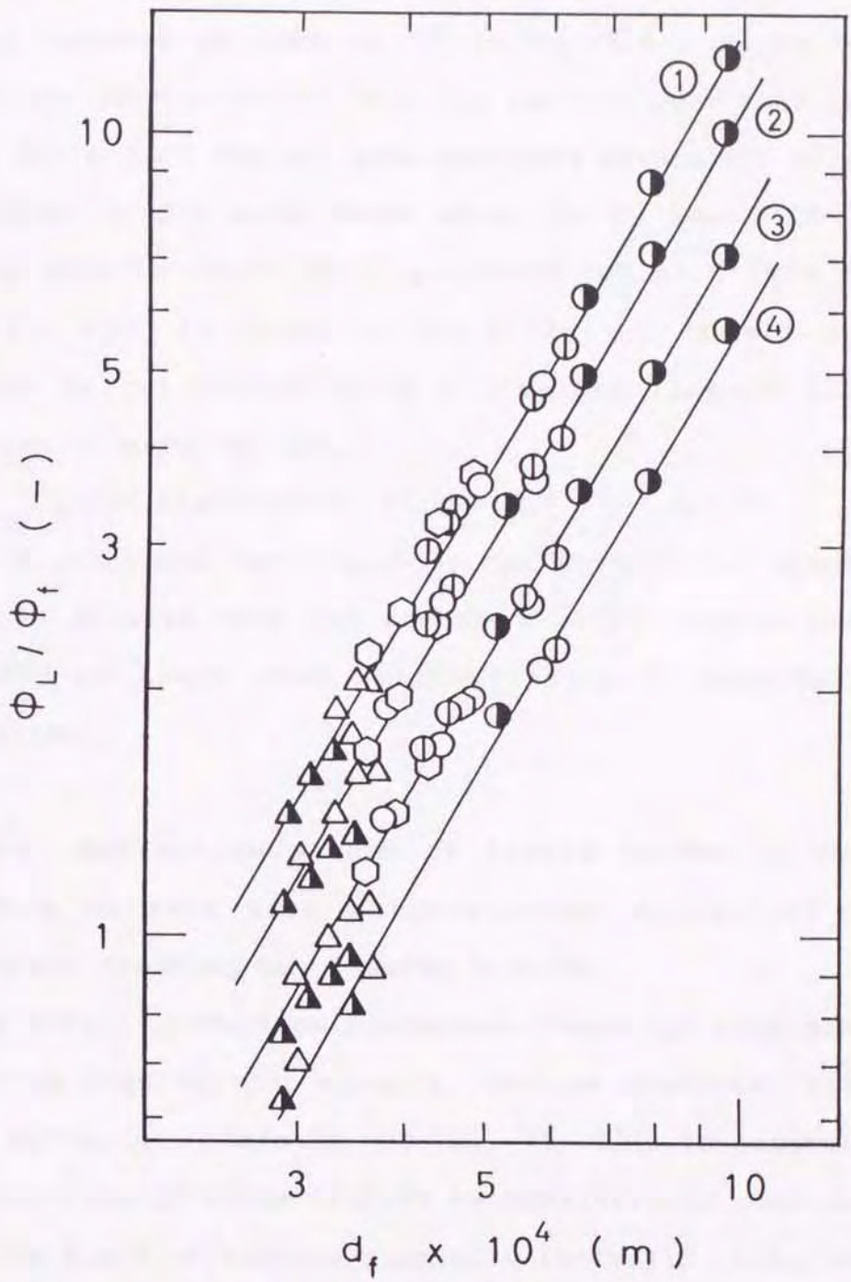

Figure 5-11. Relation between ϕ_L / ϕ_f and d_f (keys are the same as in Fig.5-3): Lines; (1) $V_L = 1.7 \times 10^{-2}$ m^3, $U_g = 5.0 \times 10^{-2}$ m/s, $W = 2.0 \times 10^{-5}$ m^3/s, (2) $V_L = 1.7 \times 10^{-2}$ m^3, $U_g = 4.0 \times 10^{-2}$ m/s, $W = 1.0 \times 10^{-5}$ m^3/s, (3) $V_L = 1.7 \times 10^{-2}$ m^3, $U_g = 1.0 \times 10^{-2}$ m/s, $W = 1.0 \times 10^{-5}$ m^3/s, (4) $V_L = 1.3 \times 10^{-2}$ m^3, $U_g = 1.0 \times 10^{-2}$ m/s, $W = 1.0 \times 10^{-5}$ m^3/s.

of the liquid on ϕ_L may be expressed in terms of $\phi_f d_f^{1.83}$, in other words, that the term $\phi_f d_f^{1.83}$ may be used instead of that of C^{β} in Eq.(5-5). Plots of ϕ_L against $10^{func.(h_f/U_g)} U_L^{0.24} \phi_f d_f^{1.83}$ were then carried out for all of the ϕ_L data observed within the effective W range in BCs with MFRDs when the D_T was 0.19-0.31m, $V_L = 1.3 \times 10^{-2} - 7.5 \times 10^{-2} m^3$, $U_g = 1.0 \times 10^{-2} - 5.0 \times 10^{-2}$ m/s and D_d 0.13-0.24m. As shown in Fig.5-12, ϕ_L in all systems could be correlated using a straight line as follows, within an error of 25%.

$$\phi_L = 7.81 \times 10^6 \, 10^{func.(h_f/U_g)} U_L^{0.24} \phi_f d_f^{1.83} \qquad (5\text{-}6)$$

It is concluded that Eq.(5-6) can be used for predicting ϕ_L in BC with MFRD for various foaming liquids independently of their kind, concentration or physical properties.

5-3-4. Estimation method of liquid holdup in foam in bubble columns with rotating-disk mechanical foam-breakers treating any foaming liquids

In actual production processes, there are many kinds of foaming liquids, for example, various mixtures, biological media, etc (Refs.17, 20, 21, 71, 73). In general, the composition of these liquids is considerably complicated. In the field of surface chemistry (Refs.115, 116), it has been suggested that of physical properties of the liquids the surface tension σ is the most important factor for the foam formation. On the other hand, It has confirmed in the previous chapter that the liquid holdup in foam, ϕ_L, can be used as a substantial measure of the dynamic

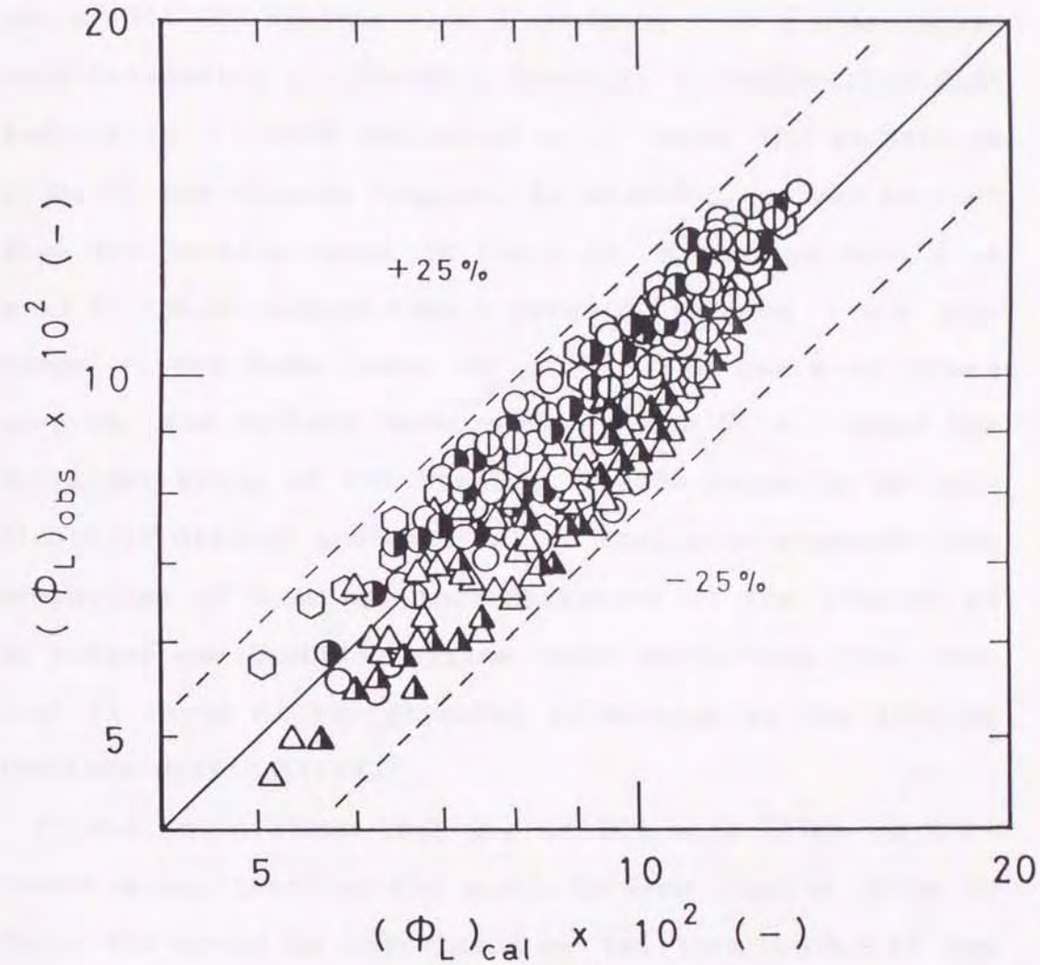

Figure 5-12. Comparison of observed and calculated values of ϕ_L (keys are the same as in Fig.5-3).

foaming capacity of the liquids in the BC with the MFRD. If σ can be applied as a measure of mechanical foam-breaking to the BC, a definite relation may be found between the values of ϕ_L and σ. Figure 5-13 shows a plot of ϕ_L against σ of the foaming liquid tested. On the whole, all the systems have a tendency that ϕ_L decreases with increasing σ. However, there is a considerable difference in ϕ_L with variation of σ among the respective kinds of the foaming liquids. In addition, as can be seen from the results shown in Fig.5-13, attention should be paid to the situation that a large difference in ϕ_L produces at the same level of σ. On the basis of these results, the surface tension dependency of ϕ_L among the different kinds of the foaming liquids seems to be difficult to discuss systematically. That also suggests that evaluation of foaming characteristics of the liquids in an actual gas-bubbling system under mechanical foam control in terms of the physical properties of the liquids involves difficulties.

It was shown above that ϕ_L in BCs with MFRDs of different sizes treating the model foaming liquids shown in Table 4-1 could be correlated by the term $\phi_f d_f^{1.83}$ and the operating conditions such as D_T, V_L, U_g, D_d, etc. According to those results, it should be noted that Eq.(5-6) for ϕ_L involves the term $\phi_f d_f^{1.83}$ determined based on the measurement results in a small apparatus different from gas-bubbling apparatus to be employed actually but the physical properties of the foaming liquids are not involved. The values of ϕ_t, v and u_f required for the

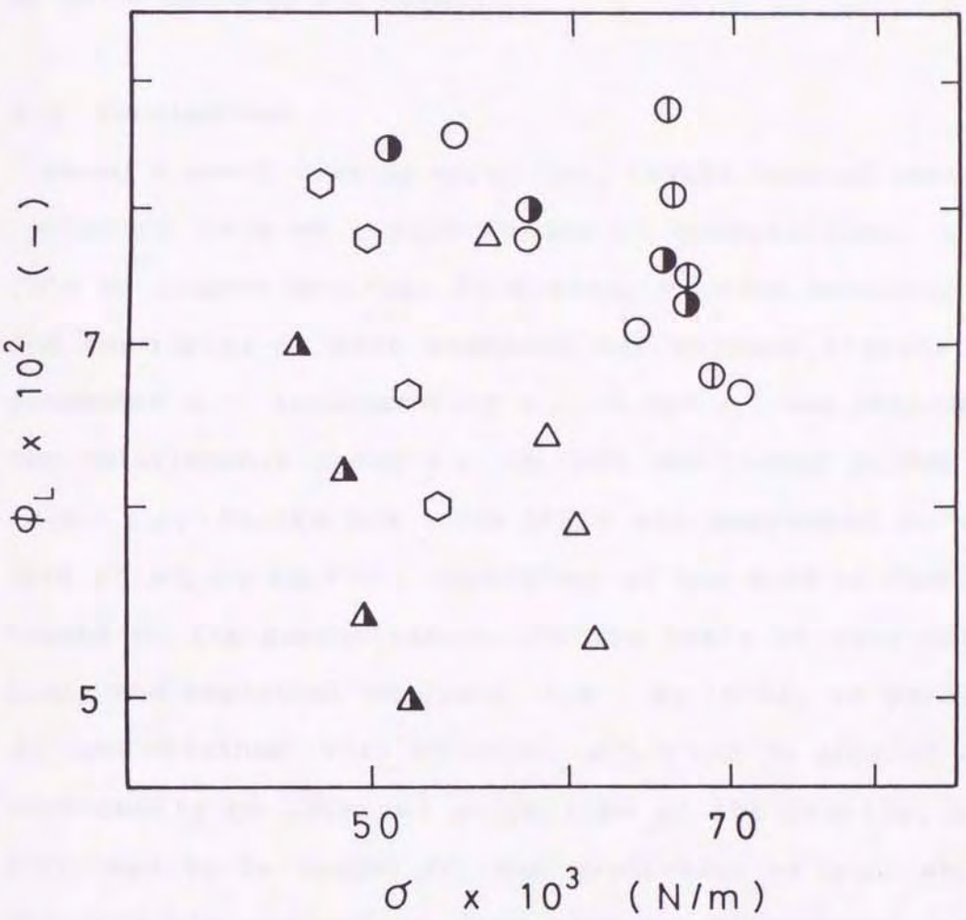

Figure 5-13. Relation between σ and ϕ_L (keys are the same as in Fig.5-3).

evaluation of ϕ_f and those of d_f can be measured for any foaming liquids, by using the present foaming apparatus. Thus, it is expected that ϕ_L under any operating conditions of the BC with the MFRD may be estimated beforehand from Eq.(5-6), provided that the values of $\phi_f d_f^{1.83}$ determined are used and the operating conditions of the BC with the MFRD are given.

5-4. Conclusions

Using a small foaming apparatus, liquid foaming characteristics such as liquid holdup in foamate flow, ϕ_t, rate of liquid drainage from foam, v, foam velocity u_f and foam size d_f were examined for various liquids. A parameter ϕ_f, incorporating ϕ_t, v and u_f, was obtained. The relationship among ϕ_f, d_f and the liquid holdup in foam, ϕ_L, in the BCs with MFRDs was expressed in the form of $\phi_L \propto \phi_f d_f^{1.83}$, regardless of the kind of foaming liquid or its concentration. On the basis of this relation, the empirical equation, i.e., Eq.(5-6), to predict ϕ_L was obtained. This equation, which can be applied independently of physical properties of the liquids, was confirmed to be useful for the prediction of ϕ_L, which reflects the mechanical foam-breaking difficulty, under any operating conditions of the BCs with the MFRDs treating various foaming liquids.

CHAPTER 6

RELATION BETWEEN CRITICAL DISK ROTATIONAL SPEED FOR FORM-BREAKING OF ROTATING-DISK MECHANICAL FOAM-BREAKERS AND FOAMING CHARACTERISTICS OF SOLUTIONS

6-1. Introduction

Although a number of methods are available for mechanical foam control, mechanical foam-breakers with rotating installations (Refs.24, 28, 51, 56, 68, 104, 119, 135, 145) are the most common among the mechanical methods. All known foam-breakers, available on the market, work on this principle. Some published reports (Refs.51, 56, 104, 145) show that a certain critical rotational speed is necessary for breaking the foam by rotating installations. Various types of empirical correlations for predicting the critical (minimum) rotational speed have been proposed so far (Refs.51, 56, 145). Most of these existing equations, however, are those obtained on the basis of the experiments where only a restricted range of foaming liquids was used. Foaming liquids actually used in production processes are multifariousness. Performance of foam-breakers is also known to differ considerably depending on the kind of foaming liquid to be treated. Taking into the consideration these facts, it can be said that the existing equations which cannot be applied to various foaming systems are of no value for practical usage.

In chapter 4, the foam-breaking characteristics of ro-

tating-disk mechanical foam-breakers (MFRDs) fitted to BCs treating various liquids were investigated from the changes in the required critical disk rotational speed (N_c) as a measure related to difficulty or ease of foam-breaking operation. Depending on the kind of foaming liquid, however, significant differences in the value of N_c were observed at identical gas bubbling conditions. This is considered to be mainly due to difference in foaming characteristics of respective liquids. In order to obtain empirical equation to predict N_c of MFRDs fitted to BCs treating any foaming liquids, independently of their kind, concentration or physical properties, further studies are necessary on the relation between the changes in N_c and those in foaming characteristics of the liquids to be treated. In this chapter, for BCs treating various foaming liquids, the relation between N_c of MFRDs and the foaming characteristics of the liquids, i.e., the foaming characteristic term $\phi_f d_f^{1.83}$ of respective liquid discussed in chapter 5, is investigated and a new correlation for predicting N_c is also sought.

6-2. Experimental

As the N_c data, those observed within the effective Γ_T range, which could be predicted by Eq.(6-1) (Ref.95), in BCs with MFRDs when the D_T was 0.19-0.31m, V_L 1.3×10^{-2}-7.5×10^{-2} m^3, U_g 1.0×10^{-2}-5.0×10^{-2} m/s and D_d 0.13-0.24m were employed.

$$N_\Gamma^+ = 0.141(Re)^{2/3}(We)^{-0.883} \qquad (6\text{-}1)$$

As the value of the liquid holdup in foamate flow, ϕ_f,

and the foam size d_f, those obtained for respective liquids in chapter 5 were employed. The kind of liquid was the same as that in the preceding chapter.

6-3. Results and Discussion

6-3-1. Prediction of critical disk rotational speed for foam-breaking based on changes in foaming characteristics of solutions

In chapter 4 which dealt with the design and operation of MFRDs fitted to BCs treating various foaming liquids, an empirical equation of the following type to predict N_c in foam-breaking regions was obtained:

$$N_c = A\Gamma^{-0.27} 10^{func.(h_f/U_g)} (D_T/D_d)^{0.90} C^B \qquad (6\text{-}2)$$

where A and B are empirical constants which depend on the kind of foaming liquid. Func.(h_f/U_g) in Eq.(6-2) was expressed by the form of Eq.(6-3), independently of the kind of foaming liquid.

$$func.(h_f/U_g) = 0.511 + 0.062 \log(h_f/U_g) - 0.144[\log(h_f/U_g)]^2 \qquad (6\text{-}3)$$

The value of h_f, which also was almost independent of the kind of foaming liquid, could be predicted by Eqs.(6-4) and (6-5).

$$h_f/D_T = U_g^{-2.54} (H_L/H_d)^{5.76} 10^{func.(H_L/H_d)} \qquad (6\text{-}4)$$

$$func.(H_L/H_d) = -2.25 - 15.30 \log(H_L/H_d) - 22.65[\log(H_L/H_d)]^2 \qquad (6\text{-}5)$$

Figure 6-1 shows the typical results of N_c plotted against the concentration C of foaming liquids. It is found that the value of N_c differs considerably depending

on the kind of foaming liquid. This result implies that Eq.(6-2) is useful for predicting N_c when the same foaming liquids as used in chapter 4 are used, but application to other liquids is difficult. The differences in N_c as seen in Fig.6-1 are considered to be mainly due to those of foaming property of respective liquids which are related to foam-breaking difficulty. Thus, a relation which is independent of the kind and concentration of liquid is required instead of C^B in Eq.(6-2). Then, this relationship will be useful for evaluating N_c in the foam control system treating any kinds of foaming liquids.

In chapter 5, using a small foaming apparatus, liquid foaming characteristics such as liquid holdup in foamate flow, ϕ_f, and foam size d_f were examined for various liquids. From the investigation of the relationship among ϕ_f, d_f and the liquid holdup in foam, ϕ_L, in BCs under mechanical foam control, it was suggested that the term $\phi_f d_f^{1.83}$ reflects the mechanical foam-breaking difficulty, i.e., the difference in ϕ_L among liquids. On the other hand, concerning the relationship between ϕ_L and N_c, it can be shown from the results in chapter 4 that the changes in ϕ_L correspond well to those in N_c, indicating that values of N_c tend to be high when the foam with larger ϕ_L is formed, as demonstrated in Fig.6-2. Considering this and the fact that the term $\phi_f d_f^{1.83}$ was useful for evaluation of the differences of ϕ_L among liquids, it is postulated that the term $\phi_f d_f^{1.83}$ may also be used to correlate N_c values obtained for BCs with MFRDs treating various liquids. In other words, the term

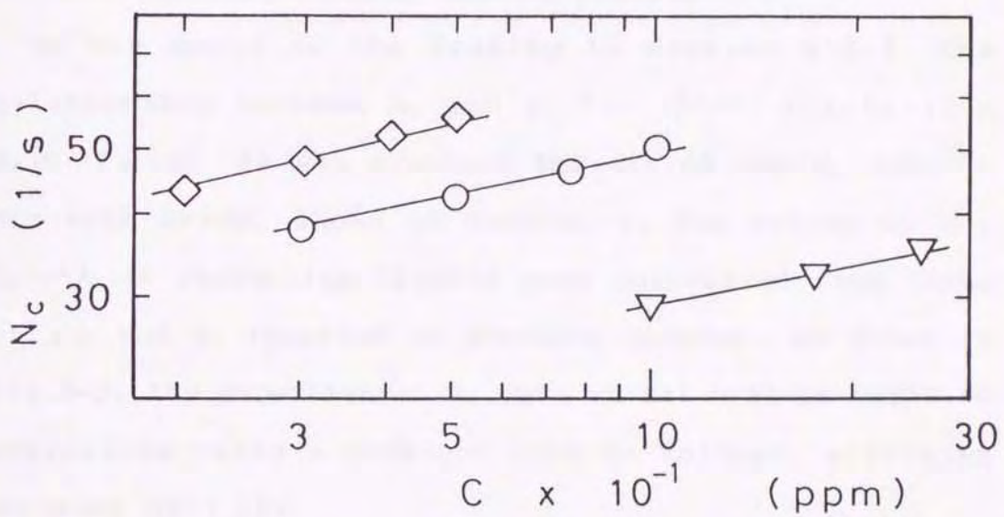

Figure 6-1. Relation between N_c and C: ○ ; F-D solutions, ▽ ; F-T60 solutions, ◇ ; F-S solutions. (operating conditions are D_T=0.19m, H_d=4.737D_T, D_d=0.789D_T, H_L=0.667H_d, U_g=3.0x10^{-2}m/s, and Γ =2.122x10^{-5}m^2/s).

$\phi_f d_f^{1.83}$ may be used instead of C^B in Eq.(6-2). This also means that N_c values may be predicted by the following form.

$$N_c = C\Gamma^{-0.27} 10^{func.(h_f/U_g)} (D_T/D_d)^{0.90} \phi_f d_f^{1.83} \qquad (6\text{-}6)$$

Where C is the constant determined empirically.

6-3-2. Correlation of critical disk rotational speed of rotating-disk mechanical foam-breakers fitted to bubble columns treating various foaming liquids

On the basis of the finding in section 6-3-1, the relationship between N_c and $\Gamma^{-0.27} 10^{func.(h_f/U_g)} (D_T/D_d)^{0.90} \phi_f d_f^{1.83}$ was examined for all of the N_c data in BCs with MFRDs, shown in chapter 4. The values of $\phi_f d_f^{1.83}$ of respective liquids were calculated from those of ϕ_f and d_f reported in previous chapter. As shown in Fig.6-3, the experimental N_c data in all systems could be correlated using a straight line as follows, within an accuracy of $\pm$ 25%.

$$N_c = 2.28 \times 10^7 \Gamma^{-0.27} 10^{func.(h_f/U_g)} \times (D_T/D_d)^{0.90} \phi_f d_f^{1.83} \qquad (6\text{-}7)$$

The above results suggest that the foaming characteristic term $\phi_f d_f^{1.83}$ of liquids proposed in the preceding chapter is also useful for evaluation of the required disk rotational speed of MFRDs fitted to BCs treating various liquids.

6-4. Conclusions

For BCs treating various kinds of foaming liquids, the critical rotational speed N_c required for foam-breaking

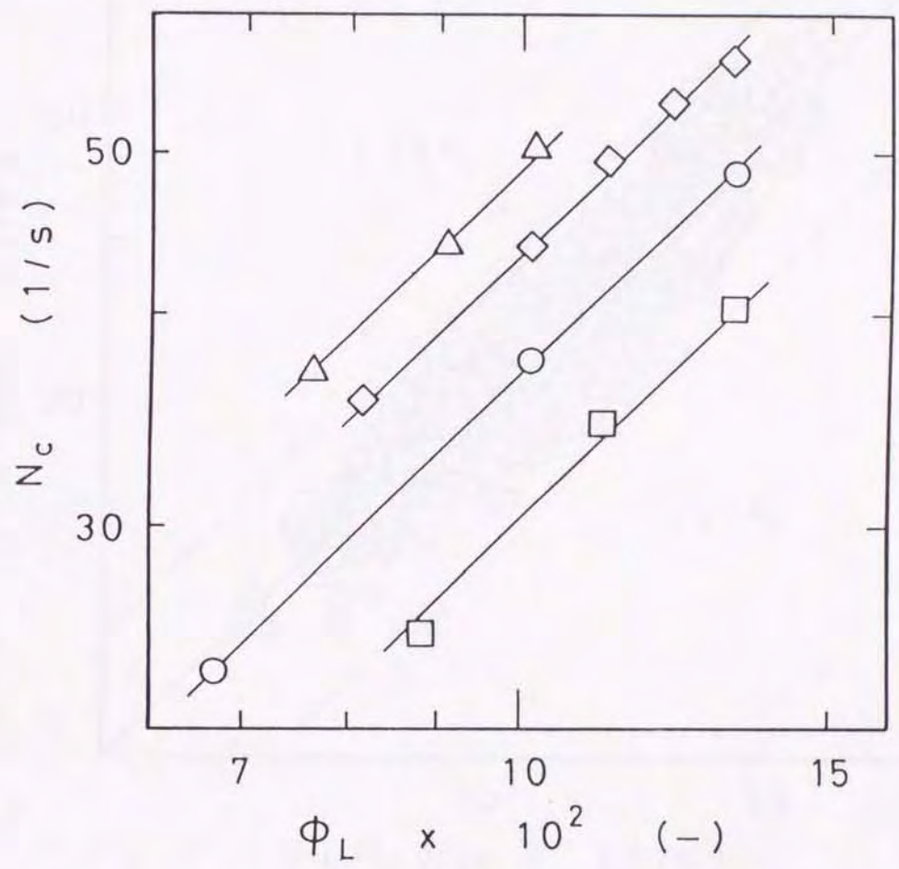

Figure 6-2. Relation between N_c and ϕ_L: ○ ; F-D(4) solution, D_T=0.31m, D_T/D_d=1.475, H_L/H_d=0.667, Γ =3.183x10^{-5}m^2/s, △ ; F-T40(4) solution, D_T=0.19m, D_T/D_d=1.357, H_L/H_d=0.667, Γ =2.122x10^{-5}m^2/s, ◇ ; F-S(3) solution, D_T=0.19m, D_T/D_d=1.267, H_L/H_d=0.667, Γ =2.122x10^{-5}m^2/s, □ ; F-E(4) solution, D_T=0.256m, D_T/D_d=1.267, H_L/H_d=0.511, Γ =4.244x10^{-5}m^2/s.

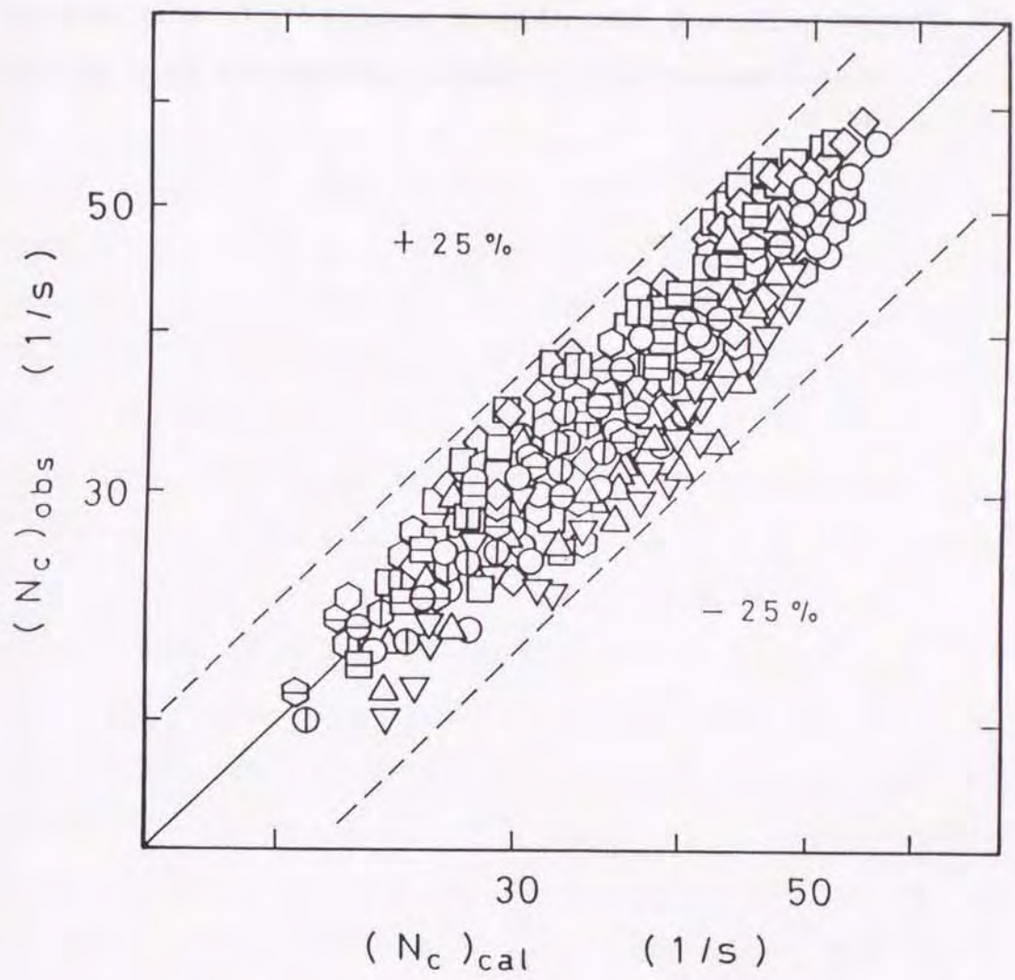

Figure 6-3. Comparison of observed and calculated values of N_c. F-D solutions; D_T(m): ○ ; 0.19, ⊖ ; 0.256, ◍ ; 0.31, F-T solutions; D_T(m): ⬡ ;0.19, ⊖ ; 0.256, ◍ ; 0.31, F-E solutions; D_T(m): □ ; 0.19, ⊟ ; 0.256, ◫ ; 0.31, F-T40 solutions; D_T(m): △ ; 0.19, F-T60 solutions; D_T(m): ▽ ; 0.19, F-S solutions; D_T(m): ◇ ; 0.19 (operating conditions are $H_d = 4.737 D_T$, $D_T/D_d = 1.267\text{-}1.475$, $H_L/H_d = 0.511\text{-}0.667$, $U_g = 1.0\text{-}5.0 \times 10^{-2}$ m/s, $\Gamma = 2.122 \times 10^{-5} - \Gamma_T$ m²/s).

of MFRDs fitted to BCs was studied in relation to the foaming characteristics of the liquids. Eq.(6-7) were obtained for N_c in foam-breaking regions. With this equation, it was found that prediction of N_c of MFRDs fitted to BCs treating various liquids was possible regardless of the kind of foaming liquid or its concentration.

CHAPTER 7

DESIGN AND OPERATION OF BUBBLE COLUMNS FITTED WITH ROTATING-DISK MECHANICAL FOAM-BREAKERS TREATING VARIOUS COMPLEX SOLUTIONS AND BIOLOGICAL MEDIA

7-1. Introduction

In the preceding chapters, it was shown that differences in the liquid holdup in foam, ϕ_L, and the critical disk rotational speed N_c required for foam-breaking among the liquids were possible to evaluate by the foaming characteristic term F_{CT} ($=\phi_f d_f^{1.83}$) of respective liquids, which is independent of the kind, concentration or physical properties of various liquids. The model foaming liquids used, however, were those contained single components such as detergent, saponin, etc. The foaming liquids encountered in actual production processes are varied and generally have complex compositions. In order to demonstrate the usefulness of the design and operation of the MFRD that utilize the foaming characteristic term F_{CT}, clarified in chapters 5 and 6, further studies using realistic liquids of multicomponent systems are necessary.

In this chapter, rotating-disk mechanical foam-breakers (MFRDs) were used in BCs treating mixed solutions and biological media so that the design and operational characteristics of BCs with MFRDs could be studied in relation to the foaming characteristics of the various liquids. For a small BC treating mixed solutions, the foam-

ing behavior of the BC and foam-breaking behavior of the MFRD were first investigated respectively in terms of changes in ϕ_L and N_c. Values of F_{CT} for mixed solutions were determined on the basis of the results measured by using the foaming apparatus, and differences in ϕ_L and N_c among the mixed solutions were discussed in relation to the values of F_{CT}. Usefulness of the empirical correlations for the prediction of ϕ_L in the small BC and N_c of the MFRD fitted to its BC was also examined. Similar investigations were then carried out for the small BC with the MFRD treating biological media. Applicability of the empirical correlations for the prediction of ϕ_L and N_c was further tested for larger BCs with MFRDs, treating mixed solutions and biological media.

7-2. Experimental

The experimental apparatus used in this experiment was the same as that in chapter 4. Three geometrical similar BCs, 0.19, 0.256 and 0.31m in diameter D_T, were used. The gas superficial velocity U_g ranged from 1.0×10^{-2} to 5.0×10^{-2}m/s. The working liquid volume was varied from 0.017 to 0.075m^3 depending on D_T. The MFRD was set in the head space of each BC to maintain the ratio of the disk height H_d to D_T (4.737 in H_d/D_T) and three rotating disks, 0.15 to 0.24m in diameter D_d, were employed. The ratio of D_T/D_d in three BCs was 1.267. The liquid feed rate W onto the rotating disk was varied from 1.0×10^{-5} to 4.8×10^{-5} m^3/s. The liquid holdup in foam, ϕ_L, the critical disk rotational speed N_c and the power consumption P_{kc} requir-

ed for foam-breaking were measured according to methods identical to those employed in the previous chapters.

In determinations of the term F_{CT} as a standard value which reflects inherent foaming characteristics of the liquid to be treated, the small foaming apparatus used was the same as that in chapter 5. Liquid holdup in foamate flow (ϕ_t), rate of liquid drainage from foam (v), foam velocity (u_f) and foam size (d_f), which reflect the foaming characteristics of liquids, were first measured for mixed solutions and biological media under constant gas-bubbling and foaming conditions. The liquid holdup in foam, ϕ_f, in the foaming column (A_f in cross-sectional area), defined by Eq.(7-1) as a function of ϕ_t v and u_f, was then evaluated.

$$\phi_f = \phi_t + v/(u_f A_f) \qquad (7\text{-}1)$$

Using ϕ_f obtained from Eq.(7-1) and size d_f of foam generated in the corresponding liquid, the value of F_{CT} ($=\phi_f d_f^{1.83}$) was determined. Further details of this equipment, including the experimental and measurement procedures, have been reported in chapter 5.

As the mixed solution, twelve kinds of solutions shown in Table 7-1 were used. As the biological medium containing foamy substances, the followings were used: (A) MY medium of ρ =1006.0kg/m^3, μ =1.08mPa·s and σ =53.6mN/m (yeast extract 3kg/m^3, malt extract 3kg/m^3, peptone 5 kg/m^3, glucose 10kg/m^3); (B) medium of ρ =1014.2kg/m^3, μ =1.12mPa·s and σ =59.1mN/m for *Penicillum chrysogenum* (Ref.131) (glucose 20kg/m^3, peptone 10kg/m^3, KH_2PO_4 5 kg/m^3, $MgSO_4 \cdot 7H_2O$ 2.5kg/m^3, $FeCl_3$ 0.001kg/m^3); (C) malt

Table 7-1 Physical Properties of Mixed Solutions at 293K.

Solution		Concentration		ρ (kg/m^3)	μ x10^3 (Pa·s)	σ x10^3 (N/m)
F-D[a] + F-S[e]	M-S (1)	1.0x10^{-2}[g] + 2.0x10^{-3}[h]		998.5	1.02	46.2
F-T40[c] + F-S[e]	M-S (2)	2.5x10^{-2}[h] + 5.0x10^{-3}[h]		998.9	1.01	42.3
F-T[b] + F-T40[c]	M-S (3)	4.0x10^{-3}[h] + 1.0x10^{-2}[h]		998.6	1.01	40.2
F-S[e] + F-E[f]	M-S (4)	5.0x10^{-3}[h] + 5.0x10^{-1}[h]		999.9	1.05	35.8
F-T[b] + F-E[f]	M-S (5)	4.0x10^{-3}[h] + 5.0x10^{-1}[h]		999.7	1.04	34.3
F-D[a] + F-E[f]	M-S (6)	1.0x10^{-2}[g] + 5.0x10^{-1}[h]		999.9	1.05	33.8
F-T40[c] + F-E[f]	M-S (7)	5.0x10^{-2}[h] + 5.0x10^{-1}[h]		1000.0	1.05	34.4
F-T[b] + F-T40[c] + F-D[a]	M-S (8)	1.0x10^{-3}[h] + 1.0x10^{-2}[h]	+ 3.0x10^{-3}[g]	998.6	1.01	45.5
F-S[e] + F-T60[d] + F-T[b]	M-S (9)	2.0x10^{-3}[h] + 1.0x10^{-2}[h]	+ 1.0x10^{-3}[h]	998.6	1.01	44.4
F-S[e] + F-T60[d] + F-D[a]	M-S(10)	2.0x10^{-3}[h] + 1.0x10^{-2}[h]	+ 3.0x10^{-3}[g]	998.7	1.01	46.7
F-E[f] + F-T40[c] + F-S[e]	M-S(11)	1.0x10^{-1}[h] + 1.0x10^{-2}[h]	+ 2.0x10^{-3}[h]	999.0	1.03	37.3
F-E[f] + F-T[b] + F-D[a]	M-S(12)	1.0x10^{-1}[h] + 1.0x10^{-3}[h]	+ 3.0x10^{-3}[g]	998.8	1.03	39.5

[a] Detergent(Lipon F, manufactured by Lipon Corp.). [b] Triton X-100. [c] Tween 40. [d] Tween 60. [e] Saponin.
[f] Egg albumin. [g] Vol.%. [h] Wt.%.

extract medium of ρ =1013.8kg/m^3, μ =1.16mPa·s and σ = 45.9mN/m (malt extract 20kg/m^3, peptone 1kg/m^3, glucose 20kg/m^3); (D) YP medium (Ref.127) of ρ =998.9kg/m^3, μ = 1.03mPa·s and σ =59.3mN/m (dry yeast 1w/v% , soluble starch 2w/v% , KH_2PO_4 0.5w/v% , $MgSO_4 \cdot 7H_2O$ 0.05w/v% , CSL 0.5w/v%); (E) medium of ρ =998.6kg/m^3, μ =1.03mPa·s and σ =61.1mN/m for yeast (Ref.107) [molasses 5wt.% , $(NH_2)_2CO$ 0.066wt.% , $(NH_4)_2HPO_4$ 0.033wt.% , H_2SO_4 0.12wt.%]. All the experiments were carried out at 293K with the gas phase being air.

7-3. Results and Discussion

7-3-1. Liquid holdup in foam in small bubble column with rotating-disk mechanical foam-breaker treating mixed solutions

In chapter 5, which dealt with the relation between mechanical foam-breaking difficulty and the foaming characteristics of liquids of single components, it was shown that the liquid holdup in foam, ϕ_L, as a measure of the foaming intensity for BCs which is related to the difficulty or ease of foam-breaking with MFRDs within the effective Γ_T range which could be predicted by Eq.(7-2) (Ref.95):

$$N_\Gamma^+ = 0.141(Re)^{2/3}(We)^{-0.883} \qquad (7\text{-}2)$$

was expressed by Eq.(7-3).

$$\phi_L = 7.81 \times 10^6 U_L^{0.24} 10^{func.(h_f/U_g)} F_{CT} \qquad (7\text{-}3)$$

As shown in the preceding chapter, the func.(h_f/U_g) was given by Eq.(7-4) for all the liquids tested.

$$\text{func.}(h_f/U_g)=0.511+0.062\log(h_f/U_g)-0.144[\log(h_f/U_g)]^2 \quad (7\text{-}4)$$

Values of h_f could also be predicted from Eqs.(7-5) and (7-6) regardless of the kind of foaming liquid or its concentration.

$$h_f/D_T=U_g^{-2.54(H_L/H_d)^{5.76}10^{\text{func.}(H_L/H_d)}} \quad (7\text{-}5)$$

$$\text{func.}(H_L/H_d)=-2.25-15.30\log(H_L/H_d)-22.65[\log(H_L/H_d)]^2 \quad (7\text{-}6)$$

Whether Eq.(7-3) is applied for the foam control system treating mixed solutions was investigated using the small BC of D_T=0.19m. The relation between ϕ_L and U_L was first examined (Fig.7-1). Although there is a difference in the value of ϕ_L, depending on the kind of mixed solution, ϕ_L was found to vary in proportion to the 0.24 power of U_L for all the solutions. The dependence of h_f/U_g on ϕ_L was then examined. Figure 7-2 shows a typical result of ϕ_L plotted vs. h_f/U_g. It was confirmed that the changes in ϕ_L with h_f/U_g were expressed in the form of $\phi_L \propto 10^{\text{func.}(h_f/U_g)}$. ϕ_t, v, u_f and d_f values for respective mixed solutions were then measured by using the small foaming apparatus, and the values shown in Table 7-2 were obtained respectively. Using the values of F_{CT} of respective solutions, ϕ_L at each operating condition was calculated from Eq.(7-3) and their values were compared with those observed. The ϕ_L values calculated agreed with those observed within 20% error. This result shows that Eq.(7-3) presented in chapter 5 for the system using the liquids of single components can be also applied for the prediction of ϕ_L in the BC with the MFRD treating mixed

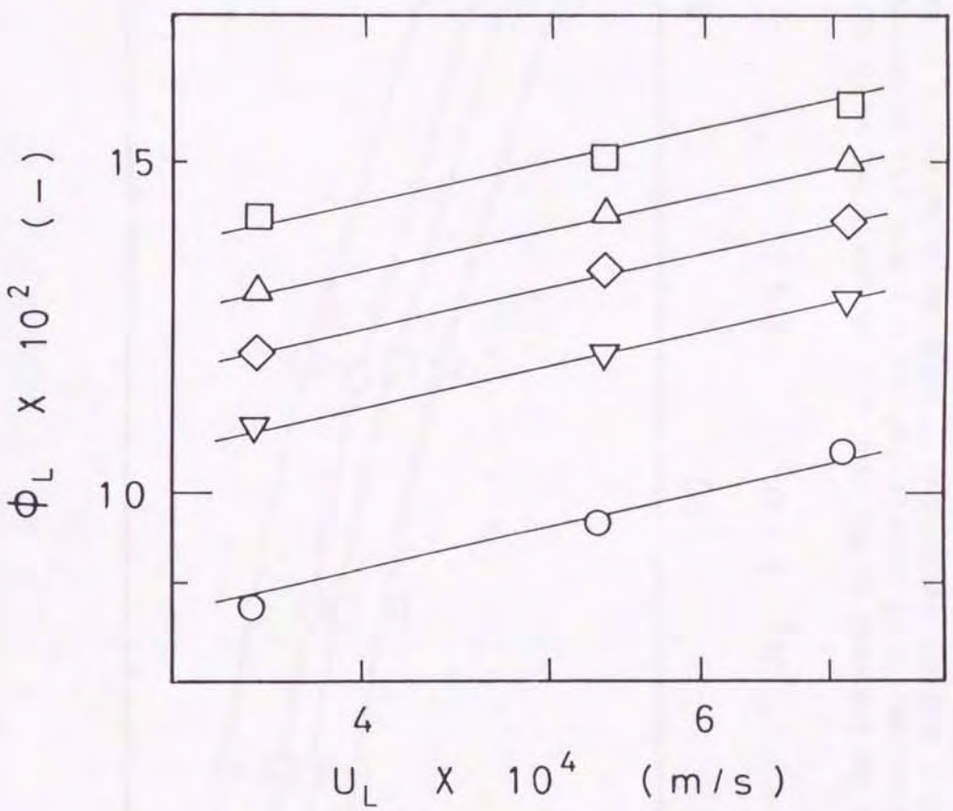

Figure 7-1. Relation between U_L and ϕ_L in small BC with $H_L = 0.667 H_d$: ○ ; M-S(6) solution, $U_g = 1.0 \times 10^{-2}$ m/s, △ ; M-S(7) solution, $U_g = 3.0 \times 10^{-2}$ m/s, □ ; M-S(2) solution, $U_g = 5.0 \times 10^{-2}$ m/s, ▽ ; M-S(9) solution, $U_g = 3.0 \times 10^{-2}$ m/s, ◇ ; M-S(12) solution, $U_g = 5.0 \times 10^{-2}$ m/s.

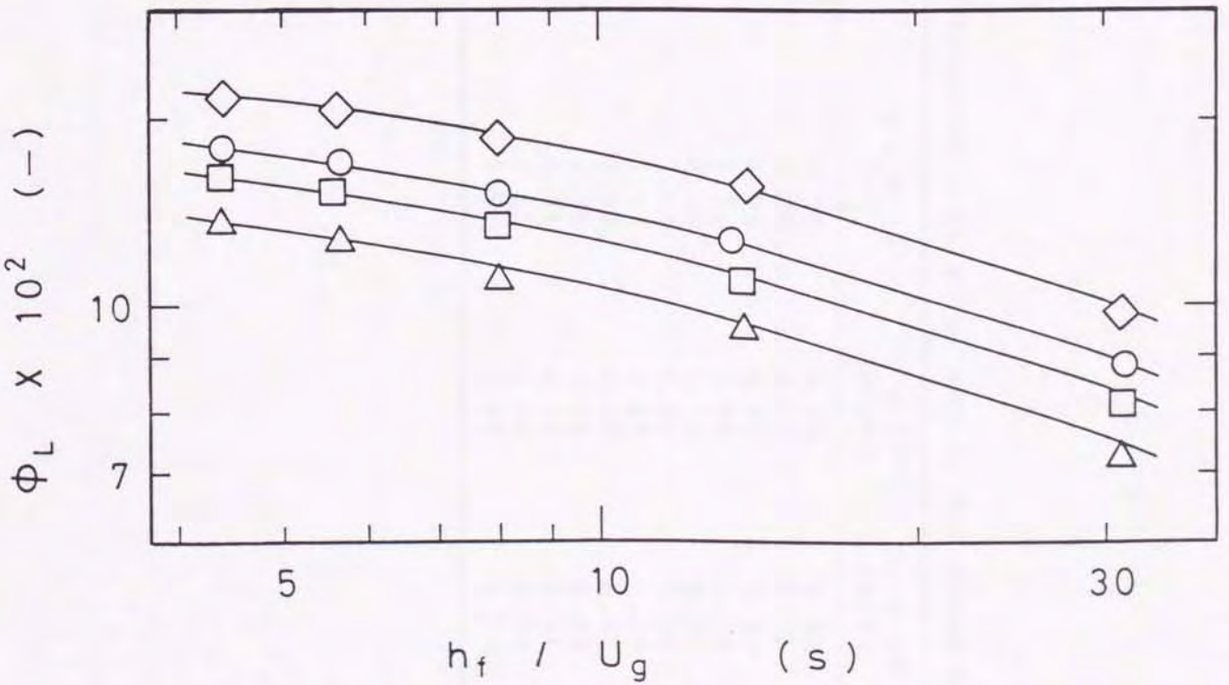

Figure 7-2. Relation between h_f/U_g and ϕ_L in small BC with H_L=0.667 H_d : □ ; M-S(2) solution, Γ =2.122x10^{-5}m^2/s, ◇ ; M-S (4) solution, Γ = 3.183x10^{-5}m^2/s, ○ ; M-S(8) solution, Γ =4.244x10^{-5}m^2/s, △ ; M-S(11) solution, Γ =2.122x10^{-5}m^2/s.

Table 7-2 Values of ϕ_t, v, u_f and d_f for Mixed Solutions.

Solution	$\phi_t \times 10^2$ (-)	$v \times 10^7$ (m^3/s)	$u_f \times 10^3$ (m/s)	$d_f \times 10^4$ (m)
M-S (1)	1.90	5.88	5.88	3.6
M-S (2)	1.98	4.91	5.71	3.9
M-S (3)	1.93	4.91	5.40	3.8
M-S (4)	1.92	2.94	5.13	4.5
M-S (5)	2.10	4.31	4.55	3.6
M-S (6)	2.14	4.91	5.56	3.8
M-S (7)	1.72	4.12	4.76	4.0
M-S (8)	2.42	4.47	6.67	3.9
M-S (9)	2.30	3.92	6.97	4.0
M-S(10)	1.91	4.37	6.67	4.1
M-S(11)	2.55	4.06	6.90	3.9
M-S(12)	1.97	2.49	6.73	4.3

solutions of complex compositions.

7-3-2. Critical disk rotational speed of rotating-disk mechanical foam-breaker fitted to small bubble column treating mixed solutions

In chapter 6, which dealt with the relation between critical disk rotating speed N_c of MFRDs and the foaming characteristics of liquids of single components, an empirical equation of the following type to predict N_c of MFRDs fitted to BCs in foam-breaking region was presented.

$$N_c = 2.28 \times 10^7 \Gamma^{-0.27} (D_T/D_d)^{0.90} 10^{func.(h_f/U_g)} F_{CT} \quad (7\text{-}7)$$

Func.(h_f/U_g) in Eq.(7-7) was expressed by the form of Eq. (7-4) for all the liquids tested and the values h_f could be predicted from Eqs.(7-5) and (7-6).

Whether Eq.(7-7) is applied for the foam control system treating mixed solutions was investigated using the small BC. For N_c values observed within the effective Γ_T range which could be predicted by Eq.(7-2), the relation among N_c, Γ and h_f/U_g values was examined. The typical relation between N_c and Γ is shown in Fig.7-3. As for the dependence of Γ on N_c, it was found that their relation was expressed in the form of $N_c \propto \Gamma^{-0.27}$ regardless of the kind of mixed solution. The effect of h_f/U_g on N_c was then examined. Figure 7-4 shows a typical result of N_c plotted vs. h_f/U_g. It was confirmed the changes in N_c with h_f/U_g were expressed in the form of $N_c \propto 10^{func.(h_f/U_g)}$ Using the values of F_{CT} of respective solutions shown in Table 7-2, N_c at each operating condition was calculated

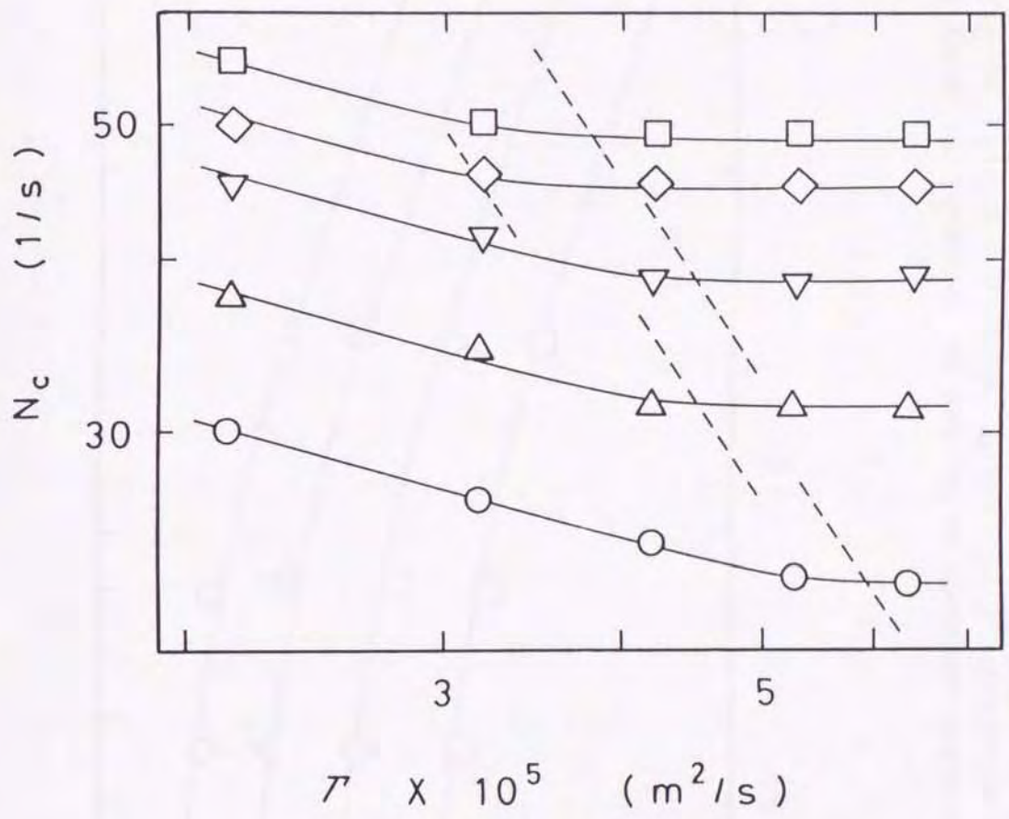

Figure 7-3. Relation between Γ and N_c in small BC with $H_L = 0.667H_d$: Dotted lines represent Eq.(4-2). △ ; M-S(3) solution, $U_g = 2.0\times10^{-2}$ m/s, ◇ ; M-S(5) solution, $U_g = 3.0\times10^{-2}$ m/s, □ ; M-S(1) solution, $U_g = 3.0\times10^{-2}$ m/s, ○ ; M-S(8) solution, $U_g = 1.0\times10^{-2}$ m/s, ▽ ; M-S(10) solution, $U_g = 5.0\times10^{-2}$ m/s.

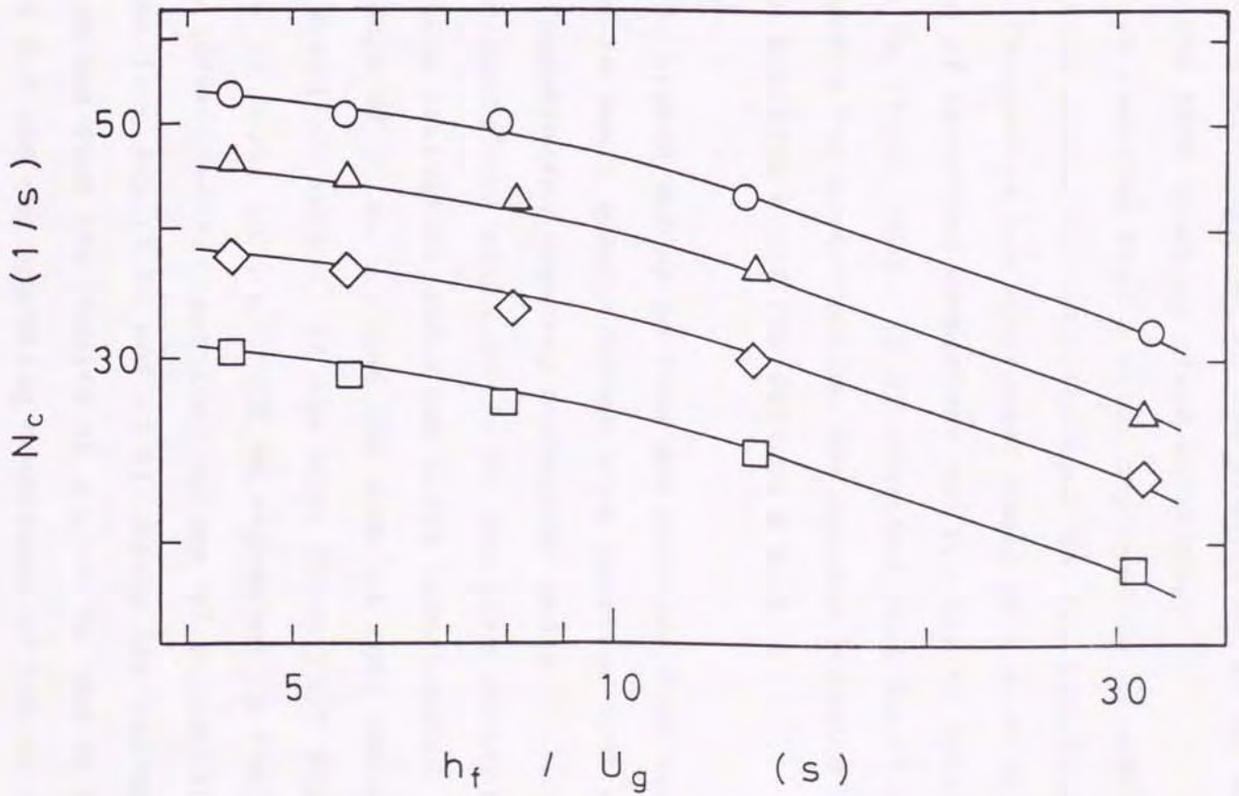

Figure 7-4. Relation between h_f/U_g and N_c in small BC with H_L=0.667 H_d : ○ ; M-S(6) solution, Γ =2.122x10^{-5}m^2/s, △ ; M-S(7) solution, Γ = 3.183x10^{-5}m^2/s, ◇ ; M-S(9) solution, Γ =4.244x10^{-5}m^2/s, □ ; M-S(12) solution, Γ =4.244x10^{-5}m^2/s.

from Eq.(7-7). Their values were compared with those observed. The N_c values calculated agreed with those observed within 20% error. It is concluded that Eq.(7-7) could be also applied to the prediction of N_c in the BC with the MFRD treating mixed solutions.

It is required that a motor employed in an actual foam-breaking operation is sufficient in its rotation capacity. Changes in the rotational speed of a disk with variation of operating conditions and F_{CT} can be easily known from Eq.(7-7). Thus, it is expected that Eq.(7-7) would be usable for preestimating the maximum rotation capacity of an electric motor for driving a disk.

7-3-3. Liquid holdup in foam and critical disk rotational speed in small bubble column with rotating-disk mechanical foam-breaker treating biological media

Applicability of Eq.(7-3) to the foam control system treating biological media was first investigated. The dependence of U_L on ϕ_L was the same as that observed for the mixed solutions. It was also found that the dependence of h_f/U_g on ϕ_L could be expressed in the form of $\phi_L \propto 10^{func.(h_f/U_g)}$ and that values of h_f could be predicted from Eqs.(7-5) and (7-6). Using the values of F_{CT} determined from the results of ϕ_t, v, u_f and d_f shown in Table 7-3 and the operating conditions of the BC with the MFRD, ϕ_L values were calculated from Eq.(7-3) and compared with those observed. The ϕ_L values calculated agreed with those observed within 20% error. That is, it was confirmed that Eq.(7-3) could be applied to the pre-

Table 7-3 Values of ϕ_t, v, u_f, and d_f for biological media.

Medium	$\phi_t \times 10^2$ (-)	$v \times 10^7$ (m^3/s)	$u_f \times 10^3$ (m/s)	$d_f \times 10^4$ (m)
(A)	1.96	14.33	3.92	2.1
(B)	2.13	12.96	3.64	2.1
(C)	4.11	7.85	5.12	2.8
(D)	2.30	8.84	4.00	2.6
(E)	2.42	8.84	4.26	2.4

diction of ϕ_L in the foaming system containing biological media.

Concerning the changes in N_c, the effects of operating variables such as Γ and h_f/U_g on N_c were first investigated. Their effects on N_c within the Γ_T range, which could be predicted by Eq.(7-2), were almost the same as those observed for the mixed solutions. A comparison of observed values of N_c with those calculated from Eq.(7-7) was then carried out. The N_c values observed agreed with those calculated within 20% error. It is concluded that Eq.(7-7) is also applicable to the foam control system treating biological media.

7-3-4. Prediction of ϕ_L and N_c in larger bubble columns with rotating-disk mechanical foam-breakers

For larger BCs with MFRDs, treating mixed solutions and biological media, applicability of the empirical correlations for ϕ_L and N_c, i.e., Eq.(7-3) and (7-7), was examined. Foam-breaking experiments were carried out using the BC of D_T=0.256m and that of D_T=0.31m. Figure 7-5 shows a typical comparison of ϕ_L values calculated by Eq.(7-3) and those observed. It is found that Eq.(7-3) can also be applied for the prediction of ϕ_L in the large BC treating mixed solutions and biological media. Comparison of N_c values estimated from Eq.(7-7) with those observed was then carried out. It was confirmed that N_c values of MFRDs fitted to these large BCs could be estimated by Eq.(7-7) within 20% error.

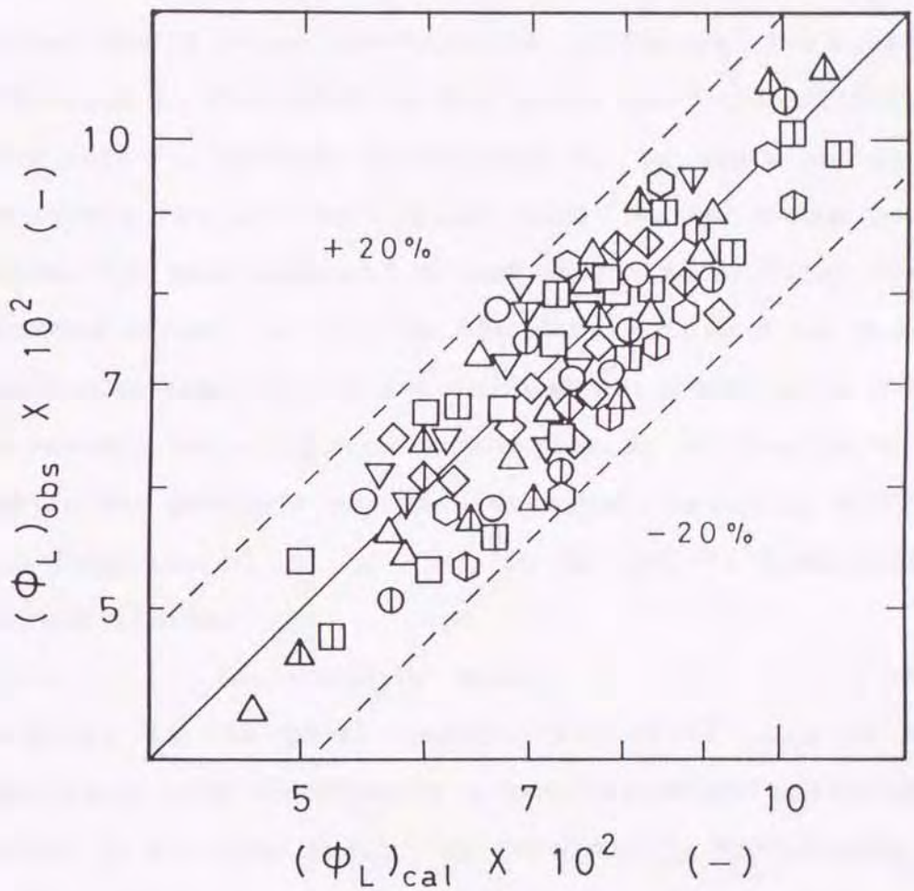

Figure 7-5. Comparison of observed and calculated values of ϕ_L: D_T=0.256m, H_L=0.511H_d: ○ ; M-S(1) solution, U_g=1.0-2.0x10^{-2}m/s, △ ; M-S(9) solution, U_g=1.0-3.0x10^{-2}m/s, □ ; M-S(11) solution, U_g=1.0-3.0x10^{-2}m/s, ▽ ; (A) medium, U_g=1.0-1.5x10^{-2}m/s, ⬡ ; (C) medium, U_g=1.0-2.0x10^{-2}m/s, ◇ ; (D) medium, U_g=1.0-2.0x10^{-2}m/s, D_T=0.31m, H_L=0.667H_d: ◍ ; M-S(1) solution, U_g=1.0-2.0 x10^{-2}m/s, ◬ ; M-S(9) solution, U_g=1.0-3.0x10^{-2}m/s, ◫ ; M-S (11) solution, U_g=1.0-3.0x10^{-2}m/s, ▽ ; (A) medium, U_g=1.0-1.5 x10^{-2}m/s, ◍ ; (C) medium, U_g=1.0-2.0x10^{-2}m/s, ◇ ; (D) medium, U_g=1.0-2.0x10^{-2}m/s.

7-3-5. Power consumption for foam-breaking

The effects of operating variables on the power consumption P_{kc} for foam-breaking (the power required for liquid dispersion by the rotating disk) at the critical state in BCs with MFRDs treating mixed solutions and biological media were investigated. Although there was a difference in the value of P_{kc} among the liquids, a tendency that P_{kc} becomes higher when U_g, D_d and W are large was common for all the systems used. By using the power consumption data measured at and above the critical foam-breaking state, as well as the data obtained in liquid dispersion experiments in which W and N varied widely, the correlation of power consumption P_k on the basis of dimensional analysis was then examined. Assuming that P_k is a function of ρ, μ, σ, N, D_d and W, dimensional analysis yields:

$$N_{Pk}=\text{const.}Fw^{a}Re^{b}We^{c} \qquad (7\text{-}8)$$

where N_{Pk} is the power number. The first term on the right-hand side represents a kind of flow coefficient defined as the flow number. By considering the effects of Fw, Re and We on N_{Pk} and completing the equation, the following equation was obtained within 20% error.

$$N_{Pk}=4.29Fw^{1.0}Re^{0.02}We^{0.06} \qquad (7\text{-}9)$$

It is concluded that Eq.(7-9) would be useful for estimating power consumption P_k for foam-breaking at and above the critical state in BCs with MFRDs treating various liquids.

7-3-6. Power consumption for foam-breaking in terms of

changes in liquid holdup in foam, dispersion distance of liquid particles and gas velocity ratio between BC and annular foam-ascending section

According to the results in chapter 4, it can be pointed out that the power consumption P_{kc} at the critical foam-breaking state becomes high when the foam with larger ϕ_L is formed. If a relation which is independent of the kind and concentration of liquid can be found between P_{kc}, ϕ_L and the operating variables, it is expected that the relationship will be useful for evaluating differences in P_{kc} due to those in ϕ_L. In chapter 4, it was shown that P_{kc} could be predicted from Eq.(7-10) as a function of ϕ_L, the dispersion distance l_f [$=\sqrt{(D_T^2-D_d^2)}/2$] of the liquid particles from the disk and the gas velocity ratio U_{ga}/U_g between the BC and the annular foam-ascending section S_a separated by the disk and the column wall.

$$P_{kc}=2.15\times10^5\,\phi_L^{2.14}\,l_f^{2.65}\,(U_{ga}/U_g)^{1.60} \qquad (7\text{-}10)$$

Applicability of Eq.(7-10) to the present foam control system was examined, by comparing P_{kc} values calculated with those observed. As the value of ϕ_L, those calculated from Eq.(7-3) were used. l_f, U_g and U_{ga} values were determined from the operating conditions. The P_{kc} values calculated by Eq.(7-10) agreed with those observed within 25% error. It is concluded that Eq.(7-10) would be useful for predicting the magnitude of P_{kc} in BCs with MFRDs treating mixed solutions and biological media, which must be varied according to changes in ϕ_L during the operation.

7-3-7. Control of foaming based on changes in foaming characteristic term F_{CT} of process solution

It is generally known that foaming behaviour in actual production processes is not constant throughout a reaction period, namely that foaming pattern in reactors changes during the operation (Ref.59). The variations in foaming pattern are mainly due to physicochemical changes in the liquid with progress of the reaction, consumption of raw materials, the formation of products, etc. According to the results shown so far, it is pointed out that these physicochemical changes are possible to evaluate as those in the foaming characteristic term F_{CT} of the liquid at each reaction period. An example of the foam control method based on changes in F_{CT} at respective times is discussed in relation to those in ϕ_L, P_{kc} and N_c.

In foam-breaking operation with the MFRD, the most important factor affecting the magnitude of P_{kc} and N_c is the liquid holdup in ascending foam, ϕ_L, in the BC. The value of ϕ_L is first calculated from Eq.(7-3) as a function of F_{CT}. P_{kc} is then evaluated from Eq.(7-10). The value of N_c corresponding to P_{kc} is further determined from Eq.(7-9). To carry out foam control in line with this flow, i.e., to operate the MFRD with the minimum power consumption and disk rotational speed, when the foaming pattern in the BC changes considerably during the operation, it becomes necessary to measure the foaming characteristic term F_{CT} of the liquid related to the difficulty or ease of foam-breaking at a proper interval, and to feed their information to a rotation control part

of the MFRD, according to the procedure as shown in an example of Fig.7-6. The foaming characteristic term F_{CT}, which is independent of the kind and concentration of liquid or their physical properties, is possible to evaluate within a short time, using small quantity of sample withdrawn from the BC actually employed. It is expected that if F_{CT} values measured at an appropriate time interval feed to a control device in which design equations such as Eq.(7-3) including the term F_{CT} and Eqs.(7-9) and (7-10) were inputted, the MFRD may be able to operate more effectively and economically.

7-4. Conclusions

Foaming behavior of the BC treating mixed solutions and biological media under mechanical foam control with the MFRD and foam-breaking behavior of the MFRD were quantitatively evaluated in relation to the changes in operating conditions of the BC with the MFRD and those in foaming characteristic term F_{CT} of respective solutions and media measured in the small foaming apparatus. The F_{CT} value proved to be useful as a parameter which reflects the difficulty or ease of mechanical foam-breaking among the liquids. The liquid holdup in foam, ϕ_b, which reflects the foaming intensity of the BC and is related to the difficulty or ease of foam-breaking, and the critical disk rotational speed N_c required for foam-breaking could be predicted respectively by Eq.(7-3) and Eq.(7-7). Power consumption P_{kc} for foam-breaking with the MFRD was also found to be predicted by Eq.(7-10). These equations,

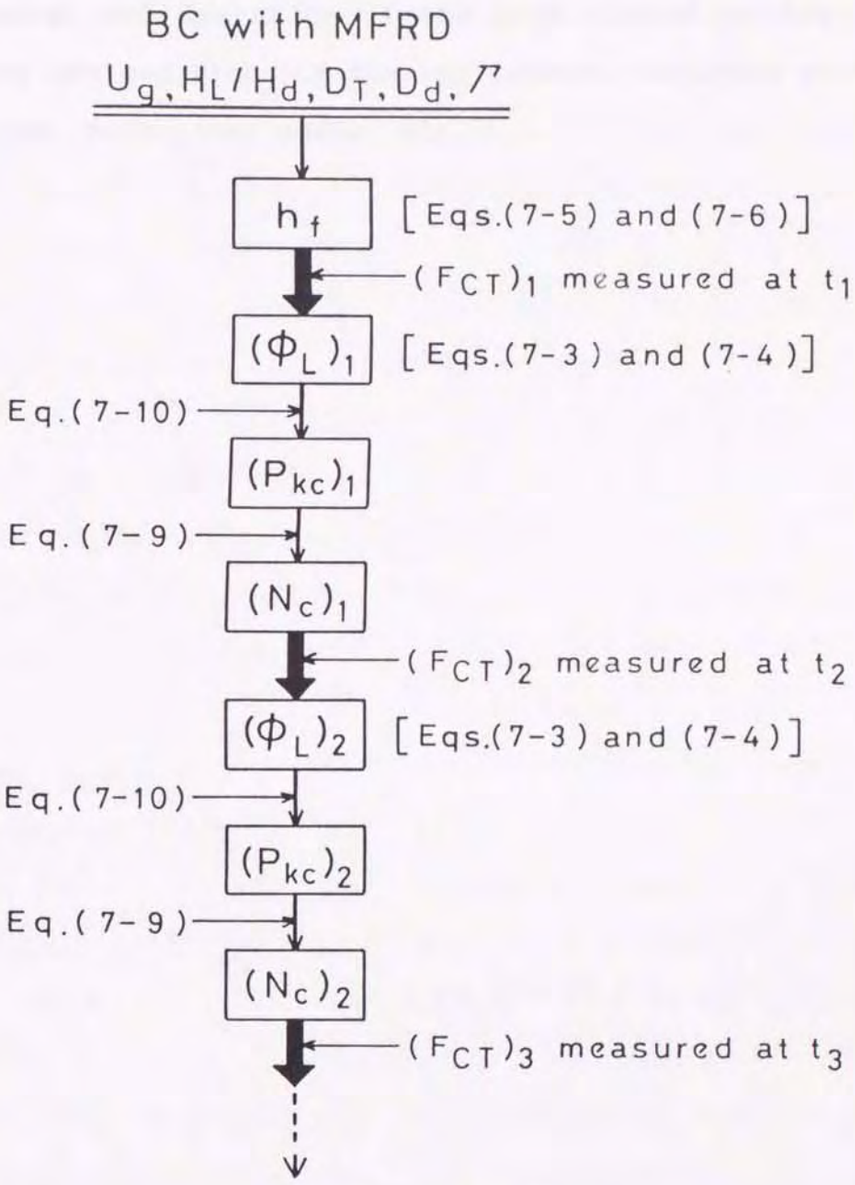

Figure 7-6. An example of operational procedure of MFRD based on changes in F_{CT} of liquid during operation.

which can be applied independently of the kind and concentration of the foaming liquid (i.e. physical properties of the liquid), are expected to be beneficial to the design and operation of the MFRD fitted to the BC treating various kinds of foaming liquids including mixed solutions, biological media, etc.

CHAPTER 8

GAS HOLDUP IN BUBBLE COLUMNS UNDER FOAM CONTROL

8-1. Introduction

The gas holdup is one of the important parameters in the design and operation of bubble columns (BCs). A number of studies on the gas holdup in BCs without foaming have been carried out so far (Refs.5, 11, 12, 44, 53, 55, 61, 62, 69, 78, 84, 87, 92, 94, 96, 121). In contrast, systematic studies on the gas holdup in BCs treating a foaming system are scarce and reliable information seem not to have hitherto been available. The gas holdup in the BC with a foaming system is difficult to predict on the basis of the results of nonfoaming systems, because of marked differences in flow behavior, bubble size, etc. Considering the fact that the oxygen transfer rate (OTR) is largely affected by the gas holdup, prior to discussion of OTR, it is important to evaluate more accurately the changes in gas holdup in the BC under foam control. In chapter 3 which dealt with the performance characteristics of the BC (0.19m diameter) with mechanical foam control, it was suggested that higher values of the gas holdup compared to those in a nonfoaming system (NS) including antifoam agents (AFs) could be expected in a mechanical foam-control system (MFS) with the MFRD. However, such demon-stration was the result produced by the experiment performed in the foaming liquid system using a soft detergent. In order to provide a generalized basis

for the prediction of the gas holdup in the BC under foam control, further studies using other liquids or BCs of different sizes are necessary.

In this chapter, the effects of operating conditions such as the air sparge rate, the liquid or the column size on the gas holdup between BCs when the foaming was controlled by the MFRD and an AF are investigated. Correlations for predicting the gas holdups in the MFS and the NS are also studied.

8-2. Experimental

The experimental apparatus used in this experiment was the same as that in chapter 4. Three geometrical similar BCs, 0.19, 0.256 and 0.31m in diameter D_T, were used. The gas superficial velocity U_g ranged from 1.0×10^{-2} to 5.0×10^{-2}m/s. The working liquid volume V_L was held constant at 1.7×10^{-2}, 4.2×10^{-2} and $7.5\times10^{-2}m^3$ respectively for BCs of D_T=0.19, 0.256 and 0.31m to maintain the ratio of the disk height H_d to the static liquid height H_L (1.5 in H_d/H_L). As the rotating disk, three disks, 0.15, 0.20 and 0.24m in diameter D_d were used. The ratio of D_T/D_d in three BCs was 1.267. The liquid feed rate W onto the rotating disk was varied from 1.0×10^{-5} to $3.2\times10^{-5}m^3/s$, corresponding to 2.12×10^{-5} to $4.24\times10^{-5}m^2/s$ as the liquid feed rate per unit disk circumference, Γ. Further details are given in chapter 4. The mean gas holdup, defined as the fraction of bubble volume relation to the clear liquid volume, was determined by a conventional manometric technique. As the foaming liquid, five kinds

of 0.15M sodium sulfite solutions containing foaming agents were used. These same solutions to which an AF, silicon oil (KM-70, Shin-Etsu Chemical Co. Ltd.), was added at a concentration of 1000ppm were used as the non-foaming liquids. Table 8-1 shows the physical properties of these foaming and nonfoaming liquids. Moreover, it was confirmed beforehand that the foaming behavior of BCs and the foam-breaking characteristics of MFRDs fitted to BCs were little affected by the addition of Na_2SO_3, namely that there were no differences in the liquid holdup in foam, ϕ_L, and the critical disk rotational speed N_c between the systems containing with and without 0.15M Na_2SO_3.

8-3. Results and Discussion

8-3-1. Gas holdup in mechanical foam control system

The effects of operating condition on the gas holdup in a mechanical foam-control system (MFS) were investigated at and above the critical foam-breaking state, represented by the changes in the disk rotational speed N. In the same manner as in chapter 3, little changes in $(\varepsilon_g)_M$ with variation of N above N_c were observed. That is, it was found that $(\varepsilon_g)_M$ was almost free from the effect of N. Figure 8-1 shows the results of $(\varepsilon_g)_M$ plotted vs. U_g with the liquid and the liquid feed rate per unit disk circumference, Γ, as parameters. Although there is a difference in the value of $(\varepsilon_g)_M$, depending on the liquids, all the systems used had a tendency that $(\varepsilon_g)_M$ be-

Table 8-1 Physical properties of liquids.

Liquid	ρ (kg/m^3)	μ x10^3 (Pas)	σ x10^3 (N/m)
0.15M sodium sulfite solution containing: Detergent[a]	1016.2	1.05	36.24
0.15M sodium sulfite solution containing: Triton X-100[b]	1016.1	1.07	41.78
0.15M sodium sulfite solution containing: Tween 40[c]	1016.1	1.09	60.51
0.15M sdium sulfite solution containing: Tween 60[d]	1016.8	1.08	51.68
0.15M sodium sulfite solution containing: Saponin[e]	1015.7	1.05	62.36
0.15M sodium sulfite solution containing: Detergent[a] and KM-70[f]	1016.4	1.05	33.87
0.15M sodium sulfite solution containing: Triton X-100[b] and KM-70[f]	1016.5	1.06	35.64
0.15M sodium sulfite solution containing: Tween 40[c] and KM-70[f]	1016.0	1.08	46.05
0.15M sodium sulfite solution containing: Tween 60[d] and KM-70[f]	1017.1	1.07	40.90
0.15M sodium sulfite solution containing: Saponin[e] and KM-70[f]	1016.3	1.04	37.67

[a] 1.0x10^{-2} vol%, [b] 4.0x10^{-3} wt%, [c] 2.5x10^{-2} wt%, [d] 5.0x10^{-2} wt%, [e] 2.0x10^{-3} %, [f] Antifoam agent (C_F=1000ppm), silicon oil, manufactured by Shin-Etsu chemical Co.Ltd.

came larger when U_g was increased. With respect to the effect of Γ , as can be seen from the results shown in Fig.8-1, the value of $(\varepsilon_g)_M$ tended to be large slightly with increasing Γ . In BCs with MFRDs, the collapsed foam liquid produced by foam-breaking flows downwards along the column wall. This flow tended to entrain foam ascending from the aerated liquid surface near the wall into the bulk liquid. The larger the value of Γ , the larger the amount of foam entrained into the liquid, which also contributes to an increase in gas holdup in the bulk liquid. The increase of $(\varepsilon_g)_M$ with Γ may be attributed to enhancement of such a foam entrainment phenomenon.

8-3-2. Correlation of gas holdup in mechanical foam control system

For the correlation of gas holdup $(\varepsilon_g)_M$ in the MFS, plots of $[1-(\varepsilon_g)_M]^{-4}$ against U_g were first carried out. the results are shown in Fig.8-2. Their relationship is linear but the slope differs according to the liquids. That is, the effect of U_g on the gas holdup was expressed in the form of Eq.(8-1).

$$[1-(\varepsilon_g)_M]^{-4} \propto U_g^{\alpha} \qquad (8\text{-}1)$$

Where α is empirical constant which depends on the liquids. The effect of Γ on $[1-(\varepsilon_g)_M]^{-4}$ was then examined. As shown in Fig.8-3, it was found that their relationship was expressed by the following form regardless of U_g, the size of BC and the liquid.

$$[1-(\varepsilon_g)_M]^{-4} \propto \Gamma^{0.06} \qquad (8\text{-}2)$$

Thus, from Eqs.(8-1) and (8-2), the following equation is

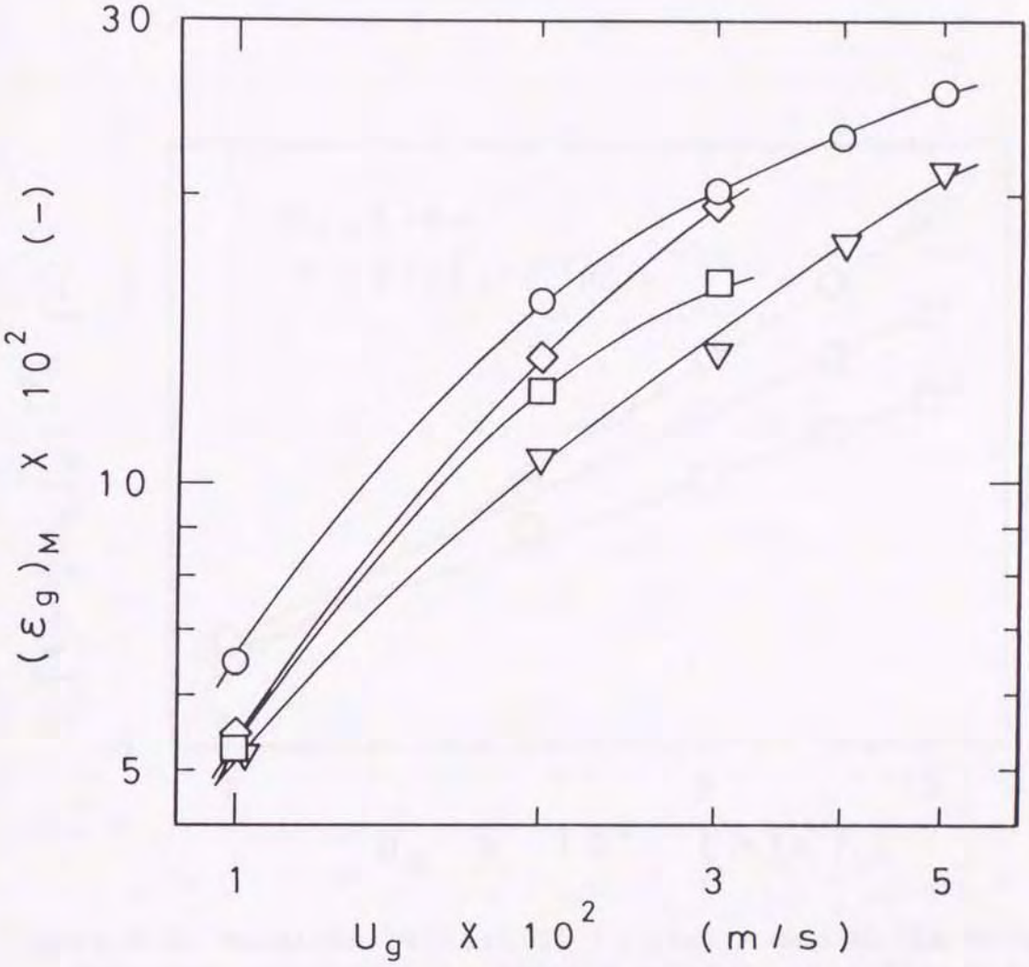

Figure 8-1. Effect of U_g on $(\varepsilon_g)_M$ in MFS: ○ ; Detergent solution, D_T=0.19m, Γ =4.244x10^{-5}m^2/s, □ ; Triton X-100 solution, D_T=0.31m, Γ =2.122x10^{-5}m^2/s, ◇ ; Saponin solution, D_T=0.256m, Γ =3.183x10^{-5}m^2/s, ▽ ; Tween 40 solution, D_T=0.19m, Γ =2.122x10^{-5}m^2/s.

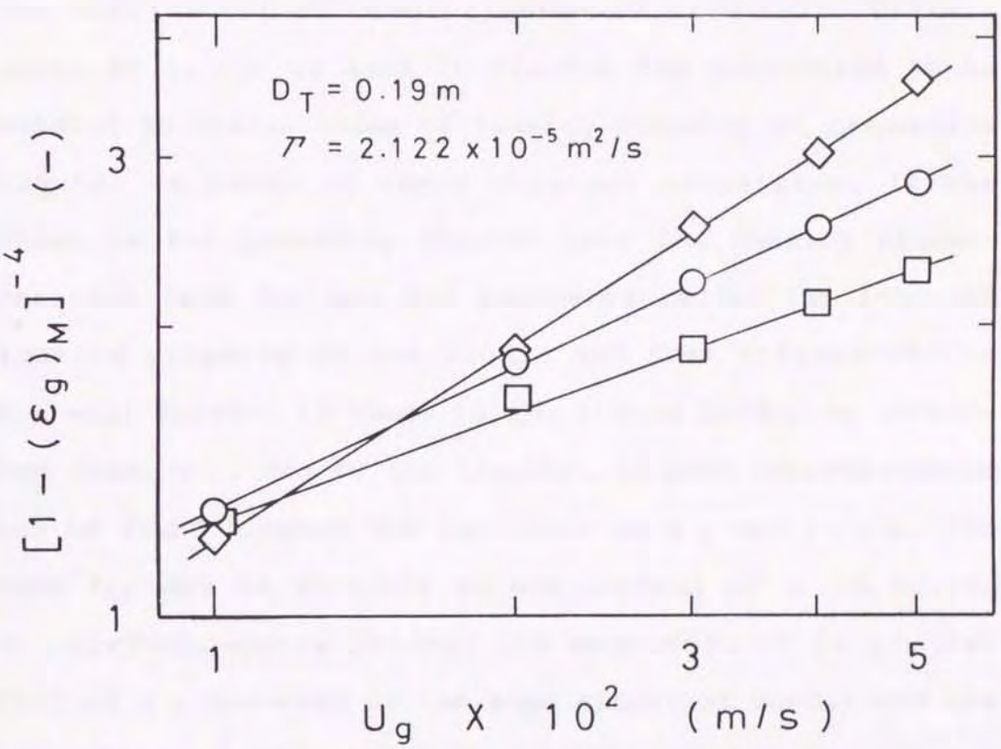

Figure 8-2. Relation between $[1-(\varepsilon_g)_M]^{-4}$ and U_g in MFS: ○ ; Detergent solution, ◇ ; Saponin solution, □ ; Triton X-100 solution.

obtained for $[1-(\varepsilon_g)_M]^{-4}$.

$$[1-(\varepsilon_g)_M]^{-4}=AU_g{}^{\alpha}\Gamma^{0.06} \qquad (8\text{-}3)$$

Where A is empirical constant which changes depending on the liquids.

Equation (8-3) is useful for predicting $(\varepsilon_g)_M$ when the same foaming liquids as used in this experiment are used, but application to other liquids is difficult. Differences in $(\varepsilon_g)_M$ as seen in Fig.8-1 are considered to be related to either those of foaming property of respective liquids or those of their physical properties. It was shown in the preceding chapter that the foaming characteristic term F_{CT} was the parameter reflecting inherent foaming property of the liquid and that differences in F_{CT} well related to those in the liquid holdup in ascending foam, ϕ_L, due to the liquids. If good correspondence can be found between the increases in ϕ_L and $(\varepsilon_g)_M$, the term F_{CT} may be possible to use instead of α in Eq.(8-3). Correspondence between the magnitude of $(\varepsilon_g)_M$ and that of ϕ_L measured at the same operating conditions was investigated. The typical results of $(\varepsilon_g)_M$ and ϕ_L plotted vs. respective foaming liquids are shown in Fig.8-4, in which corresponding P_{kc} values are also plotted for reference. It is found that an increase $(\varepsilon_g)_M$ does not correspond to that in ϕ_L, namely that the term F_{CT} which is related to ϕ_L is difficult to use instead of α. This result, in other words, also suggests that differences in $(\varepsilon_g)_M$ due to the foaming liquids may be related to those in their physical properties, in the same manner as existing cases used nonfoaming liquids.

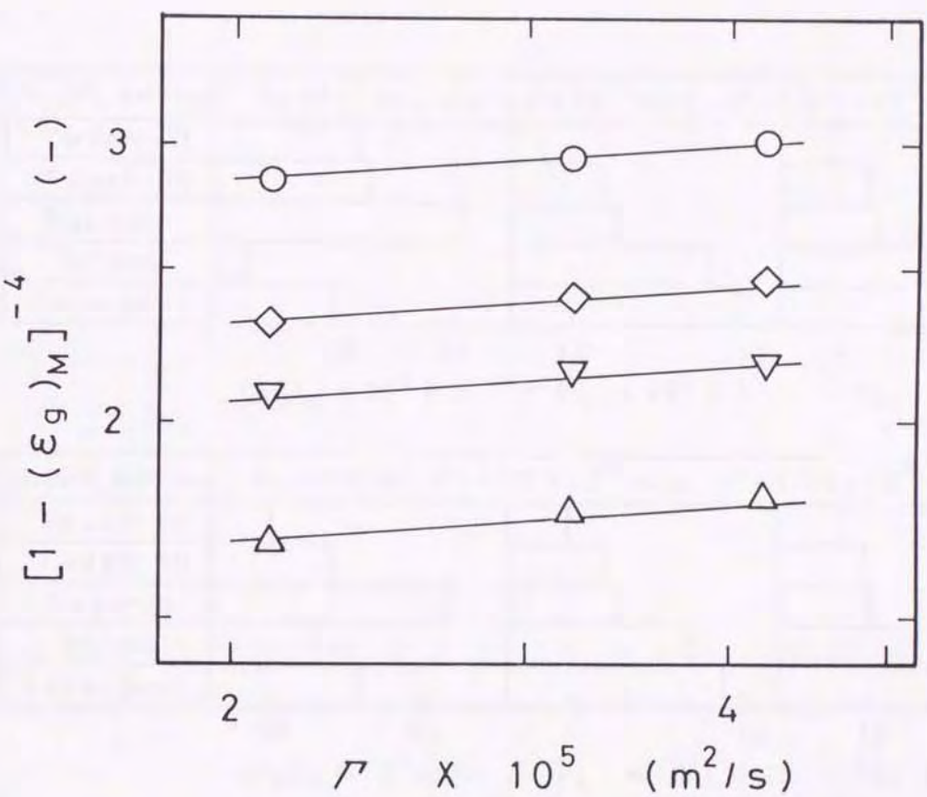

Figure 8-3. Relation between $[1-(\varepsilon_g)_M]^{-4}$ and Γ in MFS: △ Tween 40 solution, D_T=0.31m, U_g=2.0x10^{-2}m/s, ◇ ; Saponin solution, D_T=0.256m, U_g=3.0x10^{-2}m/s, ○ ; Detergent solution, D_T=0.19m, U_g=5.0x10^{-2}m/s, ▽ ; Tween 60 solution, D_T=0.19m, U_g=3.0x10^{-2}m/s.

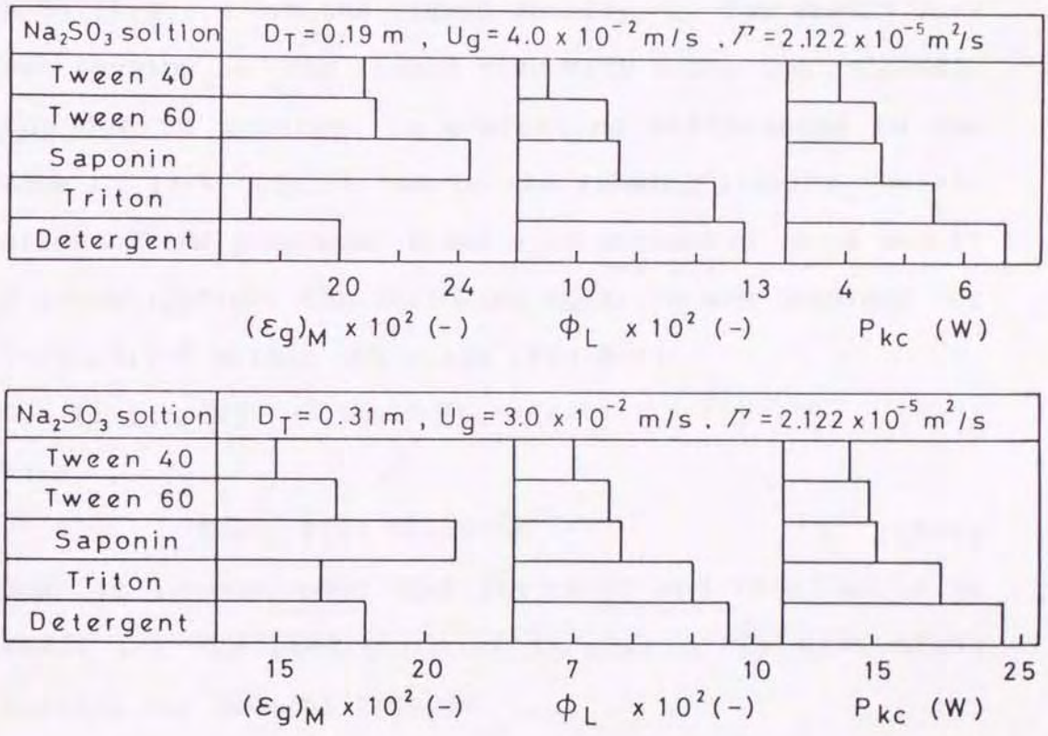

Figure 8-4. Relation among $(\varepsilon_g)_M$, ϕ_L and P_{kc}.

Gestrich and Rahse (Ref.53) have investigated the gas holdup in BCs treating different nonfoaming liquids. They showed that the dimensionless parameter K defined by Eq.(8-4), which reflects the effect of liquid property, was useful for the evaluation of differences in the gas holdup due to those of the liquid.

$$K=\rho\,\sigma^{3}/\mu^{4}g \qquad (8\text{-}4)$$

In Eq.(8-4), ρ is the liquid density, σ the liquid surface tension, μ the liquid viscosity and g the acceleration due to gravity. In evaluating differences in the value of $[1-(\varepsilon_g)_M]^{-4}$ due to the foaming liquids, utilization of the parameter K was also attempted. As a result of investigation, the following equation was obtained for $[1-(\varepsilon_g)_M]^{-4}$ within 20% error (Fig.8-5).

$$[1-(\varepsilon_g)_M]^{-4}=3.75\times10^{-7}U_g^{\,func.(K)}\Gamma^{0.06}K^{0.78} \qquad (8\text{-}5)$$

Where

$$func.(K)=1.91\times10^{-5}K^{0.44} \qquad (8\text{-}6)$$

Thus, it is concluded that Eqs.(8-5) and (8-6) would be useful for the prediction of $(\varepsilon_g)_M$ in BCs with MFRDs treating any foaming liquids.

8-3-3. Gas holdup in nonfoaming system and its correlation

For the effect of U_g on the gas holdup $(\varepsilon_g)_F$ in a nonfoaming system (NS), as seen in Fig.8-6, $(\varepsilon_g)_F$ tended to increase with increasing U_g. With respected to the effect of the liquid, in the same manner as cases observed for $(\varepsilon_g)_M$, there was a difference in the value of $(\varepsilon_g)_F$ depending on the liquids. The correlation of $(\varepsilon_g)_F$ in

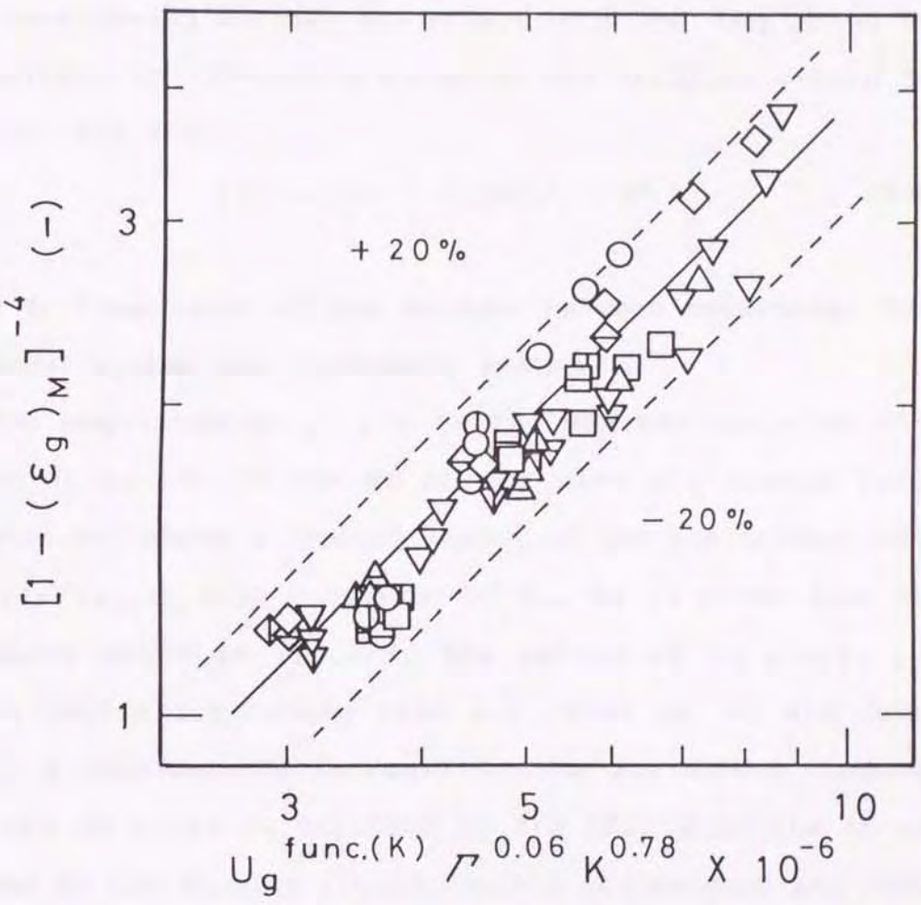

Figure 8-5. Final correlation of gas holdup in MFS: Detergent solution; D_T(m): ○ ; 0.19, ⊖ ; 0.256, ⊕ ; 0.31, Tween 60 solution; D_T(m): △ ; 0.19, ⧋ ; 0.256, ⧊ ; 0.31, Triton X-100 solution; D_T(m): □ ; 0.19, ⊟ ; 0.256, ⊞ ;0.31, Saponin solution; D_T(m): ◇ ; 0.19, ⧁ ; 0.256, ⧂ ; 0.31, Tween 40 solution; D_T(m): ▽ ; 0.19, ⧩ ; 0.256, ⧨ ; 0.31.

terms of U_g and the parameter K was then examined. Figure 8-7 shows the results of $[1-(\varepsilon_g)_F]^{-4}$ plotted vs. U_g with the liquid as a parameter. Their relationship was expressed in the form of Eq.(8-7) regardless of the liquid.

$$[1-(\varepsilon_g)_F]^{-4} \propto U_g^{0.18} \tag{8-7}$$

By considering further the effect of K and completing the equation, the following equation was obtained within 20% error (Fig.8-8).

$$[1-(\varepsilon_g)_F]^{-4}=1.04U_g^{0.18}K^{0.04} \tag{8-8}$$

8-3-4. Comparison of gas holdups between mechanical foam control system and nonfoaming system

The magnitude of $(\varepsilon_g)_M$ in the MFS was compared with that of $(\varepsilon_g)_F$ in the NS at the same air sparge rate. Figure 8-9 shows a typical result of the gas holdup ratio $(\varepsilon_g)_M/(\varepsilon_g)_F$ with variation of U_g. As is clear from the results shown in Fig.8-9, the values of $(\varepsilon_g)_M/(\varepsilon_g)_F$ were remarkably larger than 1.0. That is, it was found that a considerable increase in the gas holdup compared to the NS could be expected in the MFS. When the AF was added to the foaming liquid, bubble coalescence and large bubble formation were liable to occur. The main cause for smaller $(\varepsilon_g)_F$ compared to $(\varepsilon_g)_M$ may be attributed to the increased frequency of bubble coalescence in the NS.

8-4. Conclusions

For BCs treating various kinds of foaming liquids, the effects of operating conditions such as the U_g, D_T and the liquid on the gas holdup between BCs when the foaming

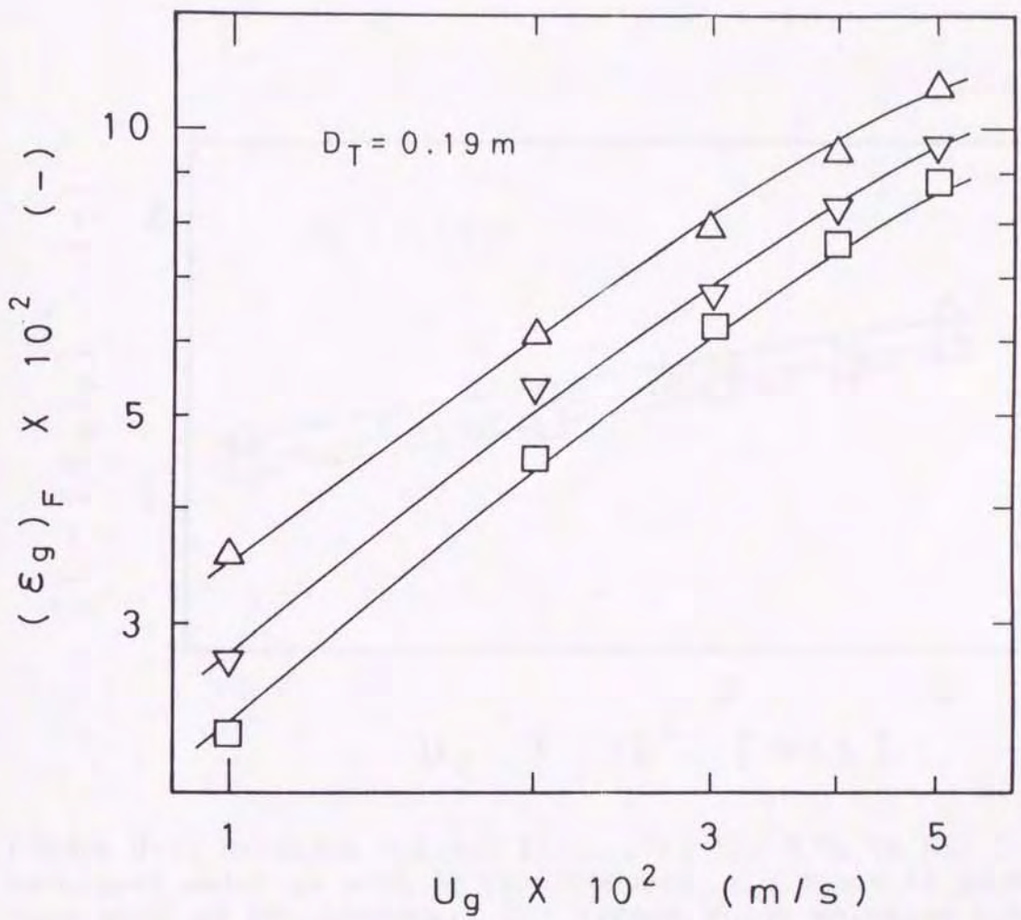

Figure 8-6. Effect of U_g on $(\varepsilon_g)_F$ in NS: D_T=0.19m: ▽ ; Tween 40 solution with AF (C_F=1000ppm), □ ; Triton X-100 solution with AF (C_F=1000ppm), △ ; Tween 60 solution with AF (C_F=1000ppm).

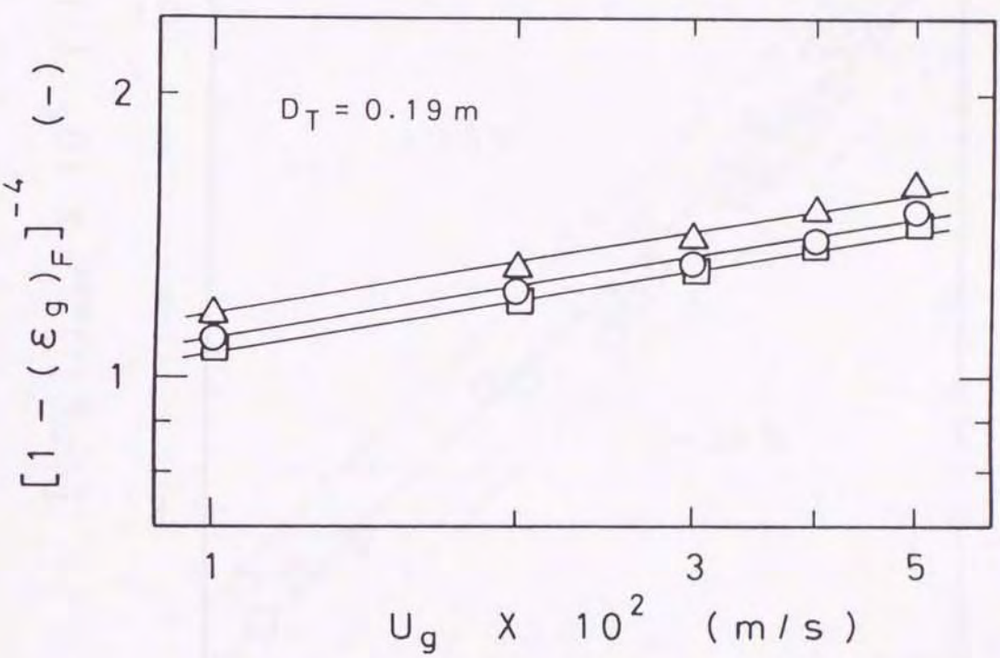

Figure 8-7. Relation between $[1-(\varepsilon_g)_F]^{-4}$ and U_g in NS: ○ ; Detergent solution with AF (C_F=1000ppm), △ ; Tween 60 solution with AF (C_F=1000ppm), □ ; Triton X-100 solution with AF (C_F=1000ppm).

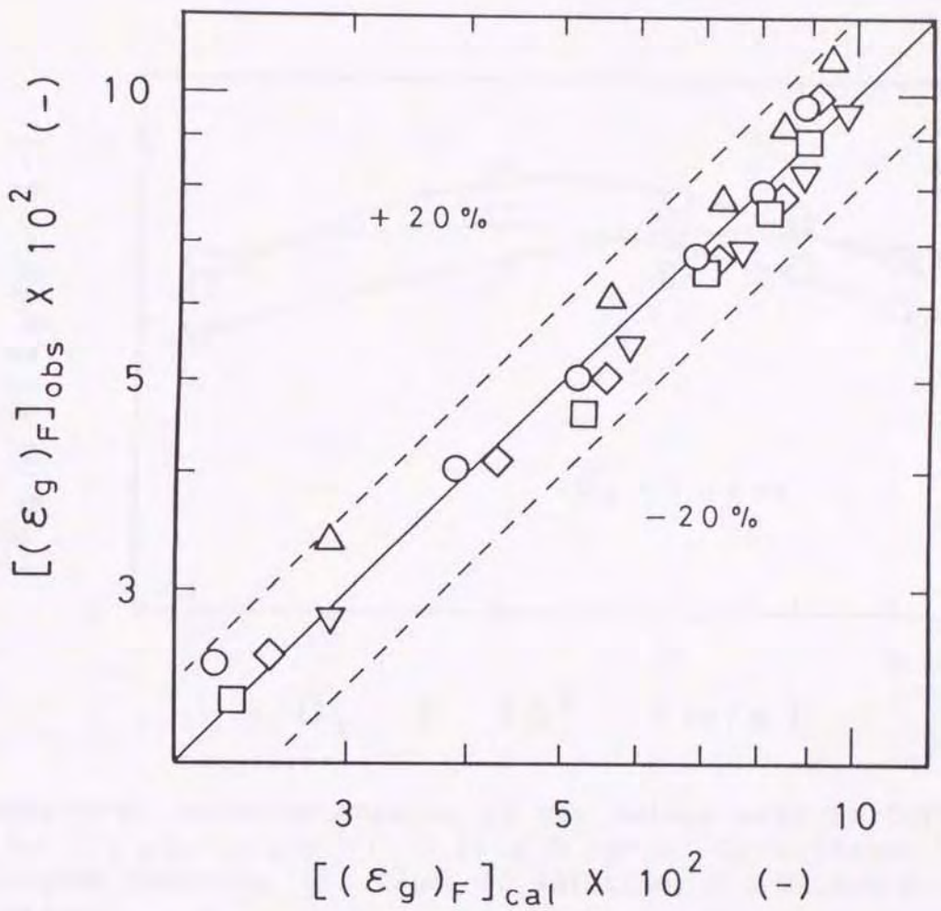

Figure 8-8. Comparison of observed and calculated values of $(\varepsilon_g)_F$ in NS: ○ ; Detergent solution with AF (C_F=1000ppm), △ ; Tween 60 solution with AF (C_F=1000ppm), ▽ ; Tween 40 solution with AF (C_F=1000ppm), □ ; Triton X-100 solution with AF (C_F=1000ppm), ◇ ; Saponin solution with AF (C_F=1000ppm).

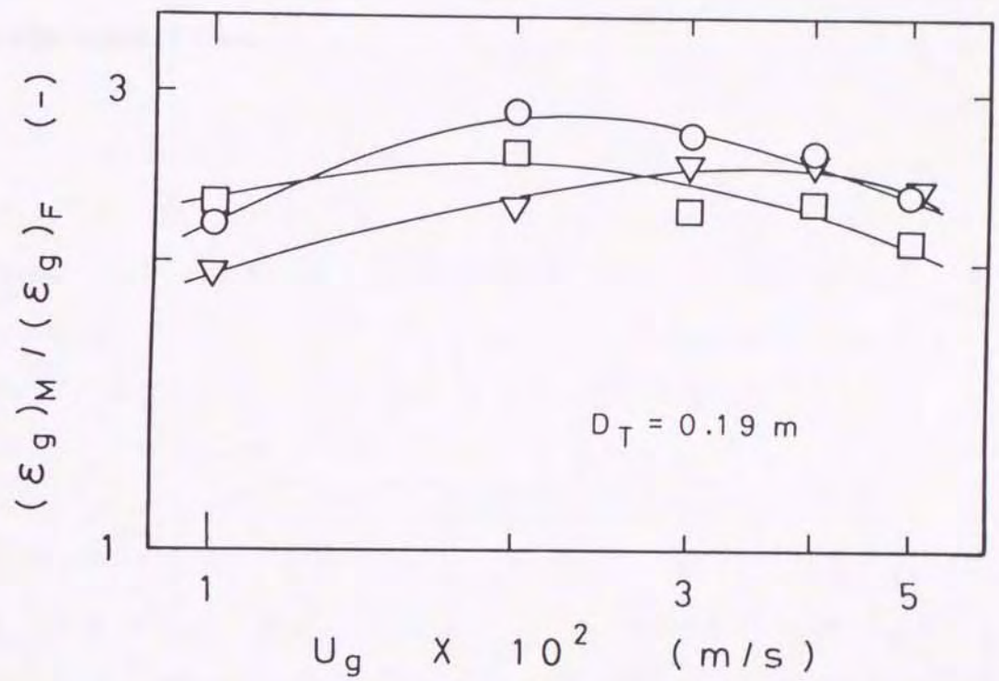

Figure 8-9. Relative changes of gas holdup with variation of U_g: $(\varepsilon_g)_M/(\varepsilon_g)_F$; Γ =2.122x10^{-5}m^2/s, C_F=1000ppm; ○ : Detergent solution, ▽ ; Tween 40 solution, □ ; Triton X-100 solution.

was controlled by the MFRD and the AF were evaluated. Eqs.(8-5) and (8-6) and Eq.(8-8) were obtained for gas holdups in the mechanical foam-control system (MFS) and those in the nonfoaming system(NS) including the AF, respectively. It was also clarified quantitatively that the gas holdup $(\varepsilon_g)_M$ in the MFS was large compared to the gas holdup $(\varepsilon_g)_F$ in the NS under the same aeration rate conditions.

CHAPTER 9

VOLUMETRIC LIQUID-PHASE MASS TRANSFER COEFFICIENTS IN BUBBLE COLUMNS UNDER FOAM CONTROL

9-1. Introduction

Many studies have been dealt with the volumetric liquid-phase mass transfer coefficient $k_L a$ in bubble columns (BCs) (Refs.4, 5, 33, 40, 48, 55, 63, 75, 79, 90, 99, 102). Reviewing these existing studies, however, most of their works were carried out in BCs without foaming. Thus, useful information is available on such nonfoaming systems. In contrast, there are few studies in which $k_L a$ in BCs with a foaming system was investigated. As for the effect of antifoam agents (AFs) on $k_L a$, studies on $k_L a$ for systems other than nonfoaming liquids are also scarce and no reliable information is yet available. Under the situation that basic information on $k_L a$ in a foaming system was lacked, BCs with a foaming system at present seen to have been operated on the basis of the results of nonfoaming systems. However, direct application of the results of nonfoaming systems to a BC with a foaming system leads to unproper design and operation of the BC under foam control. That suggests the necessity of carrying out a systematic study on $k_L a$ of the BC under foam control. In chapter 3, it was demonstrated that $k_L a$ in a mechanical foam control system (MFS) was larger than that in a nonfoaming system (NS) including AFs. However, it remains to be further investigated whether the similar results

may be obtained when various foaming liquids or BCs of different sizes were used. It is also necessary to compare $k_L a$ between the MFS and the NS when viewed from the specific power input.

In this chapter, for foaming systems using 0.15M sodium sulfite solutions containing various foaming agents, $k_L a$s when the foaming in the BC is controlled by the MFRD and an AF are examined. Their differences are also discussed in relation to those in the specific power input.

9-2. Experimental

A schematic flow diagram of the experimental set-up is shown in Fig.9-1. Three BCs, 0.19, 0.256 and 0.31m in diameter D_T, were employed. Operational conditions are the same as those in the preceding chapter. As the foaming liquids, five kinds of 0.15M sodium sulfite solutions containing foaming agents shown in Table 8-1 in the preceding chapter were used. These same solutions to which an AF, silicon oil (KM-70) was added at a concentration of 1000ppm, were used as the nonfoaming liquids.

The volumetric liquid-phase mass transfer coefficient $k_L a$ was measured by the sulfite oxidation method using 0.15M sodium sulfite solution, pH 8.0, and containing 1.0×10^{-4}M copper sulfate. Values of $k_L a$, with respect to the unit volume of clear liquid, were calculated by the following formula:

$$-dC_{ss}/dt = 2k_L ap/H \qquad (9\text{-}1)$$

where dC_{ss}/dt is the slope of the concentration-time plot, p the partial pressure of oxygen and H the Henry's

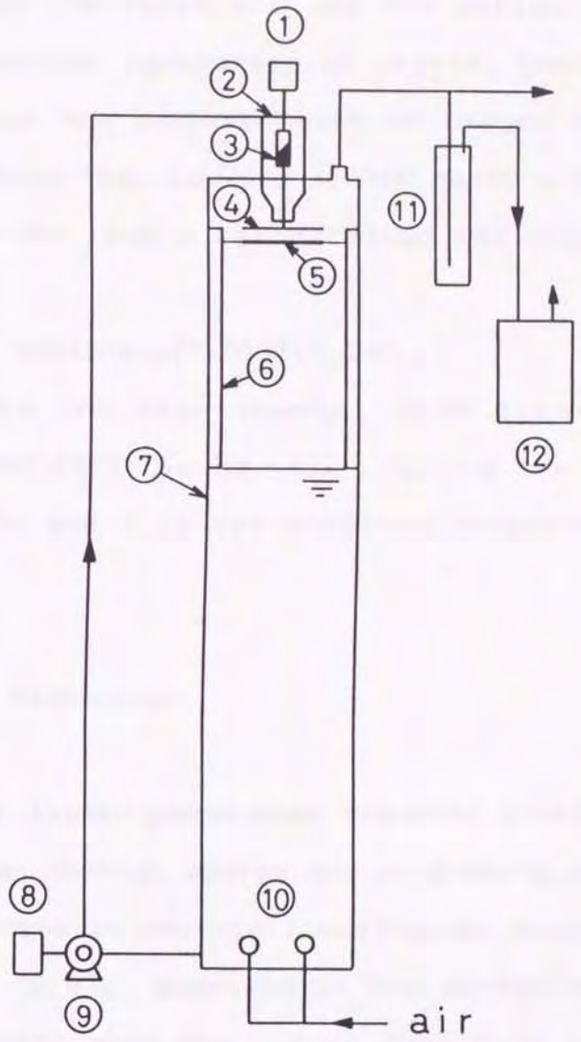

Figure 9-1. Schematic flow diagram of experimental apparatus: (1)motor, (2)liquid feeder, (3)torque meter, (4)rotating disk, (5)fixed disk, (6)baffle plate, (7)bubble column, (8)flow controller, (9)pump, (10)ball sparger, (11)drain pot, and (12)oxygen analyzer.

law constant. The concentration of Na_2SO_3 was determined by iodometry. The logarithmic mean of the partial pressure of oxygen in the inlet air and the outlet gas was adopted as the partial pressure p of oxygen. The partial pressure of oxygen was measured with an oxygen analyzer (Model LF-700, Toray Eng. Co. Ltd.). The Henry's constant H for oxygen in the liquid being tested was calculated from,

$$H=1.68\times10^{3}\exp(0.013T+0.94C_{ss}) \qquad (9\text{-}2)$$

which was fit to the experimental data reported by Richard et al (Ref.111). In Eq.(9-2), C_{ss} is the concentration of Na_2SO_3 and T is the absolute temperature of the liquid.

9-3. Results and Discussion

9-3-1. Volumetric liquid-phase mass transfer coefficients in mechanical foam control system and nonfoaming system

The results of the volumetric liquid-phase mass transfer coefficient, $(k_La)_M$, measured in the mechanical foam control system (MFS) when the liquid feed rate per unit disk circumference, Γ, was varied, are shown in Fig.9-2. The value of $(k_La)_M$ tended to increase slightly with increasing Γ. It is generally known that in BCs with liquid recirculation higher values of $(k_La)_F$ compared to those without liquid circulation can be expected. The results shown in Fig.9-2 may be attributed to the effect of the increased liquid circulation rate of the liquids in BCs due to increase of Γ.

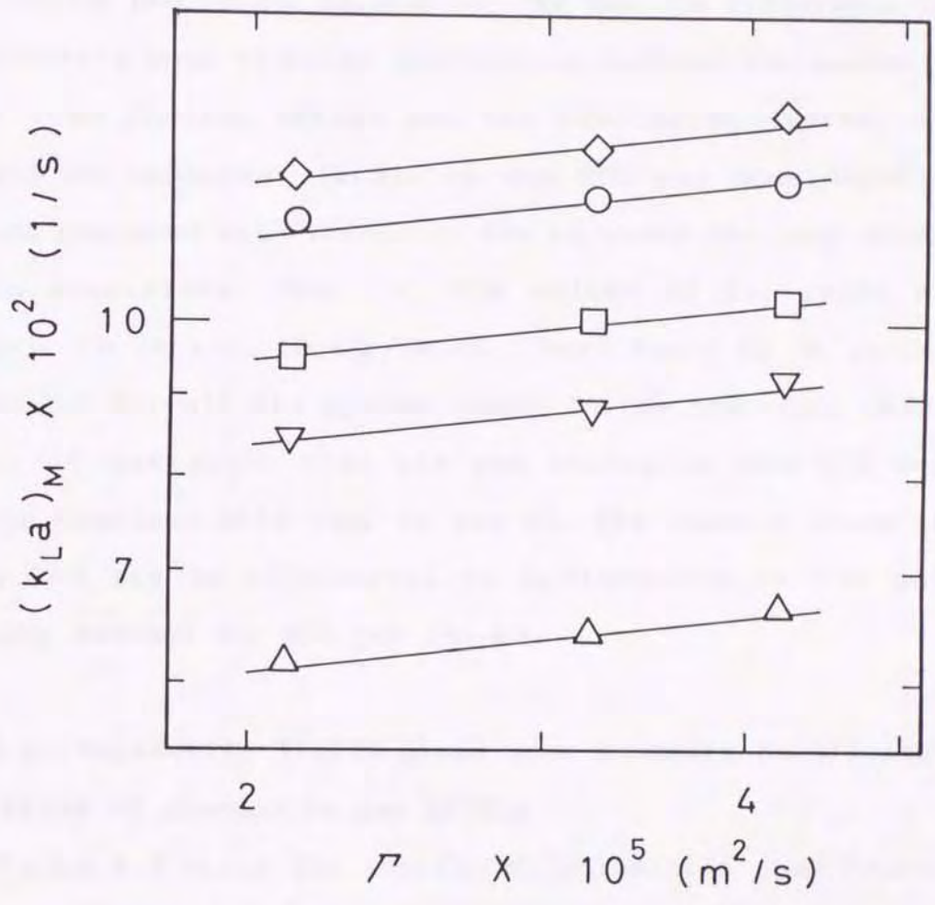

Figure 9-2. Effect of Γ on $(k_La)_M$ in MFS: △ ; Detergent solution, D_T=0.19m, U_g=1.0x10^{-2}m/s, □ ; Detergent solution, D_T=0.19m, U_g=2.0x10^{-2}m/s, ○ ; Detergent solution, D_T=0.19m, U_g=5.0x10^{-2}m/s, ◇ ; Saponin solution, D_T=0.256m, U_g=3.0x10^{-2}m/s, ▽ ; Tween 40 solution, D_T=0.31m, U_g=2.0x10^{-2}m/s.

The changes of $(k_La)_M$ with varying U_g are shown in Fig.9-3. The data of the volumetric liquid-phase mass transfer coefficient $(k_La)_F$, measured in the nonfoaming system (NS) are also shown in Fig.9-3. The effect of U_g on $(k_La)_M$ and $(k_La)_F$ is similar. As for the difference in volumetric mass transfer coefficient between the mechanical foam control system and the nonfoaming system, as might be expected, $(k_La)_M$ in the MFS was considerably large compared with $(k_La)_F$ in the NS under the same aeration conditions. That is, the values of the ratio of $(k_La)_M$ to $(k_La)_F$, $(k_La)_M/(k_La)_F$, were found to be larger than 1.0 for all the systems used. In the preceding chapter, it was shown that the gas holdup in the MFS was large compared with that in the NS. The results shown in Fig.9-3 may be attributed to differences in the gas holdup between the MFS and the NS.

9-3-2. Volumetric liquid-phase mass transfer coefficient in terms of changes in gas holdup

Figure 9-4 shows the results of volumetric mass transfer coefficients $(k_La)_M$ and $(k_La)_F$ in the MFS and the NS, in which $(k_La)_M$ and $(k_La)_F$ are plotted vs. the gas holdups $(\varepsilon_g)_M$ and $(\varepsilon_g)_F$ measured under corresponding operating conditions. It is found that k_La values in the MFS are considerably high compared with those in the NS at the same level of ε_g. In the MFS, the bubble size is considerably smaller and distribution of bubbles is almost uniform regardless of the liquids. However, in the NS, bubble coalescence occurs frequently and as a result

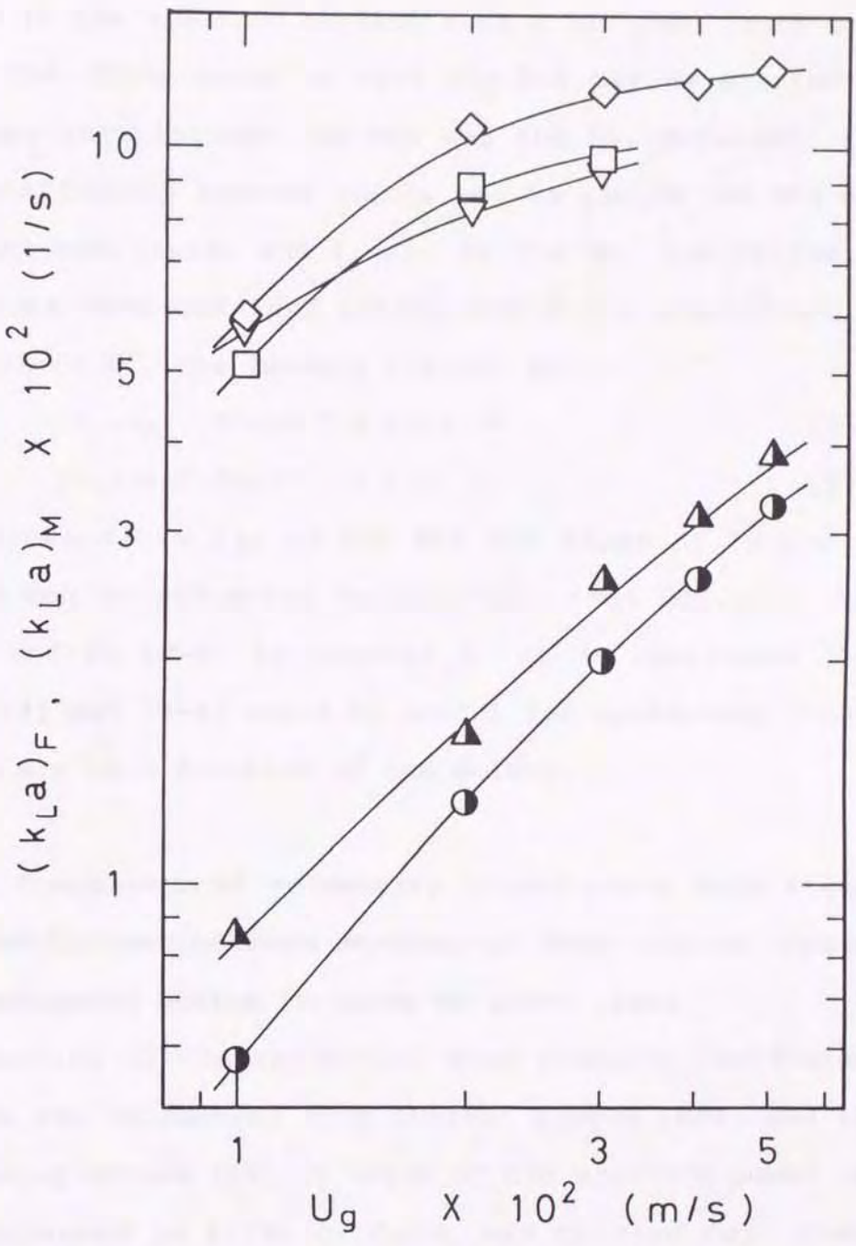

Figure 9-3. Effect of U_g on $(k_La)_M$ in MFS and $(k_La)_F$ in NS: ◇ ; Saponin solution, D_T=0.19m, Γ =2.122x10^{-5}m^2/s, □ ; Triton X-100 solution, D_T=0.31m, Γ =2.122x10^{-5}m^2/s, ▽ ; Tween 40 solution, D_T=0.256m, Γ =2.122x10^{-5}m^2/s, ◭ ; Tween 60 solution with AF (C_F=1000ppm), D_T=0.19m, ◑ ; Detergent solution with AF (C_F=1000ppm), D_T=0.19m.

large bubble formation is observed. This results in a decrease in the specific surface area a for gas-liquid contact. The differences as seen Fig.9-4 may be attributed to those in a between the MFS and the NS. Moreover, for the relationship between $(k_L a)_M$ and $(\varepsilon_g)_M$ in the MFS and that between $(k_L a)_F$ and $(\varepsilon_g)_F$ in the NS, the following equations were obtained within 20% error regardless of the size of BC, the foaming liquid, etc.

MFS; $$(k_L a)_M = 2.46 \times 10^{-1} (\varepsilon_g)_M^{0.49} \quad (9\text{-}3)$$

NS; $$(k_L a)_F = 7.35 \times 10^{-1} (\varepsilon_g)_F^{1.33} \quad (9\text{-}4)$$

The values of $(\varepsilon_g)_M$ in the MFS and those of $(\varepsilon_g)_F$ in the NS can be estimated respectively from Eqs.(8-5) and (8-6) and Eq.(8-8) in chapter 8. It is concluded that Eqs.(9-3) and (9-4) would be useful for predicting $(k_L a)_M$ and $(k_L a)_F$ as a function of gas holdup.

9-3-3. Comparison of volumetric liquid-phase mass transfer coefficient between mechanical foam control system and nonfoaming system in terms of power input

Comparison of the volumetric mass transfer coefficient between the mechanical foam control system (MFS) and the nonfoaming system (NS) in terms of the specific power input expressed as P_T/V_L or P_g/V_L was carried out. Power input P_T in the MFS was evaluated as the sum of the power P_{kc} for foam-breaking and the power P_g for gas input. The pneumatic power P_g of the gas input was taken as that due to isothermal expansion of the gas. Figure 9-5 shows the results of $(k_L a)_M$ plotted vs. P_T/V_L and those of $(k_L a)_F$ plotted vs. P_g/V_L. As seen in the figure, in the rela-

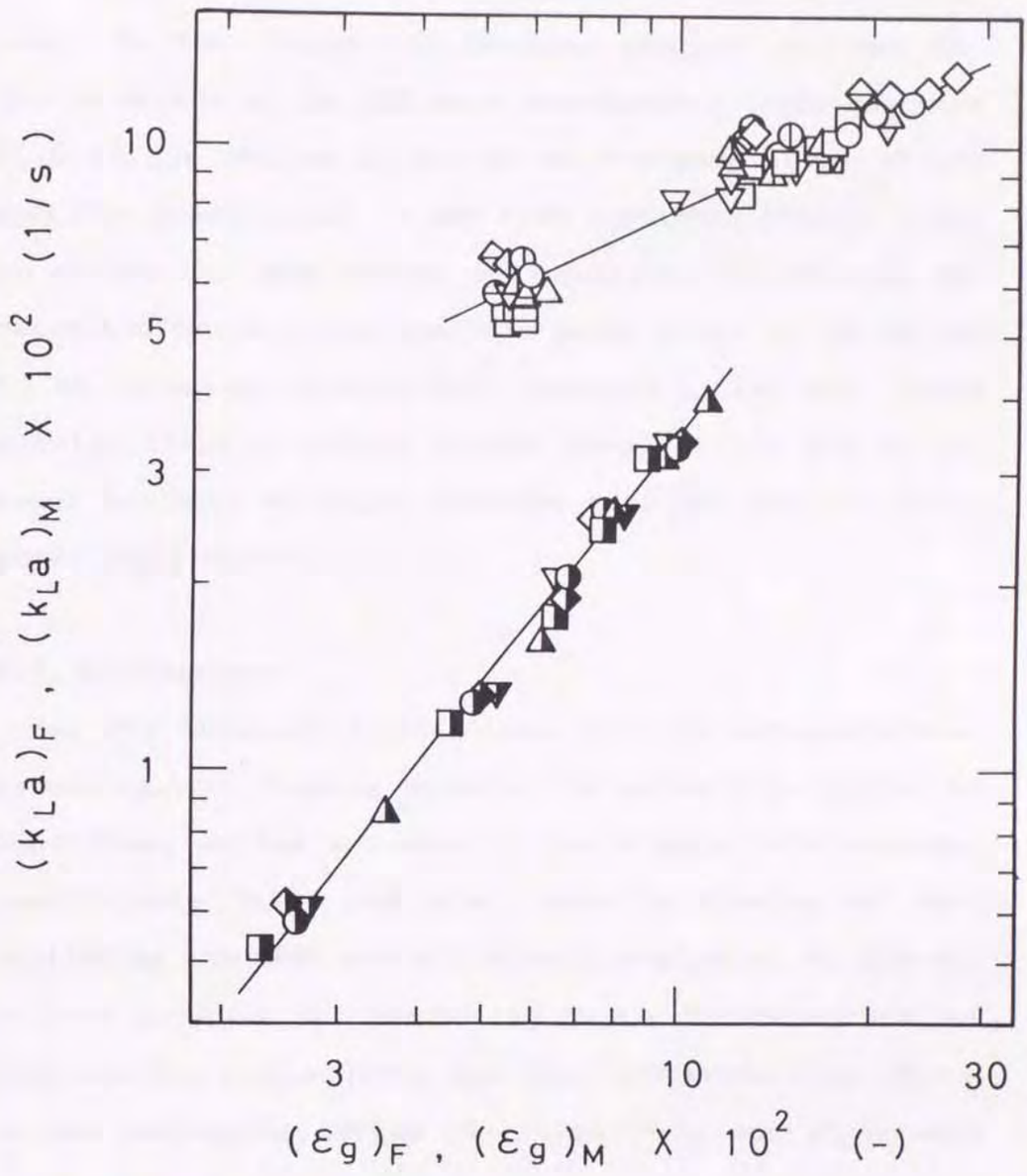

Figure 9-4. Relation between k_La and ε_g with and without addition of AF: MFS; Detergent solution; D_T(m): ○ ; 0.19, ⊖ ; 0.256, ◍ ; 0.31, Tween 60 solution; D_T(m): △ ; 0.19, ◬ ;0.256, ◭ ; 0.31, Tween 40 solution; D_T(m): ▽ ; 0.19, ▽ ; 0.256, ▼ ; 0.31, Triton X-100 solution; D_T(m): □ ; 0.19, ⊟ ; 0.256, ◫ ; 0.31, Saponin solution; D_T(m): ◇ ; 0.19, ◈ ; 0.256, ◆ ; 0.31, NS; D_T=0.19m: ◑ ; Detergent solution with AF (C_F=1000ppm), ◭ ; Tween 60 solution with AF (C_F=1000ppm), ▼ ; Tween 40 solution with AF (C_F=1000ppm), ◧ ; Triton X-100 solution with AF (C_F=1000ppm), ◆ ; Saponin solution with AF (C_F=1000ppm).

tionship between $(k_La)_M$ and P_T/V_L or that between $(k_La)_F$ and P_g/V_L, there were little differences due to the liquids. As for comparison between the MFS and the NS, $(k_La)_M$ values in the MFS were considerably large compared with $(k_La)_F$ values in the NS at the same level of the specific power input. It was also confirmed that in order to obtain the same values of volumetric coefficient between the two BCs, the specific power input in the NS had to be increased considerably compared to the MFS. These results clearly support higher level of the MFS in respect not only to oxygen transfer rate but also to saving power requirements.

9-4. Conclusions

For BCs treating 0.15M sodium sulfite solutions contained various foaming agents, the effects of operating conditions on the volumetric liquid-phase mass transfer coefficients $(k_La)_M$ and $(k_La)_F$ when the foaming was controlled by the MFRD and the AF were evaluated. As the empirical equation for predicting $(k_La)_M$ in the mechanical foam-control system (MFS) and that for predicting $(k_La)_F$ in the nonfoaming system (NS), Eqs.(9-3) and (9-4) were obtained respectively. From a comparison of the volumetric liquid-phase mass transfer coefficient between the MFS and the NS in terms of the specific power input, it was also confirmed that the MFS was superior to the NS, not only in oxygen transfer performance but also in power input economy.

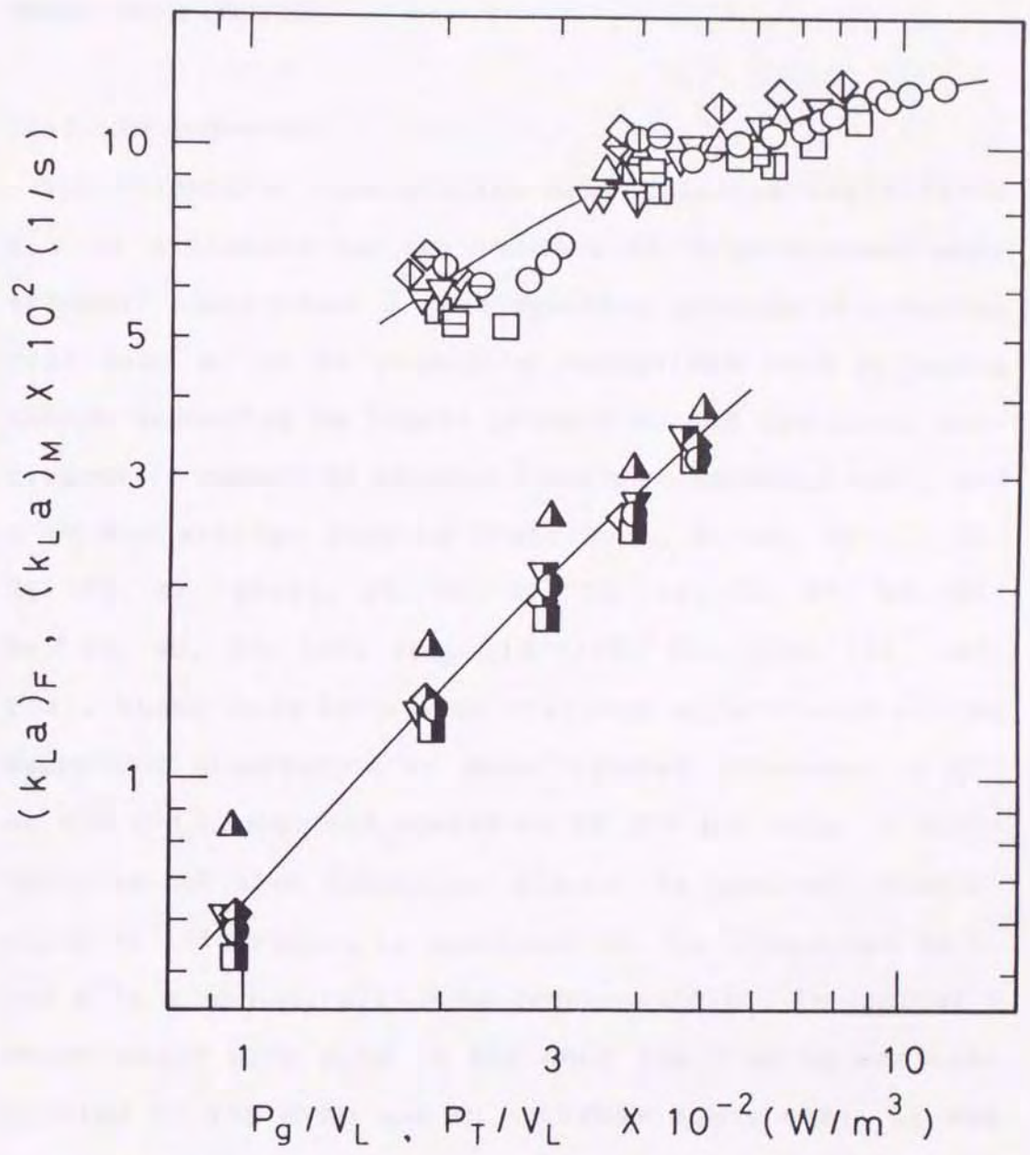

Figure 9-5. Comparison of k_La with and without addition of AF in terms of specific power input (keys are the same as in Fig.9-4).

CHAPTER 10

LIQUID-PHASE MASS TRANSFER COEFFICIENTS IN BUBBLE COLUMNS UNDER FOAM CONTROL

10-1. Introduction

The volumetric liquid-phase mass transfer coefficient k_La is expressed as the product of liquid-phase mass transfer coefficient k_L and specific gas-liquid interfacial area a. It is generally recognized that k_L and a change depending on liquid properties and operating conditions. A number of studies have been reported on k_L and a in BCs without foaming (Refs.3, 6, 8, 16, 25-27, 32, 36, 39, 41, 45-47, 50, 66, 67, 72, 74, 76, 77, 80, 83, 88, 89, 93, 97, 100, 103, 110, 118, 121, 124, 132, 142, 143). These data have been utilized effectively as the bases for elucidation of mass transfer processes in BCs or for the design and operation of BCs not only in laboratories but also industrial plants. In contrast, practically no information is available in the literature on k_L and a in a mechanically foam controlling BC. In chapter 9 which dealt with k_La as in BCs when the foaming was controlled by the MFRD and an antifoam agent (AF), it was shown that the volumetric mass transfer coefficient $(k_La)_M$ in the mechanical foam-control system (MFS) was considerably large compared with the volumetric mass transfer coefficient $(k_La)_F$ in the nonfoaming system (NS) at the same aeration rate conditions. This difference is considered to be related to either the effect of k_L or

that of a. In order to clarify their effect, however, it is necessary to discuss separately the magnitude of k_L and a which are the constituent parameters of the volumetric liquid-phase mass transfer coefficient.

In this chapter, changes in the bubble diameter in BCs when the foaming was controlled by the MFRD and an AF are first measured. The magnitude of the specific gas-liquid interfacial area in respective foam control systems are then evaluated, by using these results and those of the gas holdup measured in chapter 8. The value of the liquid-phase mass transfer coefficient k_L is also determined from the value of a and that of $k_L a$ obtained in the preceding chapter. Furthermore, on the basis of the above results, difference in the oxygen transfer performance between BCs when the foaming was controlled by the MFRD and the AF is discussed. Correlations for k_L in these mechanical foam control and nonfoaming systems are also attempted to establish.

10-2. Experimental

A schematic flow diagram of the experimental apparatus used in this experiment is shown in Fig.10-1. A BC, 0.19m in diameter D_T, were used. Operational condition, the foaming and nonfoaming liquids used, etc. are the same as those in the preceding chapter. Photographs of bubbles in the nonfoaming system (NS) including the AF were taken through a transparent viewing box filled with water. The bubble shape could be approximated by a spheroid. The volume-surface mean bubble diameter was calculated from

$$d_{vs}=6\sum_{j=1}^{n} v_{bj}/\sum_{j=1}^{n} s_{bj} \qquad (10\text{-}1)$$

In the mechanical control system (MFS), it was difficult to take photographs through the viewing box, i.e., to obtain clear picture of bubbles, because of presence of large amounts of very fine bubbles. The size of bubbles in the MFS, the shape of which was close to a sphere, was therefore measured by means of microphotography, the method of which was similar by Yoshida and Yamada (Ref. 144). Liquid samples contained fine bubbles were withdrawn through a tube from the column, and passed through a photographic section (Fig.10-1), to which a microscope and a camera were attached. It took 1 to 2 seconds for the sample to reach the photographic section. When a photograph was taken, the flow of sample was stopped for a brief period by closing the cock attached to the outlet. It was ascertained beforehand that no coalescence or break-up of bubbles occurred. The specific gas-liquid interfacial area per unit volume of the liquid was evaluated from

$$a=6\varepsilon_g/d_{vs} \qquad (10\text{-}2)$$

The liquid-phase mass transfer coefficient k_L was obtained from the following relation, using the value of a and that of $k_L a$.

$$k_L=k_L a/a \qquad (10\text{-}3)$$

10-3. Results and Discussion

10-3-1. Change in specific gas-liquid interfacial area

Using the value of the measured bubble diameter and

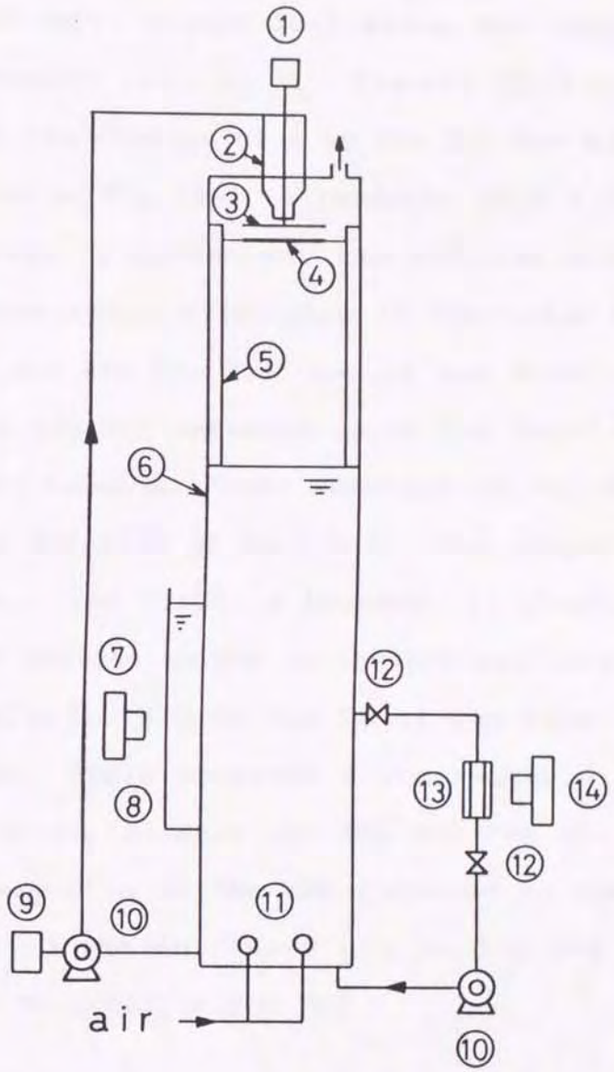

Figure 10-1. Schematic flow diagram of the experimental apparatus: (1)motor, (2)liquid feeder, (3)rotating disk, (4)fixed disk, (5)baffle plate, (6)bubble column, (7)camera, (8)viewing box, (9)flow controller, (10)pump, (11)ball sparger, (12)cock, (13)photographic section, and (14)microscope and camera.

that of corresponding gas holdup obtained in chapter 8, the specific surface area a was evaluated for the MFS and the NS respectively. Figure 10-2 shows the results of a plotted vs. the gas velocity U_g. Figures 10-2(a) and 10-2(b) represent the changes of a in the MFS and NS respectively. As seen in Fig.10-2, a tendency that a increases when U_g is large is common for the systems tested. But there was a remarkable difference in the value of a between the MFS and the NS. That is, it was found that the values of a in the MFS amounted up to the level of about thirty to sixty times as those observed in the NS. As is clear from the relation of Eq.(10-2), the larger ε_g and the smaller d_{vs}, the larger a becomes. In chapter 8, it was shown that the gas holdup in the MFS was considerably large compared with that in the NS at the same aeration rate conditions. There observed a remarkable difference in the value of d_{vs} between the MFS and the NS. Remarkably high values of a in the MFS compared to the NS may be attributed to the increased gas holdup and the decreased bubble diameter in the MFS.

10-3-2. Change in liquid-phase mass transfer coefficient

The liquid-phase mass transfer coefficient k_L was separated from k_La using the measured specific gas-liquid interfacial area. Figure 10-3 shows the results of liquid-phase mass transfer coefficient observed in the MFS and the NS plotted vs. the gas velocity U_g. The data observed in BCs without foaming are also shown for comparison. As seen in the figure, the effect of U_g on k_L in the present

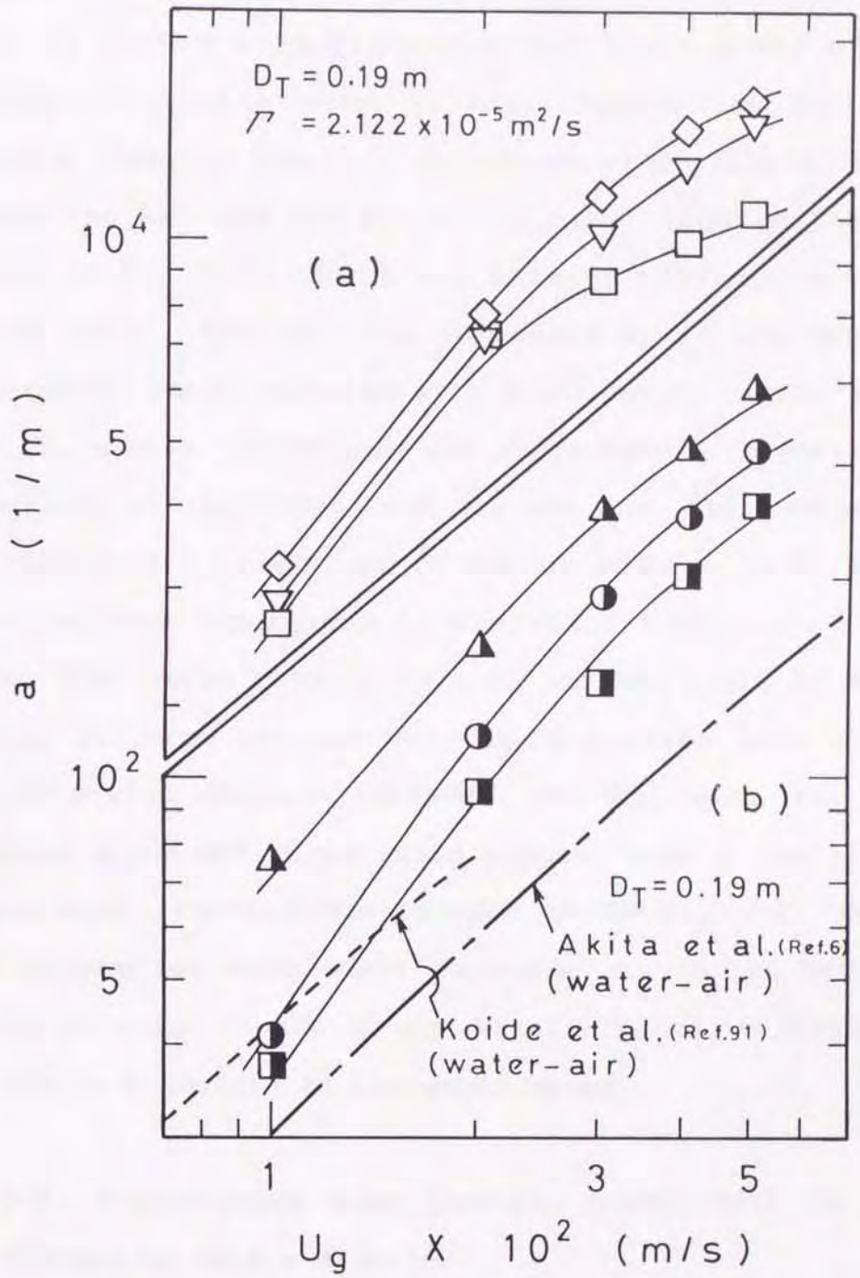

Figure 10-2. (a) Relation between a and U_g in MFS: ◇ ; Saponin solution, □ ; Triton X-100 solution, ▽ ; Tween 40 solution. (b)Relation between a and U_g in NS. ◭ ; Tween 60 solution with AF (C_F=1000ppm), ◑ ; Detergent solution with AF (C_F=1000ppm), ◨ ; Triton X-100 solution with AF (C_F= 1000ppm).

system is similar to that observed by Akita and Yoshida (Ref.6). It is also found that k_L in the NS is smaller than k_L in BCs without foaming but their order of magnitude is roughly equal to that observed by Akita and Yoshida (Ref.6). However, concerning comparison of k_L between the MFS and the NS, as is clear from the results shown in Fig.10-3, there was a large difference in the value of k_L. That is, the values of k_L in the MFS were remarkably small compared with those of k_L in the NS. In the NS, bubble coalescence and large bubble formation are observed. On the other hand, in the MFS, the bubble size is considerably small and distribution of bubbles is almost uniform regardless of operation conditions. It is known that large bubbles have no surface rigidity due to mobile surfaces whereas very small bubbles have surface rigidity with immobile surfaces, and that such very small bubbles which behave as solid spheres have a low liquid-phase mass transfer coefficient (Refs.80, 124). One of the causes for very small values of k_L in the MFS compared to those in the NS may be attributed to difference in bubble diameters as discussed above.

10-3-3. Liquid-phase mass transfer coefficient in terms of changes in bubble diameter

Figure 10-4 shows liquid-phase mass transfer coefficients in the MFS and the NS plotted vs. d_{vs}, compared with the data of other authors (Refs.6, 8, 27, 45, 46, 93) who dealt with the system using nonfoaming liquids. As can be seen from the results shown in Fig.10-4, the

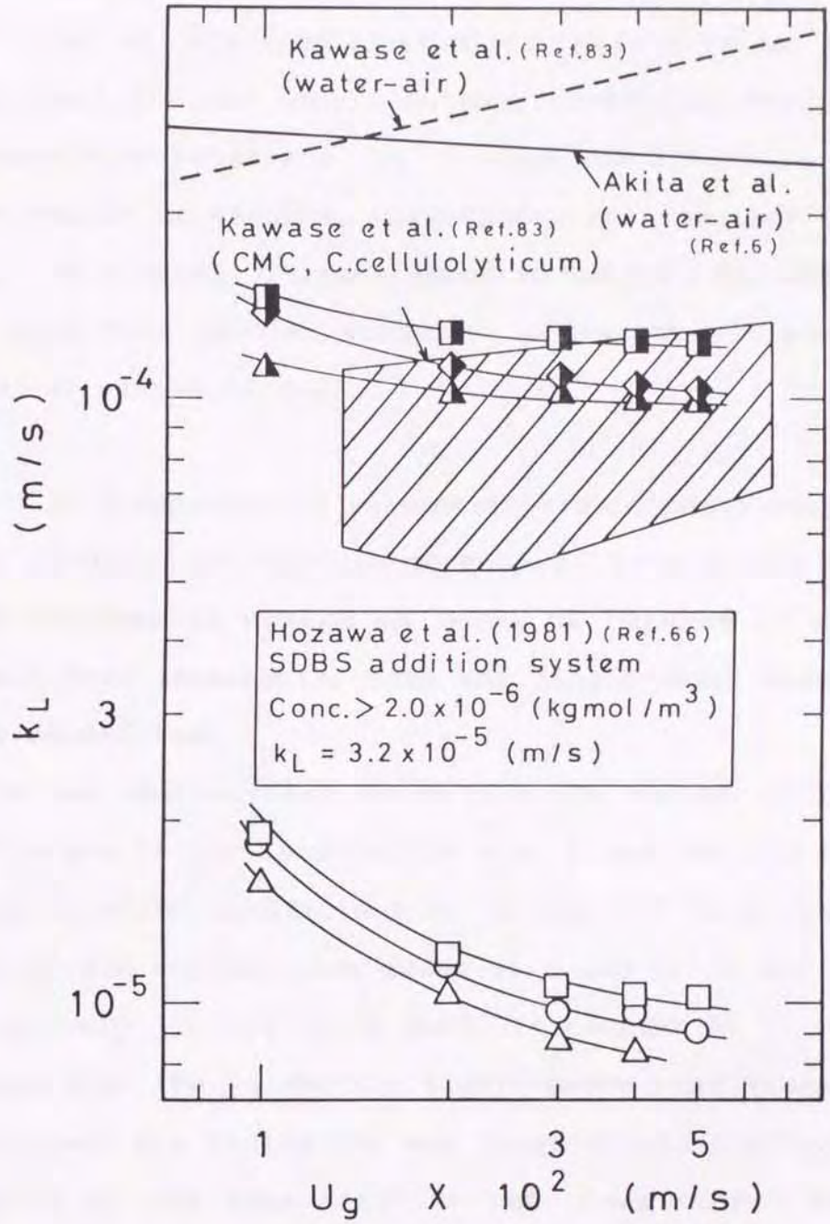

Figure 10-3. Relation between k_L and U_g in MFS and NS: MFS; D_T=0.19m, Γ =2.122x10^{-5}m^2/s: ○ ; Detergent solution, △ ; Tween 60 solution, □ ; Triton X-100 solution, NS; D_T=0.19m: ◑ ; Saponin solution with AF (C_F=1000ppm), ◨ ; Triton X-100 solution with AF (C_F=1000ppm), ◭ ; Tween 60 solution with AF (C_F=1000ppm).

changes in k_L with variation of d_{vs} in the NS are similar to those observed by Akita and Yoshida (Ref.6), Fujie et al. (Ref.46) who used electrolytic solutions and Koide et al. (Ref.93) who used solutions containing various surface-active materials. It is also found that in the MFS the region of small k_L corresponds well to that of small d_{vs}. This result is considered to support the above discussion that smaller values of k_L in the MFS are due to smaller values of d_{vs}.

10-3-4. Comparison of volumetric liquid-phase mass transfer coefficient between mechanical foam control system and nonfoaming system in terms of changes in specific gas-liquid interfacial area and liquid-phase mass transfer coefficient

It was demonstrated above that the values of the specific gas-liquid interfacial area a and the liquid-phase mass transfer coefficient k_L in the MFS were remarkably larger and smaller than those of a and k_L in the NS, respectively. On the other hand, in chapter 9, it was also shown that the volumetric liquid-phase mass transfer coefficient k_La in the MFS was large compared with that in the NS at the same aeration rate conditions. The difference in k_La are determined according to either those in a or those in k_L. Combining the k_La difference between the MFS and the NS and the above comparative results on a and k_L, the following is concluded: higher values of k_La in the MFS compared to the NS is mainly due to the effect of increased specific gas-liquid interfacial area.

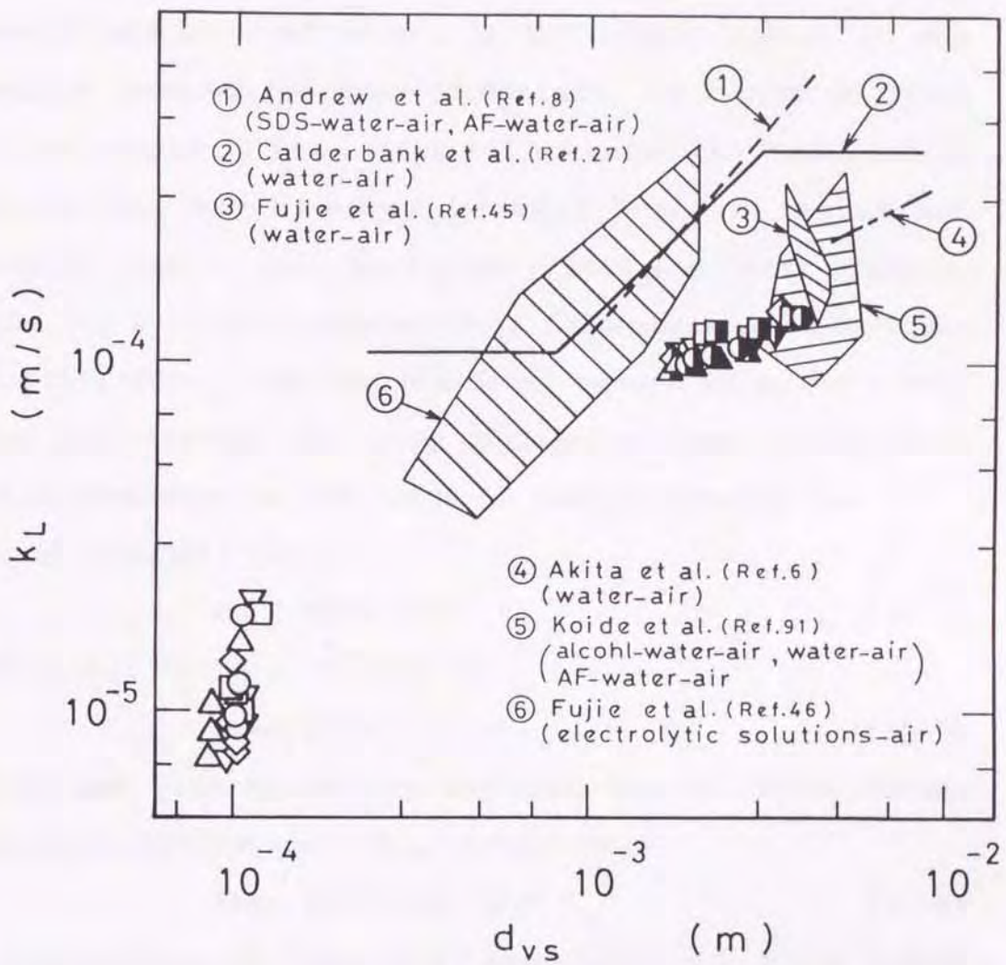

Figure 10-4. Relation between k_L and d_{vs} in MFS and NS: MFS; D_T=0.19m, Γ =2.122x10^{-5}m^2/s: ○ ; Detergent solution, △ ; Tween 60 solution, ▽ : Tween 40 solution, □ ; Triton X-100 solution, ◇ ; Saponin solution, NS; D_T=0.19m: ◑ ; Detergent solution with AF (C_F=1000ppm), ▲ ; Tween 60 solution with AF (C_F=1000ppm), ▼ ; Tween 40 solution with AF (C_F= 1000ppm), ◧ ; Triton X-100 solution with AF (C_F=1000ppm), ◭ ; Saponin solution with AF (C_F=1000ppm).

10-3-5. Correlation of liquid-phase mass transfer coefficient in mechanical control system and nonfoaming system

Although various types of correlations (Refs.6, 27, 67, 118) are available for the estimation of liquid-phase mass transfer coefficient k_L in bubble swarms in BCs without foaming (or foam formation), as listed in Table 2-5 of chapter 2, the empirical correlations developed by Calderbank and Moo-Young (Ref.27) and by Akita and Yoshida (Ref.6) have been widely used and their application has also been recommended. Calderbank and Moo-Young (Ref.27) found that two distinct regimes of k_L were evident and proposed two types of dimensionless correlations which dependent on the range of bubble diameter d_{vs}:

For $d_{vs} > 2.5\times10^{-3}$m;

$$Sh=0.42Sc^{1/2}Gr^{1/3} \qquad (10\text{-}4)$$

For $0.2\times10^{-3}\text{m} < d_{vs} < 0.6\times10^{-3}$m;

$$Sh=0.31Sc^{1/3}Gr^{1/3} \qquad (10\text{-}5)$$

Akita and Yoshida (Ref.6) obtained the following dimensionless correlation ($d_{vs} > 1.0\times10^{-3}$m):

$$Sh=0.5Sc^{1/2}Ga^{1/4}Bo^{3/8} \qquad (10\text{-}6)$$

Correlations of Eqs.(10-4) and (10-6) are first tested for the NS in Figs.10-5(a) and 10-5(b), respectively. The liquid-phase diffusivity D_L for oxygen in the liquid used was calculated from;

$$D_L=4.93\times10^{-14}\exp(3.61\times10^{-2}T - 2.44\times10^{-1}C_{ss}) \qquad (10\text{-}7)$$

which fitted to the experimental data reported by Richard et al (Ref.111).

For the changes of Sh in the NS, as can be seen from the results demonstrated in Figs.10-5(a) and 10-5(b),

direct application of Eq.(10-4) or (10-6) was difficult. Instead of them, by utilizing the results shown in each figure, Eq.(10-8) in terms of Sc and Gr or Eq.(10-9) in terms of Sc, Ga and Bo was obtained within 15% error, respectively.

$$Sh=3.34\times10^{-2}Sc^{1/2}Gr^{4/9} \qquad (10\text{-}8)$$

$$Sh=0.28Sc^{1/2}Ga^{1/4}Bo^{3/8} \qquad (10\text{-}9)$$

Antifoam agents has very complicated effects on oxygen transfer rates in bioreactors. The recent studies (Refs. 82, 137) have suggested that they may reduce mass transfer coefficient in the following two ways:

(1) interfacial blockage (increase in mass transfer resistance);

(2) hydrodynamic change (suppression of mobility of the surface).

The cause for lower values of Sh in the NS compared with those predicted with Eq.(10-4) or (10-6) is considered to be probably due to the difference of solutions used (solution with or without an added antifoam agent). Moreover, Eqs.(10-8) and (10-9) obtained in the above should be regarded as tentative correlations since they are based on limited data. In order to determine which type is more general correlation, further studies using a wider range or larger scales of liquid-phase physicochemical properties in the NS are needed.

On the other hand, as for the correlation of k_L in the MFS, as seen in Figs.10-6(a) and 10-6(b), it was difficult to correlate the observed data by Eq.(10-5) or Eq. (10-6). The same was also observed when the existing cor-

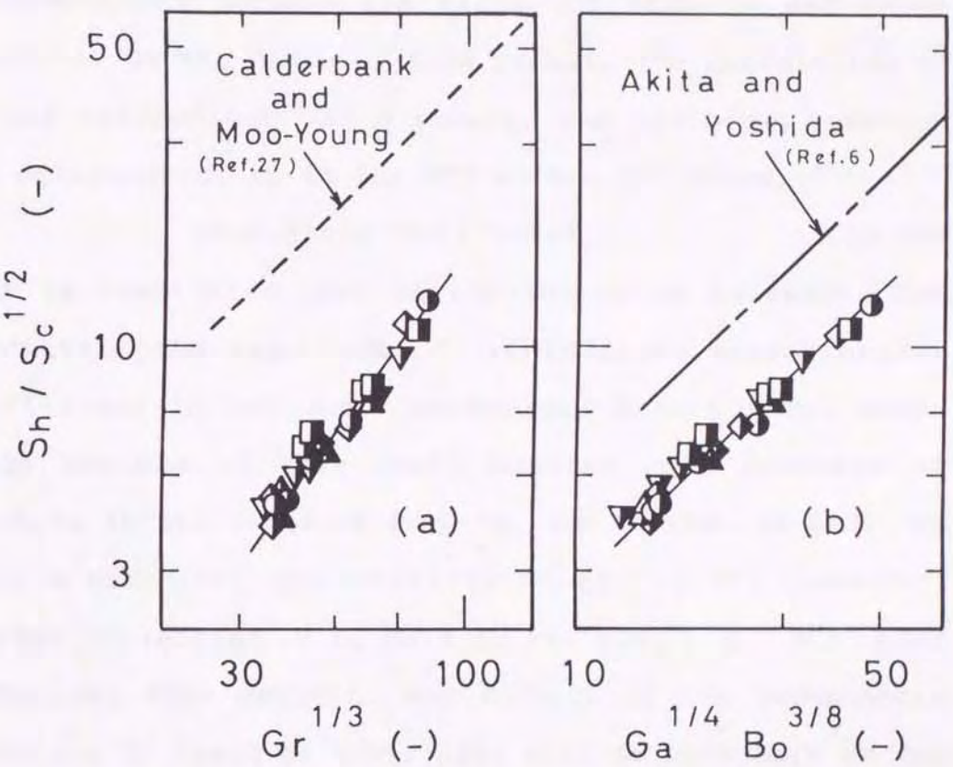

Figure 10-5. Correlation of k_L in NS. (a) Correlation of k_L with Eq.(10-4) (keys are the same as in Fig.10-4). (b) Correlation of k_L with Eq.(10-6) (keys are the same as in Fig.10-4).

relations other than Eqs.(10-5) and (10-6) were tested. These suggest that a new correlation equation for k_L in the MFS must be sought. According to the plot shown in Fig.10-6(a), it is found that although the number of data is not necessary sufficient there is a relatively good correspondence between the values of $Sh/Sc^{1/3}$ and those of $Gr^{1/3}$. On the basis of this result, the correlation of k_L was carried out. As a result, the following equation was obtained for k_L in the MFS within 35% error.

$$Sh=4.31\times10^{-3}Sc^{1/3}Gr^{4/3} \qquad (10\text{-}10)$$

It is considered that Eq.(10-10) would be usable for predicting the magnitude of liquid-phase mass transfer coefficient in BCs under mechanical foam control where large amounts of very small bubbles, the diameter of which is in the range of 1×10^{-4}m, are formed. In order to confirm universal applicability of Eq.(10-10), however, further collection of k_L data in the MFS, i.e., BCs under mechanical foam control, and recheck of the dependences of Sc and Gr based on their data will be necessary in the future.

10-4. Conclusions

The volumetric liquid-phase mass transfer coefficient k_La in BCs when the foaming was controlled by the MFRD and the AF was split into the specific gas-liquid interfacial area a and the liquid-phase mass transfer coefficient k_L. A comparative investigation of the magnitude of a and k_L between the MFS and the NS demonstrated that the values of a and k_L in the MFS were remarkably large and

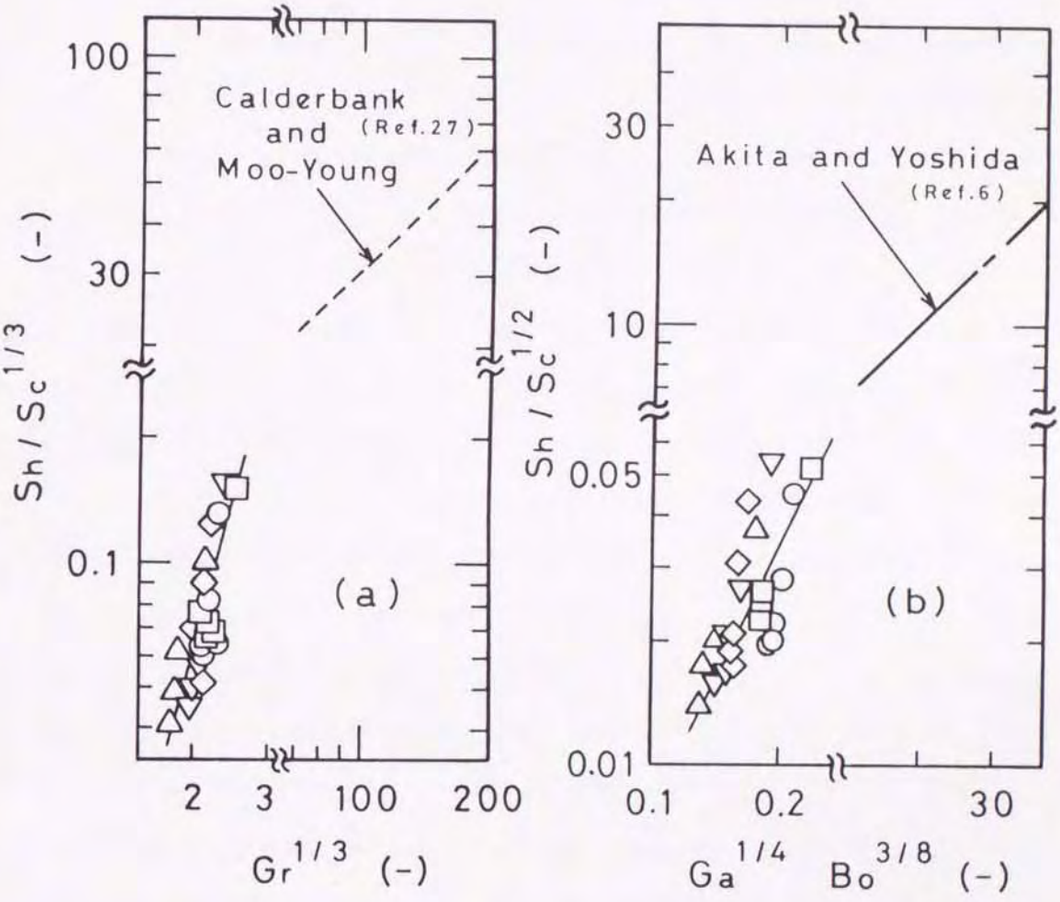

Figure 10-6. Correlation of k_L in MFS. (a) Correlation of k_L with Eq.(10-5) (keys are the same as in Fig.10-4).(b) Correlation of k_L with Eq.(10-6) (keys are the same as in Fig.10-4).

small compared with those of a and k_L in the NS respectively. It was also found that higher values of k_La in the MFS compared to the NS were due to the increased specific gas-liquid surface area. As the correlation for predicting k_L in the MFS and the NS, Eqs.(10-8) and (10-9) and Eq.(10-10) were obtained respectively.

CHAPTER 11

CONCLUDING REMARKS

Bubble column fermentors, i.e., bubble columns, have a wide range of applications in microbial process industries. These fermentors are especially preferred because of simplicity in construction and operation, low operating costs, etc. In aerobic fermentation operations using such a fermentor, a considerable amount of air is generally sparged into a process solution, which also results in formation of foam. Foam formation in submerged fermentation is not only a nuisance and health hazard but also adversely affects productivity and downstream processing. Therefore, it is essential to control the foam in some way. Mechanical control of fermentation foams has attracted fermentologic interest as the method that allows foam control without incurring the defects and disadvantages experienced in chemical foam control which is achieved with the addition of antifoam agents (AFs). Nevertheless, systematic studies seem not to have yet been carried out. As compared with remarkable progress in other fields of biotechnology and bioengineering, studies on design and operation of bubble column fermentors when the foaming is controlled by a mechanical foam-breaker are also lagged far behind. Under the circumstances, existing studies are almost none that can provide basic and practical data on the effect of factors such as the air sparge rate, the kind of foaming liquid, the nature of foam, etc. or on

the various characteristics such as the gas holdup, the volumetric liquid-phase mass transfer coefficient and the liquid-phase mass transfer coefficient in bubble column fermentors under foam control. This is also obvious from the fact that the usage of mechanical foam-breakers in bubble column fermentors is at present mostly empirical. The absence of basic approach naturally does not permit correct choice and operation of practical foam-breakers to be used actually. The lack of information on operational characteristics of bubble column fermentors under foam control results also in failure of their rational and successful design or effective operation.

In this study, systematic investigation into the above-mentioned fundamental and practical problems was undertaken from the engineering point of view in bubble column fermentors (i.e., bubble columns) using a rotating-disk mechanical foam-breaker (MFRD) which facilitated foam-breaking action by the impact between the dispersed liquid particles from the disk and the ascending foam. The results obtained in each chapter are first summarized, and the prospect of further studies as derived from a series of data obtained in this study is then outlined.

11-1. Conclusion of the study

Chapter 1 described the purpose and plan of the present study on the design and operation of bubble column fermentors under foam control and the construction of this thesis.

Chapter 2 reviewed the outline of the existing studies

on mechanical foam-breaking, various characteristics such as the gas holdup ε_g, the volumetric liquid-phase mass transfer coefficient k_La and the liquid-phase mass transfer coefficient k_L of bubble column fermentors (i.e., bubble columns) under foam control and so on. It revealed problems to be studied and showed the significance of the present study.

In chapter 3, as a step forward to a series of studies on various characteristics of bubble columns (BCs) under foam control, foam-breaking performance of a rotating-disk mechanical foam-breaker (MFRD) fitted to the BC and its usefulness as a foam control apparatus in the BC with a foaming system were studied. Comparison of flow and mass transfer characteristics between BCs when the foaming is controlled by the MFRD and an antifoam agent (AF) was also attempted. For a BC treating diluted detergent solutions and those containing corn-syrup and baker's yeast, foaming behavior of the BC and foam-breaking behavior of the MFRD under various operating conditions were first examined in terms of the changes in the liquid holdup in the foam, ϕ_L. In order to reveal the superiority of mechanical foam control system, the characteristics such as the gas holdup ε_g and volumetric liquid-phase mass transfer coefficient k_La of the BC with the MFRD were then compared with those in the BC with an AF. The MFRD proved to be useful in controlling foam in the BC without the addition of AFs. That is, it was found that the MFRD was sufficient as a foam control apparatus in the BC with a foaming system. It was also confirmed

that ϕ_L was a typical measure which reflected the foaming intensity of the BC and was also related to the difficulty or ease of mechanical foam-breaking in terms of the power required for foam-breaking. As for the difference in gas holdups, $(\varepsilon_g)_M$ and $(\varepsilon_g)_F$, between the two BCs when the foaming was controlled by the MFRD and an AF, $(\varepsilon_g)_M$ was observed to be large compared with $(\varepsilon_g)_F$ at the same aeration rate conditions. It was also shown that $(k_La)_M$ in a mechanical foam control system (MFS) were considerably large compared with those in a nonfoaming system (NS) including an AF. Furthermore, a comparative investigation of k_La between the MFS and the NS in terms of the specific power input demonstrated higher level of the mechanical foam control system (MFS) in respect not only to the oxygen transfer performance but also to saving power requirements.

In chapter 4, design and operational characteristics of MFRDs fitted to BCs of different sizes were studied using various kinds of foaming liquids. The foam-breaking capacity of MFRDs, represented by the changes in the critical disk rotational speed N_c required for foam-breaking, that changes depending on the operational conditions were first evaluated. The effects of operational variables such as the liquid feed rate per unit disk circumference, Γ, the concentration of solute in the liquid, C, the column to rotating-disk diameter ratio, D_T/D_d, and the ratio of the foam-ascending distance from aerated liquid surface to the gas superficial velocity, h_f/U_g, on N_c were then clarified. On the basis of the results obtained

above, the correlation of N_c with operational variables was attempted. As a result, N_c under any operating conditions of BCs with MFRDs treating each kind of foaming liquid was found to be correlated by Eq.(4-4) - (4-12), respectively. The foaming behavior of BCs was then examined in terms of the changes in the liquid holdup in foam, ϕ_L, which reflects the foaming intensity of BCs and is related to the difficulty of foam-breaking as a function of N_c. The relationship between ϕ_L and the operational parameters such as liquid superficial velocity U_L, C, D_T/D_d and h_f/U_g was evaluated. The values of ϕ_L in BCs with MFRDs treating each kind of foaming liquid could be predicted by Eq.(4-12) and Eqs.(4-14) - (4-19), respectively. The level of required foam-breaking power P_{kc} of MFRDs was also examined in relation to the changes in ϕ_L, the dispersion distance l_f of liquid particles dispersed from the rotating disk and the gas velocity ratio between the BC and the annular foam-breaking section separated by the disk and the column wall, U_{ga}/U_g. As a result, P_{kc} were found to be correlated by Eq. (4-20) independently of the kind and concentration of foaming liquids. Estimation of the performance of a MFRD fitted in a BC and that of the operational range which foaming can be controlled effectively and economically by the MFRD were further carried out. It was shown that the effective operational range of the MFRD in such a BC could be predicted by using Eq.(4-2) and Eqs.(4-4) - (4-12), respectively.

In chapter 5, the mechanical foam-breaking difficulty,

represented by the changes in liquid holdup in foam, ϕ_L, was studied in terms of changes in foaming characteristics of liquids. Using a small foaming apparatus which is different from the gas bubbling apparatus actually employed, i.e., BCs, the foaming characteristics of various liquids were first evaluated. Liquid foaming characteristics such as liquid holdup in foamate flow, ϕ_t, rate of liquid drainage from foam, v, foam velocity u_f and foam size d_f were measured for respective liquids under constant gas-bubbling and foaming conditions. To investigate whether respective foaming characteristic values obtained can be used as a measure of foam-breaking difficulty, these values were then compared with those of ϕ_L observed in BCs with MFRDs. ϕ_L was difficult to correlate independently by individual factors such as ϕ_t, v, u_f and d_f measured in the foaming apparatus. Therefore, evaluation of the overall foaming characteristics of liquids as a function of respective factors was then attempted. A new parameter ϕ_f, incorporating ϕ_t, v and u_f, was derived. From investigation of the relationship among ϕ_f, d_f and ϕ_L, the relationship $\phi_L/\phi_f \propto d_f^{1.83}$ regardless of the kind of foaming liquid or its concentration was obtained. On the basis of this relation, the term $\phi_f d_f^{1.83}$ was employed instead of the concentration term in empirical equations for ϕ_L proposed in chapter 4, and the new correlation of ϕ_L was attempted. It was found that ϕ_L in BCs with MFRDs treating various liquids could be predicted Eq.(5-6) independently of the kind of foaming liquid and its concentration.

In chapter 6, the required critical disk rotational speed N_c of MFRDs fitted to BCs treating various foaming liquids was evaluated in relation to the foaming characteristics of liquid. As could be derived from the results discussed in chapter 4, the values of N_c were found to differ depending on the kind of foaming liquid. On the basis of the facts that the changes in ϕ_L corresponded well to those in N_c and that the term $\phi_f d_f^{1.83}$ was useful for evaluation of the difference of ϕ_L among the liquids, the term $\phi_f d_f^{1.83}$ was utilized to correlate N_c values of MFRDs fitted to BCs. Equation (6-7) was obtained as the equation which could be applied for the prediction of N_c in foam-breaking regions independently the kind of foaming liquids and its concentration.

Chapter 7 dealt with design and operation of BCs with MFRDs treating mixed solutions and biological media whose composition is complex. For a small BC treating mixed solutions, the foaming behavior in BC were first examined in terms of the changes in ϕ_L. The effects of operating conditions such as U_L and h_f/U_g on ϕ_L, were the same as those observed in the system using the liquids of single component. Foaming characteristic values such as ϕ_f, v, u_f and d_f for each mixed solution were then measured in the small foaming apparatus. Using the values of foaming characteristic term F_{CT} ($=\phi_f d_f^{1.83}$) for respective solutions, ϕ_L at each operating condition was calculated from Eq.(7-3). From a comparison between ϕ_L values calculated and those observed, it was confirmed that Eq.(7-3) proposed for the single component system could be also

applied for the prediction of ϕ_L in the BC with the MFRD treating mixed solutions. N_c values of MFRD fitted to small BC treating mixed solutions were also evaluated. The dependences of operating variables on N_c were the same as those in the system using the liquids of single component. Comparison between N_c values calculated from Eq.(7-7) and those observed was carried out. N_c in the foam control system treating mixed solutions was found to be possible to predict from Eq.(7-7). Similar investigations were carried out for the small BC with the MFRD treating biological media. It was confirmed that Eq.(7-3) and (7-7) could be also applied to the prediction of ϕ_L and N_c in the foam control system treating biological media. For larger BCs with MFRDs treating mixed solutions and biological media, applicability of the empirical correlations for ϕ_L and N_c was further examined. It was also found that ϕ_L and N_c values of MFRDs fitted to large BCs could be estimated respectively by Eq.(7-3) and Eq.(7-7). Power consumption P_{kc} for foam-breaking with MFRDs was further confirmed to be predicted by Eq.(7-10). The equations, i.e., Eqs.(7-10), (7-3) and (7-7), which can be applied independently of the kind and concentration of the foaming liquids, are expected to be beneficial to the design and operation of MFRDs fitted to BCs treating various kinds of foaming liquids including mixed solutions, biological media, etc.

In chapter 8, gas holdups in BCs of different sizes under foam control were studied for the system using various liquids. The effects of operating conditions on the

gas holdup $(\varepsilon_g)_M$ in a mechanical foam control system (MFS) were first investigated. $(\varepsilon_g)_M$ was almost free from the effect of the disk rotational speed N. Although there was a difference in the value of gas holdup depending on the liquid, $(\varepsilon_g)_M$ became larger with increasing U_g for all the systems. As for the effect of Γ, $(\varepsilon_g)_M$ tended to be slightly large with increasing Γ. The correlation of $(\varepsilon_g)_M$ in the MFS was then attempted. $(\varepsilon_g)_M$ in BCs treating any foaming liquids was found to be predicted by Eqs.(8-5) and (8-6). Similar investigations were also carried out for BCs in a nonfoaming system (NS) including an antifoam agent (AF). The gas holdup $(\varepsilon_g)_F$ in the NS could be correlated by Eq.(8-8). Comparison of gas holdups between the MFS and the NS at the same aeration rate conditions was further carried out. The values of gas holdup ratio $(\varepsilon_g)_M/(\varepsilon_g)_F$ were found to be remarkably larger than 1.0. That is, it was found that a considerable increase in the gas holdup compared to the NS could be expected in the MFS.

In chapter 9, mass transfer characteristics of BCs treating various foaming liquids when the foaming was controlled by MFRDs and an antifoam agent (AF) were studied. The volumetric liquid-phase mass transfer coefficient was measured by the sulfite oxidation method. The effects of operating conditions on the volumetric liquid-phase mass transfer coefficient $(k_La)_M$ in the mechanical foam-controlling system (MFS) and $(k_La)_F$ in the nonfoaming system (NS) including an AF were first examined. $(k_La)_M$ tended to increase slightly with increase Γ. The

effect of U_g on $(k_L a)_M$ and $(k_L a)_F$ was similar. It was also observed that $(k_L a)_M$ was considerably large compared with $(k_L a)_F$ under the same aeration rate conditions. The volumetric liquid-phase mass transfer coefficients in the MFS and the NS were then evaluated in relation to the changes in gas holdup. $(k_L a)_M$ and $(k_L a)_F$ could be predicted by Eqs.(9-3) and (9-4) as a function of gas holdup, respectively. Comparison of $k_L a$ between the MFS and NS in terms of the specific power input was further carried out. It was shown that in order to obtain the same values of $k_L a$ between the two BCs, the specific power input in the NS had to be increased considerably compared to the MFS. That is, the superiority of the MFS in respect not only to oxygen transfer rate but also to power input economy was confirmed.

Chapter 10 dealt with liquid-phase mass transfer coefficients in BCs under foam control. The bubble diameters in BCs when the foaming was controlled by the MFRD and an AF were first measured. Using these results and those of the gas holdup measured in chapter 8, the specific gas-liquid interfacial area a was then evaluated for the MFS and the NS, respectively. An increasing tendency of a with U_g was common for both systems, but the values of a in the MFS were found to be remarkable large compared with those of a in the NS. The liquid-phase mass transfer coefficient k_L was separated from $k_L a$ using the values of a. Changes in k_L were then investigated in relation to those in bubble diameter. A comparative investigation of the magnitude of k_L between the MFS and the NS demon-

strated that k_L in the MFS was remarkably small compared with k_L in the NS. It was concluded that higher values of k_La in the MFS were mainly due to the effect of increased specific gas-liquid interfacial area caused by the presence of fine bubbles in the bulk liquid. Furthermore, on the basis of the results obtained above, the correlation of liquid-phase mass transfer coefficients in terms of the dimensionless parameters such as the sherwood number Sh, the Schmit number Sc, the Galilei number Ga, the Grashof number Gr and the Bond number Bo was also carried out. As the equations for predicting k_L in the MFS and the NS, Eqs.(10-8) and (10-9) and Eq.(10-10) were obtained respectively.

In the present study, investigation by chemical engineering and apparatus engineering approaches was carried out on operational characteristics of bubble column fermentors under foam control. This paper, as summarized in the above, thus provided a large number of useful and practical data through fundamental and systematic investigation on foam control by rotating-disk mechanical foam-breakers or on the design and operation of bubble column fermentors equipped with MFRDs, treating various kinds of foaming liquids. A collection of the data and information obtained in the present study is anticipated to contribute as a significant and basic guide-line for the methodology of mechanical foam-breaking in bubble column fermentors, and for designing and operation of bubble column fermentors having a foam-breaking mechanism best suited for microbiological reaction processes in a foam-

ing system.

11-2. Prospect of further study

The ultimate goal of the study is a successful design, operation and control of the bubble column fermentor under mechanical foam control and a reliable prediction of the bubble column fermentor performance over a wide range of operating conditions. In order to accomplish the purpose completely, some works still remain to be done. Further themes which are expected to be solved on bubble column fermentors with mechanical foam-breakers are as follows:

1) Evaluation of the effect of liquid temperature on foam-breaking characteristics of rotating-disk mechanical foam-breakers (MFRDs) fitted to bubble column fermentors, i.e., bubble columns (BCs).
2) Clarification of the effect of gas sparger types on characteristics of BCs with MFRDs.
3) Analysis of foam-breaking, flow and mass transfer characteristics of BCs with mechanical foam-breakers different from the MFRD.
4) Evaluation of performance of various bubble column fermentors with MFRDs or other types of mechanical foam-breakers and analysis of their design and operational characteristics based on changes in foaming characteristics of liquids.
5) Extensive application of bubble column fermentors equipped with various types of mechanical foam-breakers to fermentations or development of mechani-

cal foam-breakers having an auto-control mechanism.

In this study, all the experiments were carried out at the liquid temperature of 20℃ which was considered standard. In actual production processes, however, temperature of the process solution used in fermentations is varied over a wide range, according to the conditions best suited for cultivation of microorganisms. If the temperature of liquids to be treated is below or above 20 ℃ , it is assumed that foaming characteristics of liquids may differ from those at 20℃ and as a result foam-breaking characteristics of MFRDs fitted to BCs also change. In this study, it was shown that the foaming characteristic term F_{CT} measured for respective liquids by using a small foaming apparatus was useful for the prediction of the liquid holdup in foam, ϕ_L, and the required critical disk rotational speed N_c as related to mechanical foam-breaking difficulty. Taking into consideration the fact that this characteristic term was independent of the kind of foaming liquid, its concentration or physical properties, it is expected that foam-breaking characteristics of MFRDs fitted to BCs treating liquids of various temperatures will also be able to evaluate by utilizing the term F_{CT}. In order to confirm this, further experimental works using liquids of different temperatures are necessary.

Evaluation of the effects of gas sparger types on various characteristics of BCs with MFRDs was not studied in this study. For sparging of air into bubble column fermentors, different types of gas spargers such as

single nozzle, perforated plate, porous plate, etc. have frequently been utilized. Hence, clarification of the effect of gas sparger types on various operational characteristics in BCs with MFRDs are indispensable for practical and wide-spread use of this type of bubble column fermentor. It is also desired to confirm usefulness of the foaming characteristic term F_{CT}, that is, to examine applicability of the term F_{CT} to the prediction of the liquid holdup in foam and the required critical disk rotational speed in these systems.

A number of mechanical foam-breakers utilizing the impact force or the shear and centrifugal force such as whirling paddle, conical rotor, spray, nozzle, etc. other than the MFRD have been proposed so far for the control of foaming in fermentors (Refs.24, 28, 29, 51, 54, 56, 57, 59, 68, 134, 135, 145). Quantitative performance data, however, are scarce, and our understanding of mechanisms of the operation is far from adequate. In other words, the usage of these mechanical foam-breakers is at present mostly empirical. To select a practical and effective foam-breaker for foam control in BCs, performance of available foam-breakers must first be evaluated quantitatively. Analysis of foam-breaking characteristics of the existing foam-breakers utilizing the foaming characteristic term F_{CT} is also desired. And then, it will also be necessary to evaluate flow and oxygen transfer characteristics in BCs with these available foam-breakers and to compare their results with those observed in BCs with MFRDs.

In microbial process industries, various types of bubble column fermentors or their improved types have been employed (Refs.30, 52, 98, 120, 122). In order to clarify which fermentor type is most effective for the treatment of a foaming system, it is first important to evaluate foam-breaking performance of MFRDs or other types of foam-breakers fitted to various BCs and then to evaluate characteristics such as the foam-breaking, the gas holdup and the volumetric mass transfer coefficient in each BC fitted with any foam-breakers. Establishment of design and operational procedures of various types of BCs with mechanical foam-breakers, in which the foaming characteristic term of liquids is utilized, is also desired.

In industrial production processes, there are many microbial reaction systems with foam formation. Thus, studies on application of bubble column fermentors having a foam-breaking mechanism to various microbiological processes with foaming, in which useful materials such as cell mass, metabolites, etc. are produced, are especially important, which also are expected to be beneficial to the development of bubble column fermentors, useful for effectively treating a foaming system without using antifoam agents. An important theme to be further studied after confirmed practical value of bubble column fermentors having a foam-breaking mechanism is the problem of auto-control of mechanical foam-breakers employed actually. It is generally known that the foaming pattern in bubble column fermentors changes considerably during the

fermentation. To operate effectively the foam-breaker with the minimum rotational speed and power consumption, it is necessary to control the foaming automatically in accordance with the changes in foaming pattern (i.e., intensity) of the process solution during the operation. Development of a bubble column fermentor fitted with a mechanical foam-breaker having an auto-control mechanism has hitherto been received little attention. However, it should be recognized that auto-control of foaming brings about considerable reduction of running costs for the operation of a mechanical foam-breaker. Development of the mechanism for controlling the foaming automatically is also anticipated to contribute to wide-spread use of mechanical foam-breakers in microbial production processes using bubble column fermentors.

Nomenclature

a	specific surface area per unit volume of the liquid	[1/m]
A_f	cross-sectional area of foaming column	[m^2]
A_t	cross-sectional area of tube for discharging foamate	[m^2]
Bo	Bond number ($=gd_{vs}^2 \rho / \sigma$)	[-]
C	concentration of solute in liquid	[ppm]
C_{DO}	dissolved oxygen concentration	[kg/m^3]
C_{DO}^*	dissolved oxygen concentration at saturation	[kg/m^3]
C_F	concentration of antifoam agent	[ppm]
C_{ss}	concentration of sodium sulfite	[$kmol/m^3$]
d_b	individual bubble diameter	[m]
d_f	size of foam ascending through column in small foaming apparatus	[m]
d_p	particle diameter	[m]
d_{vs}	volume-surface mean bubble diameter	[m]
D_d	rotating disk diameter	[m]
D_L	liquid-phase diffusivity	[m^2/s]
D_T	bubble column diameter	[m]
f	frequency of impact between liquid particles and ascending foam	[1/s]
F	liquid flow rate	[m^3/s]
Fr	Froude number ($=\mu^2/gD_T$)	[-]
g	gravitational constant	[m/s^2]
Ga	Galilei number ($=gd_{vs}^3 \rho^2/\mu^2$)	[-]
Gr	Grashof number ($=d_{vs}^3 \rho \triangle \rho / \mu^2$)	[-]
h_f	foam-ascending distance from aerated liquid	

	surface to MFRD in bubble column	[m]
h_l	liquid level in foaming column after stopping air-sparging	[m]
H	Henry's law constant	[Pam^3/mol]
H_d	rotating disk height in bubble column	[m]
H_f	height of aerated liquid surface from the bottom of bubble column	[m]
H_L	static liquid height in bubble column	[m]
k_L	liquid-phase mass transfer coefficient	[m/s]
k_La	volumetric liquid-phase mass transfer coefficient	[1/s]
K	dimensionless parameter defined by Eq.(8-4)	[-]
l_f	dispersion distance of liquid particles from disk	[m]
L_b	baffle length	[m]
n	number of gas bubbles observed	[-]
N	disk rotational speed	[1/s]
N_c	critical disk rotational speed required for foam-breaking	[1/s]
N_{PK}	power number ($=P_k/\rho N^3 D_d^5$)	[-]
N_Γ^+	dimensionless transition liquid feed rate per wetted perimeter from ligament to filmy formation ($=\Gamma_T/D_d\sqrt{\mu N/\rho}$)	[-]
p	partial pressure of oxygen	[Pa]
P	pressure	[Pa]
P_g	pneumatic power of gas input	[W]
P_k	power consumed for liquid dispersion	[W]
P_{kc}	power consumed for liquid dispersion at critical state for foam-breaking	[W]

P_T	power input in MFS, defined by $P_{kc}+P_g$	[W]
Q_g	volumetric gas flow rate in foaming column	[m^3/s]
Q_L	volumetric rate of liquid in foamate flow discharging from foaming column	[m^3/s]
R	oxygen uptake rate by cell	[kg/s]
Re	Reynolds number ($=\rho ND_d^2/\mu$)	[-]
s_b	surface area of bubble	[m^2]
S	cross-sectional area of bubble column	[m^2]
S_a	annular foam-breaking section [$=\pi (D_T^2-D_d^2)/4$]	[m^2]
Sc	Schmidt number ($=\mu/\rho D_L$)	[-]
Sh	Sherwood number ($=k_L d_{vs}/D_L$)	[-]
t	time	[s]
T	absolute temperature of liquid	[K]
u_f	foam velocity in foaming column	[m/s]
u_L	liquid superficial velocity	[m/s]
U_b	terminal single bubble rise velocity	[m/s]
U_g	gas superficial velocity in bubble column	[m/s]
U_{ga}	gas superficial velocity passing through S_a	[m/s]
U_L	liquid superficial velocity when liquid dispersed from disk is assumed to flow downwards through the foam layer in bubble column	[m/s]
v	volumetric rate of liquid drainage from foam	[m^3/s]
v_b	bubble volume	[m^3]
v_f	volume of liquid in foamate collected in container	[m^3]
v_F	foam volume	[m^3]
v_L	net liquid volume in v_F	[m^3]
V_f	net liquid volume in foam layer in bubble column	[m^3]

V_l	net liquid volume in bulk liquid layer in bubble column	[m^3]
V_L	working liquid volume in bubble column	[m^3]
W	liquid feed rate onto rotating disk	[m^3/s]
W_b	baffle width	[m]
We	Weber number ($=\rho N^2 D_d^3/\sigma$)	[-]
W_f	absolute amount of cells existed in foam layer	[kg]
W_l	absolute amount of cells existed in bulk liquid layer	[kg]
X_d	dry cell concentration per working liquid volume	[kg/m^3]
X_l	wet cell concentration in bulk liquid layer	[kg/m^3]
X_L	wet cell concentration per working liquid volume	[kg/m^3]
$\overline{X}_f$	mean wet cell concentration in foam layer	[kg/m^3]
ε_g	gas holdup relative to clear liquid volume	[-]
ε_{gm}	gas holdup relative to aerated liquid volume [$=\varepsilon_g/(1+\varepsilon_g)$]	[-]
μ	viscosity of liquid	[Pas]
μ_{ef}	effective viscosity calculated with the help of power law model	[Pas]
μ_g	viscosity of gas	[Pas]
ν	kinematic viscosity	[m^2/s]
ρ	density of liquid	[kg/m^3]
ρ_g	density of gas	[kg/m^3]
σ	surface tension of liquid	[N/m]
ϕ_f	liquid holdup in foam ascending through foaming column defined by Eq.(5-4)	[-]
ϕ_L	liquid holdup in foam in bubble column under	

	mechanical foam control	[-]
$\overline{\phi}_L$	mean liquid holdup in foam in foam layer	[-]
ϕ_t	liquid holdup in foamate discharging through tube in foaming column	[-]
Γ	liquid feed rate per unit disk circumference ($=W/\pi D_d$)	[m^2/s]
Γ_T	transition liquid feed rate per wetted perimeter from ligament to filmy formation, calculated by Eq.(4-2)	[m^2/s]
$\Delta\rho$	density difference ($=\rho - \rho_g$)	[kg/m^3]

Subscripts

cal	calculated
cen	center part in foaming column
i	plane of 2.0×10^{-1} m height from aerated liquid surface in foaming column
in	inlet value
obs	observed
out	outlet value
t	tube for discharging foamate from foaming column
F	chemical foam-controlling system or antifoam addition system
M	mechanical foam-controlling system
wall	wall in foaming column
W	water
1	value at time t_1
2	value at time t_2
3	value at time t_3

Literature Cited

1) Abe, S., T. Hamada and H. Tanaka: 42nd Annual Meeting of Soc. Chem. Engrs. Japan, April, Hiroshima, Paper E209 (1977).

2) Adler, I., U. Eberhard, W. D. Haberman and K. Schugerl: Eur. J. Appl. Microbiol. Biotechnol., 12, 212 (1981).

3) Aiba, S. and K. Toda: J. Gen. Appl. Microbiol., 9, 443 (1963).

4) Akiba, T. and T. Fukimbara: J. Ferment. Technol., 50, 414 (1972).

5) Akita, K. and F. Yoshida: Ind. Eng. Chem. Process Des. Develop., 16, 76 (1973)

6) Akita, K. and F. Yoshida: Ind. Eng. Chem. Process Des. Develop., 13, 84 (1974).

7) Anderson, J. L. and J. A. Quinn: Chem. Eng. Sci., 25, 373 (1970).

8) Andrew, B. and J. H. William: Biotechnol. Bioeng., 13, 663 (1971).

9) Astarita, G.: Ind. Eng. Chem. Fundam., 4, 236 (1965).

10) Atkinson, B. and F. Marituna: Biochemical Engineering and Biotechnology Handbook, The Nature Press, New York (1983).

11) Bach, H. F. and T. Pilhofer: Germ. Chem. Eng., 1, 270 (1978).

12) Begovich, J. M. and J. S. Watson: *Fluidization*, Proc. 2nd Eng. Found. Conf., ed., J. F. Davidson,

and D. L. Keairns, 190 (1978).

13) Bello, R. D., C. W. Robinson and M. Moo-Young: Biotechnol. Bioeng., 27, 369 (1985).

14) Benedik, A. and W. J. Heideger: Biotechnol. Bioeng., 13, 663 (1971).

15) Berovič, M. and A. Cimerman: Eur. J. Appl. Microbiol. Biotechnol., 7, 313 (1979).

16) Bhavaraju, S. M., T. W. F. Russell and H. W. Blanch: AIChE J., 24, 454 (1978).

17) Bikerman, J. J.: Foams, Springer-Verlag, New York (1973).

18) Brown, D. E. and M. A. Zainudeen: Biotechnol. Bioeng., 20, 1045 (1978).

19) Bryant, J.: In "Methods in Microbiology", Academic Press, New York, 187 (1970).

20) Bumblis, W. and K. Schugerl: Eur. J. Appl. Microbiol. Biotechnol., 11, 106 (1981).

21) Bumblis, W., K. Kalischewski and K. Schugerl: Eur. J. Appl. Microbiol. Biotechnol., 11, 110 (1981).

22) Bull, D. N. and L. L. Dempe: Biotechnol. Bioeng., 13, 529 (1971).

23) Bungay, H. R., C. F. Simons and P. Hosler: J. Biochem. Microbiol. Technol. Eng., 2, 143 (1960).

24) Burnner, C. A. and R. Lemlich: Ind. Eng. Chem. Fundam., 2, 297 (1963).

25) Calderbank, P. H.: Trans. Instn. Chem. Engrs., 36, 443 (1958).

26) Calderbank, P. H.: Trans. Instn. Chem. Engrs., 37, 173 (1959).

27) Calderbank, P. H. and M. Moo-Young: Chem. Eng. Sci., 16, 39 (1961).

28) Chechura, A. A.: USSR Patent No.512, 231 (1976).

29) Chemap A. G.: "Booklet No.h-997,9-78." Chemap A. G., Mannedorf, Switzerland, (1978).

30) Chisti, M. Y.: "Airlift Bioreactors", Elsevier Applied Science, New York (1989).

31) Davies, J. T., A. A. Kilner and G. A. Ratcliff: Chem. Eng. Sci., 19, 583 (1964).

32) Davies, J. T.: AIChE J., 18, 169 (1972).

33) Deckwer, W. D., K. Nguyen-tien, A. Schumpe and Y. Serpemen: Biotechnol. Bioeng., accepted (1981).

34) Deindoefer, F. H. and E. L. Gaden: Appl. Microbiol., 3, 253 (1955).

35) Dorsey, A. E.: J. Biochem. Microbiol. Technol. Eng., 1, 289 (1959).

36) Downing, A. L. and G. A. Truesdale: J. Appl. Chem., 7, 590 (1957).

37) Ebner, H., K. Pohl and A. Enenkel: Biotechnol. Bioeng., 9, 357 (1967).

38) Evans, J. I. and M. J. Hall: Process Biochem., 6, 23 (1971).

39) Eckenfelder Jr. W. W. and E. L. Barnhart: AIChE J., 7, 631 (1961).

40) Fair, J. R.: Chem. Eng., 74, 67 (1967).

41) Figueiredo, M. and P. H. Calderbank: Chem. Eng. Sci. 34, 1333 (1979).

42) Finn, R. K.: Bacterial Rev., 18, 254 (1954).

43) Fowler, M. W.: Prog. Ind. Microbiol., 16, 207 (1982).

44) Friedel, L., P. Herbrechtsmeier and R. Steiner: Ger. Chem. Eng., 3, 342 (1980).

45) Fujie, K., M. Takaine, H. Kubota and Y. Miyaji: J. Chem. Eng., 13, 188 (1980).

46) Fujie, K., N. Ishihara and H. Kubota: J. Ferment. Technol., 58, 477 (1980).

47) Fujinawa, K., M. Mogi and T. Hanzawa: Kagaku Kogaku, 31, 584 (1967).

48) Fukuda, H., T. Shiotani, W. Okada and H. Morikawa: J. Ferment. Technol., 56, 619 (1978).

49) Fukuda, H.: J. Ferment. Technol., 59, 259 (1981).

50) Fukushima, S. and K. Kusaka: J. Chem. Eng. Japan, 10, 468 (1977).

51) Furchner, B. and A. Mersmann: Chem. Eng. Technol., 13, 86 (1990).

52) Furusaki, S., I. Endo and R. Matsuno: "Biochemical Engineering for 2001", Springer-Verlag (1992).

53) Gestrich, W. and W. Krauss: Chem. Ind. Tech., 47, 360 (1975).

54) Ghildyal, N. P., B. K. Lonsane and N. G. Karanth: Adv. Appl. Microbiol., 33, 173 (1988).

55) Godbole, S. P., A. Schumpe, Y. T. Shah and N. L. Carr: AIChE J., 30, 213 (1984).

56) Goldberg, M. and E. Rubin: Ind. Eng. Chem. Proc. Design. Dev., 6, 195 (1967).

57) Guerra-Santos, L., O. Kappeli and A. Fiechter: Proc. 1982 Int. Conf. Microb. Enhance., 12 (1983).

58) Hall, M. J. and C. H. Hassall: Appl. Microbiol., 19, 109 (1970).

59) Hall, M. J., S. D. Dickinson, R. Pritchard and J. I. Evans: Prog. Ind. Microbiol., 12, 170 (1973).
60) Hass, P. A. and H. F. Johnson: AIChE J., 11, 319 (1965).
61) Hikita, H. and H. Kikukawa: Chem. Eng. J., 8, 191 (1974).
62) Hikita, H., S. Asai, K. Tanigawa, K. Segawa and M. Kitao: Chem. Eng. J., 20, 59 (1980).
63) Hikita, H., S. Asai, K. Tanigawa, K. Segawa and M. Kitao: Chem. Eng. J., 22, 61 (1981).
64) Hobbs, S. Y. and C. F. Pratt: AIChE J., 20, 178 (1974).
65) Howe, R. H. L.: Process Biochem., 13, 28 (1978).
66) Hozawa, H., H. Yokohata, N. Imaishi and K. Fujinawa: Kagaku Kogaku Ronbunshu, 7, 138 (1981).
67) Hughmark, G. A.: Ind. Eng. Chem. Proc. Des. Dev., 6, 218 (1967).
68) Ibragimov, R. I.: USSR Patent No.422, 464 (1974).
69) Iordache, M. and O. I. Muntean: Ind. Eng. Chem. Fund., 20, 204 (1981).
70) Ishida, Y. and M. Isano: J. Antibiot., 7, 381 (1952).
71) Ito, M. and A. Abe: *In* Soc. Chem. Engrs. Jpn. (ed.), Kiho-Ekiteki Kogaku, Nikkankogyo Shinbunsha, Tokyo, 181 (1969).
72) Kalischewski, K. and K. Schugerl: Ger. Chem. Eng., 1, 140 (1978).
73) Kalischewski, K., W. Bumblis and K. Schugerl: Eur. J. Appl. Microbiol. Biotechnol., 7, 21 (1979).
74) Kargi, F. and M. Moo-Young: Comprehensive Biotech-

nology, vol-2, Pergamon Press, Oxford, UK, 5 (1985).

75) Kastanek, F: Collect. Czech. Chem. Comm., 42, 2491 (1977).

76) Kataoka, H. and T. Miyauchi: Kagaku Kogaku, 36, 888 (1972).

77) Kataoka, H., H. Takeuchi, K. Nakao, H. Yagi, T. Tadaki, T. Otake, T. Miyauchi, K. Washimi, K. Watanabe and F. Yoshida: J. Chem. Eng. Jpn., 12, 105 (1979).

78) Kato, Y. and A. Nishiwaki: Int. Chem. Eng., 12, 182 (1972).

79) Kawagoe, M., K. Nakao and T. Otake: J. Chem. Eng. Jpn., 8, 254 (1975).

80) Kawase, Y., B. Halard and M. Moo-Young: Biotechnol. Bioeng., 42, 1609 (1987).

81) Kawase, Y. and M. Moo-Young: Appl. Microbiol. Biotechnol., 27, 159 (1987).

82) Kawase, Y. and M. Moo-Young: Bioprocess Eng., 5, 169 (1990).

83) Kawase, Y., B. Halard and M. Moo-Young: Biotechnol. Bioeng., 39, 1133 (1992).

84) Kelkar, B. G., S. P. Godbole, M. F. Honath, Y. T. Shah, N. L. Carr and W. D. Deckwer: AIChE J., 29, 361 (1983).

85) Kitai, A., S. Goto and A. Ozaki: J. Ferment. Technol., 47, 356 (1969).

86) Kitchener, J. A. and C. F. Cooper: Q. Rev. Chem. Soc. 13, 71 (1959).

87) Kito, M., M. Shimida, T. Sakai, S. Sugiyama and C.

Y. Wen: *Fluidization*, 411 (1976).

88) Koide, K., T. Hayashi, K. Sumino and S. Iwamoto: Chem. Eng. Sci., 31, 963 (1976).

89) Koide, K., T. Hirahara and H. Kubota: Kagaku Kogaku, 30, 712 (1966).

90) Koide, K., H. Sato and S. Iwamoto: J. Chem. Eng. Japan, 16, 407 (1983).

91) Koide, K., S. Yamazoe and S. Harada: J. Chem. Eng. Japan, 18, 287 (1985).

92) Kumar, A., T. T. Dagaleesan, G. S. Laddha and H. E. Hoelscher: Can. J. Chem. Eng., 54, 503 (1976).

93) Lavery, M. and A. W. Nienow: Biotechnol. Bioeng. 30, 368 (1979).

94) Marrucci, G.: Ind. Eng. Chem., Fundam., 4, 224 (1965).

95) Matsumoto, S., K. Saito and Y. Takashima: J. Chem. Eng. Japan, 7, 13 (1974).

96) Mersmann, A.: Ger. Chem. Eng., 1, 1 (1978).

97) Moo-Young, M., B. Halard, D. G. Allen., R. Burrell and Y. Kawase: Biotechnol, Bioeng., 30, 746 (1987).

98) Moser, A.: "Bioprocess Technology", Springer-Verlag, New-York (1988).

99) Nakanoh, M. and F. Yoshida: Ind. Eng. Chem. Proc. Des. Dev., 19, 190 (1980).

100) Nakanoh, M. and F. Yoshida: Ind. Eng. Chem. Proc. Des. Dev., 22, 577 (1983).

101) Nunokawa, Y., H. Toba and K. Ouchi: J. Ferment. Technol., 49, 959 (1971).

102) Odawara, Y., T. Yamaguchi, Y. Suganuma and H.

Fukumori: J. Ferment. Technol., 59, 253 (1981).

103) Oels, U., J. Lucke, R. Buchholz and K. Schugerl: Ger. Chem. Eng., 1, 115 (1978).

104) Ohkawa, A., M. Sakagami, N. Sakai, N. Futai and Y. Takahara: J. Ferment. Technol., 56, 428 (1978).

105) Ohkawa, A., N. Sakai, H. Imai and K. Endoh: Biotechnol. Bioeng., 26, 702 (1984).

106) Onodera, M., H. Nishibori, H. Tanaka, N. Ogasawara and A. Ohkawa: Biosci. Biotech. Biochem., 57, 486 (1993).

107) Phillips, K. L., J. F. T. Spencer, H. R. Sallans and J. M. Roxburgh: J. Biochem. Microbiol. Technol. Eng., 2, 81 (1960).

108) Pirt, S. J. and D. S. Callow: J. Appl. Bacteriol., 21, 211 (1958).

109) Plichon, B., A. Decq and J. B. Guillaume: Ann. Microbiol. (Inst. Pasteur), 127A, 521 (1976).

110) Raymond, D. R. and S. A. Zieminski: AIChE J., 17, 57 (1971).

111) Richard, G. R. and L. B. Eugene: Chem. Eng. Sci., 41, 2629 (1986).

112) Rollinson, G. N. and M. Lumb: J. Gen. Microbiol., 8, 265 (1953).

113) Ross, S.: Chem. Eng. Prog., 63, 41 (1967).

114) Rubin, E., C. R. LaMantia and E. L. Gaden Jr: Chem. Eng. Sci., 22, 1117 (1967).

115) Sasaki, T.: Kogyokagaku Zasshi, 58, 809 (1955).

116) Sasaki, T.: Kaimengensho no Kiso, *In* Sasaki, T., Y. Tamai, T. Hisamatsu and M. Maeda (ed.), Hyomenkogaku

koza 3, Asakura Shoten, Tokyo, 155 (1973).

117) Sawada, T., H. Kamikawa and K. Sugata: J. Ferment. Technol., 55, 276 (1977).

118) Schügerl, K., U. Oels and J. Lucke: Advances in Biochem. Eng., 17, Springer Verlag (1977).

119) Schügerl, K., J. Lucke, J. Lehman and F. Wagner: Adv. Biochem. Eng., 8, 63 (1978).

120) Schügerl, K.: "Bioreactor Engineering", vol.2, John Wiley & Sons, New York (1991).

121) Schumpe, A., W. D. Deckwer: Ind. Eng. Chem. Process Des. Dev., 21, 706 (1982).

122) Shah, Y. T., B. G. Kelkar., S. P. Godbole and W. D. Deckwer: AIChE J., 28, 353 (1982).

123) Sheppard, J. D. and D. G. Cooper: J. Chem. Tech. Biotechnol., 48, 325 (1990).

124) Shirotsuka, T. and A. Hirata: Kagaku Kogaku, 35, 123 (1971).

125) Solomons, G. L.: Process Biochem., 2, 47 (1967).

126) Solomons, G. L. and M. P. Perkins: J. Appl. Chem., 8, 251 (1958).

127) Sugimoto, H., S. Ishi-i, T. Iwasa and T. Yokotsuka: J. Agr. Chem. Soc., Japan, 40, 93 (1966).

128) Sukan, S. S. and A. Guray: Biotechnol. Lett., 7, 451 (1985).

129) Takahara, Y.: Hakko to Kogyo, 36, 288 (1978).

130) Takahashi, H. and F. Yoshida: J. Ferment. Technol., 57, 349 (1979).

131) Takahashi, J., K. Yamada and T. Asai: J. Agr. Chem. Soc., Japan, 33, 707 (1959).

132) Towell, G. D., C. P. Strand and G. H. Ackerman: AIChE Inst. Chem. Eng., Symp. Ser., 10, 10 (1965).

133) Vanett Riet, K., A. Prins and J. A. Nieuwenhuijse: Eur. Congr. Biotechnol., 3rd, 2, 521 (1984).

134) Viesturs, U. E., M. Z. Kristason and E. S. Levitans: Adv. Biochem. Eng., 21, 169 (1982).

135) Walling, C., E. E. Ruff and J. L. Thornlon: J. Phys. Chem. 56, 989 (1952).

136) Weber, M. E.: Chem. Eng. Sci., 30, 1507 (1975).

137) Yagi, H. and F. Yoshida: J. Ferment. Technol., 52, 287 (1974).

138) Yasukawa, M., K. Yamagiwa and A. Ohkawa: Bull. Chem. Soc. Jpn., 63, 3307 (1990).

139) Yasukawa, M., M. Onodera, K. Yamagiwa and A. Ohkawa: J. Chem. Eng. Japan, 24, 188 (1991).

140) Yasukawa, M., M. Onodera, K. Yamagiwa and A. Ohkawa: J. Chem. Eng. Japan, 24, 531 (1991).

141) Yasukawa, M., M. Onodera, K. Yamagiwa and A. Ohkawa: Biotechnol. Bioeng., 38, 629 (1991).

142) Yoshida, F. and Y. Miura: Ind. Eng. Chem. Process Des. Develop., 2, 263 (1963).

143) Yoshida, F. and Y. Miura: AIChE J., 9, 331 (1963).

144) Yoshida, F. and T. Yamada: J. Ferment. Technol., 49, 235 (1971).

145) Zlokarnik, M.: Ger. Chem. Eng., 9, 314 (1986).

ADDITIONAL REMARK

This thesis was arranged based on the research papers which were reported in the following journals.

1) Takesono, S., M. Yasukawa, M. Onodera, K. Izawa, K. Yamagiwa and A. Ohkawa:
Performance Characteristics of a Tower Fermenter with Mechanical Foam Control.,
J. Chem. Tech. Biotechnol., 56, 97-107 (1993).

2) Takesono, S., M. Onodera, J. Nagai, K. Yamagiwa, A. Mori and A. Ohkawa:
Relation between Mechanical Foam-Breaking Difficulty and the Foaming Characteristics of Solutions.,
J. Ferment. Bioeng., 75, 314-318 (1993).

3) Takesono, S., M. Onodera, K. Yamagiwa and A. Ohkawa:
Design and Operation of Rotating-Disk Foam-Breakers Fitted to Tower Fermenters.,
J. Chem. Tech. Biotechnol., 57, 237-246 (1993).

4) Takesono, S., M. Onodera, K. Yamagiwa, A. Mori and A. Ohkawa:
Relation between Critical Disk Speed for Foam-Breaking of Rotating-Disk Mechanical Foam-Breakers and Foaming Characteristics of Solutions.,
J. Ferment. Bioeng., 77, 221-223 (1994).

5) Takesono, S., M. Onodera, K. Yamagiwa and A. Ohkawa:
Mechanical Control of Foaming in Tower Reactors.,
to be appeared in J. Chem. Tech. Biotechnol.

ACKNOWLEDGMENT

The author wishes to express his deep gratitude to Professor Akira Ohkawa, Professor Akihiko Mori, Lecturer Kazuaki Yamagiwa and Research Associate Masayuki Onodera who directed this research with the continuing suggestion which led to the completion of the research.

The author is greatly indebted to Professor Makoto Inagaki, Professor Masato Tanaka, Professor Hirosato Tanaka, Professor Koji Isogai and Associate Professor Akira Ito, Niigata University, for their valuable advice and discussion on this research. Professor Makoto Inagaki and Professor Masato Tanaka also offered unsparing cooperation and suggestive advice for presentation and compilation of the thesis.

He is also grateful to Associate Professor Yoji Taguchi, Niigata University, for his opportune advice and encouragement.

Thanks are also due to the members of Professor Ohkawa's laboratory; in particular, Messrs. Masami Yasukawa, Junichi Nagai, Koji Izawa, Barry Mamadou Dian, Kozo Akai and Miss Chieko Toyoshima, who cooperated with the author in the experimental and constructional works, and to Mr. Katsumi Takahashi, who in various ways helped the author.